REPUBLIQUE ALGERIENNE DEMOCRATIQUE ET POPULAIRE

MINISTERE DE L'ENSEIGNEMENT SUPERIEUR ET DE LA RECHERCHE SCIENTIFIQUE

Université des frères Mentouri Constantine1

Faculté des Sciences de la Nature et de la Vie

Département de Biologie animale

N° d´ordre :23/Ds/2018
N° de série :01/Boi.A/2018

Thèse de Doctorat :

EN VUE DE L'OBTENTION DU DIPLOME DE DOCTORAT EN SCIENCE EN BIOLOGIE ANIMALE
Spécialité : Biologie Moléculaire et Cellulaire
Option : Toxicologie Cellulaire

Intitulé:

Neurodegeneration, inflammation, oxidative stress and behavioral deficit following bilateral short term adrenalectomy in the nervous system of albino Wistar rats

Présentée par:

Naserddine Hamadi

Devant le jury :

Présidente :	**Pr. AMEDAH SOUAD**	**Université des frères Mentouri Constantine1**
Directrice de thèse :	**Pr. KHELIFI-TOUHAMI FATIMA**	**Université des frères Mentouri Constantine1**
Examinateurs:	**Pr. BAGHIANI ABDERRAHMANE**	**Universite Abbas Ferhat setif-1**
	Pr. ARRAR LEKHMICI	**Université Abbas Ferhat Sétif-1**
	Pr. KHENNOUF SEDDIK	**Université Abbas Ferhat Sétif-1**
	Dr. CHETTOUM AZIEZ	**Universite des freres mentouri Constantine1**

Année Universitaire: 2017-2018

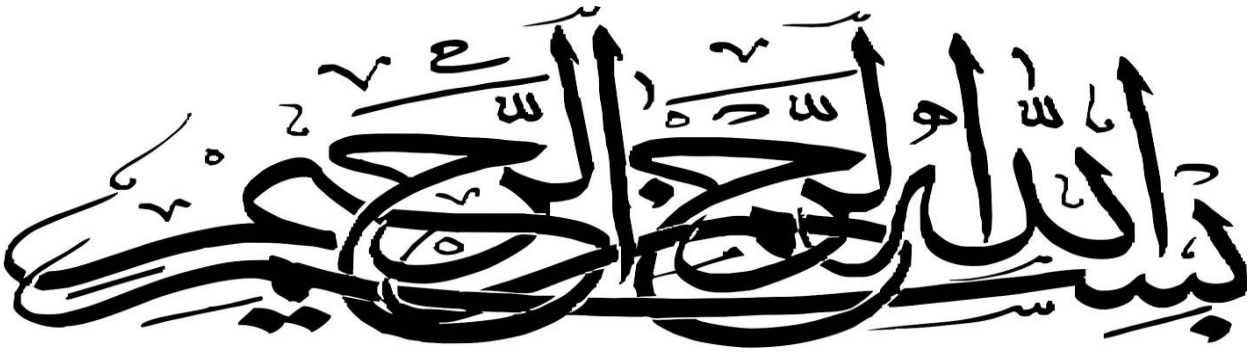

Dedication

First, my praises and thanks to "Allah" for his guidance and support in every step of my journey of success that I have achieved in my life.

I dedicate this work

To the greatest woman in my life, My *Mother*.

To the greatest caring and supporting man in my life, My *Father*.

I would like to dedicate this work to my dear wife *Cherine Charifa*.

To all my brothers *Hichem*, *Norou* with a special thanks and acknowledgement to my hero *Rida* for their endless support and encouragement.

To the most beautiful girls of my life my sisters *Dalel, Hala, Hajer, Nora* and with a special dedication to my little sister *Chahinaze.*

THANK YOU ALL FOR YOUR UNCODITIONAL LOVE

Acknowledgments

I offer my gratitude and appreciation to my supervisors without them this thesis might not have been completed. I would like to thank Prof. **Fatima Khelifi-Touhami** my main supervisor and director of Ethnobotany-Palynology and Ethnopharmacology-Toxicology laboratory for believing in me and honoring me by her supervision and accepting me to be one of her student, for the constant support and encouragement all along the way in achieving this work and for her guidance and patience.

I wish to express my special thanks and deep appreciation to ***Prof. Abdu Adem,*** Department of Pharmacology, College of Medicine and Health Sciences, United Arab Emirates University for allowing me to work in his lab, suggesting the topic of this work and standing behind it financially and scientifically.

I am so glad and thankfull to the president of the jury ***Pr. Amedah Souad*** and all the examiners ***Pr. Baghiani Abderrahmane, Pr. Arrar Lekhmici, Pr. Khennouf Seddik and Dr. Chettoum Aziez*** for accepting to judge my work and honor me by their blessed presence on the day of my thesis defense.

I am thankful so deeply to ***Dr. Loay lubbad,*** Department of surgery, College of Medicine and Health Sciences, UAE University for his constant technical support.

I am also so grateful to ***Prof. Abderrahim Nemmar,*** Department of Physiology. CMHS.UAEU for his priceless support and guidance.

I am so grateful to ***Prof. Safa Sheheb,*** Department of Anatomy, CMHS. UAEU for introducing me to the world of histology.

Very special thanks and gratitude to ***Prof. Adnan Kermandji,*** Constantine-1 University for the support, guidance and inspirational motivation along the way in producing the current work.

Special thanks to ***Mr. Rasheed Hameed,*** Department of Anatomy, CMHS. UAEU for the emotional, humoral, and technical support.

Without a doubt I am thankful to ***Azimullah Sheikh*** and ***Naheed Amir,*** Department of Pharmacology, CMHS. UAEU for teaching me different techniques in the first place and their endless technical support.

I am so grateful to have very wonderful great friends along the process of achieving this work and having wonderful time together: ***Khalid Cheleghema (El IBCHINI), Karim Doha, Aws Rashed Diab, Mohamed Mahjoub, Dr.Mustafa Ardah, Dr. Salah Alzajali, Muhamad Shafiullah, Ali Saad, Jamel Ziane, Houari Sherit and Hani Bouziane.***

LIST Of ABBREVIATIONS

AD: Alzheimer’s disease.

ALS: amyotrophic lateral sclerosis.

BDNF: brain derived growth factor.

CRF: corticotrophin-releasing factor.

EAE: experimental auto-immune encephalitis.

EIA: enzyme immunoassay.

DTNB: 5, 5′-dithio-bis-(2-nitrobenzoic acid).

DG: dentate gyrus.

GCL: granule cell layer.

GFAP: glial fibrillary acidic protein.

GSH: reduced glutathione.

HRP: horseradish peroxidase.

FTD: Fronto-temporal dementias.

Iba1: ionizedcalcium-binding adaptor molecule 1.

IL-1β: intrleukin-1.

IL-6: intrleukin-6.

iNOS: inducible nitric oxide synthase.

IGF-1: insulin-like growth factor.

MDA: malondialdehyde.

ML: Molecular layer.

MPTP: 1-methyl-4-phenyl-1,2,3,6-tetrahydropyridine.

MS: multiple sclerosis.

NF-kB: nuclear factor- kB.

NeuN: neuronal nuclear antigen.

NGF: nerve growth factor.

NO: nitric oxide.

NT: neurotrophin.

PBS: phosphate-buffered saline.

PD: Parkinson’s disease.

PL: polymorphous layers.

PUFA: polyunsaturated fatty acids.

ROS: reactive oxygen species.

RT: Room Tempurature.

SEM: Standard error of the mean.

SPSS: statistical package for the socialsciences.

SL: stratum lucidum

SOD: superoxide dismutase.

TMT: trimethyl tin.

TBA: thiobarbituric acid.

TNF-α: tumor necrosis factor

List of Figures:

Figure-22: Bar graphs showing TNF-α level in the hippocampus of adrenalectomized and sham operated rats over course of time (4h, 24h, 3days, 1week and 2weeks).

Figure-23: Images of coronal sections of the hippocampus stained with Fluoro-Jade B.

Figure-24: Representative confocal images of with Fluoro-Jade B staining.

Figure-25: Electron micrographs of dentate gyrus upper blade of ADX rats compared to sham operated three days postoperatively.

Figure-26: Electron micrographs of CA4 pyramidal cells of ADX compared to sham operated rats three days following surgery.

Figure-27: Electron micrographs showing degeneration in different areas of the hippocampus of ADX rats compared to sham operated were taken seven days postoperatively.

Figure-28: Electron micrographs taken from the upper blade of the dentate gyrus two weeks following adrenalectomy.

Figure-29: High power microscopy of degenerated granule cell in the hippocampus of adrenalectomized rats two weeks following adrenalectomy.

Figure-30: High power microscopy taken from CA4 area of the hippocampus following two weeks of adrenalectomy.

Figure-31: Electron micrograph showing CA3 pyramidal cells at different stage of degeneration two weeks following adrenalectomy.

Figure-32: Images of microgliosis in the hippocampus.

Figure-33: Bar graphs showing the comparison between the number of Iba-1 positive cells in the hippocampus of adrenalectomized and sham operated rats.

Figure-34: Representative images of coronal sections of the whole hippocampus.

Figure-35: Images of astrogliosis in the hippocampus.

Figure-36: Bar graphs showing the comparison between the number of GFAP positive cells in the hippocampus of adrenalectomized and sham operated rats.

Figure-37: Representative images of coronal sections of the whole hippocampus stained with NeuN (red) and GFAP (green) antibodies showing astrogliosis after two weeks of adrenalectomized rats compared to bilateral sham operated rats.

Figure-38: Representative images of coronal sections of the whole hippocampus approximately from -4.68mm relative to bregma stained with NeuN (red) and Iba-1 (green) showing microgliosis after two weeks of adrenalectomized rats compared to bilateral sham operated rats.

Figure-39: Representative images of coronal sections of the whole hippocampus approximately from -5.5mm relative to bregma stained with NeuN (red) and Iba-1 (green) showing microgliosis after two weeks of adrenalectomized rats compared to bilateral sham operated rats.

Figure-40: Representative confocal images of triple staining of hippocampal sections.

Figure-41: Reduced glutathione Standard Curve.

Figure-42: Bar graphs showing GSH levels in the hippocampus of adrenalectomized and Sham operated rats over course of time (4h, 24h, 3days, 1week and 2weeks).

Figure-43: Superoxide dismutase Standard Curve.

Figure-44: Bar graphs showing SOD activity in hippocampus of adrenalectomized and sham operated rats over the course of time (4h, 24h, 3days, 1week and 2weeks).

Figure-45: Malondialdehyde Standard Curve.

Figure-46: Bar graphs showing MDA levels in the hippocampus of adrenalectomized and Sham operated rats.

Figure-47A: Bar graphs showing latency time of adrenalectomized and Sham operated rats following three days of bilateral adrenalectomy.

Figure-47B: Bar graphs showing latency time of adrenalectomized and Sham operated rats following one week of bilateral adrenalectomy.

Figure-47C: Bar graphs showing latency time of adrenalectomized and Sham operated rats following two weeks of bilateral adrenalectomy.

Figure-48: summary of our findings.

LIST OF TABLES:

Table-13A: latency time of adrenalectomized rats compared to the sham operated rats after three days of adrenalectomy.

Table-13B: latency time of adrenalectomized rats compared to the sham operated rats after one week of adrenalectomy.

Table-13C: latency time of adrenalectomized rats compared to the sham operated rats after two weeks of adrenalectomy.

TABLE OF CONTENTS

Abstract

Bilateral adrenalectomy has been shown to damage the hippocampal neurons. Although the effects of long-term adrenalectomy have been studied extensively there are few publications on the effects of short-term adrenalectomy. In the present study we med to investigate the effects of short-term bilateral adrenalectomy on the levels of pro-inflammatory cytokines IL-1β, IL-6 and TNF-α; neurodegeneration, the response of microglia and astrocytes to neuronal cell death, animal behavior as well as oxidative stress markers GSH, SOD and MDA over the course of time (4h, 24h, 3days, 1week and 2weeks) in the hippocampus of Wistar rats.

Our results showed a transient significant elevation of pro-inflammatory cytokines IL-1β and IL-6 from four hours to three days in the adrenalectomized compared to sham operated rats. After one week, the elevation of both cytokines returns to the sham levels. Surprisingly, TNF-α levels were significantly elevated at four hours only in adrenalectomized compared to sham operated rats. The occurrence of neuronal cell death in the hippocampus following adrenalectomy was confirmed by Fluoro-Jade B staining and electron microscopy. Our results showed a time dependent increase in degenerated neurons in the dorsal blade of the dentate gyrus from three days to two weeks after adrenalectomy. Our results revealed an early activation of microglia on day three whereas activation of astroglia in the hippocampus was observed at one week postoperatively. A progression of microglia and astroglia activation all over the dentate gyrus and their appearance for the first time in CA3 of adrenalectomized rats hippocampi compared to sham operated was seen after two weeks of surgery. Quantitative analysis revealed a significant increase in the number of microglia (3, 7 and 14 days) and astrocytes (7 and 14 days) of ADX compared to sham operated rats. Our

study revealed no major signs of oxidative stress until two weeks after adrenalectomy when a significant decrease of GSH levels and SOD activity as well as an increase in MDA levels were found in adrenalectomized compared to sham rats. In the current study we used passive avoidance test to evaluate the cognitive functions of the ADX rats, we have found that the removal of the adrenal gland cause a behavioral deficit in the adrenalectomized rats compared to the shams over the time (3, 7 and 14 days).

Our study showed an early increase in the levels of pro-inflammatory cytokines followed by neurodegeneration and activation of glial cells as well as oxidative stress and all these changes manifested in a behavioral deficit in the adrenalectomized rats. Taking these findings together it could be speculated that the early inflammatory components might contribute to the initiation of the biological cascade responsible for subsequent neuronal death in the current neurodegenerative animal model. These findings suggest that inflammatory mechanisms precede neurodegeneration and glial activation.

Keywords: Adrenalectomy, hippocampus, neuroinflammation, neurodegeneration, oxidative stress.

OVERVIEW

Glucocorticoids are steroid hormones produced in the adrenal gland and secreted in the blood stream in response to the circadian rhythm as well as in stress situations (Dickmeis, 2009). The human and rodent versions of these hormones are cortisol and corticosterone respectively. It is well known since the second half of the last century that the hippocampus is the main target of these hormones due to the high level of their receptors in this area of the brain (McEwen et al., 1968)**.** In addition, several other brain areas such as the amygdala, neocortex and hypothalamus are targets of the adrenal hormones because of the abundance of mineralo and/or glucocorticoid receptors (Reul et al., 2015).

Immunohistochemical studies showed glucocorticoid receptors in the brain are of two types, mineralocorticoid or type 1 and glucocorticoid or type 2 receptors (Reul and de Kloet, 1985)**.** The abundance of these receptors in the hippocampus differs from one neuronal population to another where the granule cells are rich in type 1 and pyramidal neurons in type 2 receptors. In addition to their suppressive effect a inflammatory mediators (MacLennan et al., 1998)**.** In the brain such hormones play a major role in the production of neurotrophin-3 (NT-3), Brain Derived Growth factor (BDNF) and Nerve Growth Factor (NGF) (Barbany and Persson, 1992; Nichols et al., 2005; Smith et al., 1995; Vollmayr et al., 2001).

At the hippocampal level, several studies showed dual effect of these hormones. It has been reported chronic administration of high dose of glucocorticoids results in degeneration of pyramidal neurons (Sapolsky and Pulsinelli, 1985). However, multiple studies have demonstrated that adrenalectomy (ADX) induced massive and selective degeneration of the granule cells of the dentate gyrus (Sloviter et al., 1989, 1993a, 1993b.,Gould et al., 1990; Nichols et al., 2005; Spanswick et al., 2011; Stienstra et al., 1998). Moreover, in addition to granule cells degeneration, pyramidal cells degeneration were observed in the

hippocampus after long-term adrenalectomy (Sapolsky et al., 1991;Adem et al., 1994).

The discovery made by Sloviter et al.1989 (Sloviter et al., 1989) that adrenalectomy induces hippocampal granule cell loss and the duplication of this finding by several groups (Krugers et al., 1994; Nichols et al., 2005; Sousa et al., 1997; Sugama et al., 2013) as well as the findings by Sapolsky et al. 1991 (Sapolsky et al., 1991) and Adem et al. 1994 (Adem et al., 1994) that showed hippocampal pyramidal cell loss after long-term adrenalectomy have established this model as a neurodegenerative model to study of hippocampal cell death. Moreover, the neurodegeneration and glial response to the cell death that takes place in this model is comparable to what is seen in other established neurodegenerative models such as ischemia (Rothwell, 2003; Zhu et al., 2006), surgical injury (Tchelingerian et al., 1993), TMT (Trimethyltin) (Liu et al., 2005) KA (Kainic acid) (Minami et al., 1991) and cis-2,4-methanoglutamate (MGlu) (Pearson et al., 1999). Hence the ADX model can be used as an experimentally controlled neuronal cell death in the hippocampus which might be a relevant model to what is happening in neurodegenerative disorders.

Pro-inflammatory cytokines interleukin-1β (IL-1β) (Rothwell and Luheshi, 2000; Touzani et al., 1999; Vitkovic et al., 2000)**,** Intrleukin-6 (IL-6) (Gadient and Otten, 1994; Godbout and Johnson, 2004) and tumor necrosis factor alpha (TNF-α) (Perry et al., 2002; Sternberg, 1997; Vitkovic et al., 2000) have been shown to be produced by different cells in the brain (Rothwell, 2003)**.** Elevated levels of such cytokines have been found in numerous degenerative diseases such as Alzheimer's disease (AD) (Rubio-Perez and Morillas-Ruiz, 2012; Veerhuis et al., 1999)**,** Amyotrophic lateral sclerosis (ALS) (Rothwell and Luheshi, 2000) and Parkinson's disease (PD) (Blum-Degen et al., 1995; Nagatsu et al., 2000)**.**

Different studies showed the early expression of cytokines in various neurodegenerative animal models in which kainic acid (Yabuuchi et al., 1993)**,** trimethyltin (TMT) (Fiedorowicz et al., 2001)**,** ischemia-reperfusion (Sairanen et al., 1997; Yabuuchi et al., 1994)**,** 1-methyl-4-phenyl-1,2,3,6-tetrahydropyridine (MPTP) (Kumar et al., 2012; Selley, 2005) treatments were used. It has been reported that these inflammatory mediators are involved in the initiation of the morphological changes which occur during neuronal death and exacerbation of the damage induced by different insults (Allan et al., 2000; Apelt and Schliebs, 2001; Berti et al., 2002; Botchkina et al., 1997; Knoblach et al., 1999; Touzani et al., 2002).

Oxidative stress is well-known as a cytotoxic phenomenon when imbalance between the antioxidants and oxidants occurs leading to different aspects of tissue endangerment and subsequently the contribution to the neurodegenerative process (Halliwell, 2006; Lee et al., 2010; Li et al., 2004; Murakami et al., 2011). Reactive oxygen species (ROS) have important physiological functions (Hsieh and Yang, 2013; Schieber and Chandel, 2014)**.** Production of high levels of ROS can cause oxidative stress. Since oxidative stress can induce cell damage and promote inflammation (Haddad, 2002), cells have a battery of anti-oxidizing molecules and enzymes to prevent the accumulation of ROS (van Horssen et al., 2011).

INTRODUCTION

Chapter1: Cytoarchitecture and functions of the hippocampus

1-Neuronal populations in the hippocampus:

1-1-Pyramidal cells:

Pyramidal neurons of the cornu Amonis are characterized by two sets of dendritic arborsation, the apical dendrites emerge from the apex of the neuron heading towards stratum lacunosum through the stratum radiatum where they give off a few fine branches at the right angles toward CA1. At the Contrary, the basal dendrites emerge not only from one spot of the cell body but from several places (Isaacson et al., 1974, Spruston,2014 ; Ito et al.2008). The axons of these giant cells emerge either from the soma (Rasband. 2010 ; Höfflin et al.2017) or the proximal segment of one of the dendrites (Lorincz and Nusser, 2010).

Pyramidal cells are considered as essential cells in the hippocampal circuitry (Babateenet al.2017) and they are one of the most studied neurons in the brain. It has been shown that these cells are excitatory neurons generating the glutamate as neurotransmitter and play a crucial role in the integration of spatial, contextual and emotional information. In addition to their role in transferring all hippocampal output to various targets all over the brain (Graves et al., 2012).

1-2-Granule cells:

Before we discuss the morphology and physiology of these small cells. It is interesting to indicate that the granule cells are the only cells capable of proliferating and generating new neurons during the adulthood, such discovery was

one of the enormous breakthroughs in the nineties of the last century by Elizabeth Gould at Rockefeller University (Gould et al., 1997).

The granule cells considered the smallest cells that can be found in different regions of the brain such as olfactory bulb (Egger et al., 2005), cerebellum (Duguid et al., 2015) and the dentate gyrus (Claiborne et al.,1990). The histological examination of the hippocampus and more precisely the dentate gyrus revealed that the granule cells are the principal cells of the dentate gyrus. They are densely packed to form the primary layer of the dentate gyrus. In most cases, there is no glial sheath interposed between the cells and the ultrastructure examination of the dentate gyrus demonstrated the rise of their apical dendrite in the molecular layer; this later was bordered by the hippocampus fissure. (Figure-1a) (Amaral et al., 2007).

Studies have shown that granule cells play a major role in spatial memory and integration of the information because they are considered as the major gate of communication between the hippocampus and the parahippocampal structures (kee et al., 2007). The physiological studies of these cells revealed that they are glutamergic neurons and play a major role in the trisynaptic circuit of the hippocampus (Gutiérrez. 2003). In epileptic patient, granule cells become hyperactive due to the development of the basal dendrite which they lack naturally. Such an abnormality allowed them to increase the area of contact with input fibers and eventually increase their activation which in return will push the granule cells to activate the pyramidal cells of the CA3 and create a state of electric seizure results in the behavior alteration that we see in these patients (Figure-1b) (Dudek et al., 2004).

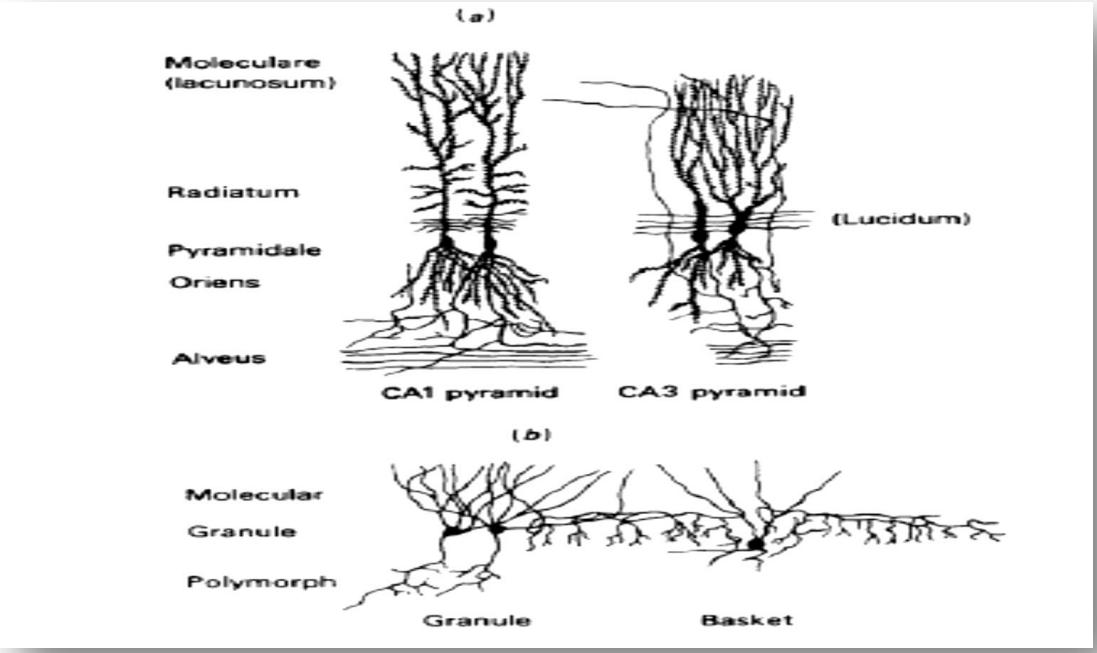

Figure-1: Structure of different cells of the hippocampus (O'Keefe and Nadel., 1974)

2-Cytoarchitecture:

Ramon y Cajal in 1914 is considered one of the pioneering figures in the determination of the hippocamppal cyto-architecture, followed by the exquisite work of his student Lorente de No 1934 by using silver and Nissl staining (Turner et al., 1998; El Falougy et al., 2008).The hippocampal formation comprises dentate gyrus, hippocampus proper (CA1, CA2 and CA3) and the adjacent parahippocampal cortices (Cao et al.2017). the hippocampus is organized in a laminar fashion and its connectivity is mostly unidirectional (Lopez-Rojas and Kreutz. 2016).

The double horseshoe shape of the hippocampus imposes a tri-synaptic paradigm of connections between different parts and facilitates the flow of the

information in and out of the hippocampus. The perforant pathways that originated in the entorhinal cortex considered the most prominent input to the hippocampus. These projections intersect with apical dendrites of the granule cells in the molecular layer of the dentate gyrus (Witter. 1993). In return, the granule cells send their axons laterally to the stratum lacunosum where they get connected with apical dendrites of the pyramidal cells of the CA3 (Swanson et al.,1978; Witter. 1993). These latters are characterized by long axons, organized in two bundles called the Schaffer collaterals, the major input to the small pyramidal cells of the CA1 and CA2 (Stepan et al.2015). Currently it became a general census that the trisynapatic model is the real demonstration how the information flows in the hippocampus (Figure-2) (Nakashiba et al., 2008; Neves et al., 2008).

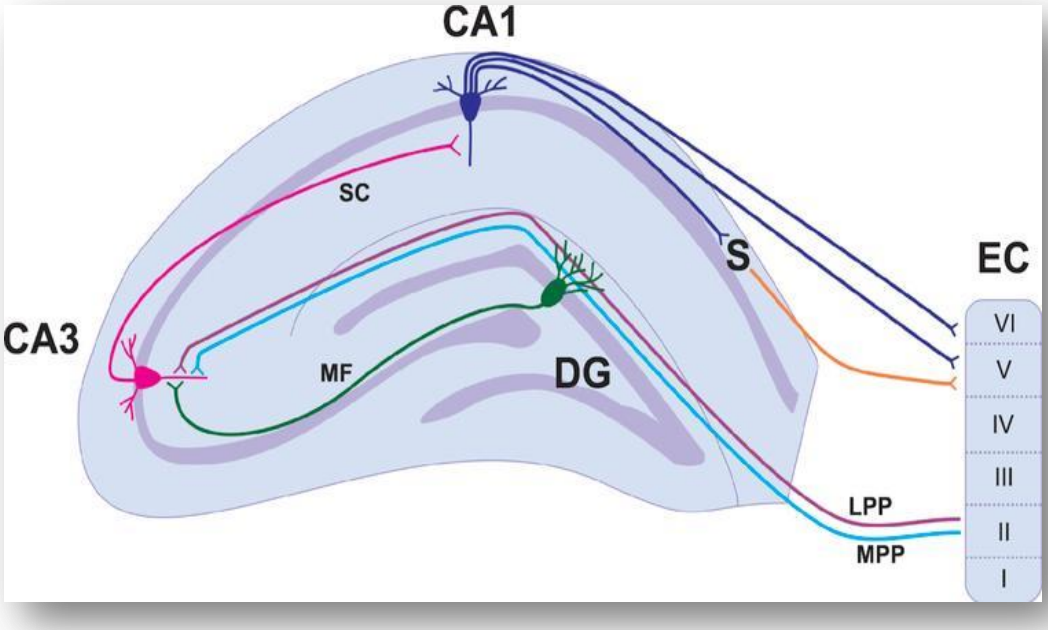

Figure-2: The trisynaptic paradigm in the hippocampus.Entorhinal Cortex (EC), Dentate Gyrus (DG), Perforant Path (PP - split into lateral and medial). Mossy Fibres (MF).Schaffer Collateral Pathway (SC).(Patten et al., 2015).

3-Functions of the hippocampus:

It has been a big fallacy in most people's believe of linking the role of hippocampus merely with learning and memory. Studies have shown this part of the brain plays a major role in stress response feedback, motor and emotions control. It was very hard for us to resume the function of the hippocampus in one or two pages since hundreds of books have been written about this subject.

3-1-Learning and memory:

The hippocampus is considered the center of acquiring and learning new experiences which called short term memory (Burgess et al, 2002). It is worthy to note that the hippocampus plays a major role in the embedding, storing and consolidation of of the information for a long period in the isocortex to form another different kind of memory that called long-term memory (Dudai, 2012, Adam et al.2014). Also the hippocampus plays a major role in processing, storing and retrieving different kind of memory such as episodic memory, a memory that permits conscious recollection of different events (Squire, 2007; Eichenbaum, 2000; Kopelman, 1993). In addition, the hippocampus plays a chief role in spatial memory that involves spatial location recognition (Squire, 2007; Herman et al., 1989).

3-2-Stress responses:

Today it is proofed and well known that the hippocampus plays an important role in the regulation of stress response (Kjelstrup et al.2008), via the regulation of the hypothalamic–pituitary–adrenal axis (HPA) axis and suppression of the ACTH secretion from the hypothalamus, a direct inducer of production and secretion of

glucocorticoids in the adrenal gland (Lathe.2001, Gutiérrez. 2003). Furthermore, since the early 1960s it has been known that hippocampal removal (or section of the fornix) precipitates adrenal hypersecretion of glucocorticoids (Fendler et al., 1961; Knigge, 196 1; Moberg et al., 1971).

3-3-Motor activity:

Since James Papez in 1947 defined the hippocampus as part of the limbic system (Arszovszki et al.2014), a common believe started to emerge about the involvement of the hippocampus in the control of ventral striatal loop, a group of brain areas responsible for motility control (Humphries and Prescott., 2010).

The ventral striatum is not only important for spatial processing and contextual cues (Hauber and Sommer.2011; Ferretti et al., 2010), processes the information relevant to effort (Hauber and Sommer.2011). The nucleus accumbens, the main structure of the ventral striatum, can be divided into core and shell subregions. The shell receives hippocampal inputs predominantly from ventral CA1 and subiculum, whereas the core receives them from dorsal CA1, subiculum and parahippocampal regions (Voorn et al., 2004).

Chapter 2: Neuroinflammation

1-Astrocytes:

1-1-Origin:

The german neuropathologist Rudolf Virchow was the first scientist that described the astrocytes as nerve glue in the second half of the nineteenth century (Scheller et al., 2011). Astrocytes are the most abundant neuroglial cells in the central nervous system, generally they outnumber neurons by five folds and they can be found all over the brain (Romero et al., 2014). It is now clear that astrocytes are of two types, white matter abundant astrocytes called fibrous and grey matter located astrocytes called protoplasmic (Parpura et al.,2012). The two types differ widely in their anatomy and physiology (Shigetomi et al., 2008).

The astrocytes processes ensure thousands of contacts with neural synapses per cell. Despite the large number of the processes that astrocytes possess, these cells tile the entire central nervous system in extraordinary network-like fashion where no overlapping between the cells can be seen, using the gap junctions as an essential way of communication between each other to meet the transportation of different mediators between the cells (Giaume et al., 2010).

1-2-Morphology:

The morphology of astrocytes differs from one region of the brain to another where we can find fibrous astrocytes with the processes oriented along the fiber tracts in the white matter (Wang et al., 2008). Protoplasmic astrocytes abundant in the grey matter such as the dentate gyrus of the hippocampus and corpus callosum, their processes are oppositely directed against the nerve fibers (Oberheim et

al.,2012;Bushong et al., 2003). The possession of multiple processes enable astrocytes to envelope the pre and postsynaptic terminals and play a remarkable role in fluid, ions, PH and neurotransmitters homeostasis in the synaptic space which is very crucial for the synaptic functioning and transmission (Brown and Ransom, 2007).

Interestingly, the heterogeneous nature of astrocytes population based on their morphology, expression of different sets of receptors, transporters, ions channels and other proteins raises the intriguing possibility that different subtypes of astrocyte are implicated in distinct metabolic/homeostatic functions (Matyash and Kettenmann, 2010).

1-3-Role in the CNS:

Astrocytes play a pivotal role in maintaining the homeostasis of the central nervous system (Placone et al., 2015), through ensuring a constant equilibrium of ions and water levels in the neuronal surrounding where a quick internalization of potassium ions by astrocytes during action potential takes place to maintain extracellular low levels of potassium according to the physiological needs (Sofroniew et al., 2010).

In addition, in order to sustain the energy demands and due to their possession of lactate shuttle, astrocytes supply neurons by lactate during critical moment where the oxygen is not sufficient for energy production (Magistretti, 2006; Tsacopoulos and Magistretti, 1996). In line with this, it has been shown that astrocytes play an important role in neurovascular and neurometabolic coupling. Indeed, neuronal activity triggers the release of a variety of vasoactive substances by astrocytes such as prostaglandins (PGE), nitric oxide (NO) and arachidonic acid (AA) to maintain the harmony in the nervous system (Gordon et al., 2007; Iadecola

and Nedergaard, 2007). In addition, there is a growing evidence that astrocytes influence directly neuronal communication through monitoring the release of multiple substances including glutamate, purines (ATP and adenosine), (γ-Aminobutyric acid) (GABA) (Halassa et al., 2009; Nedergaard et al., 2003; Perea et al., 2009; Shigetomi et al., 2008). Considering the metabolic relation between the two cells, we can assume the dependence of neurons on astrocytes to maintain the homeostasis and the integrity of the brain. It also permits us to predict any defection in the astrocyte machinery may lead to serious consequences in the brain (Figure-3).

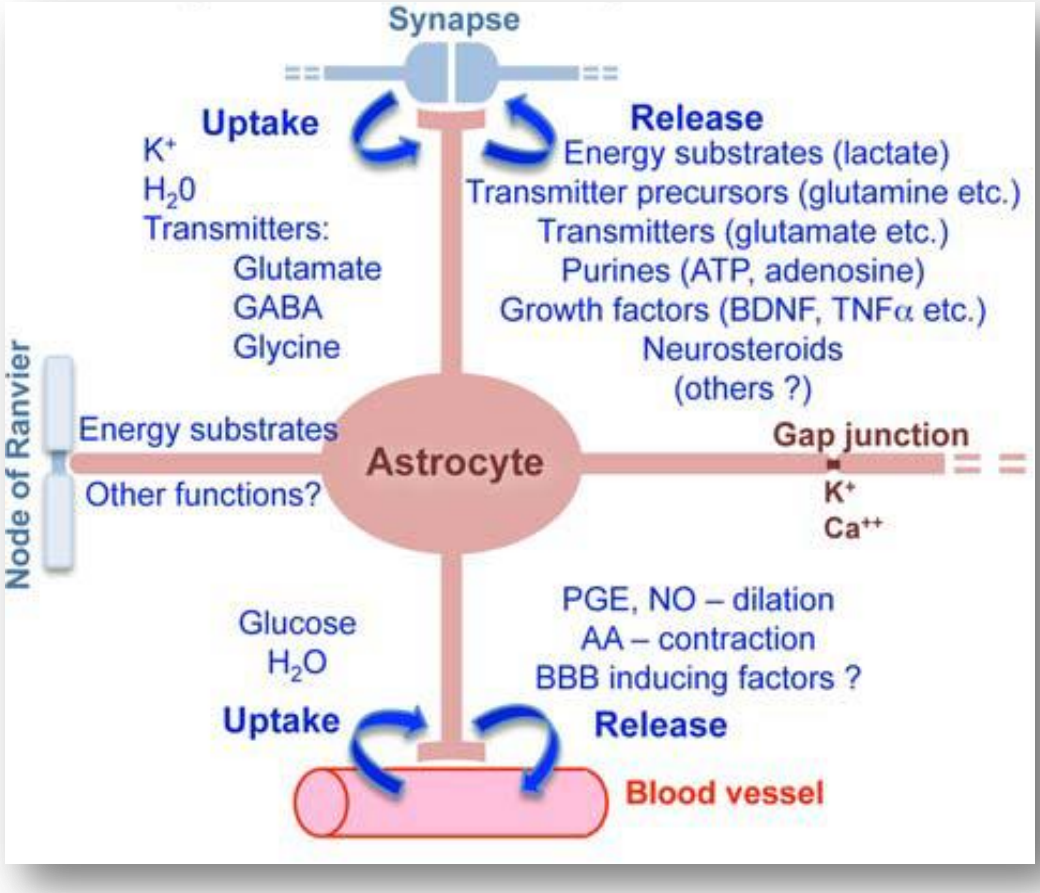

Figure-3: Role of astrocytes in the brain (Sofroniew and Vinters.2010)

It has been demonstrated that these metabolic relations between neurons and astrocytes qualified the later to play a very important role in brain physiology and ultimately in one of its sophisticated activities such as breath controlling (Gourine et al., 2010) and sleep homeostasis (Halassa et al., 2009).

Furthermore, several studies have evidenced the contribution of astrocytes in cognitive functions of the brain such as memory consolidations (Gibbs et al., 2008). Numerous homeostatic functions of astrocytes have been observed including defense against oxidative stress, energy storage in the form of glycogen and tissue repair. In addition they play a great role in the formation and remodeling of synapses (Perea et al., 2009; Shigetomi et al., 2008).

2-Microglia:

2-1-Origin:

Parallel to the periphery, the central nervous system has its own immune cells called microglia, The discovery of microglia returned to the twenties of the last century where the Spanish pioneer Pio del Rio-Hortega was able to describe the microglia differently from the astrocytes (Kettenmann et al., 2011). Microglia are known as CNS resident macrophage due to the huge similarity between the two cells in terms of function and phenotype (Habib and Beyer, 2015; Benedek et al., 2017).

Both macrophage and microglia cells express major histocompatibility complex (MHC) antigens, as well as T and B cell markers such as various cluster of differentiation (CD) proteins (McGeer and McGeer, 1995; Perry et al., 1985; Williams et al., 1994). However, still some differences that distinguish the two cells, contrary to the macrophages that are in constant contact with serum proteins, a slightest disruption in blood-brain barrier which ultimately results in leakage of

serum protein can induce the activation of microglia (Ransohoff and Perry, 2009). Another distinction, unlike the macrophages that are continuously replaced by new myeloid progenitors, microglia cells are generated upon activation which could be represented by an ultimate activation (Kettenmann et al., 2011; Ransohoff and Perry, 2009).

2-2-Morphology:

Microglia cells represent 15-20% of the total number of cells in the brain (Carson et al., 2006) and it is worthy to note that the density of these immune cells are slightly different from one region to another across the brain where up to 12% of substantia nigra cells are microglia, this applies to only 5% of cells in corpus callosum. Similarly, microglia morphology varies considerably where in the white matter they have elongated somata and the processes are preferentially oriented along the fiber tracts. On the contrary, microglia in the circumventricular organs, a region characterized by a leaky blood–brain barrier they exhibit a compact morphology with a few short processes. In the gray matter the microglia exhibit many elaborate radially oriented arbors (Harry and Kraft, 2012).

There has been a long debate concerning the origin of these cells when the common believe that these cells are originated in the neuroectoderm (Fedoroff et al., 1997). However, today due to the cutting edge technology it has become a general consensus that microglia are the descents of progenitors that have been originated from embryonic mesoderm in the periphery and migrated to the brain during the development (Kettenmann et al., 2011).

2-3-Role in the CNS:

Microglial cells are considered the first barrier of defense in the brain parenchyma (Piirainen et al., 2017). They play a very important roles in the regulation of neuronal processes development, maintenance of the neural environment, response to injury and subsequent repair. Microglia cells are similar to monocyte, actively surveying and shaping the structure and function of the neuronal circuit (Wake et al., 2013).

Phagocytosis is the process of terminal removal of cellular debris by microglia (Tremblay et al., 2011). The postnatal regulation of the number of neurons in the brain requires the induction of apoptosis in wide number of neurons which leads to the accumulation of cellular debris that requires its clearance by phagocytosis (Lee et al., 2010), this phenomena followed by synaptic remodeling and arrangement. Activated microglia were seen at different regions of the brain where synaptic remodeling is active like thalamus, cerebellum, olfactory bulb and hippocampus revealing the contribution of microglia in the development of the neuronal circuitry at early stage (Figure-4) (Dalmau et al., 1998; Fiske and Brunjes, 2000; Perry et al., 1985).

Furthermore, electron microscopy observation proofed the involvement of these cells in synaptic network remodeling (Wake et al., 2013) through phagocytosis in the developed brain. In addition, microglia cells were observed near to dendritic spines in mouse cortex in an experience-dependent manner indicating the contribution of such cells in synaptic plasticity (Schafer and Stevens, 2015).The discovery of neurogenesis during adulthood in the subgranular layer of the dentate gyrus of the hippocampus (Gouldet al., 1997), revealed another activity of microglia during this process where studies showed the majority of newborn

neurons pruned early during their development and undergo apoptosis which requires the involvement of microglia, this suggests the pivotal role of these cells in the progression of neurogenesis and spare these area the inflammation (Tremblay et al., 2011), In the healthy brain, microglia cells display a "homeostatic" phenotype, which continually monitor the surrounding environment, where studies have shown microglia react rapidly to any modifications of their environment (Davalos et al., 2005; Nimmerjahn et al., 2005). During infections or injuries, microglia behavior showed a great similarity to the macrophages in blood or tissues where they acquire the active amoeboid phenotype and secrete a wide range of cytokines (Shechter et al., 2013; Sica and Mantovani, 2012). Furthermore, in multiple neurodegenerative diseases, studies have shown that microglia are typically characterized by overt pro-inflammatory activation (Orihuela et al., 2016).

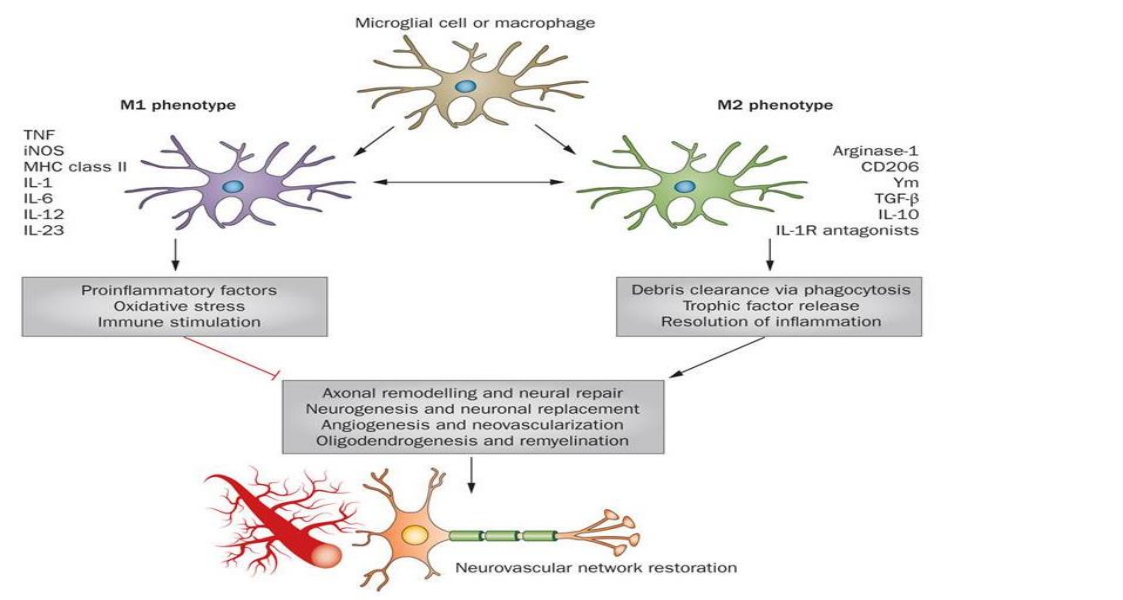

Figure-4: Role of microglia in the brain (Hu et al.2014)

3-Inflamatory Cytokines:

3-1-Interleukin-1:

First described as lymphocytes activating cytokine in 1972 (Gery and Waksman, 1972). Interleukin-1, is a term used to designate a class of three proteins interleukin-1α, interleukin-1β and interleukin-1ra (receptor antagonist), encoded by three separate genes located on the chromosome 2.

The morphological examination of the primary structure of IL-1α and IL-1β revealed a slight similarity between the two molecules that does not exceed 26% of homology. However, they share a quite similarity for the tertiary structure (Murzin et al., 1992) which enables the two molecule to have a common affinity for the two IL-1 receptors. In addition to morphological similarity, both cytokines can be regulated by the same regulatory machine and exert quite the same biological activities (Auron et al., 2007). The main producers of these cytokines are macrophages. However, many other cellular sources have been identified like neutrophils, lymphocytes, dendritic cells, keratinocytes, endothelial cells, hepatocytes, fibroblasts (Vicenová et al., 2009) and tumor cells (Miller et al., 2000; Wolf et al., 2001).

It is worthy to note that IL-1α is continuously produced by cells. However, in the case of IL-1β unless the cells receive a stimulatory factors during inflammation they are not able to produce it (Pelegrin and Surprenant, 2006). The principal targets of IL-1 are primarily cells of the immune system such as monocytes, lymphocytes, granulocytes and dendritic cells. The effects of these cytokines are not merely immune but they may have an influence on non- immune cells such as epithelial cells, fibroblasts and endothelial cells (Vicenová et al., 2009). In the brain, IL-1 is constantly expressed at low levels in healthy adult brain by a variety of cell types both neuronal and glial cells (Vitkovic et al., 2000).

Due to the close similarity of the general effect of IL-1α and IL-1β, it is important to emphasize here that when we mention IL-1β only, we are referring to the effect shared by the two cytokines. IL-1β is a pluripotent, proinflammatory factor that exert and orchestrate inflammatory responses in the periphery (Dinarello, 1996). Interleukin 1 is considered one of the most potent activators of T cells and indirectly influences the activation of B cells. Such cytokine exerts a regulatory effect on different components of the inflammatory cascade such as nuclear factor kappa B (NF-κB) and activator protein-1 (AP-1). Furthermore, it has the capacity to promote the activation of certain genes involved in cell division, survival and development of the vascular system (Schneider et al., 1998).

It has been shown that IL-1 molecule has a pluripotent effects on multiple brain functions including normal regulation of non-rapid eye movement (slow-wave) during sleep (Krueger et al., 2001), normal synaptic remodeling (Schneider et al., 1998), modulation of the hypothalamic pituitary-adrenal hormonal axis (Rothwell and Luheshi, 2000) and the appetite-suppressing hormone, leptin (Friedman and Halaas, 1998). It has been found in response to neuronal insult the microglia increase the production of IL-1 in the brain.

3-2-Interleukin 6:

At the beginning IL-6 was known as differentiation factor for B-cells through promoting the differentiation of these cells from it active form to an antibody producing cells (Hirano et al., 1986; Mihara et al., 2012).The majority of the immune cells (T and B cells, monocytes) produce IL-6. In addition, multiple non-immune cells like fibroblasts, keratinocytes, endothelial cells, meningeal cells, adipocytes and some tumor cells have the capacity to produce such proinflammatory cytokine (Scheller et al., 2011). In the nervous system both glial

and neuronal cells are expressing IL-6 and its receptors (Gadient and Otten, 1993; Schöbitz et al., 1993).

IL-6 exerts its effects through attachment to its transmembrane receptor, this latter is associated to a signaling receptor protein gp130 and it is worthy to note that IL-6 influences multiple cells by triggering different effects via its unique receptor and gp130 (Mihara et al., 2012). Several studies have shown that IL-6 plays a major role in the brain in different perspectives such as neurogenesis, a phenomenon which neurons are able to produce new cells (Bauer et al., 2007; Deverman and Patterson, 2009). In addition to its promoting effect in the production of new neurons, IL-6 has the capacity to influence the determination of cholinergic neurons phenotype (Fann and Patterson, 1994; März et al., 1998).

The influence of this cytokine is not restricted only to neurons but it shows a major effect on non-neuronal cells like astrocytes and microglia where an overexpression of such cytokine in transgenic mice displays a massive prominent astrogliosis and microgliosis (Campbell et al., 1993; Chiang et al., 1994; Fattori et al., 1995; Giralt et al., 2002). On the flip side, IL-6 knockout mice showed alteration of both cell populations activity in different models of neuronal injury (Cardenas and Bolin, 2003; Galiano et al., 2001; Penkowa et al., 1999a; Sugiura et al., 2000). Also it promotes sprouting and functional recovery of organ typical cultures of the hippocampus (Hakkoum et al., 2007).

IL-6 is famously known as pro-inflammatory cytokine which refers to its early production during infection and injuries. Such effect returns to the expression of IL-6 by the damaged or infected area. IL-6 along with IL-1β or TNF-α induce attraction of neutrophils to the site of injury, Down regulation of such cytokine halts such activity (Hurst et al., 2001; Jones, 2005; Scheller et al., 2011). In addition, to the neuronal and inflammatory activities of IL-6, other effects have been attributed to this cytokine such as metabolic activity where they showed

during exercise the level of IL-6 increases significantly (Pedersen and Febbraio, 2008; Pedersen et al., 2003). Furthermore, IL-6 knockout mice develop glucose intolerance and insulin resistance (Matthews et al., 2010).

3-3-Tumor necrosis factor (TNF-α):

Tumor necrosis factor (TNF, also known as TNF-α) was first described as a physiological agent that has the capacity to induce hemorrhagic necrosis into tumors transplant in mice (Carswell et al., 1975). Since then, it has been recognized as a potent player in inflammation (Bradley, 2008). Similar to IL-1β and IL-6, TNF-α is produced by different types of cells; the main sources of this cytokine are immune cells such as T cells, macrophages and natural killer cells (Sedger and McDermott, 2014).

The expression of TNF-α was observed in the brain by microglia cells in 1986 (Frei et al., 1987) and since then it becomes well known that the majority of the CNS cells have the capacity to produce it (Sternberg, 1997).

Two transmembrane receptors have been identified for such cytokine TNF-R1 (p55) and TNF-R2 (p75) and almost all the cells express at least one of the two receptors (Wiens and Glenney., 2011). Interestingly, this cytokine induces different effects on different cells and this referred to non-homology of the two receptors where the structural examination revealed a minor similarity between the two receptors. The genetic manipulation to the two receptors in mice revealed different impact on the physiology (Pfeffer et al., 1993). It has been reported that TNF-α acts as multifunctional cytokine exerting a variety of immunological functions by up-regulating the production of immune cytokines, synthesis of prostaglandin E2 and reactive oxygen species (Pfeffer., 2003).

It is worthy to note that TNF-α induces a contradictory actions on different cells, studies have shown the diversity of the actions of such cytokine depends on the kind of intracellular signaling induced where TNF-α has the ability to induce cell death through the activation of both caspase-3 and caspase-8 on one hand (Nicholson and Thornberry, 1997). On the other hand, the same cytokine plays a pivotal role in cell survival through the activation of NF-kB and mitogen-activated protein kinase (MAPK)(Liu and Han, 2001; Van Antwerp et al., 1996).

TNF-α is a pro-inflammatory cytokine that has a central role in the protection against microbial agents in different animals. In addition to its physiological effect on promoting T cells proliferation and the anticoagulant properties of endothelial cells (Beutler et al., 1988; Tracey et al., 1993). It has been found an excessive expression of such cytokine leads a pathogenesis of both acute and chronic inflammatory diseases like AIDS, arthritis and cancer (Beutler et al., 1988; Tracey et al., 1993). In the central nervous system, TNF-α is produced primarily by microglia and astrocytes in response to a wide range of pathological processes including infection, inflammatory disease, ischemia and traumatic injury (Liuet al.1994).

Chapter 3: Oxidative Stress

It has been said that, "A disturbance in the pro-oxidant/antioxidant systems in favor of the former may be denoted as an oxidative stress" (Davies, 2000). Since pro-oxidant or reactive oxygen species are natural byproduct of our metabolism, the body develops an antioxidant system to antagonize the damage that may result from their excessive formation (Halliwell, 1999). In this section different kinds of reactive oxygen species and mechanisms of defense that are able to neutralize their deleterious effects will be discussed.

1-Definition of Reactive oxygen species (ROS):

Reactive oxygen species (ROS) is a collective term used for a group of oxidants, which are either free radicals or molecular species capable of generating free radicals (Kunwar and Priyadarsini, 2011). Free radicals are chemical species that lack an electron that made them unstable and became highly reactive in order to pair up with other molecules and gain a state of stability.

2-Lipid Peroxidation:

Lipids are essential components of cell membrane that maintain structure and control the function of the cell. They are primary targeted by ROS such as oxygen free radicals. The oxidation of lipids is associated with various pathological states (Esterbauer, 1993). Lipid peroxidation, or interaction of lipids with reactive oxygen species has been an intensive area of research for decades (Pratt et al., 2011).

Lipid peroxidation is initiated by hydrogen abstraction or addition of an oxygen radical resulting in oxidative damage of polyunsaturated fatty acids

(PUFA). The free radical chain reaction propagates until two free radicals conjugate with each other to terminate the chain. The reaction can also be terminated in the presence of a chain-breaking antioxidant such as vitamin E (α-tocopherol) (Halliwell and Gutteridge, 1984). In the presence of transition metal ions, ROOH can give rise to the generation of radicals capable of re-initiating lipid peroxidation by redox-cycling of these metal ions (Halliwell and Gutteridge, 1984). Lipid peroxidation causes a decrease in membrane fluidity and in barrier functions of the membranes. Many products of lipid peroxidation such as hydroperoxides or their aldehyde derivatives inhibit protein synthesis, blood macrophage actions, alter chemotactic signals and enzyme activity (Fridovich and Porter, 1981).

The complex nature of the lipid peroxidation process and its potential biological significance has attracted the attention of scientists from different fields ranging from chemistry and biochemistry to biology and clinical sciences. Such attention results in to the elucidation that lipid peroxidation is implicated in several human diseases like atherosclerosis (Berliner and Heinecke, 1996), cancer (Hammad et al., 2009; Wu et al., 2010), diabetes (Silverstein and Febbraio, 2009), chronic alcohol exposure (Yang et al., 2010), acute lung injury (Imai et al., 2008; Nonas et al., 2006) as well as neurodegenerative disorders like Alzheimer's (Montine et al., 2005) and Parkinson's diseases (Porter et al., 2010).

3-Reduced glutathione (GSH):

Considered the most abundant thiol compound in all cells (Meister and Anderson, 1983), GSH is a tri-peptide antioxidant found in all compartment of the cell (Meister and Anderson, 1983).The importance of such antioxidant manifests in its capacity to interact and neutralize the deleterious effect of reactive oxygen

species, serving as a supplier of protons to antioxidant enzymes. The ratio between reduced-GSH / oxidized-GSSG plays a major role as mirro to the oxidative status of the cell (Jones, 2002). As mentioned above reduced glutathione plays at different levels in the protection of the cell against reactive oxygen species. GSH acts as a donor of proton to the oxidized lipids in the membrane during lipid peroxidation and thereby stops the propagation of such deleterious phenomena throughout the cell membrane which might lead to serious damage to the cell (Curello et al., 1985).

In addition, it plays a role as co-substrate for glutathione peroxidase and transferases during peroxidation (Gregus et al., 1996). Another antioxidant role of GSH appears through the reduction of major non enzymatic oxidants such as vitamin C. Furthermore, it is involved in the detoxification process of certain xenobiotics (Gregus et al., 1996; Halliwell and Gutteridge, 1984).

4-Catalase:

Catalase is one of the important enzymes in the defenses against free radicals. It was first noticed unknowingly in 1811 when Louis Jacques Thénard discovered hydrogen peroxide and proposed that an unknown substance is causing its breakdown (Loew, 1900). More than one century later, catalase from beef liver was crystalized by B. Sumner and A. Dounce (Sumner and Dounce, 1937). Catalase is an ubiquitous enzyme found almost in all living cells and considered one of the most active enzyme, studies have shown the turnover of such enzyme is more than multiple millions of hydrogen peroxide molecules to water and oxygen in each second.

The hydrogen peroxide detoxification feature of catalase plays an important role in the protection against one of the dangerous reactive species and spares the

cell from the damage that might result from the attack of cellular components of hydrogen peroxide. In addition, it has been found that the survival rates was extended after CAT containing liposomes were injected after exposure to 100% of oxygen (Speranza et al., 1993). Catalase plays an important role in the management of oxidative stress during certain pathophysiological conditions, inflammatory diseases, aging and cancer (Kim et al., 2002).

5-Superoxide Dismutase (SOD):

Superoxide dismutase (EC 1.15.1.1) is a class of oxide-reductase enzymes and one of the most important antioxidant enzymes in the neutralization of reactive oxygen species due to its capacity to dismute the superoxide anion and made less reactive species such as H_2O_2, thereby reducing the likelihood of superoxide anion interacting with nitric oxide to form reactive peroxynitrite. There are three isoforms for SOD named after their localization in the cell where we can distinguish cytosolic Cu/Zn-SOD, mitochondrial Mn-SOD and extracellular SOD (EC-SOD). Interestingly it has been observed that through all over the body, the amount of Cu/Zn-SOD are double as large as the Mn-SOD (Marklund, 1980). Isoforms of SOD are variously located within the cell. CuZn-SOD is found in both cytoplasm and nucleus. Mn-SOD is confined to the mitochondria, but can be released into extracellular space (Reiter et al., 2000).

Extracellular superoxide dismutase (EC-SOD) is a secretory, tetrameric, copper and zinc containing glycoprotein with a high affinity for certain glycosaminoglycans such as heparin and heparin sulfate. EC-SOD was found in the interstitial spaces of tissues and also in extracellular fluids, accounting for the majority of the SOD activity in plasma, lymph and synovial fluid (Marklund, 1980; Sandström et al., 1994).

Chapter 4: Relation between neurodegeneration, neuroinflammation and oxidative stress

1-Gliosis and cell death:

The traditionally perceived of the passive role of microglia in the brain as maintenance cells has been questioned and microglia are now accepted as active mediators of neurodegeneration (Block and Hong, 2005). It has been demonstrated in Alzheimer's disease, Aβ is responsible for the activation and recruitment of microglia in-vitro (Davis et al., 1992; Sasaki et al., 1997). In line with this observations Craft et al., 2004 demonstrated in AD animal models, the intraventricular infusion of Aβ1–42 peptide along with inhibition of glial activation by aminopyridazines led to the reduction of neuropathlogical symptoms seen in this model. The degeneration of the nigro-striatal dopaminergic (DA) pathways is the major feature in the brain of Parkinson's disease (PD) patients (Olanow and Tatton, 1999). Substantia niagra is recognized as the richest region with microglia in the brain which contains 4.5 fold compared to neocortex and other regions (Kim et al., 2000). It has been shown beside the direct toxicity of the neurotoxin, rotenon to dopaminergic neurons, this substance has the ability to recruit and involve the microglia in the neurodegeneration occurring in such PD model (Gao et al., 2003). Frontal and anterior temporal loss of neurons is typical feature of Fronto-temporal dementia (FTD) (Munoz et al., 2003). In an attempt to investigate the involvement of the inflammatory process in neurodegeneration in such diseases, the work of Schofield et al., 2003 showed the activation of microglia at early stages of the disease, providing a rare evidence of an early and perhaps initiating role of microglial inflammation in fronto-temporal dementia (Figure-5).

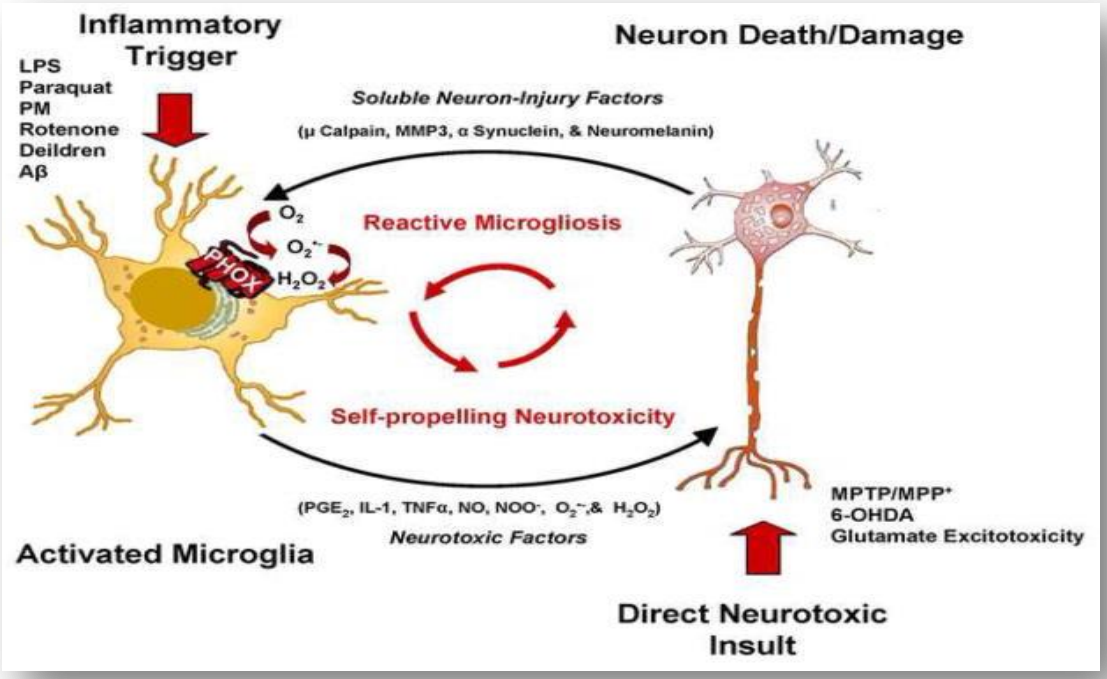

Figure-5: Role of Reactive microgliosis in neuronal cell death (Lull and Block. 2010).

Astrocytes are known as supportive cells to neurons, studies have shown these cells play an important role in the clearance and degradation of Aβ (Koistinaho et al., 2004; Li et al., 2011; Wyss-Coray et al., 2003) and have the ability to phagocyte the fibers of Aβ (Jiang et al., 1998; Niino et al., 2001). In support of this hypothesis many reports have shown the accumulation of the Aβ1–42 and the amount of this material correlates positively with the extent of local AD pathology (Nagele et al., 2003). In vitro, the Aβ peptide decrease the uptake of the neurotransmitter glutamate by astrocytes and neurotoxin substance likewise. In addition, they found such peptide promotes the mitogen-activated protein kinase cascades in astrocytes that triggers a state of astrogliosis (Agostinho et al., 2010; Matos et al., 2008). Several studies showed while the astrocytes performing their

assisting and repairing activity in the brain, their direct involvement in neural damage (Pekny et al., 2014; Placone et al., 2015). From pathological examinations, an increase in the number of astrocytes as well as in GFAP expression is observed in PD (Ciesielska et al., 2009; Muramatsu et al., 2003). There are abundant evidences that astroglial abnormalities and physiological dysfunction precede clinical disease. These changes include reactive astrocytosis that can be seen many months before motor neuron degeneration (Bruijn et al., 1997).

Multiple Sclerosis is a chronic inflammatory demyelinating disease of the central nervous system in which glial cells play a prominent role. In murine experimental autoimmune encephalomyelitis (EAE), an established animal model of multiple sclerosis, astrocyte hypertrophy coincided with manifestation of axonal damage (Wang et al., 2005).

2-Cytokines and cell death:

In this work the focus was was on a subset of cytokines called interleukins, substances that play a major role in the inflammatory process and the host defenses. In the last three decades there are growing evidences concerning the implication of the interleukins in the endangerment of the cell survival and ultimately in cell death or neurodegeneration.

One of the most studied cytokines and its involvement in neurodegeneration is IL-1β, such cytokine presents at high rate in postmortem tissue of AD and PD patients. In addition to that, different studies have proven the induction of an array of responses such as damage to the cerebral vasculature, activation of glia, amyloid precursor protein, adhesion molecules and corticotrophin-releasing factor (CRF) (Betz et al., 1996; Rothwell, 1997; Rothwell et al., 1997, 1996). Related findings showed the involvement of such cytokine in the endangerment of the neuronal

survival where its levels raise in few hours following the administration of multiple neurotoxins. If the only conclusion that can be drawn from those studies is the possibility of such cytokine in the initiation of the endangerment of the cell survival and even indirectly the activation of the glial cell that may contribute to the cell death later on (Allan and Rothwell, 2001; Boutin et al., 2001; Griffin and Mrak, 2002; Lawrence et al., 1998; Pearson et al., 1999; Perry et al., 2003).

Accumulating evidences from both animal and human studies have indicated that chronic inflammatory processes contribute to the pathogenesis of neurodegenerative diseases and IL-6 is one of the cytokines that is strongly correlated to the onset and progression of the disease. Accordingly in IL-6 deficient mice the inflammatory response is significantly reduced during pathological conditions of the brain (Eugster et al., 1998; Klein et al., 1997; Mendel et al., 1998; Penkowa et al., 1999b; Raivich et al., 1999).

Studies have shown the knockout of IL-6 gene in mice causes a significant decrease in the activity and recruitment of microglia and astrocytes after brain injury (Penkowa and Hidalgo, 2000; Penkowa et al., 1999a). Similar observation has been made during facial nerve transaction (Klein et al., 1997). It is estimated that IL-6 plays a major role in the induction of acute-phase proteins (APP) and the presence of these proteins (i.e. α1-anti-chymotrypsin, α2-macroglobulin, and C-reactive protein (CRP) proteins) involved in the alteration of the normal process of the key proteins that caused cell death in the neurodegenerative disease such as levy body, amyloid precursor protein (APP) and mitochondrial dysfunction in Amyotrophic lateral sclerosis (Graeber and Streit, 2010; Hofmann et al., 2009).

TNF-α is considered one of the major cytokine in the immune defense and plays an important role in the activation of immune cells in the brain but studies have shown a double effect of such cytokine where TNF-α positive astrocytes have been found in all over the areas of the lesion reflecting the possibility of its

contribution in neuronal death in the lesioned area (Okuda et al., 1995; Probert et al., 1997; Renno et al., 1995; Selmaj et al., 1991).

A study showed a very elevated concentration of TNF-α in activated microglia that are in proximity of the amyloid plaque in the brain of Alzheimer disease patients (Blasko et al., 1999; Meda et al., 1995). In addition, the increase in the concentration of such cytokine has been found only after 30 min of ischemia and such an increase has been shown to be damaging to the neuronal cells (Buttini et al., 1996; Forloni et al., 1997; Lavine et al., 1998; Wallach et al., 1997).

3-Oxidative stress and neurodegeneration:

The deleterious effects of the oxidative stress in neurodegeneration have received a lot of attention from the scientific community and a new kind of thinking started to emerge like considering the anti-oxidative therapy as an alternative in the treatment of neurodegenerative disease. In this section different diseases and different neurodegenerative models where oxidative stress played a decisive role in the neuronal survival will be discussed.

Several researchers considered the brain to be abnormally sensitive to oxidative damage and many studies demonstrate the vulnerability of the brain to lipid peroxidation (Chance et al., 1979; Floyd and Carney, 1992; Zaleska and Floyd, 1985) and this could be due to the abundance of fatty acids in the brain (Butterfield et al., 2002).

In addition to that, the brain is not well equipped with very strong antioxidant machinery which makes the fight against the reactive oxygen species not an easy mission. Studies have shown that brain contains 10 % of antioxidant compared to the liver (Uttara et al., 2009). Furthermore, 20% of the oxygen of the body is consumed by the brain (Zaleska and Floyd, 1985). It have been found an

increase in the amount of H_2O_2 and $O_2^{\bullet-}$ production in the mitochondria in aged mouse brain. The kainic acid model has been used extensively to study different ways of neurodegeneration and multiple studies have showed a significant link between the cell death and the raise in the levels of reactive oxygen species in such model (Bondy and Lee, 1993; Ueda et al., 1997). Peroxidation of the plasma membrane is one of the major signs of oxidative stress due to its impact on the cell survival and the induction of apoptotic markers, studies have shown the implication of the lipid peroxidation in the toxic effects of many chemicals in many tissue injuries and disease processes. Free radicals have been reported for their great contribution to neuronal loss in cerebral ischemia, seizure disorders, schizophrenia, Parkinson's disease and Alzheimer's disease (Uttara et al., 2009). Concerning the implication of oxidative stress in different neurodegenerative diseases different studies have shown through the examination of postmortem tissue of AD patients a significant increase in lipid peroxidation in specific areas of the brain (Lovell et al., 1995; Pappolla et al., 1998).

MATERIALS AND METHODS

Aim of the study:

The regional ethical committee of the College of Medicine and Health Sciences (UAE University) approved this study (RECA/01/05).

The aim of the current study was to examine the impact of short-term bilateral adrenalectomy on neuronal cell death in different regions of the hippocampus, production of pro-inflammatory cytokines IL-1β, IL-6 and TNF-α, the activation of different glial cells astrocytes and microglia, oxidative stress MDA, GSH and SOD, the impact of the absence of such glucorticoids on the animal's behavior and the possibility of their association with neurodegeneration.

2- Animals and adrenalectomy surgery:

Eight-week old male Wistar rats 170–220g obtained from the animal facility of College of Medicine and Health Sciences, United Arab Emirates University (Al ain, United Arab Emirates) were used in the current study. All animals were placed in Plexiglas cages (Techniplast, Milan, Italy); four rats per cage, maintained in a temperature (22°C) and 12:12 light–dark cycle conditions, animals received ad libitum access to food (National feed and flour production and marketing company, Abu Dhabi, UAE) and water throughout the experiment.

Adrenalectomized rats were provided with 0.9% saline instead of drinking water in order to maintain electrolyte balance and prevent the deleterious effects of sodium chloride (Sigma-Aldrich, Missouri, USA) insufficiency.

Under Pentobarbital (Ilium-Troy Laboratories, New South Wales, Australia) anesthesia (35 mg/kg body weight), rats were subjected either to adrenalectomy or to sham operations (laparotomy) as described by Sloviter et al. 1989. Shaving the back of the animals was done by using an electric shaving machine (Wahl, Illinois,

USA). The rat was placed on the surgical table ventrally and in order to perform an aseptic surgery the back of the animals was cleaned with 70% ethanol (Sigma-Aldrich, Missouri, USA).

Bilateral incisions were made into the skin and the dorsal muscle to access the peritoneal cavity. The size of the muscle incision was just big enough to expose the adrenal gland on the top of the kidney and some free space to remove it without leaving any intact residuals of the gland. The peri-adrenal fat was grasped using a blunt forceps and the adrenal gland was exteriorized and with a tipped-blunt ceaser a cut was made at the connective tissue between the kidney and the adrenal gland. After that the incision was sutured and the animal was returned to the cage. The same procedure was applied for the sham operated animal except the removal of the adrenal gland.

3-Determination of serum corticosterone levels by Enzyme Immunoassay (EIA):

The levels of corticosterone in the serum were used to assess the effectiveness of adrenalectomy, approximately 1 ml of blood samples were taken directly from the heart at the time of sacrifice. For both biochemical and histological assessments (n=120) rats were sacrificed by decapitation after surgery at different times: 4h (n=24), 24h (n=24), 3days (n=24), 1week (n=24) and 2weeks (n=24). The sera samples were stored at -80°C until corticosterone levels were measured by Enzyme Immunoassay (EIA) Kit (Life sciences, Lausen, Switzerland). The assay is based on the competitive binding technique. Briefly, a polyclonal antibody specific for corticosterone becomes bound to the donkey anti-sheep antibody coated onto the micro- plate. Following a wash to remove excess polyclonal antibody, corticosterone present in the serum competes with a fixed

amount of horseradish peroxidase (HRP)-labeled corticosterone for sites on the polyclonal antibody. This is followed by another wash to remove excess of the conjugate and unbound sample. A substrate solution is added to the wells to determine the bound enzyme activity. The color development is stopped and the absorbance is read at 450 nm (Figure-6). The intensity of the color is inversely proportional to the concentration of corticosterone in the sample. A standard curve in the range 32 to 20,000 pg/ml was constructed to calculate corticosterone concentrations in the samples.

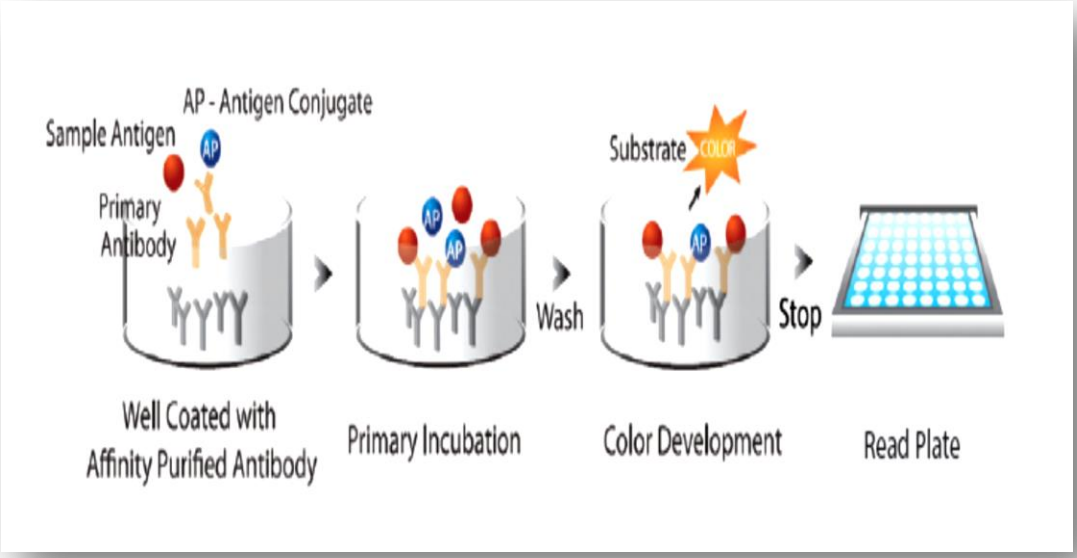

Figure-6: Scheme of Enzyme Immunoassay (EIA) (Life sciences, Lausen, Switzerland).

4-Biochemistry

4-1-Samples preparation:

Animals (n=80) were sacrificed by decapitation after surgery at different times: 4h (Sham=8, ADX=8), 24h (Sham=8, ADX=8), 3days (Sham=8, ADX=8), 1week (Sham=8, ADX=8) and 2weeks (Sham =8, ADX=8). The brain was removed, the hippocampus was immediately dissected out on ice, frozen in liquid nitrogen (Sharjah Oxygen Company, Sharjah, United Arab Emirates) and stored at −80°C until assayed. Thawed hippocampal tissues were homogenized in ice-cold T-PER Tissue Protein Extraction buffer (Thermo Fisher Scientific, Massachusetts, USA), supplied with 1:100 protease inhibitor cocktail (Sigma-Aldrich, Missouri, USA). After sonication, the samples were centrifuged at 16000 rpm for 30 min at 4°C and the supernatant was collected and stored at −80°C until use. Protein concentrations were determined using Bradford's protein assay kit (Bio-Rad, California, USA)and levels of cytokines (IL-1β, IL-6 and TNF-α) were assessed by ELISA using the commercially provided antibodies and standard proteins (R&D Systems; Minneapolis, USA).

4-2-Determination of Total protein:

A set of standards is created in duplicate from a stock of Bovine serum albumin (BSA) (Sigma-Aldrich, Missouri, USA) solution ranging from 0.2 to 1.4mg/ml. The 5X Bradford Reagent was diluted 1:4 with distilled water followed by filtration using wattman1 filter paper (Whatman, Maidstone, United Kingdom). A volume of 1.25ml of Bradford Reagent was added to each disposable polystyrene tube. Our samples were diluted in the homogenation buffer 1:10 and the same buffer was used as a blank for the assay. We added 25µl of the standards

and the samples into the labeled tubes containing the Bradford Reagent after the time of incubation 5min. the absorbance was measured at 595nm.

4-3-Determination of hippocampal cytokines (IL-1β, IL-6 and TNF-α) levels by Enzyme-Linked Immunosorbent Assay (ELISA):

Materials:

Equipment:

- Micro-plates 96-well flat-bottom (NUNC, Roskilde, Denmark).
- Plate Sealers
- Plate reader (Tecan, Zürich, Switzerland)
- Micro-plate autowasher (Tecan, Zürich, Switzerland).
- Micro-plates shaker (Stuart, Staffordshire, United Kingdome).
- ELISA Software (Magellan, version7,Tecan, Zürich, Switzerland)
- Micropipette of different type (P10, P20, P200, p1000) and multichannel Pipettes (BioHit healthcare, Helsinki, Finland).
- Nylon Membrane Filters (0.2 µm) (Corning, New York. USA).

Reagents:

- Deionized water
- PBS (Phosphate-buffered saline) (Sigma-Aldrich, Missouri, USA), PH 7.2-7.4, 0.2 µm filtered.

  137 mM NaCl

  2.7 mM KCl, 8.1 mM

Na2HPO4

1.5mM KH2PO4

- Wash Buffer: 0.05% Tween®20 (Promega, Madison USA) in PBS, pH 7.2-7.4
- Reagent diluent: 1% BSA in PBS, pH 7.2-7.4, 0.2 µm filtered.
- Substrate Solution (Sigma-Aldrich, Missouri, USA): One to one mixture of Color Reagent A (hydrogen peroxide H_2O_2) and Color Reagent B (41.6 mM Tetramethylbenzidine).
- Stop Solution: 2 N H_2SO_4 (sulfuric acid) (Sigma-Aldrich, Missouri, USA).

Antibodies: All the antibody from (R&D Systems, Minnesota, USA)

- Capture Antibody: Mouse Anti-Rat IL-6 of concentration 4µg/ml in PBS.
- Detection Antibody: Biotinylated goat Anti-Rat IL-6 of concentration 400ng/ml dissolved in Reagent diluent.
- Streptavidin conjugated to horseradish peroxidase (HRP) dissolved in Reagent diluent.
- Standard antibody: Recombinant rat IL-6 290ng/ml dissolved in Reagent diluent.

Methods: the Elisa test was performed through two main steps

Plate Preparation:

1. The micro-plate was coated (100µL) per well with the capture antibody that was freshly diluted.

2. The micro-plate was sealed and left for incubation (time for capture antibody to attach on the walls of each well) overnight at room temperature (RT).
3. The following day the micro-plate was washed three times in the plate autowasher machine by filling each well with Wash Buffer (400µL) and aspiring it immediately afterward.
4. The complete removal of the wash buffer is very critical for the better performance of ELISA and in order to ensure that the plate was inverted and blotted gently against clean paper towels.
5. The micro-plate was blocked by adding to each well a (300µL) freshly and filtered blocking buffer (BSA) and was left 1 hour for incubation at room temperature (Optimal time found in our laboratory for the BSA to occupy all the inter spaces that was not attached to capture antibody)
6. The third and fourth steps were repeated for the second washing to remove all the additional molecule of BSA and by then the plate became ready for samples addition.

Assay Procedure:

Seven Standards were prepared through 2-fold serial dilution of the desired recombinant Interleukin IL-1β, IL-6 and TNF-α see figure-7 for IL-6.

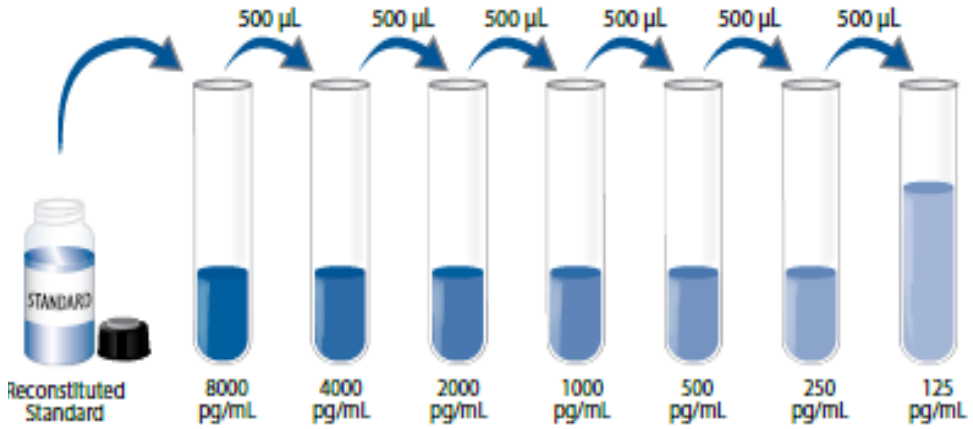

Figure-7: Two-fold serial dilution of IL-6 (R&D Systems, Minnesota, USA)

However, each interleukin has its own range of standards see table-1 for the serial dilution of IL-1β and TNF-α.

Table -1: Serial dilution of IL-1β, IL-6 and TNF-α Standards preparation

	1	2	3	4	5	6	7
IL-1β pg /ml	2000	1000	500	250	125	67.5	33.75
TNF-α pg /ml	500	250	125	62.5	31.25	15.62	7.81
IL-6 pg /ml	8000	4000	2000	1000	500	250	125

1. Once the standards prepared we started to add 100µL from the Blank, standards and hippocampal samples to each well of the coated plate. The microplate was sealed and left for 2 hours incubation at room temperature (Optimal time for the samples and standards to attach to the capture antibody).

2. The third and fourth steps were repeated for the third washing to remove all the non-adhered samples and standards.

4. At this stage the micro-plate is ready for detection, (100µL) of detection antibody per well was added. The plate was sealed and left for 2 hours incubation (Optimal time for the detection antibody to attach to the capture antibody and form a SANDWICH) at room temperature.
5. The third and fourth steps were repeated for the fourth washing to remove the non-adhered molecules of detection antibody.
6. Away from the light (100µL) of Streptavidin-HRP per well was added and left for 20min incubation at room temperature (Optimal time for Streptavidin-HRP to attach to the detection antibody).
7. The third and fourth steps were repeated for the fifth washing to remove the non-adhered molecules of Streptavidin-HRP.
8. At this step, the plate is ready to develop the color that reflect the amount of the desired cytokine by adding (100µL) per well and away from light the plate left for 20min at room temperature (optimal time for the HRP to react with the substrate to generate the yellow color).
9. In order to stop the reaction (50µL) added of stop solution per well followed by gentle shaking.
10. Immediately the optical density for each well was determined at 450 nm using plate reader see Figure-8.

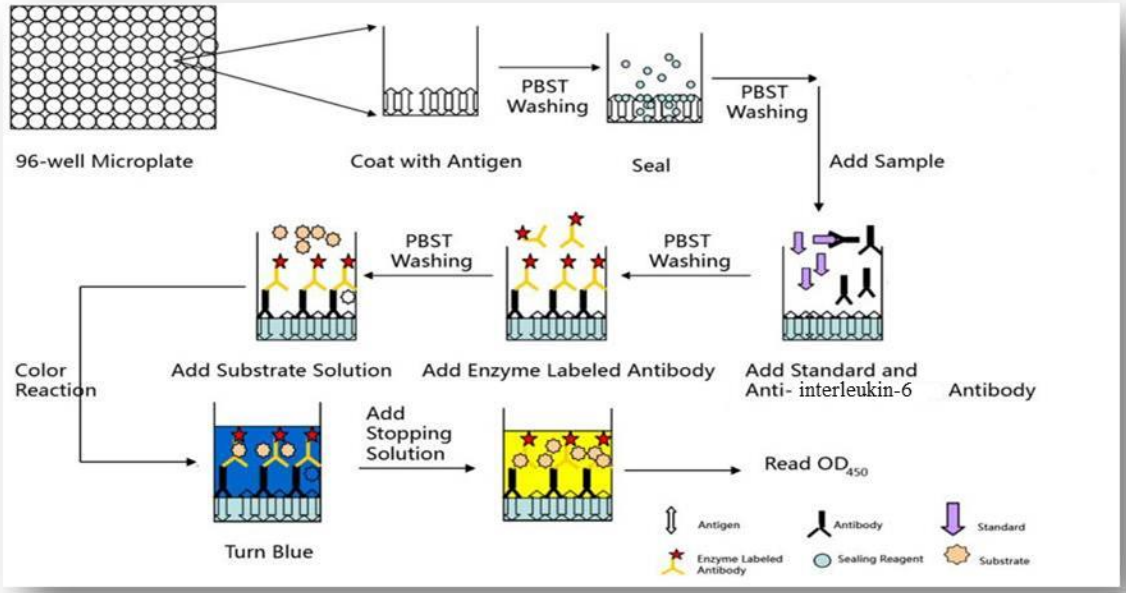

Figure-8: Scheme of Enzyme-Linked Immunosorbent Assay (ELISA) (R&D Systems, Minnesota, USA).

The levels of IL-1β, IL-6 and TNF-α were evaluated by comparison with the regression standard curve for each cytokine. The cytokine protein concentration was divided by the total protein concentration obtained in the Bradford's protein assay to correct the differences in tissue volumes. Cytokine concentration is reported as pg of cytokine/mg of protein.

4-4-Determination of the levels of oxidative stress markers (GSH, SOD, and MDA) by colorimetric assay:

It is worthy to note here that the same homogenate that was used for the evaluation of cytokines by ELISA was used for the colorimetric assay to determine the levels of oxidative stress markers GSH, SOD and MDA.

4-4-1-Superoxide dismutase (SOD):

Materials:

Equipement:

- Micro-plates 96-well flat-bottom (NUNC, Roskilde, Denmark).
- Plate reader
- Software.
- Micropipette of different type (P10, P20, P200, p1000)
- Multichannel Pipettes
- Glass test tube.

Reagents: The kit was purchased from (Cayman chemical, Michigan, USA)

- Deionized water
- Assay buffer (50mM Tris-HCL, pH 8, containing 0.1mM Diethylenetriaminepentaacetic acid (DTPA) and 0.1 mM hypoxanthine)
- Sample buffer 50mM Tris-HCL, pH 8.
- Radical detector: Tetrazolium salt solution
- Superoxide dismutase standards: Bovine erythrocyte SOD (Cu/Zn).
- Xanthine oxidase

Methods:

SODs are metalloenzymes that catalyze the dismutation of the superoxide radical ($O_2^{\bullet-}$) into hydrogen peroxide (H_2O_2) and molecular oxygen (O_2). The measurement of the SOD amount in the hippocampal homogenate is based on the use of the tetrazolium salt for detection of superoxide radicals generated by xanthine oxidase and hypoxanthine.

Assay procedure:

Standards preparation: Seven Standards were prepared from the stock solution (20 µL of Bovine erythrocyte SOD with 1.98 of sample buffer) as follow (Table -2),(figure-9).

Table -2: Serial dilution of SOD Standards preparation

Tube	SOD Stock (µI)	Sample Buffer (µI)	Final SOD Activity (U/ml)
A	0	1000	0
B	20	980	0.005
C	40	960	0.01
D	80	920	0.02
E	120	880	0.03
F	160	840	0.04
G	200	800	0.05

1. A volume 10µl of each sampleand standard were added to the designated wells of the microplate
2. Followed by adding 200 µl of diluted radical detector (diluted solution of 50 µl of tetrazolium salt with 19.95ml of distilled water).
3. Once the previous steps was completed, a volume of 20 µl of xanthine oxidase was added to all the wells in order to initiate the reaction.
4. The plate was covered and incubated on the shaker for 20min at RT.
5. The plate was read at 440nm using plate reader.

6. SOD activity was calculated by using the equation obtained from the linear regression of the standard curve substituting the linearized rate (LR) for each sample. One unit of SOD is defined as the amount of enzyme needed to exhibit 50% dismutation of the superoxide radical.

SOD (U/ml) = [(Sample LR-y-intercept/slope) × (0, 23/0.01)] ×sample dilution

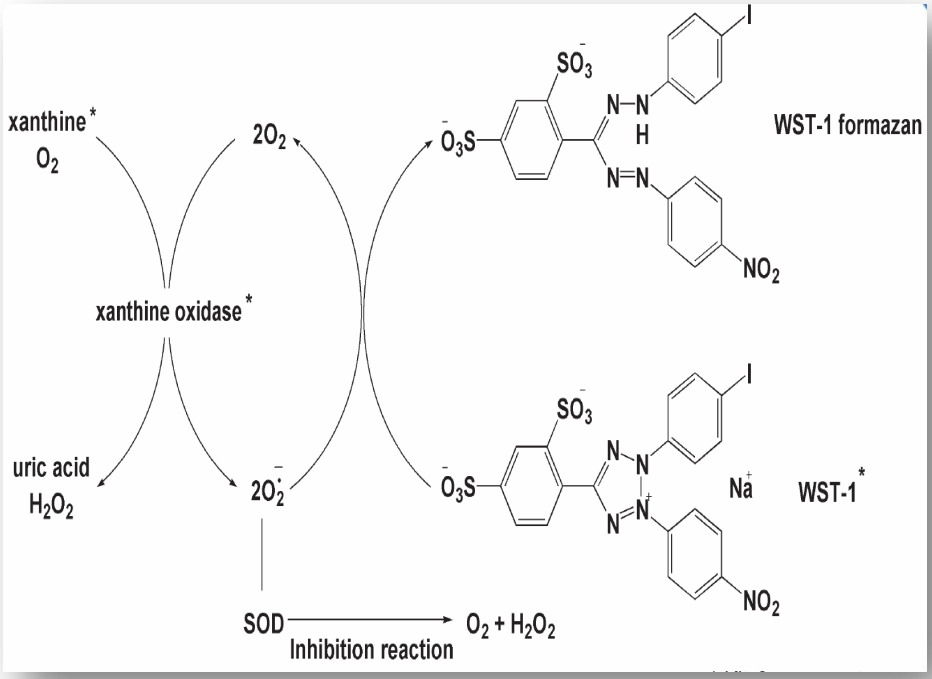

Figure-9: Scheme of Superoxide dismutase assay, (Cayman chemical, Michigan, USA)

4-4-2-Malondialdehyde (MDA):

The measurement of the TBARS amount in the hippocampal homogenate is based on the interaction of thiobarbituric acid (TBA) with malondialdehyde (MDA) under acidic conditions (acetic acid) and high temperature (95°C) using a kit purchased from (Cayman chemical, Michigan, USA).

Materials:

Equipement:

- Micro-plates 96-well flat-bottom (NUNC, Roskilde, Denmark).
- Plate reader
- Software.
- Micropipette of different type (P10, P20, P200, p1000)
- Multichannel Pipettes
- boiler
- 5ml polypropylene crew-cap centrifuge tubes

Reagents:

Thiobarbituric Acid (TBA)

TBA Acetic acid used to prepare the color reagent.

TBA sodium hydroxide used to prepare the color reagent.

TBA malondialdehyde standard 500µM

TBA-SDS (sodium dodecyl sulfate) solution.

Assay procedure:

Standards preparation: A volume of 250µl of the MDA standard was mixed with 750µl to obtain a stock solution of 125µM. Eight standards made out of the stock solution see table-3.

Table -3: Serial dilution of MDA Standards preparation

Tube	MDA (µI)	Water (µI)	MDA Concetration (µM)
A	0	1000	0
B	5	995	0.625
C	10	990	1.25
D	20	980	2.5
E	40	960	5
F	80	920	10
G	200	800	25
H	400	600	50

1. A volume of 100µl of the hippocampal homogenate and standards were mixed very well with the same amount of Sodium dodecyl sulfate (SDS) solution.
2. A volume of 4ml of color reagent (2120mg of thiobarbituric acid (TBA) dissolved in a mixture of 200 ml TBA acetic acid and 200 ml TBA sodium hydroxide) was added.
3. The mixture of the capped 5ml tube was boiled for one hour.
4. Once the incubation completed, the tubes quickly transferred to an ice bath for 10min in order to stop the reaction immediately.
5. The tubes were centrifuged at 16000g at 4°C for 10min.
6. Volume of 150µl of the resultant supernatant was taken and added to micro-plate see figure-10.
7. The formed TBA-MDA adduct was measured calorimetrically at 530-540nm. The MDA level was evaluated by comparison with the regression curve for standard.

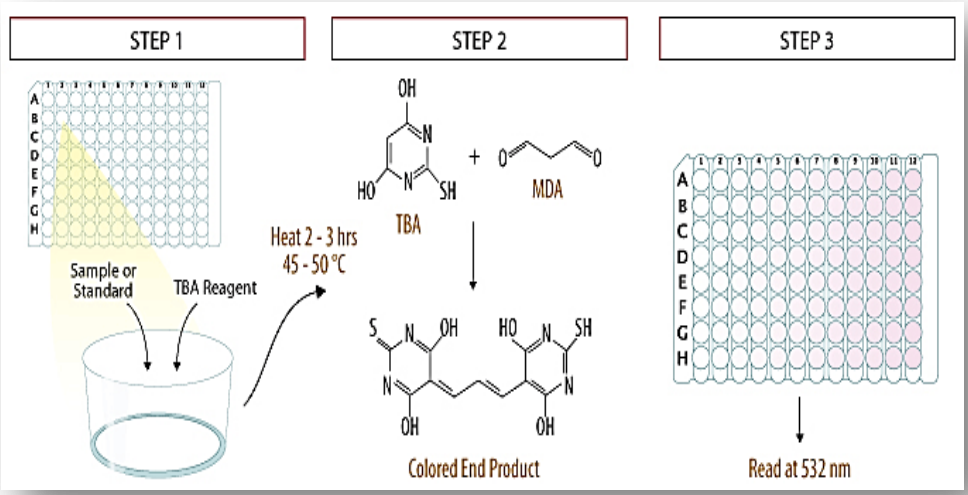

Figure-10: Scheme of the TBARS assay, (Cayman chemical, Michigan, USA)

4-4-3- Reduced glutathione (GSH):

The concentration of reduced glutathione (GSH) was determined in the hippocampal homogenate using the commercial kit (Sigma-Aldrich, Missouri, USA).

Materials:

Equipement:

- Micro-plates 96-well flat-bottom (NUNC, Roskilde, Denmark).
- Plate reader
- Software.
- Micropipette of different type (P10, P20, P200, p1000)
- Multichannel Pipettes
- Glass test tube.

Reagents:

- Deionized water
- Assay buffer: 500mM potassium phosphate, pH 7 containing 500mM Ethylenediaminetetraacetic acid (EDTA).
- Glutathione reductase: 400 units of glutathione reductase from baker's yeast in 3.6M ammonium sulfate, pH 7 containing 0.1 mM dithiothreitol diluted in assay buffer.
- Glutathione Reduced, Standard (10mM)
- 5,5'-Dithiobis(2-nitrobenzoic acid) [DTNB] solution: 1.5mg/ml of Dimethyl Sulfoxide (DMSO) diluted in assay buffer.
- 5% 5-Sulfosalicylic Acid
- Nicotinamide adenine dinucleotide phosphate NADPH solution: 40mg/ml diluted in assay buffer.
- Dimethyl Sulfoxide (DMSO)

Assay procedure:

Standards preparation: A volume of 50µl of the GSH standard as stock solution of 50µM. Five standards made out of the stock solution see Table -4.

Table -4: Serial dilution of GSH Standards preparation

Standards	1	2	3	4	5
GSH Concentration (µl)	50	25	12.5	6.25	3.125
GSH Solution (µl)	50	25 from (1)	25 from (2)	25 from (3)	25 from (4)
5% sulfosalicylic acid (µl)	None	25	25	25	25
nmoles GSH in a 10 µl sample	0.5	0.25	0.125	0.0625	0.0312

1. The hippocampal samples were first deproteinized with the 5% of 5-sulfosalicylic acid solution followed by centrifugation to remove the precipitated protein and then assayed for glutathione evaluation.
2. The measurement of GSH uses a kinetic assay in which catalytic amounts (nmoles) of GSH cause a continuous reduction of 5,5'-dithiobis (2-nitrobenzoic acid) (DTNB) to TNB.
3. The GSSG formed is recycled by glutathione reductase and NADPH.
4. The yellow product, 5-thio-2-nitrobenzoic acid (TNB) is measured spectrophotometrically at 412 nm see figure-11.
5. The assay uses a standard curve of reduced glutathione to determine the amount of glutathione in the sample (Ellman, 1959).

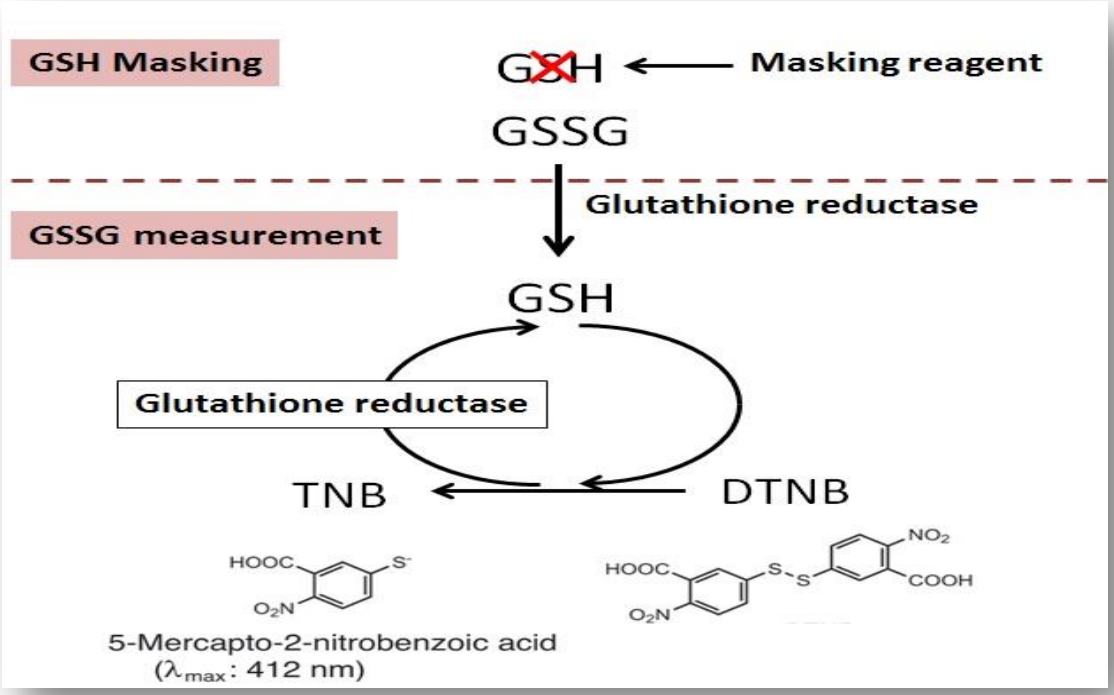

Figure-11: Scheme of Reduced glutathione assay (Sigma-Aldrich, Missouri, USA).

5-Histology:

5-1-Hippocampal tissue preparation:

5-1-1-Perfusion-fixation:

The purpose of such procedure is to obtain rapid and uniform fixation on one hand and maintain the integrity of the epitopes of the targeted protein in the immunohistochemistry staining.

In order to avoid any kind of blood clotting and ensure the smooth flow of our fixative, the animal was kept alive through a deep anesthesia with single intraperitoneal dose 35mg/kg of pentobarbital, after that animal was placed on its back on the dissection board.

Using a blunt scissor, an incision through the abdomen was made to get access to the diaphragm membrane and carefully a cut in this later was made to expose the rib cage. In order to expose the heart, another incision through the sternum was made. A cut was made in the right atrium with a small scissor and quickly 1ml blood was collected for later determination of the corticosterone levels in the serum. Once the blood is collected, a blunt needle that already connected to two bottles; one contains freshly prepared 0.1 PBS (PH 7.4) and the other 10% formalin (PH 7.4) (Sigma-Aldrich, Missouri, USA), was inserted properly through the apex of the heart until it can be seen in the aorta to begin the perfusion. The animal was perfused with 50ml of 0.1 PBS until the liver turn pale and almost the blood has been cleared from the body. Then the perfusion was stopped and we switch to the fixation with (10% formalin) for an amount 300ml per animal. It is worthy to mention that the flow of both solutions was fixed 20ml/min which is equal the blood flow in the rat (Figure-12).

Once the amount designated to the fixation finished, we remove the head of the animal and immediately dissect the brain out of the skull. In a 10-20 times volume of the brain size of same fixative, the brain was placed and left for one week (the optimal period that we found through optimization that gives us a better immunostaining)

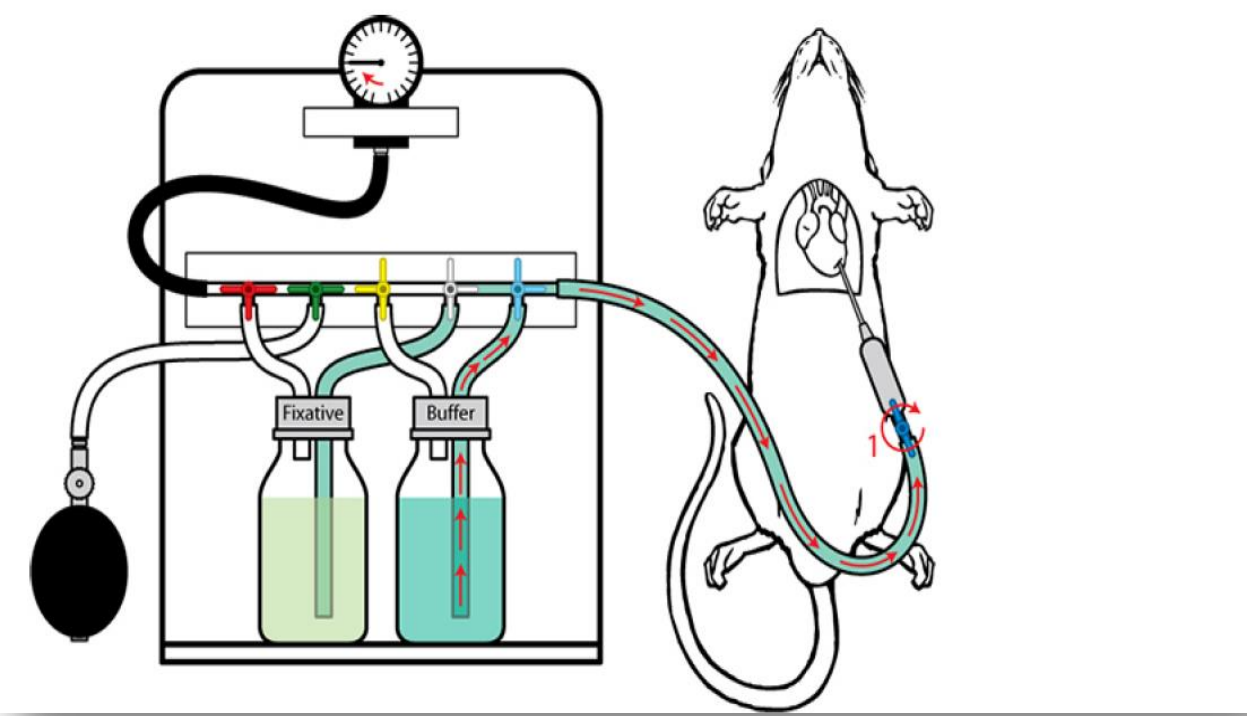

Figure-12: Scheme demonstrating the perfusion-fixation procedure.
http://voltagegate.blogspot.ae/2013/07/at-heart-of-matter-introduction-to.html

5-1-2-Paraffin Embedding:

There are two aims of such process, first is to dehydrate gradually the brain tissue and replace it with paraffin and second to make the tissue solid and easy to handle for microtome sectioning. In order to achieve the aforementioned purposes we performed the following procedure.

A-Dehydration: Through this step we made sure the tissue is gradually was water free through three changes in gradual concentration of ethanol (50, 70 and 90%) each one hour followed by three changes in absolute ethanol each 2 hours.

B-Clearing: This step is to replace the alcohol that is in the tissue with the xylene (Sigma-Aldrich, Missouri, USA), through three changes each two hours, because the alcohol and paraffin (Thermo Fisher Scientific, Massachusetts, USA) are immiscible and it is considered a preparatory step to the next one by that the paraffin will be able to infiltrate the tissue.

C-Waxing: This is last step before embedding where the brain placed in fresh paraffin at 60°C to get rid of all the xylene in the tissue through three changes in fresh xylene each two hours.

D-Embedding: The actual embedding takes place when the paraffin infiltrated the brain. The brain is adjusted in the mold in a manner where coronal section can be taken.

5-1-3-Brain sections preparation:

The excess of paraffin was removed and extra brain tissue was trimmed using the microtome (Thermo Fisher Scientific, Massachusetts, USA) (Figure-13), until we reach the area of our interest which is commonly called the mustache area that is approximately -3.7 mm relative to bregma according to Paxinos and Watson. 2005. The reason of choosing such area of the hippocampus is at this part of the brain the different parts of the hippocampus (Dentate gyrus, CA1, CA2, CA3 and CA4) are well defined and easy to be distinguished. To make sure that we are at the designated area we used the toluidine blue (Agar scientific, Essex, United Kingdom) as a quick staining. Coronal sections 1µm thick were taken. In order to

flatten the brain section, immediately the sections transferred to water bath (Thermo Fisher Scientific, Massachusetts, USA) at 50°C . Once we made sure that the section wrinkles free, using slide coated by gelatin (Sigma-Aldrich, Missouri, USA). The sections were picked and left to dry by keeping the slide vertically on a tissue paper. Once the sections were dried. The slide was transferred to a heating plate (Kunz Instruments AB, Nynashamn, Sweden) to make sure that the section is free of water and properly dried. All the slides were kept in a slide box at RT till use for different histology staining.

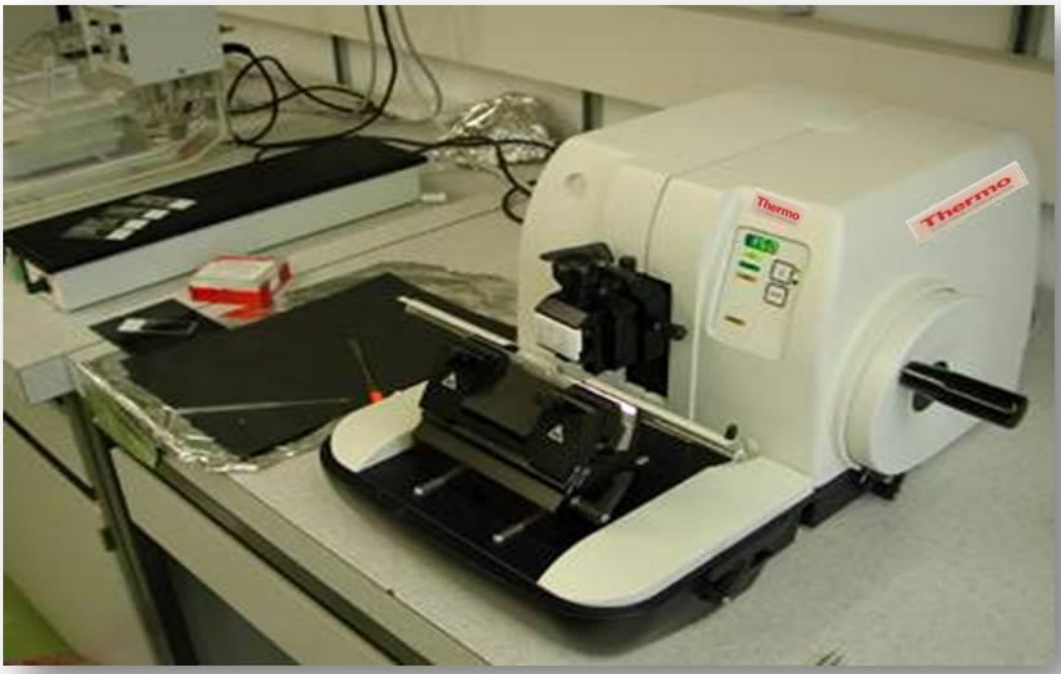

Figure-13: The set for microtome with a water bath.

5-2-Neuronal cell death examination using Fluoro-Jade B (FJB) staining:

Fluoro-Jade B staining was performed as described by Schmued and Hopkins (Schmued and Hopkins, 2000). 32 animals, 4h (Sham =4, ADX=4), 24h (Sham =4, ADX=4), 3days (Sham =4, ADX=4), 1week (Sham =4, ADX=4) and 2weeks (Sham =4, ADX=4) were used for this staining.

5-2-1-Materials:

Equipement:

- A set of jars of graduated ethanol (70, 80 90 and 100%) and absolute xylene.
- Humide chamber.

Reagents:

- Distilled water.
- PBS (Phosphate-buffered saline): PH 7.2-7.4, 0.2 µm filtered.

  137 mM NaCl

  2.7 mM KCl, 8.1 mM

  Na_2HPO_4

  1.5 mM KH_2PO_4
- 1% sodium hydroxide
- 5% NaOH
- Ethanol
- Xylene
- 0. 6% potassium permanganate
- 0.0004% Fluoro-Jade B solution (Millipore, Massachusetts, USA).

- Mounting media DPX (Sigma-Aldrich, Missouri, USA).

5-2-2-Method:

1. The coronal sections of the brain were first deparaffinized through two changes of xylene each 10min.
2. Then rehydrated through a graduated alcohol series (100, 90, 80 and 70 %) for a period of 5min for each.
3. Once the slides rehydrated, were ready to be immersed in 1% sodium hydroxide in 80% alcohol (20ml of 5% NaOH added to 80ml absolute alcohol) for 5min.
4. The slides were kept in 70% alcohol for dehydration and in distilled water for 2min respectively.
5. Fllowing dehydration the slides were transferred to a solution of 0. 6% potassium permanganate for 10min.
6. In order to get rid of any remaining of potassium permanganate the slides were rinsed in distilled water for two min and immersed in 0.0004% Fluoro-Jade B (Darmstadt, Germany) for 20min.
7. The slides were then rinsed for one min in each of three distilled water washes and placed on a slide warmer for 10min.
8. The dried slides were cleared by immersion in xylene for at least 1min and were then cover slipped with DPX and at this stage they were ready for examination.

5-3-Electron microscopy:

5-3-1-Materials:

Equipement:

- Rota mixer (Agar scientific, Essex, United Kingdom).
- Oven (Thermo Fisher Jouan, , Massachusetts, USA)
- Transmission electron microscope (Tecan, Zürich, Switzerland)
- Ultra microtome (Leica EMUC7, Wetzlar, Germany).
- 200 mesh copper grids (Agar scientific, Essex, United Kingdom).
- Molds (Agar scientific, Essex, United Kingdom).

Reagents:

- KARNOVSKY'S fixative at PH 7.2

  0.2 M phosphate buffer

  0.1 M phosphate buffer

  Paraformaldehyde (Sigma-Aldrich, Missouri, USA).

  Glutaraldehyde (EM grade; 50% solution) (Sigma-Aldrich, Missouri, USA)

  1 N sodium hydroxide (NaOH)
- 0.1M PB
- 1% osmium tetroxide (Agar scientific, Essex, United Kingdom).
- Propylene oxide (Agar scientific, Essex, United Kingdom).
- Ethanol
- Agar 100 (Agar scientific, Essex, United Kingdom).
- Resin (Agar scientific, Essex, United Kingdom).
- Uranyl acetate (Agar scientific, Essex, United Kingdom).
- Lead citrate (Agar scientific, Essex, United Kingdom).

5-3-2- Method:

The hippocampus was removed and transferred into KARNOVSKY'S fixative at PH 7.2 in glass vials for overnight at 4°C.

The next day the tissue was washed three times in 0.1M PB for 30min each. A volume of 1ml of buffered 1% osmium tetroxide was added to each vial and mixed for 1h at RT on Rota mixer. The osmium tetroxide was removed and followed by three distilled water washes for 2 min each. The samples were dehydrated as showed in table-5.

Table-5: Dehydration of brain tissue for electron microscopy.

Ethanol concentration	Timing
30% Ethanol	15min
50% Ethanol	15min
70% Ethanol	15min
80% Ethanol	15min
90% Ethanol	15min
95% Ethanol	15min
100% Ethanol I	15min
100% Ethanol II	15min
Propylene oxide I	15min
Propylene oxide II	15min

During the last Propylene oxide, the Agar100 epoxy resin was prepared to be ready for the following processing:

Agar 100Resin: Propylene oxide 1:1 for 1h.

Agar 100Resin: Propylene oxide 2:1 for 1h.

Agar 100Resin: Propylene oxide 3:1 for 1h.

Agar 100Resin for overnight at 4°C.

The next day the blocks embedded in resin were retrieved from the fridge and warmed up in the oven at 60°C for 20min and the procedure was carried out as follows; the molds were filled with freshly prepared resin and kept for 3-4 hours to remove all air bubbles and proper infiltration. The samples were rested and embedded in the molds and left in the oven for 24h at 64°C.

Blocks were trimmed and ultrathin sections were selected approximately -3.7 mm relative to bregma according to Paxinos and Watson (2005). For cutting coronal section of the hippocampus, ultra microtome was used. The semithin sections (1μm) were stained with 1% aqueous toluidine blue on glass slides. The ultrathin sections (95nm) were transferred on 200 mesh copper grids were contrasted with uranyl acetate followed by lead citrate double stain. The grids were examined and photographed under a Philips CM10 transmission electron microscope and the photo were taken from different area of the hippocampus in order to examine the occurrence of neuronal cell death in the current model.

5-4-Immunoflurescent labeling:

Animals (n=32) were sacrificed after surgery at different times: 4h (Sham =4, ADX=4), 24h (Sham =4, ADX=4), 3days (Sham =4, ADX=4), 1week (Sham =4, ADX=4) and 2weeks (Sham =4, ADX=4).

5-4-1-Materials:

Equipement:

- Humid chamber.
- Microwave (Daewoo electronics crop, Seoul, Korea).
- Microtome (Thermo Fisher Scientific, Massachusetts, USA).
- Liquid blocker (Daido Sangyo,Tokyo.Japan).
- Fluorescent microscope (Zeiss, Oberkochen, Germany).
- Confocal microscope (Nikon, Tokyo, Japan).
- Adobe PhotoShop (CS6 version, USA).

Reagents:

- Xylene.
- Ethanol.
- Distilled water.
- 10mM sodium citrate (pH 6) (Sigma-Aldrich, Missouri, USA).
- 0.1 M phosphate buffered saline (PBS, pH 7.4).
- 1% BSA.
- Primary antibodies:

- Rabbit polyclonal anti-ionized calcium-binding adaptor molecule 1 (Iba1, Wako, Massachusetts, USA 1:2000).
- Mouse monoclonal anti-neuronal nuclear antigen antibody (Neun, Millipore, Massachusetts,USA, 1:1000).
- Rabbit polyclonal anti-glial fibrillary acidic protein (GFAP, Dako, Copenhagen, Denmark, 1:1000).
- Goat Iba1 (Abcam, Massachusetts,USA 1:1000).

- Secondary antibodies:

  - Donkey anti-rabbit conjugated to Alexa488 (Invitrogen,Paisley, UK, 1:200).
  - Donkey anti-mouse conjugated to Rhodamine (Jakson, Pennsylvania, USA, 1:100).
  - Donkey anti-goat conjugated to cy5 (Jakson, Pennsylvania, USA, 1:100).
  - PBS-Triton X-100 0.3% (Sigma-Aldrich, Missouri, USA).

5-4-2-Method:

For all fluorescence labeling, the paraffin-embedded tissue sections were deparaffinized with xylene, rehydrated with ethanol (100, 90, 80, and 70%) and finally washed in distilled water. To unmask the epitopes and obtain efficient immunostaining, the brain sections were subjected to an antigen retrieval procedure with 10mM sodium citrate (PH 6) followed by heating for 1 min at high power and 10 min at low power in microwave. After this procedure the samples

were washed with 0.1 M phosphate buffered saline (PBS, pH 7.4) and cooled down at RT.

For double-immunofluorescence labeling, the sections were blocked by 1% BSA at room temperature for 30 min and then were incubated with each primary antibody at 4°C overnight. The primary antibodies used were rabbit polyclonal anti-ionized calcium-binding adaptor molecule 1 (Iba1, 1:2000) mixed with mouse monoclonal anti-neuronal nuclear antigen antibody (Neun, 1:1000) and rabbit polyclonal anti-glial fibrillary acidic protein (GFAP, 1:1000) mixed with mouse monoclonal anti-neuronal nuclear antigen (Neun, 1:1000). After washing three times in PBS, tissue sections were incubated with donkey anti-rabbit conjugated to Alexa488 (1:200) mixed with donkey anti-mouse conjugated to Rhodamine (1:100) all diluted in PBS-Triton X-100 0.3% for 1h at room temperature. Afterwards, the sections were washed several times in PBS; slides were cover slipped with fluoromount medium (Thermo Fisher Scientific, Massachusetts, USA).

Similar procedure was used for triple-immunofluorescence labeling in order to define the localization of microglia, astroglia and neurons in the same brain section, the mixture of the following primary antibodies was used, rabbit GFAP (1:1000) mixed with mouse Neun (1:1000) and goat Iba1 (1:1000) at 4°C overnight. Regarding the secondary antibody, tissue sections were incubated with donkey anti-rabbit conjugated to Alexa 488 (1:200) mixed with donkey anti-mouse conjugated to Rhodamine (1:100) and donkey anti-goat conjugated to cy5 (1:100). Representative digital images were captured using a Zeiss AxioCamHRc Digital camera with AxioVision 3.0 software (Carl Zeiss, Germany). Some sections were also examined with a C1 laser scanning confocal microscope (Nikon,Tokyo, Japan). 4X and 20X objectives were used to capture confocal images for the preparation of figures 32, 35 and 36 respectively where only one optical section

was utilized. The resulting files were used to generate the figures in Adobe PhotoShopCS6 where the photomicrographs were adjusted for contrast and brightness in order to determine the relationship between labeled neurons, astrocytes and microglia.

5-5-Quantitative analysis of the Iba-1 and GFAP positive cells:

Both microglia and astrocytes undergo morphological changes and became reactive cells in response to CNS injury. In this study we investigated the response of both these glial cells in the hippocampus after ADX. Typically, reactive microglia show shortening and widening of their processes and some of them they show amoeboid shape by losing their processes. Reactive astrocytes show increased size of their processes. These features can be easily visualized in sections stained with Iba1 and GFAP antibodies as markers for microglia and astrocytes respectively. In this study, only positively stained Iba1-positive microglia and GFAP-positive astrocytes with visible cell body at the focal plane were counted. Three ADX and three sham rats were used for each time point. Three sections of the hippocampus separated by 30µm were used from each rat. From each section three optical fields were selected for cell counting. Images of stained sections were taken at 20X magnification using an AxioCam HRc Digital camera with AxioVision 3.0 software (Carl Zeiss, Germany). In order to avoid being biased, the parameters of acquiring images like the time of exposure and the gain were first fixed for labeled microglia and astroglia and kept constant for all the examined time points. Cells matching the above mentioned criteria were counted manually using cell counter software (Heracle BioSoft SRL, Romania). A comparison was then carried out between the number of microglia and astrocytes in ADX and sham operated rats.

6-Animal behavior test:

All animals were handled daily for at least 3 days before the experiments. The Passive Avoidance task was conducted as described by (Misane and Ogren 2000; Ahlander-Luttgen et al., 2003) using a two-compartment standard shuttle box (51x25x24 cm) (Harvard Apparatus, Massachusetts, USA).

The two communicating (7x7 cm sliding door built in the separating wall) compartments were of equal size and had a stainless-steel bar floor. The right-hand compartment (shock compartment) was painted black to obtain a dark chamber, while the left-hand compartment was illuminated by a bulb (24 V; 5 W) installed on the top Plexiglas cover. PA training was conducted in a single session (day 1).

Rats were placed in the lighted compartment (with no access to the dark compartment) and were allowed to explore for 60s. During the exploration period in the PA apparatus. When 60s expired, the sliding door was automatically opened and the rat was allowed to cross over into the dark compartment. Once the rat had entered the dark compartment with all four paws, the sliding door was automatically closed and a weak electrical current (constant current, scrambled, duration 3s, 0.3 mA) was delivered through the grid floor. Latency to cross into the dark compartment (training latency) was recorded. If a rat failed to move into the dark compartment within 300 s (cut off latency), the door was reopened and the rat was gently moved into the dark compartment, where it received the foot shock.

After exposure to the foot shock, the rat was allowed to stay for 30 s in the dark compartment before it was removed from the PA apparatus to its home cage. Retention was tested 24 h after training (day 2). The animal was again placed in the lighted (safe) compartment with access to the dark compartment for a period of 300s. The latency to enter the dark compartment with all four paws was automatically measured (retention latency). If the rat failed to enter the dark

compartment within 300 s, it was removed and assigned a maximum test latency score of 300s (Figure-14).

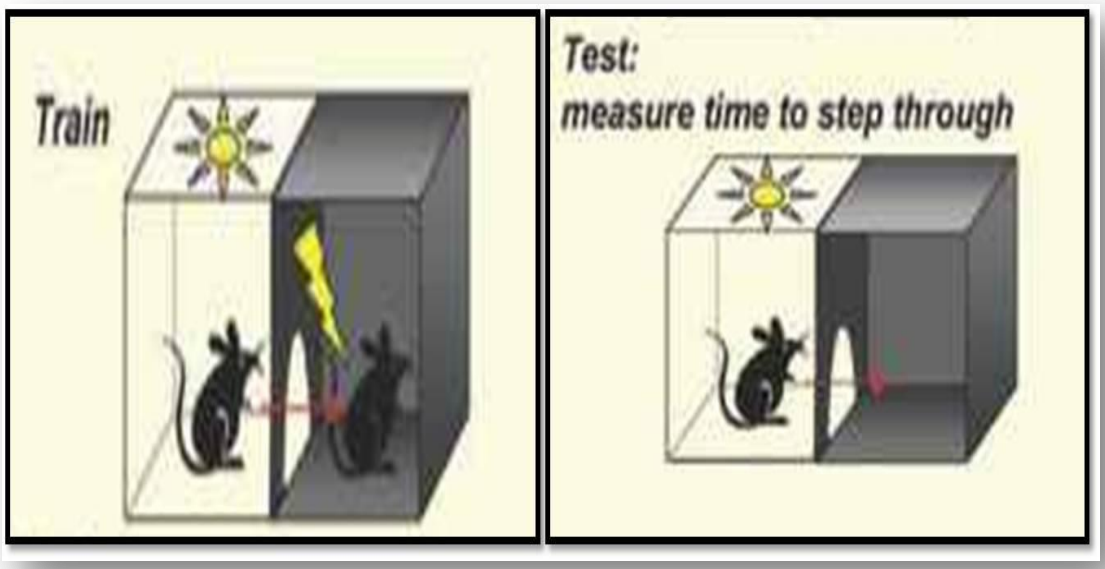

Figure-14: Passive avoidance task

(https://www.radiantthinking.us/memory-theory/ii-behavioral-assessments-in-rodents.html)

7-Statistical analysis:

All data are reported as the mean ± standard error of the mean and the analysis was considered significantly different if $P \leq 0.05$. Results for (IL-1β, IL-6 and TNF-α)و (GSH, SOD and MDA) and microglia and astrocytes counting were analyzed by two-tail Student using t test SPSS version 20 (IBM, USA).

RESULTS

1-Concentration of corticosterone

The efficacy of adrenalectomy was confirmed post-mortem by analysis of plasma corticosterone levels. The concentration of corticosterone was measured using Logit-Log paper plot Percent bound versus concentration of corticosterone for standards that ranges from 32-20000 pg/ml and by interpolation the concentration of corticosterone in the sera of adrenalectomized and sham operated rats was determined see the (Figure-15).

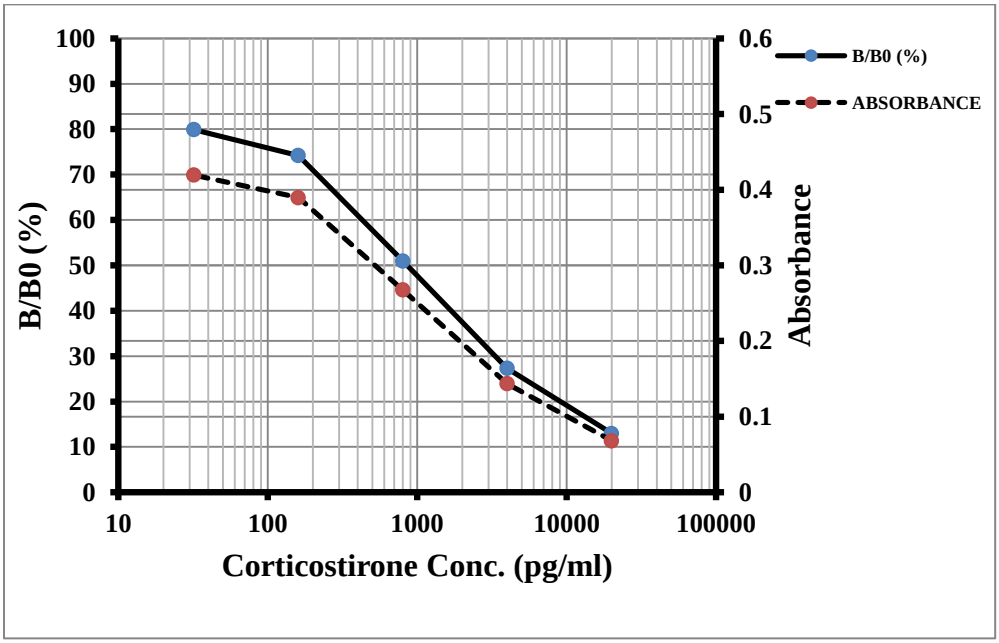

Figure-15: Standard curve used in the determination of corticosterone levels in the sera of adrenalectomized and sham operated rats.

We found the levels of corticosterone were significantly decreased after 4h ($P=0.001$) in the serum of adrenalectomized compared to bilateral sham operated rats and continued in the same trend after 24h ($P<0.001$), 72h ($P<0.001$), 1week ($P<0.001$) and 2weeks ($P<0.001$) following the surgery see (Figure-16) and (Table-6).

Table-6: Concentration of corticosterone in the serum of adrenalectomized rats compared to sham operated rats over the course of time (4h, 24h, 3days, 1week and 2weeks). ***P<0.001. Data are expressed as mean ±SEM.

Time / Groups	SHAM	ADX	Statistical significance
4H	24493.6±1732.3	7503.3±860.0	***P=0.001
24H	18629.9±3668.8	199.4±59.0	***P<0.001
72H	12527.5±1914.6	126.5±33.8	***P<0.001
1 Week	16291.5±2770.2	224.6±94.3	***P<0.001
2 Weeks	16123.7±2835.8	163.6±49.4	***P<0.001

Unit of measurement: pg/ml

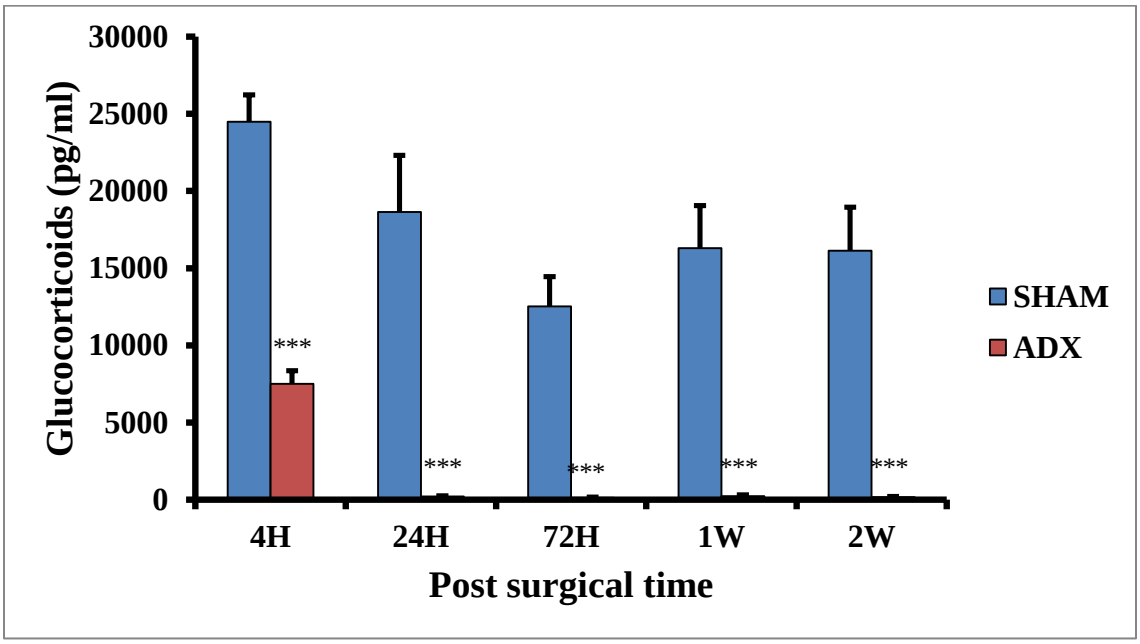

Figure-16: Bar graphs showing levels of serum corticosterone. Levels of corticosterone were measured by EIA in the serum of adrenalectomized rats compared to the sham operated rats over the course of time (4h, 24h, 3days, 1week and 2weeks). ***P<0.001. Data are expressed as mean ± SEM.

2-Neuroinflammation

2-1-Interleukin-1 beta (IL-1β):

The pro-inflammatory cytokines IL-1β, IL-6 and TNF-α are the major players in multiple responses to different insults and injuries. In addition they play a significant role in different neurodegenerative diseases. In the current neurodegeneration model we intended to evaluate the levels of these cytokines in the hippocampus of Wistar rats subjected either to bilateral adrenalectomy or to sham operation using ELISA.

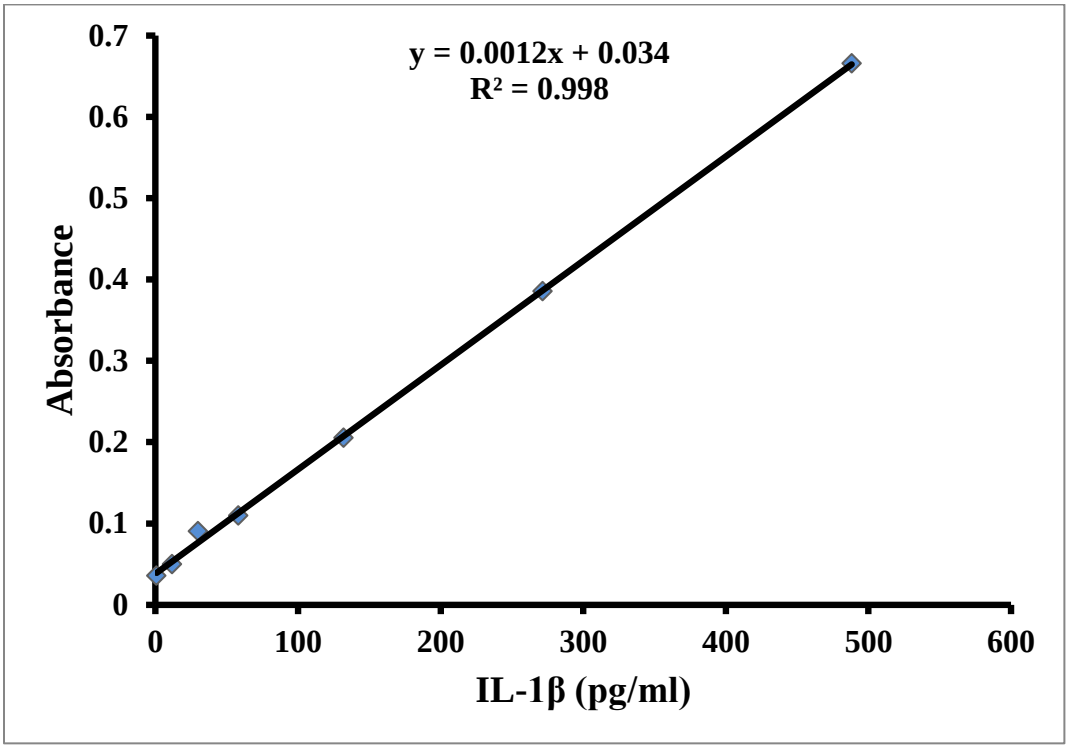

Figure-17: Interleukin-1β Standard Curve. The curve obtained from the absorbance at 450nm of varying concentrations of IL-1β standards ranging from 12.5-600 pg/ml (R^2: Pearson Coefficient of Determination).

The levels of pro-inflammatory cytokine Interleukin-1β in the hippocampal homogenates of adrenalectomized and sham operated rats were examined over the course of time (4h, 24h, 3days, 1week and 2weeks). In order to determine the

concentration of IL-1β by ELISA, a standard curve in the range 12.5-600 pg/ml was constructed and the levels of IL-1β in the samples was determined by interpolation see (Figure-17).

Our results showed that the levels of IL-1β were significantly increased in the hippocampus of adrenalectomized rats compared to bilateral sham operated rats after 4h ($P<0.05$), 24h ($P<0.05$) and 3days ($P<0.01$) of surgery. However, one and two weeks after adrenalectomy no statistical difference in the hippocampal levels of IL-1β were found between the two groups, see (Table-7) and (Figure-18).

Table-7: Concentration of Interleukin-1β levels in the hippocampal homogenates of adrenalectomized rats compared to the sham operated rats over the course of time (4h, 24h, 3days, 1week and 2weeks). Data are expressed as mean ± SEM.

Time / Groups	SHAM	ADX	Statistical significance
4H	114.25±11.17	155.87±12.51	*P<0.05
24H	108.98±6.55	129.67±4.40	*P<0.05
72H	112.60±4.12	133.72±5.53	**P<0.01
1 Week	121.84±7.38	102.03±7.41	P>0.05
2 Weeks	76.62±5.85	72.86±4.65	P>0.05

Unit of measurement: pg/mg of total protein

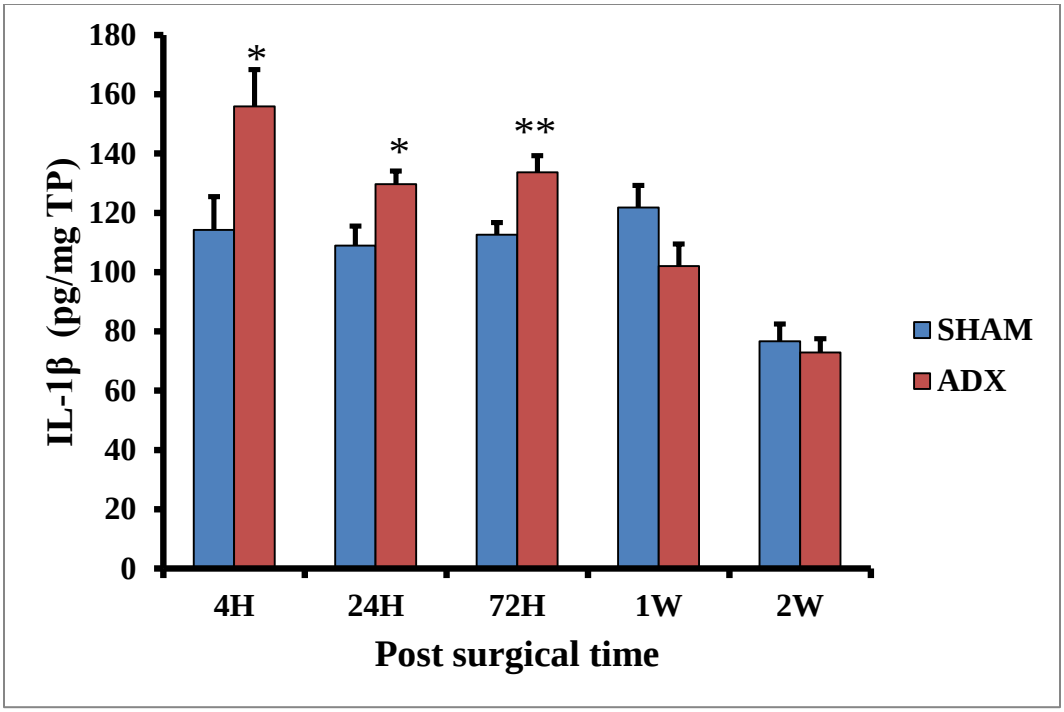

Figure-18: Bar graphs showing IL-1β level in the hippocampus of adrenalectomized and sham operated rats over course of time (4h, 24h, 3days, 1week and 2weeks) .*P<0.05. **P<0.01.Data are expressed as mean ± SEM.

2-2-Interleukin-6:

The levels of pro-inflammatory cytokine Interleukin-6 in the hippocampal homogenates of adrenalectomized and sham operated rats were examined over the course of time (4h, 24h, 3days, 1week and 2weeks). In order to determine the concentration of IL-6 by ELISA, a standard curve in the range 125-8000 pg/ml was constructed and the levels of IL-6 in the samples were determined by interpolation (Figure-19).

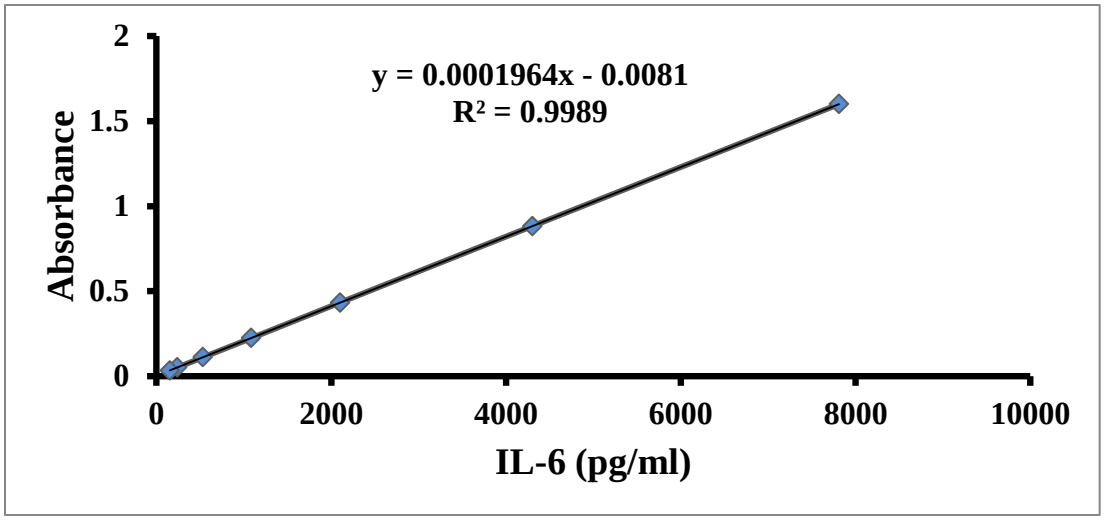

Figure-19: Interleukin-6 Standard Curve. The curve obtained from the absorbance at 450nm of varying concentrations of IL-6 standards ranging from 125-8000 pg/ml (R^2: Pearson Coefficient of Determination).

A significant increase in IL-6 levels was observed in the hippocampus 4h ($P<0.01$), 24h ($P<0.01$) and 3days ($P<0.05$) after ADX, however, no change was seen in IL-6 levels after one and two weeks postoperatively (Table-8) and (Figure-20).

Table-8: Concentration of Interleukin-6 levels in the hippocampal homogenates of adrenalectomized rats compared to the sham operated rats over the course of time (4h, 24h, 3days, 1week and 2weeks). Data are expressed as mean ± SEM.

Time / Group	SHAM	ADX	Statistical significance
4H	621.77±35.80	802.74±30.62	**P<0.01
24H	543.59±21.45	656.24±17.45	**P<0.01
72H	580.95±20.90	644.39±17.00	*P<0.05
1 Week	643.80±59.05	520.00±24.61	P>0.05
2 Weeks	560.83±29.41	587.01±41.52	P>0.05

Unit of measurement: pg/mg of total protein

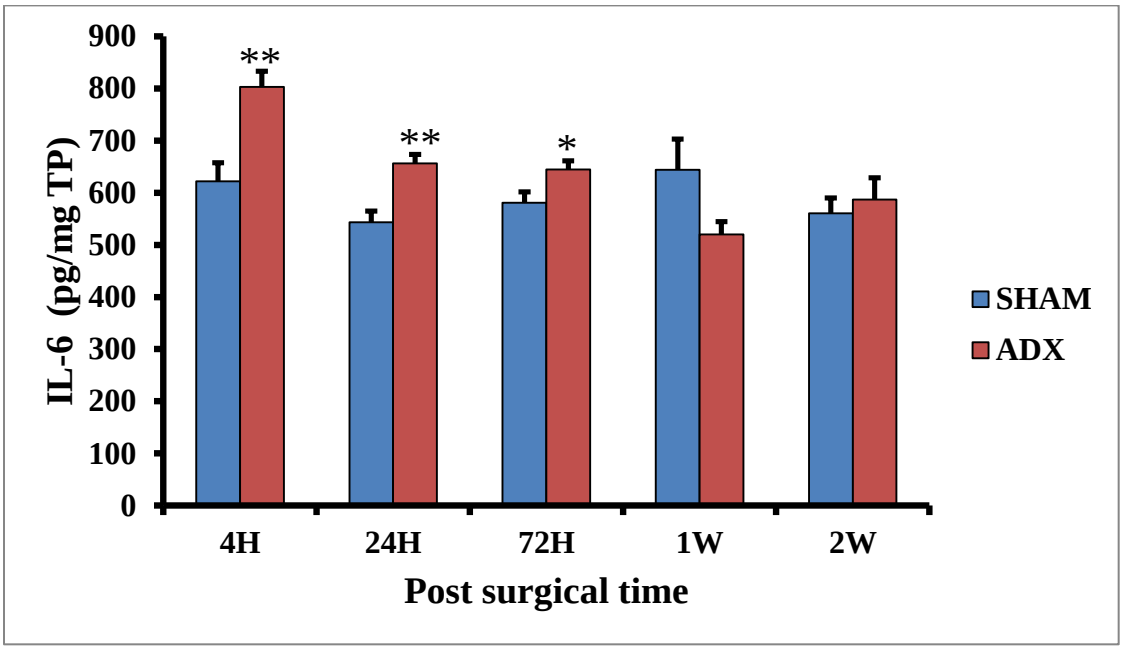

Figure-20: Bar graphs showing IL-6 levels in the hippocampus of adrenalectomized and sham operated rats over course of time (4h, 24h, 3days, 1week and 2weeks).*P<0.05. **P<0.01.Data are expressed as mean ± SEM.

2-3-Tumor Necrosis Factor-α (TNF-α):

The levels of pro-inflammatory cytokine TNF-α in the hippocampal homogenates of adrenalectomized and sham operated rats were examined over the course of time (4h, 24h, 3days, 1week and 2weeks). In order to determine the concentration of TNF-α by ELISA, a standard curve in the range 3.9-500 pg/ml was constructed and the levels of TNF-α in the samples was determined by interpolation (Figure -21).

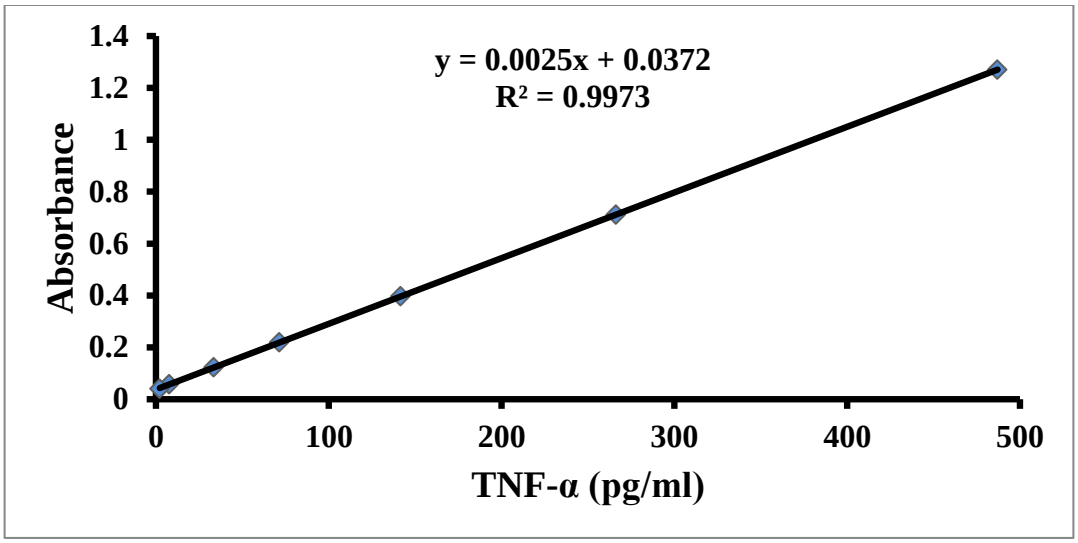

Figure -21: Tumor Necrosis Factor-α Standard Curve. The curve obtained from the absorbance at 450nm of varying concentrations of TNF-α standards ranging from 3.9-500 pg/ml (R^2: Pearson Coefficient of Determination).

The levels of TNF-α were significantly increased in the hippocampus of adrenalectomized rats compared to bilateral sham operated rats after 4h only ($P<0.01$) and remain unchanged after 24h, 72h, 1week, 2weeks of surgery see (Table-9) and (Figure-22).

Table-9: Concentration of TNF-α levels in the hippocampal homogenates of adrenalectomized rats compared to the sham operated rats over the course of time (4h, 24h, 3days, 1week and 2weeks). Data are expressed as mean ± SEM.

Time / Group	SHAM	ADX	Statistical significance
4H	21.39±0.99	29.31±1.33	**P<0.01
24H	16.90±0.63	17.33±0.89	P>0.05
72H	16.58±0.71	16.52±1.07	P>0.05
1 Week	18.30±0.93	15.52±1.11	P>0.05
2 Weeks	18.19±2.04	18.47±1.62	P>0.05

Unit of measurement: pg/mg of total protein

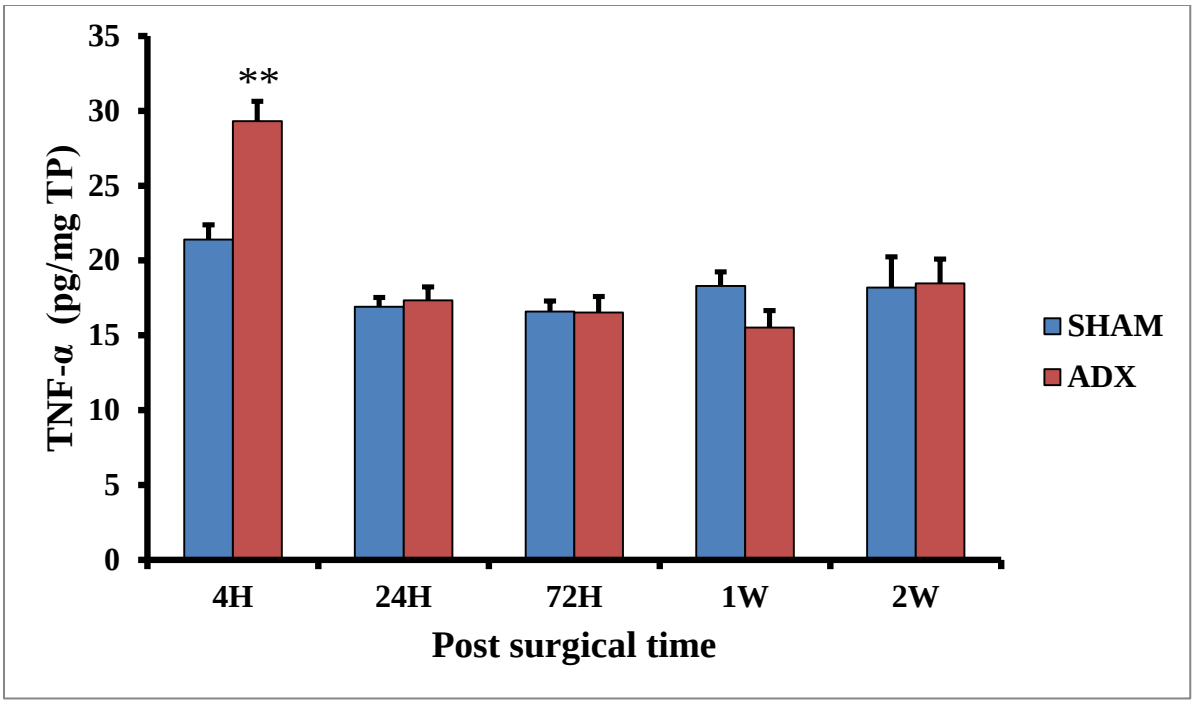

Figure-22: Bar graphs showing TNF-αlevels in the hippocampus of adrenalectomized and sham operated rats over course of time (4h, 24h, 3days, 1week and 2weeks). **P<0.01.Data are expressed as mean ± SEM.

3-Neurodegeneration

3-1-Neuronal cell death using FJB:

In order to examine the occurrence of neuronal cell death in the hippocampus following adrenalectomy over a course of time (4h, 24h, 3days, 1week and 2weeks), a Fluoro-Jade B staining was performed. FJB staining is a specific staining for neurons undergoing degeneration, regardless of the specific insult or mechanism of cell death.

After four hours (results not shown) and 24h following adrenalectomy our results showed no positive staining for degenerated neurons in both groups ADX and sham rats (Figure-23A', A, E', E). Three days after adrenalectomy we observed a few degenerated neurons in the dorsal blade of the dentate gyrus in the hippocampii of adrenalectomized rats only (Figure-23B', B, F', F). Moreover, one week after adrenalectomy, more degenerated neurons were seen on the dorsal blade of the dentate gyrus (Figure-23C', G') whilst no positive FJB staining was observed in sham operated rats (Figure-23C, G). After two weeks of adrenalectomy, we observed a progression of cell death throughout the dorsal blade of the dentate gyrus (Figure-23D', H') where an intense FJB staining was seen. In addition, less intense staining was observed in the ventral blade indicating that differential effect of the adrenal gland removal on both blades of the dentate gyrus (Figure-24). No positive FJB staining was observed in sham operated rats (Figure-24) and (Figure-23D, H).

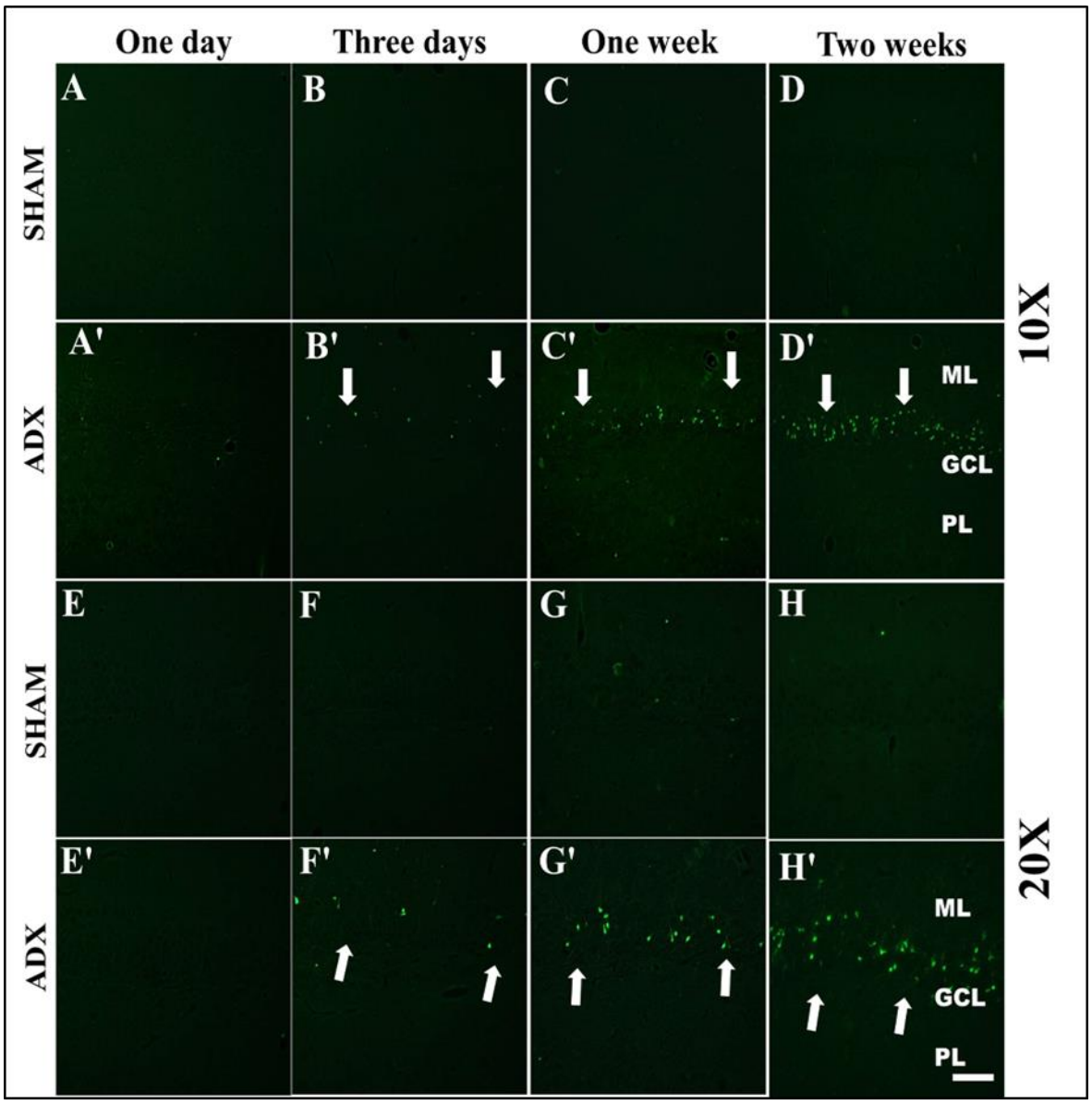

Figure-23: Images of coronal sections of the hippocampus stained with Fluoro-Jade B showing the progression of neuronal cell death over the course of time (1day, 3days, 1week and 2weeks) in the dentate gyrus of the hippocampus of adrenalectomized rats compared to sham operated rats .Absence of cell death was noticed in the dentate gyrus (A, B, C, D) and (E, F, G, H) of sham operated rats during the different time points (1day, 3days, 1week and 2weeks). One day after adrenalectomy the rats showed no signs of neuronal cell death in the dentate gyrus (A') and (E'). A progression of neuronal cell death was seen in the dentate gyrus three days (B'), one week (C'), and two weeks (D') after adrenalectomy. Molecular layer (ML), granule cell layer (GCL), polymorphous layers (PL). Scale bar=50µm.

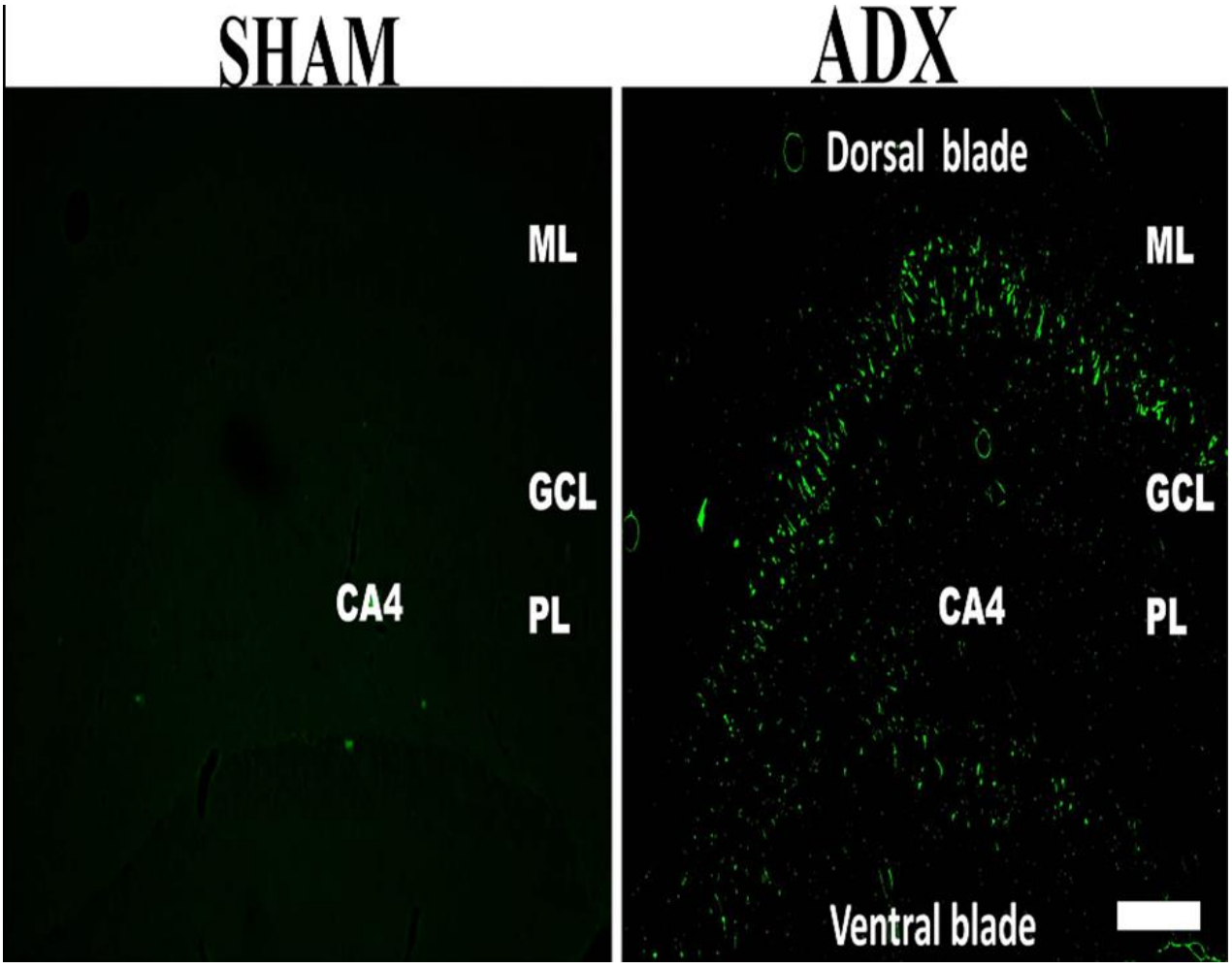

Figure-24: Representative confocal images of with Fluoro-Jade B staining (green) showing the occurrence of neurodegeneration after two weeks in both blades of the dentate gyrus of the hippocampus of adrenalectomized rats compared to sham operated rats. Molecular layer (ML), granule cell layer (GCL), polymorphous layers (PL). Scale bar=50µm.

3-2-Neuronal cell death using electron microscopy:

The motive behind the current ultrastructural study was to determine the impact of the absence such hormones on different cells of the hippocampus after short-term adrenalectomy at different time points (3, 7 and 14 days). In addition, Prof. Adem and his team in previous study reported the absence of glucocorticoids

after long period of time (5 months) induces degeneration in the different parts of the hippocampus where different neuronal populations exhibited signs of abnormalities and different types of cell death.

The examination of the thin section under the electron microscope three days following adrenalectomy showed granule cells degeneration of dorsal blade of the dentate gyrus of adrenalectomized rats hippocampus where the cells showed condensed chromatin and irregular cell membrane and the beginning of vacuolation in the cytoplasm. Interestingly we have not noticed cell abnormalities in the rest of the dentate gyrus (Figure-25B, D). Concerning different areas of the Cornu Ammonis (CA), solely CA4 pyramidal cells displayed signs of cell damages following the removal of the adrenal gland(Figure-26) while the big CA3 pyramidal cells, small pyramidal CA1 and CA2 cells did not show any signs of neurodegeneration after three days of adrenalectomy (Figure-25B,D). The examination of the hippocampus of the sham operated rats revealed no signs of neurodegeneration in different parts of the hippocampus (Figure-25A, 1C, 2A, 2C).

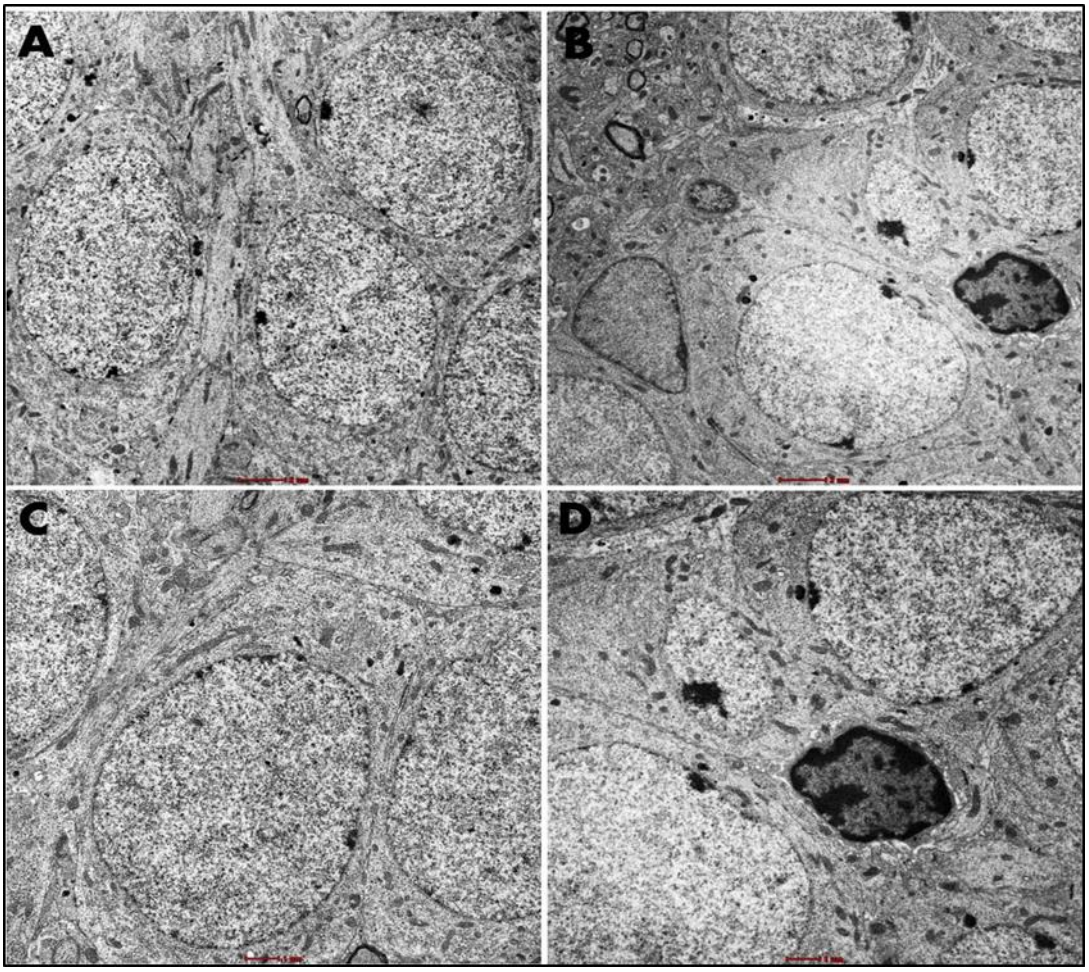

Figure-25: Electron micrographs of dentate gyrus upper blade of ADX rats compared to sham operated three days postoperatively. (A) Usually the granule cells of the dentate gyrus of the hippocampus have a round shape and a big nucleus occupies the whole cell body, in such cell the nucleus surrounded by thin layer of cytoplasm. (B) In adrenalectomized rats, few degenerated granule cells were seen in the upper blade where deformation of the cell morphology was seen. In addition the shrinkage of the cell body condensation of chromatin and reduction of the nucleus size . Scale bar = 2 µm. Higher magnification of granule layer of dentate gyrus of (D) ADX rats compared to (C) sham operated respectively . Scale bar = 1 µm.

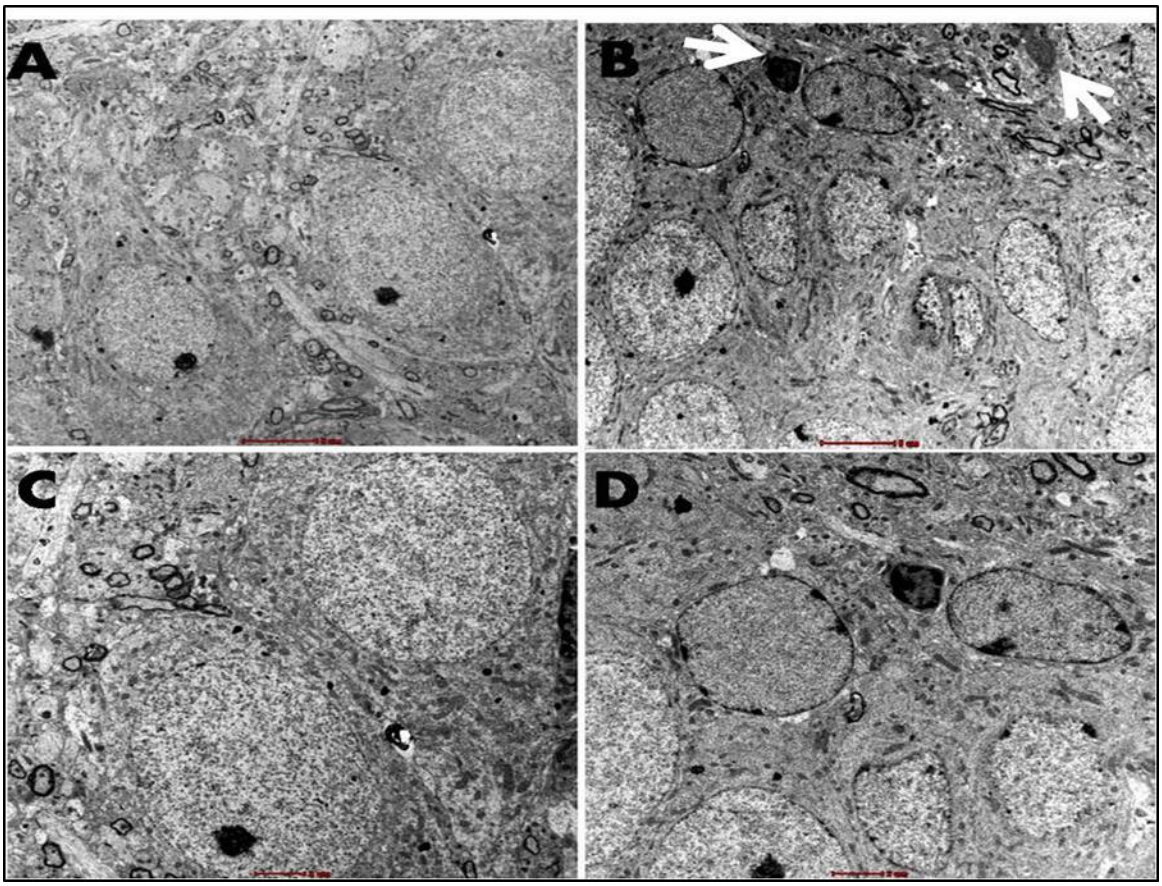

Figure-26: Electron micrographs of CA4 pyramidal cells of ADX compared to sham operated rats three days following surgery. (A) Healthy pyramidal cells showing well-defined nucleolus (Nl) and nucleus (nuc) and homogenous karyoplasm. Cytoplasmic organelles are normal in distribution and morphology. (B) multiple degenerated pyramidal neurons of the CA4 with irregular nucleus membrane and beginning of the chromatin condensation, the arrow showing already degenerated neurons where reduction the nucleus volume and dark compacted chromatin are apparent. Scale bar = 5 µm.(C) and (D) higher magnification of pyramidal layer of CA4 of sham operated compared to ADX rats respectively. Scale bar = 2 µm.

Seven days following the removal of adrenal gland, ultra-structural examination of the hippocampus revealed a progressive neurodegeneration compared to the third day of adrenalectomy where cell death was seen all over the dentate gyrus revealing more exacerbation of the neurodegenerative process

(Figure-27A'). In addition to what we have seen on the third day after adrenalectomy more degenerative cells were observed in the CA4 (Figure-27B'). In addition, EM observation of the neuropil in the CA3 area of hippocampus of adrenalectomized rats revealed cell death of the CA3 Pyramidal cells for the first time (Figure-27C'). No sign of degeneration was seen in the CA1 of the adrenalectomized rats. The hippocampus of the sham rats did not show any abnormalities in different neuronal populations (Figure-27A, B, and C)

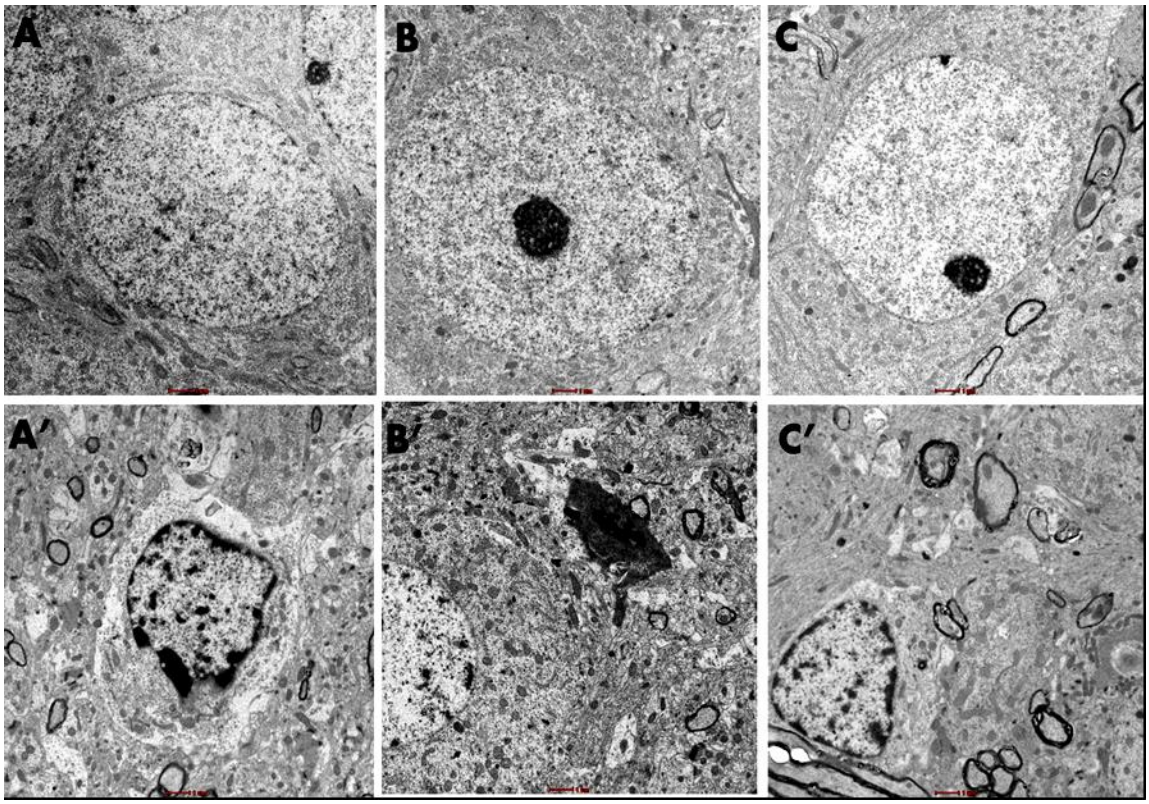

Figure-27: Electron micrographs showing degeneration in different areas of the hippocampus of ADX rats compared to sham operated were taken seven days postoperatively. (A) Intact granule cell with well defined nucleus and cell membrane of sham rats. (A') degenerated granule cell of the dentate gyrus with condensed chromatin and irregular cell membrane. (B) and (C) healthy pyramidal cells of CA4 and CA3 respectively. (B') showing ultrastructural of CA4 dead neurons with disintegration of the cell body, condensation of the chromatin and nucleus volume reduction. (C') multiple degenerated CA3 pyramidal neurons with irregular nucleus membrane and beginning of the chromatin condensation. Scale bar = 1 µm.

Our results exhibited an extensive cell death on the dorsal blade of the dentate gyrus compared to less degree of cell death in ventral blade after two weeks of adrenalectomy. A thorough examination of granule layer of the dentate gyrus showed differences in the gross appearance of the neuropil between the adrenalectomized and sham operated rats. In the adrenalectomized animals, the granule layer showed empty areas with multiple ‘‘blank’’ spaces that indicated already degenerated cells. In addition to the changes in the neuropil, we observed ultrastructural changes in the upper and lower blade of the dentate gyrus (Figure-28).

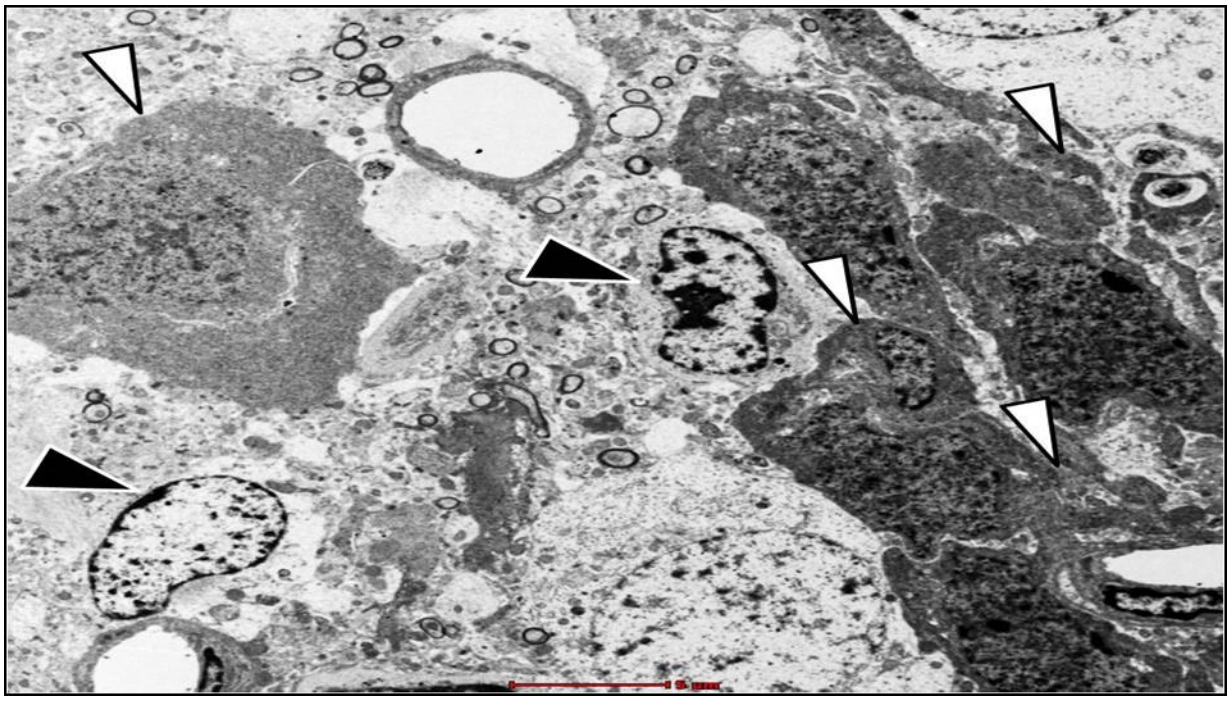

Figure-28: Electron micrographs taken from the upper blade of the dentate gyrus two weeks following adrenalectomy showing granule cells engulfed by microglia (white arrows), in addition, it shows undergoing degeneration of granule cells where fragmentation of the nucleus and appearance of vacuolation in the cytoplasm (black arrow). Scale bar = 5 µm.

A condensation of chromatin was seen in addition of the cell body shrinkage revealing both apoptotic and necrotic process occurring in this part of the hippocampus and major vulnerability of such cell type to the absences of glucocorticoids (Figure-29). In contrast, in the sham rats the neuropil was continuous with abundant, tightly packed granule cells. As the granule cells are small neurons, the nucleus occupied most of the cell body with only a thin rim of cytoplasm surrounding it.

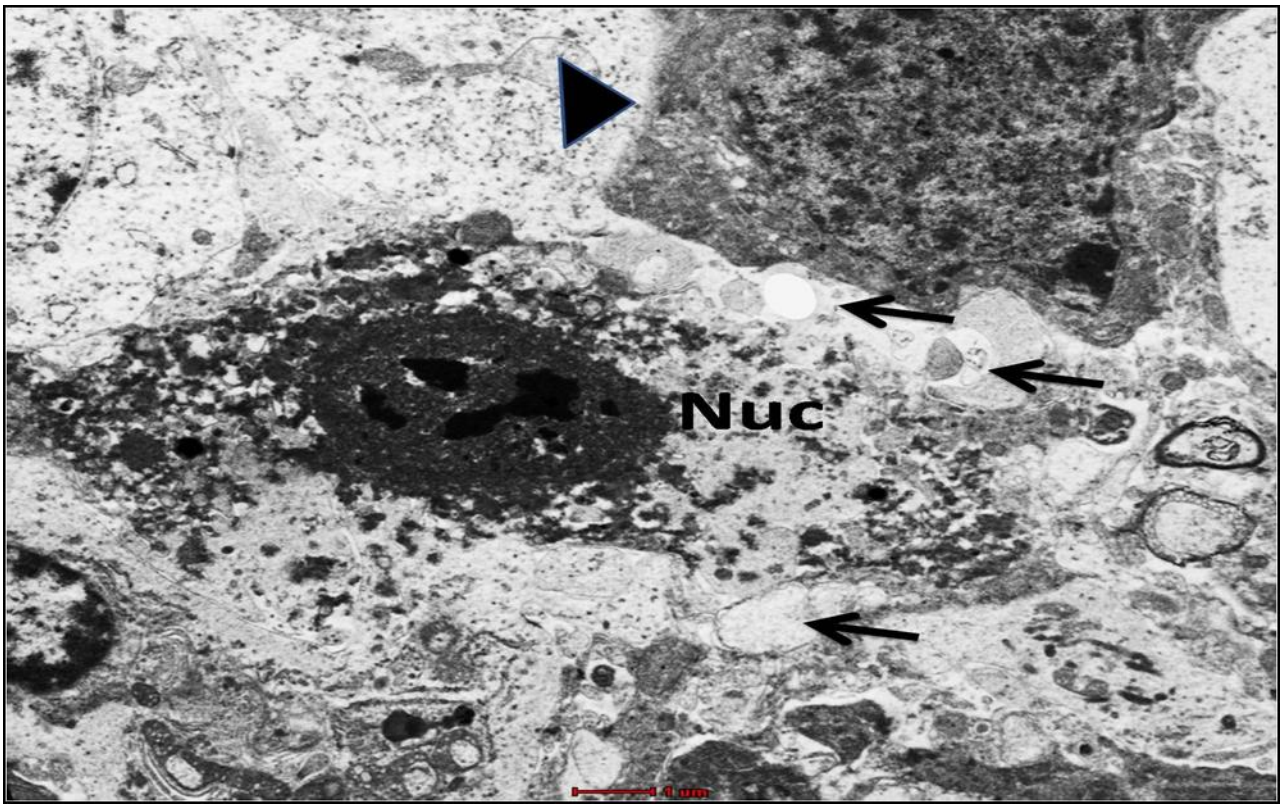

Figure-29: High power microscopy of degenerated granule cell in the hippocampus of adrenalectomized rats two weeks following adrenalectomy. Appearance of vacuolation in the cytoplasm with condensed chromatin (thin arrow) and adjacent granule cell in the process to be phagocytosed by microglia (big arrow). Scale bar = 1 µm.

The examination of the Cornu Ammonis of the adrenalectomized rats revealed an extensive cell death in the CA4 area where chromatin condensation and vacuolation were seen (Figure-30).

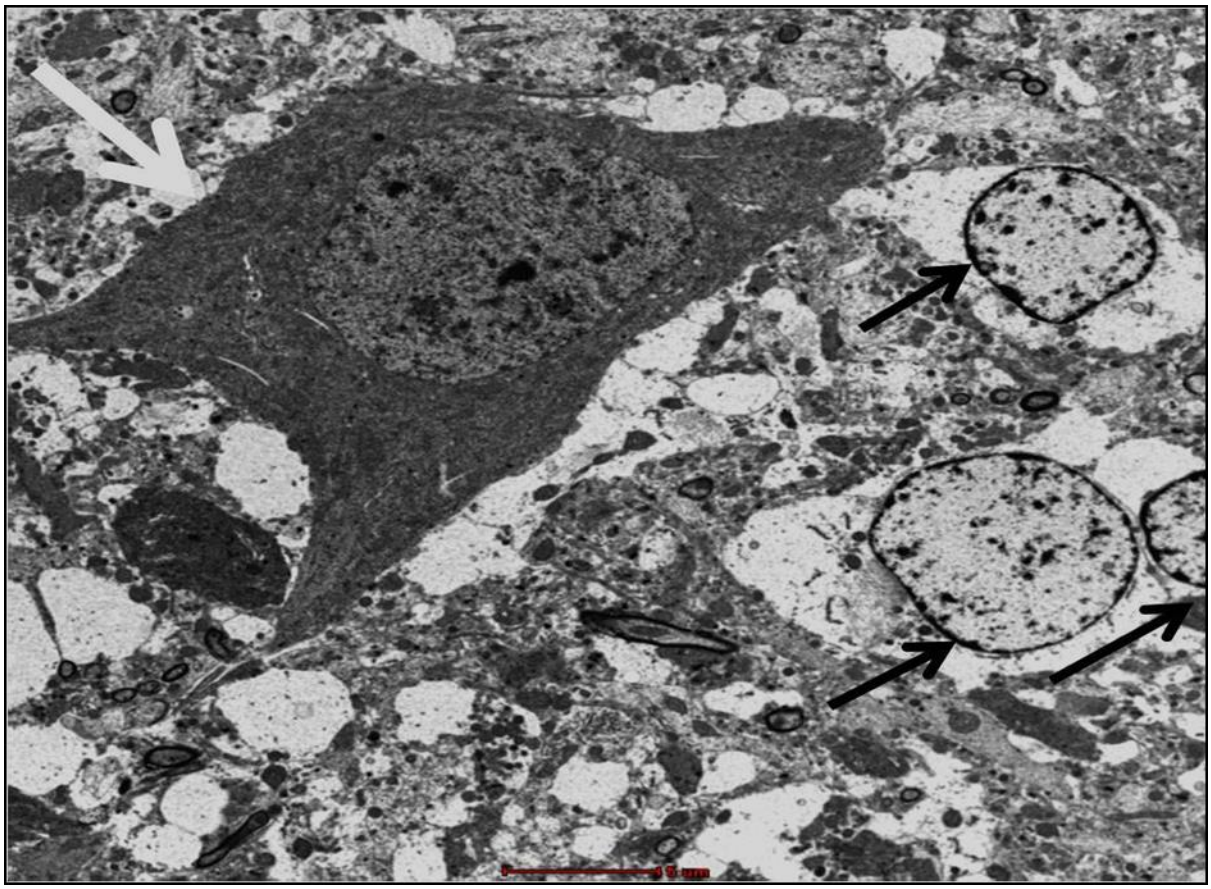

Figure-30: High power microscopy taken from CA4 area of the hippocampus following two weeks of adrenalectomy showing empty space in pyramidal layer. In addition, many neurons with compacted chromatin surrounded by irregular nucleus membrane (black arrow).A glial cell in the process to phagocyte Pyramidal cell of the CA4 (white arrow).Scale bar = 5 µm.

Electron microscopy examination of the CA3 area of ADX rats revealed the occurrence of cell death of pyramidal cells along the principal layer of such area where extensive chromatin condensation, and reduction of the soma volume and the wavy shrinkage of the nuclear membrane and the vacuolization of mitochondria where seen (Figure-31). Sham operated rats displayed healthy

clustered granule cells with regular plasma membrane and well defined nucleus with regular dispersed chromatin. More importantly, our results showed no ultrastructural abnormalities of the CA1pyramidal cells of both groups.

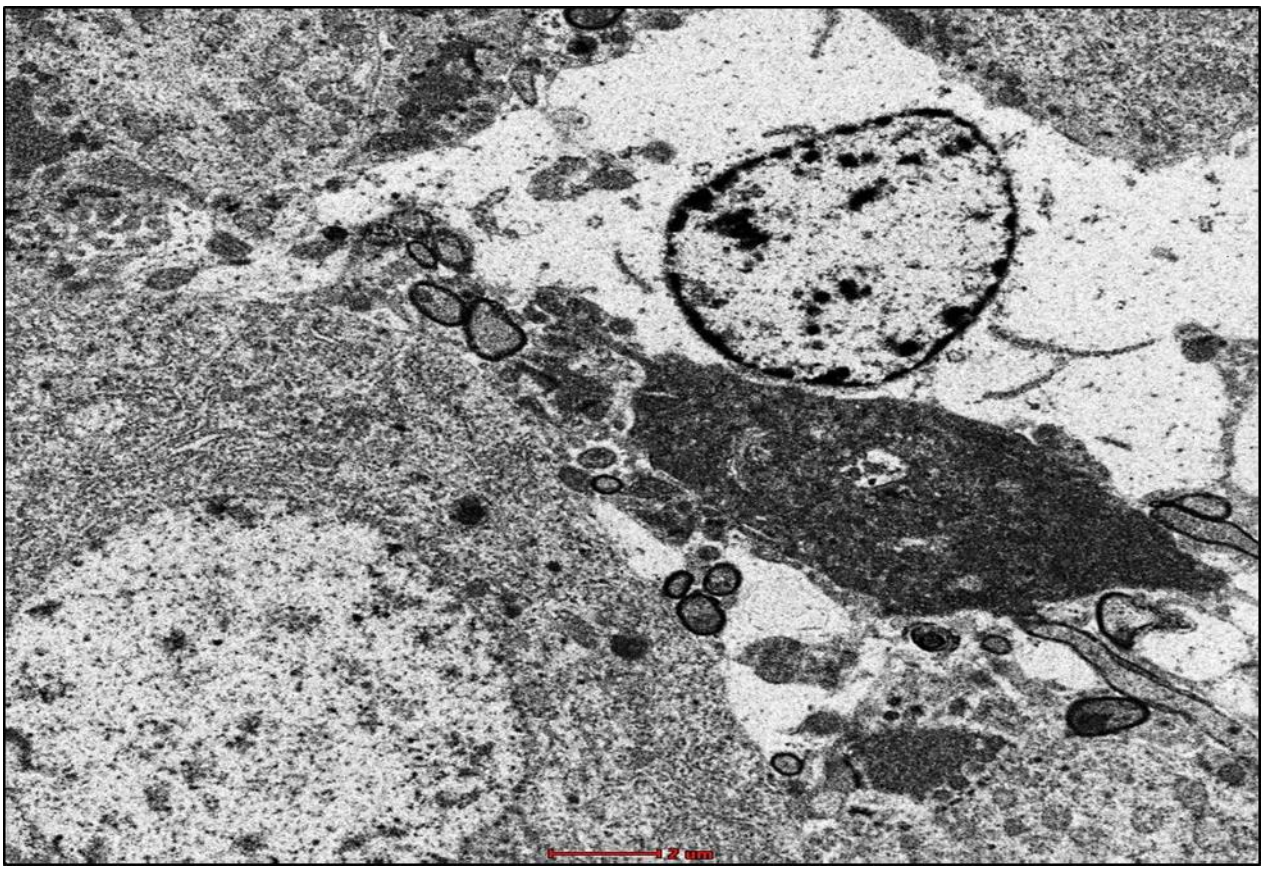

Figure-31: Electron micrograph showing CA3 pyramidal cells at different stage of degeneration two weeks following adrenalectomy confirming that withdrawal of glucocorticoids by adrenalectomy is not selective where different neuronal populations in the hippocampus are subject of substantial degeneration. Scale bar = 2µm.

4-Microgliosis and astrogliosis

4-1-Activation of microglia:

The activation of microglia is one of the major signs of neurodegeneration. In order to investigate the activation of these cells in response to neurodegeneration occurring after short-term adrenalectomy, a double immunofluorescent labeling of neurons (Neun) and microglia (Iba-1) over the course of time (4h, 24h, 3days, 1week and 2weeks) was performed.

Immunofluorescence staining with Iba-1 antibody after four hours and one day of adrenalectomy did not show activated microglia in adrenalectomized and sham operated groups (Figure-32A' and A). However, after three days we observed few activated microglia in the dorsal blade of the dentate gyrus of adrenalectomized rats while no sign of activation was seen in the sham operated rats (Figure-32B' and B). One week following the adrenal gland removal, activated microglia were seen in the whole dorsal blade of the dentate gyrus indicating a progression of microgliosis (Figure-32C'). In contrast, no sign of activated microglia were observed in the hippocampus of sham operated rats (Figure-32C).

Fluorescent double immunostaining of neurons and microglia of brain sections after two weeks postoperatively revealed a strong Iba-1 immunoreactivity in the hippocampus of adrenalectomized rats most particularly in the dentate gyrus (Figure-32D') and stratum lucidum of CA3 (Figure-32H') areas compared to the corresponding regions in the sham operated rats (Figure-32D and H).

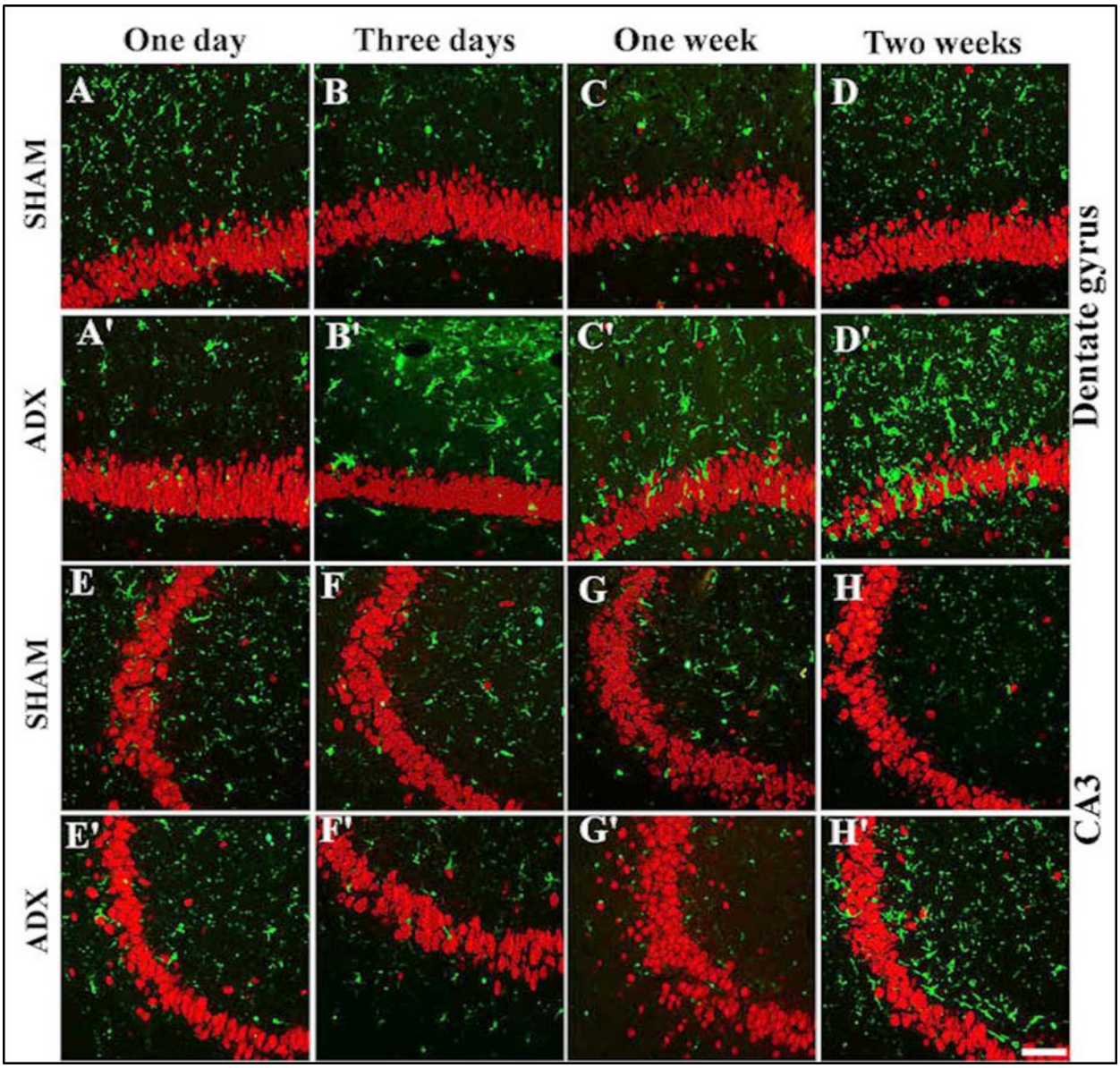

Figure-32: Images of microgliosis in the hippocampus. Coronal sections of the hippocampus stained with NeuN antibody (red) as a neuronal marker and Iba-1 antibody (green) as a microglia marker showing the progression of microgliosis over the course of time (1day, 3days, 1week and 2weeks) in the dentate gyrus and CA3 of the hippocampus of adrenalectomized rats compared to sham operated rats. Absence of microgliosis in the dentate gyrus (A, B, C, D) and CA3 (E,F,G,H) of sham operated rats during 1day, 3days, 1week and 2weeks. The adrenalectomized rats showed no signs of microgliosis in the dentate gyrus (A') and CA3 (E') after one day. However, a progression of microgliosis was seen in the dentate gyrus after three days (B'), one week (C') and two weeks (D'). In comparison, the microgliosis in the CA3 of adrenalectomized rats did not appear until after 2 weeks as the Iba1 immunoreactivity (H') after 1day, 3days and 1 week was not significantly different from that in sham operated rats(E',F',G'). Molecular layer (ML), granule cell layer (GCL), polymorphous layers (PL) and (SL) stratum lucidum. Scale bar =50µm.

The quantitative analysis showed that the number of Iba-1-positive microglia in the hippocampus of ADX rats was significantly higher in days 3 ($P<0.01$), 7 ($P<0.001$) and 14 days ($P<0.001$) compared to the sham operated rats. The results showed progressive increase in the number of microglia in the hippocampus from day three with a further increase one and two weeks after adrenalectomy (Figure-33).

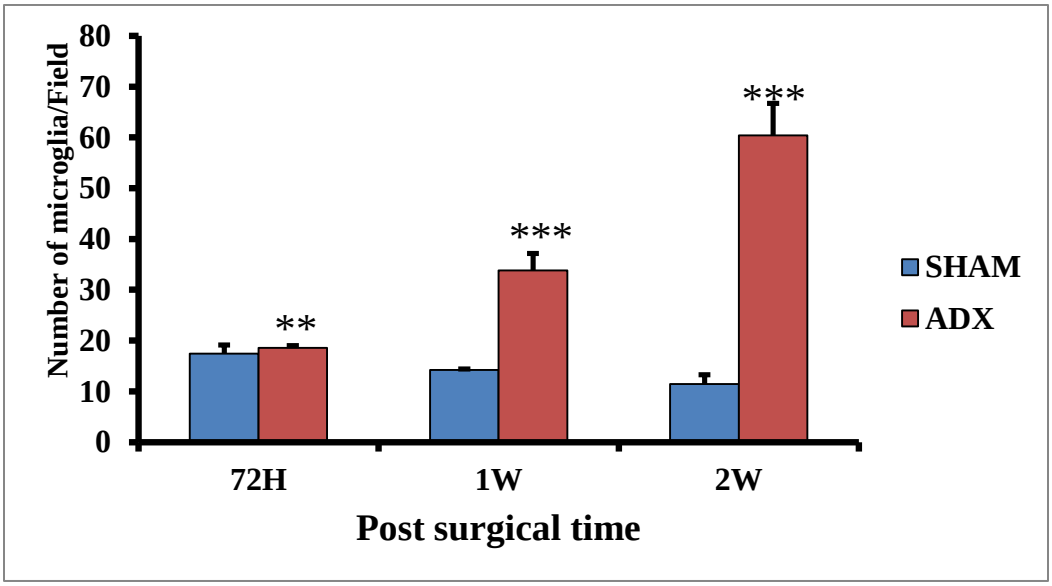

Figure-33: Bar graphs showing the comparison between the number of Iba-1 positive cells in the hippocampus of adrenalectomized and sham operated rats. The number of microglia was significantly and progressively increased in adrenalectomized rats 3 days, 1 week and 2 weeks postoperatively. **P<0.01. ***P<0.001. Data are expressed as mean (±SEM).

Iba-1 labeling exhibited a differential distribution throughout the dentate gyrus where it shows an intensive microgliosis in the molecular and granular layer of the dorsal blade and predominately at the tip where the Neun staining shows apparent absence of neurons compared to the ventral blade two weeks postoperatively (Figure-34). Interestingly, at the same time point, two weeks after adrenalectomy, we observed for the first time a strip of Iba-1 positive cells in the stratum lucidum layer of the CA3 area (Figure-34) and (Figure-32D'). No sign of microgliosis was seen in CA3 area of sham operated rats over the course of time (Figure-32E, F, G, and H).

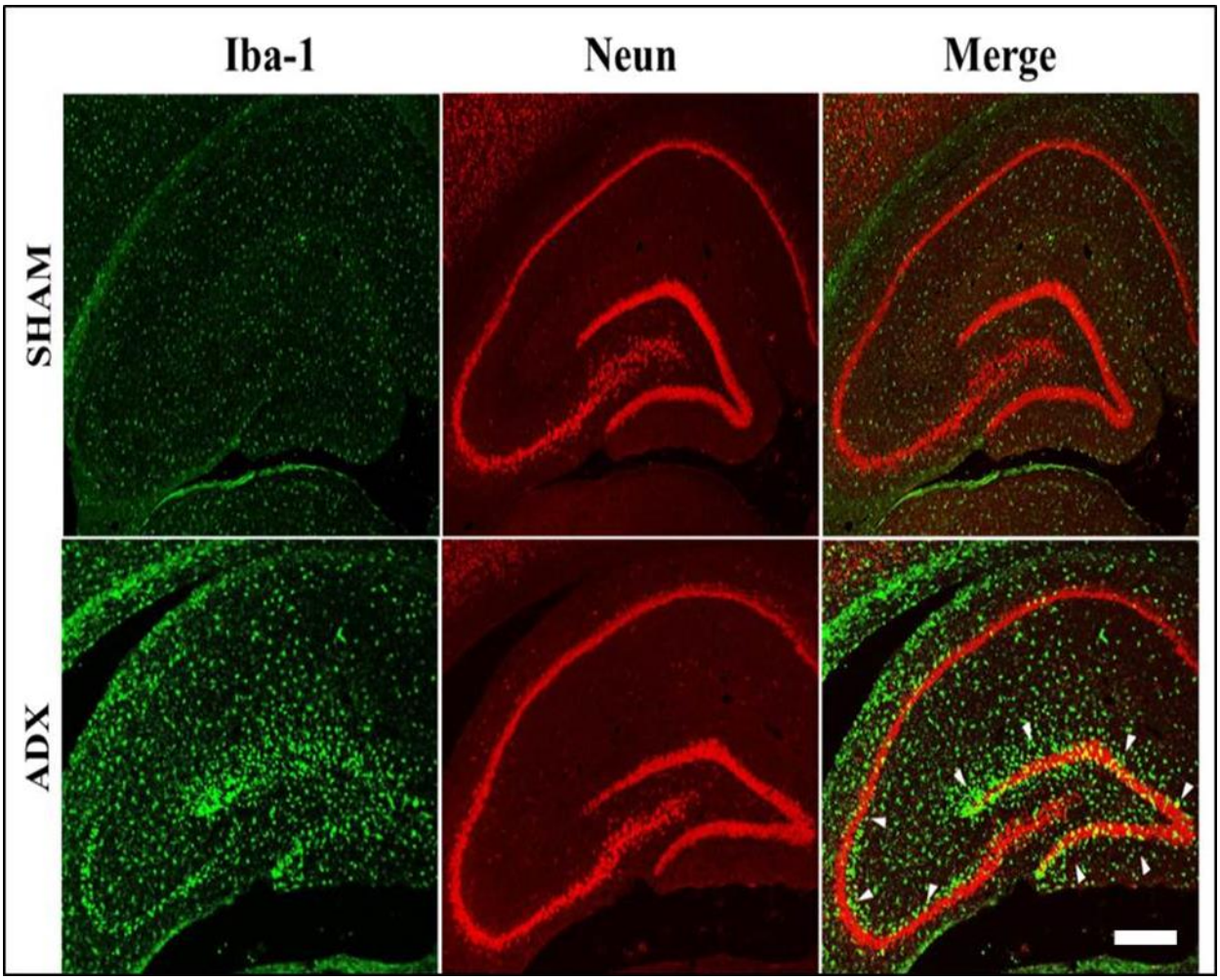

Figure-34: Representative images of coronal sections of the whole hippocampus stained with NeuN (red) and Iba-1 (green) antibodies showing microgliosis after two weeks of adrenalectomized rats compared to bilateral sham operated rats. Molecular layer (ML), granule cell layer (GCL), polymorphous layers (PL) and (SL) stratum lucidum. Scale bar=100µm.

4-2-Activation of astrocyte:

In order to examine the effect of adrenal gland removal on astrocyte immunoreactivity in the hippocampus over a course of time (4h, 24h, 3days, 1week and 2weeks), a double immunofluorescent labeling of neurons (Neun) and astrocytes (GFAP) was performed. After four hours (results not shown), one and three days of adrenalectomy, we did not observe an apparent difference in the GFAP immunoreactivity in the hippocampii of adrenalectomized and sham groups (Figure-35A', A, B', B). However, one week after adrenalectomy, activated astrocytes were seen in the dentate gyrus (Figure-35C') whilst no difference in the GFAP immunoreactivity was observed in sham operated rats (Figure-35C).

An intense GFAP immunoreactivity was observed, two weeks after adrenalectomy, throughout the hippocampus most particularly in the dentate gyrus (Fig.37) where the astrocytes undergo morphological changes and appeared hypertrophic and showed intense GFAP immunoreactivity (Figure-35D'). The GFAP immuno-labeling exhibited extensive astrogliosis in the molecular and polymorphous layers of the dentate gyrus; however less intense astogliosis was seen in the granular layer (Figure-37). The stratum lucidum of CA3 area of adrenalectomized rats showed an increase in GFAP immunoreactivity (Figure-35H').

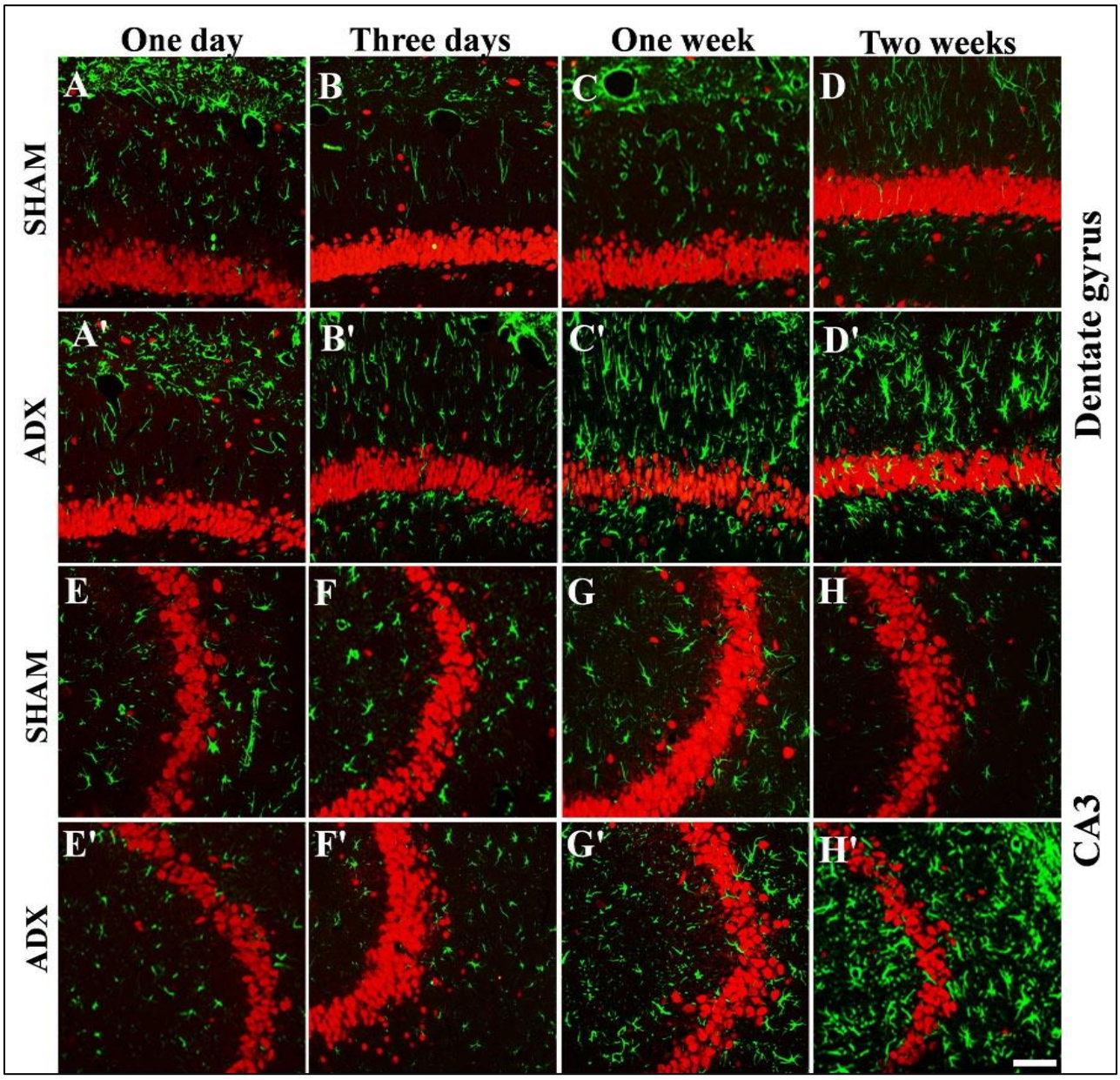

Figure-35: Images of astrogliosis in the hippocampus. Coronal sections of the hippocampus stained with NeuN antibody (red) as a neuronal marker and GFAP antibody (green) as an astrocytes marker showing the progression of microgliosis over the course of time (1day, 3days, 1week and 2weeks) in the dentate gyrus and CA3 of the hippocampus of adrenalectomized rats compared to sham operated rats .Absence of astrogliosis was noticed in the dentate gyrus (A, B, C, D) and CA3 (E, F, G, H) of sham operated rats during the different time points (1day, 3days, 1week and 2weeks). One day after adrenalectomy the rats showed no signs of astrogliosis in the dentate gyrus (A') (B') and CA3 (E') (F') respectively.

A progression of astrogliosis was seen in the dentate gyrus after one week (C') and two weeks (D') whilst no immunoreactivity was seen in CA3 after one week (G').However appearance. On the other hand, there was no significant difference between the number of GFAP-positive astrocytes in the hippocampus of ADX and sham operated rats three days following adrenalectomy. However, a significant increase (P< 0.001) in the number of astrocytes was observed one and two weeks after adrenalectomy in the ADX compared to sham operated rats (Figure-36).

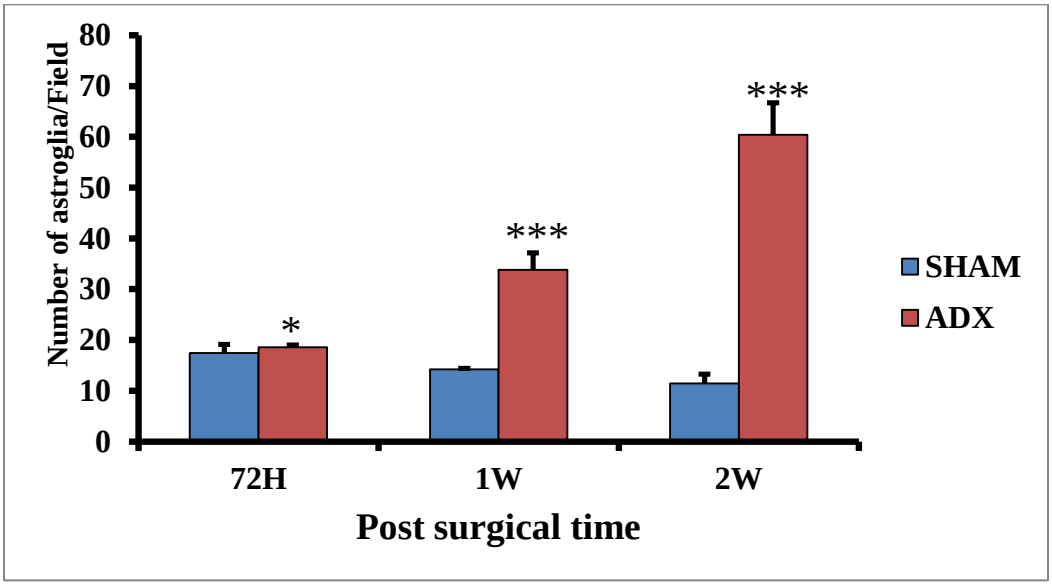

Figure-36: Bar graphs showing the comparison between the number of GFAP positive cells in the hippocampus of adrenalectomized and sham operated rats. No difference in the number of astrocytes revealed after 3 days but significantly increased 1 and 2 weeks following adrenalectomy. ***P<0.001. Data are expressed as mean (±SEM).

Moreover, GFAP immunostaining also showed extensive astrogliosis in the CA4 but not in the CA1 area of the adrenalectomized hippocampus (Figure-37).The dentate gyrus (Figure-35A, B, C, and D), CA3 (Figure-35E, F, G, and H). CA4, CA2 and CA1 (Figure-37) areas in the hippocampi of bilateral sham operated rats did not show astrogliosis.

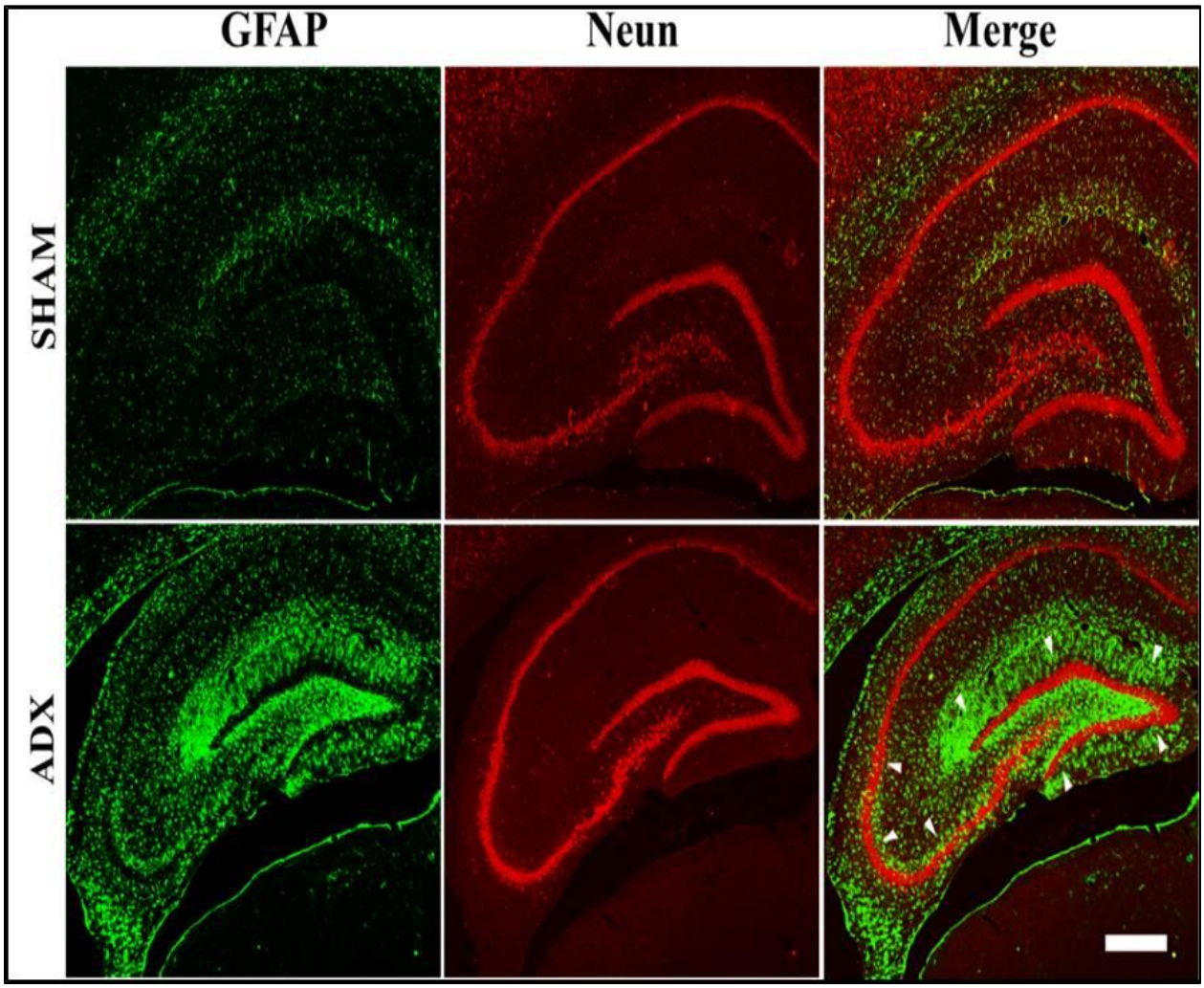

Figure-37: Representative images of coronal sections of the whole hippocampus stained with NeuN (red) and GFAP (green) antibodies showing astrogliosis after two weeks of adrenalectomized rats compared to bilateral sham operated rats. Molecular layer (ML), granule cell layer (GCL), polymorphous layers (PL) and (SL) stratum lucidum. Scale bar=100µm.

It was very interesting idea that came from one of the reviewers of our manuscript that to check at different levels through the rostral-caudal axis of the hippocampus whether the effect of the removal of the adrenal gland is consistent or not. Deciding to do that we choose to perform double immunofluorescence with

NeuN (red) and Iba-1 antibodies for neurons and microglia respectively on brain coronal sections at two levels -4.68mm and -5.5mm relative to bregma according to Paxinos and Watson.2005. Indeed we have found similar to the effect that we have observed at the level -3.7 where activated microglia on both blades of the dentate gyrus and predominantly on the dorsal blade of the ADX rats (Figure-34). Similar to the level -3.7 no sign of microgliosis were seen in the sham operated rats at two levels -4.68mm (Figure-38) and -5.5mm (Figure-39). In addition our results showed the activation of microglia at CA4 which is similar what was found at the -3.7 levels and no signs in the sham rats. Regarding the CA3 area we observed the microglia activation bordering the pyramidal cells of the CA3 at stratum lucidum which is a total similarity to what have been seen at the other levels and no signs in sham operated rats.

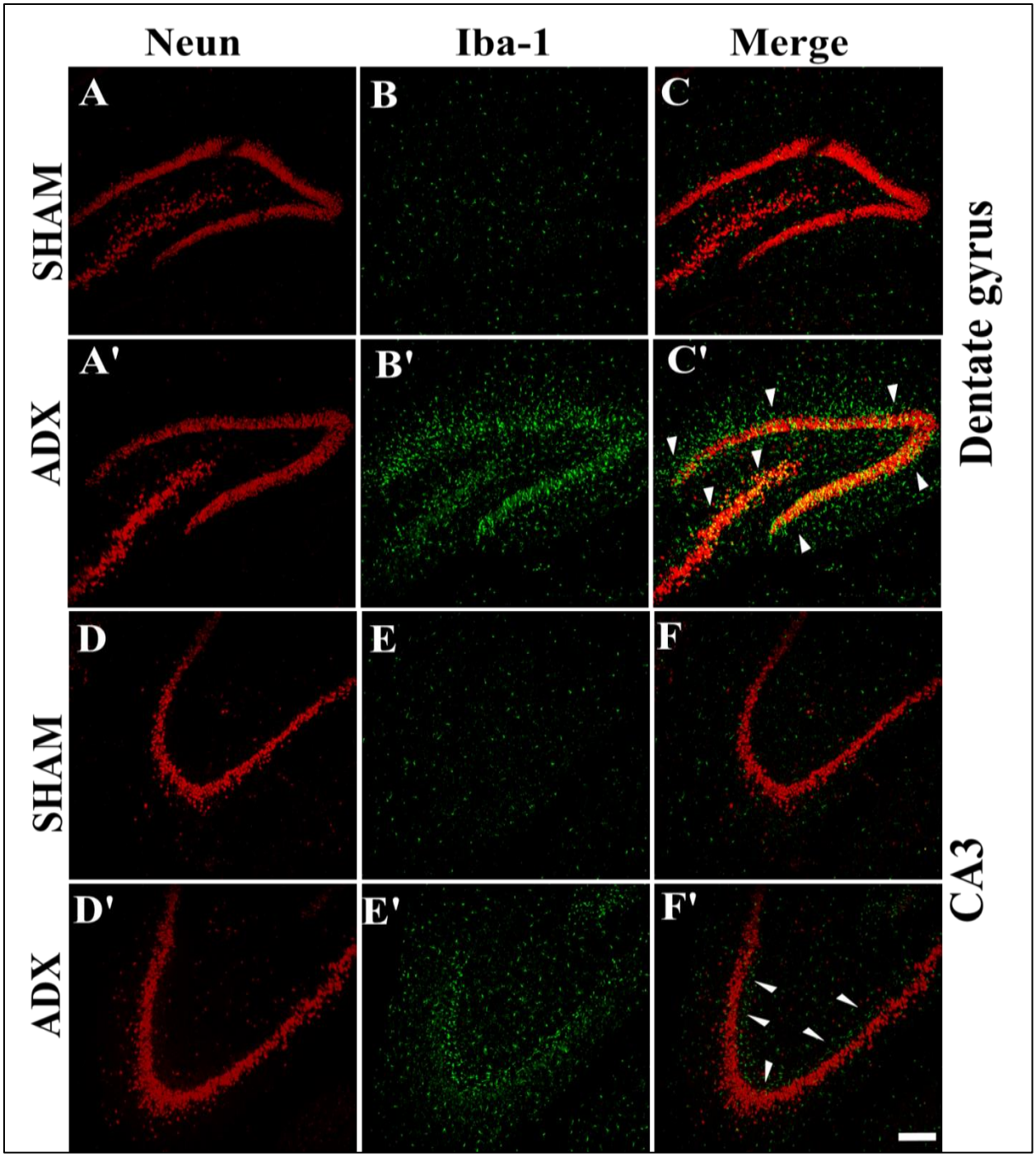

Figure-38: Representative images of coronal sections of the whole hippocampus approximately from -4.68mm relative to bregma stained with NeuN (red) and Iba-1 (green) antibodies showing activation of microglia the throughout the dentate gyrus (A',B', C') and CA3 gyrus (D',E', F') after two weeks of adrenalectomized rats compared to the dentate gyrus (A,B, C) and CA3 area (D,E, F) of bilateral sham operated rats. Scale bar=100µm.

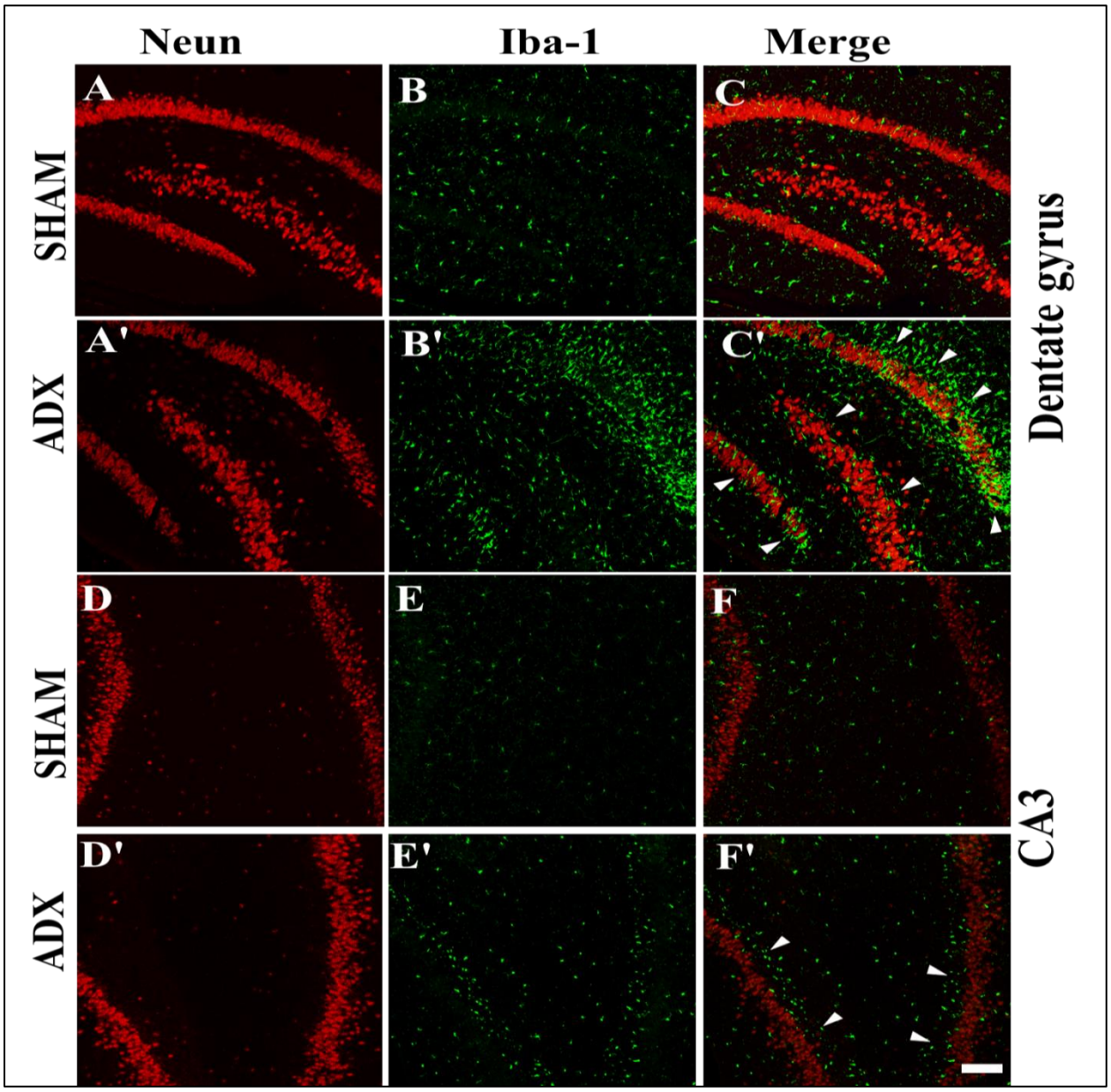

Figure-39: Representative images of coronal sections of the whole hippocampus approximately from -5.5mm relative to bregma stained with NeuN (red) and Iba-1 (green) antibodies showing activation of microglia the throughout the dentate gyrus (A',B', C') and CA3 gyrus (D',E', F') after two weeks of adrenalectomized rats compared to the dentate gyrus (A,B, C) and CA3 gyrus (D,E, F) of bilateral sham operated rats. Scale bar=100µm.

In order to investigate the localization of the activated microglia and astrocytes simultaneously after two weeks of adrenalectomy a triple immunostaining, of neurons (Neun), microglia (Iba-1),and astrocytes (GFAP) was performed and the sections were examined with a confocal microscope. We observed co-localization of the microglia and astrocytes in different layers of the dentate gyrus (Figure-40).

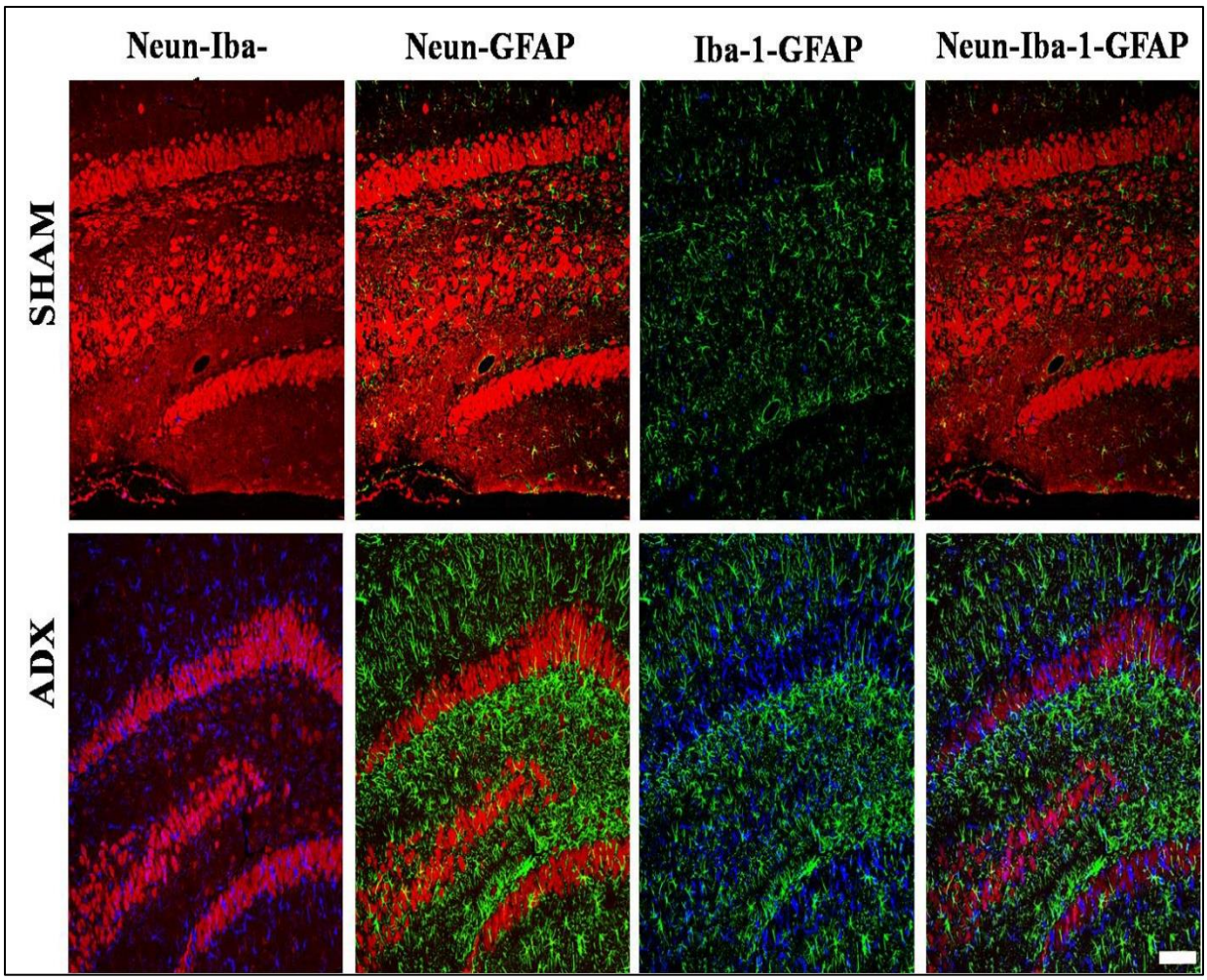

Figure-40: Representative confocal images of triple staining of hippocampal sections stained with Neun (red), Iba1 (blue) and GFAP (green) showing the localization of activated microglia and astroglia after two weeks throughout the dentate gyrus of the hippocampus of adrenalectomized rats compared to sham operated rats. Scale bar=50µm.

5-Oxidative stress

5-1-Reduced glutathione (GSH):

Reduced glutathione (GSH) is the major source of proton for biochemical reaction and detoxification of free radicals in the cell. In order to determine the concentration of GSH by colorimetric assay, a standard curve in the range 1.56-50 nmol/ml was constructed and the levels of GSH in the samples was determined by interpolation see (Figure-41).

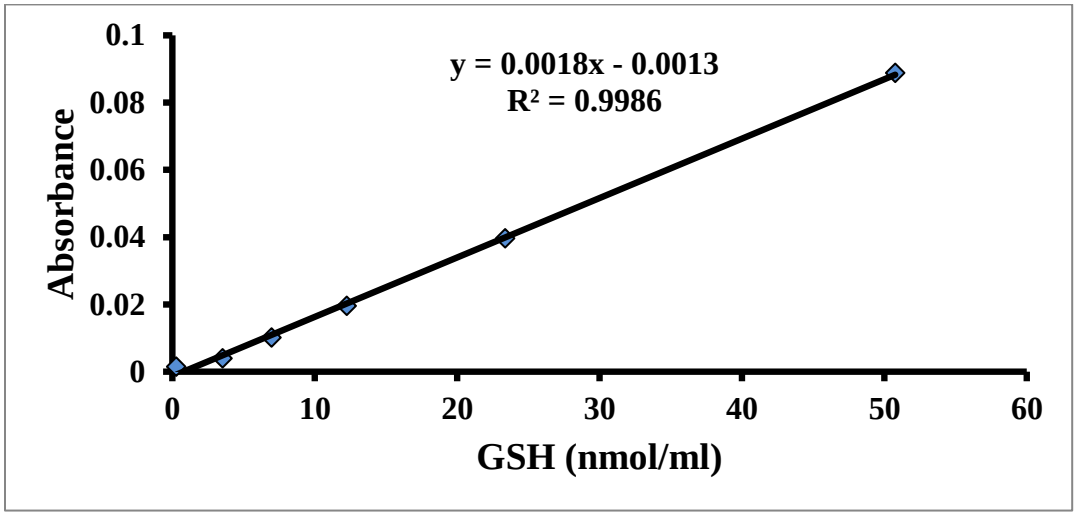

Figure-41: Reduced glutathione Standard Curve. The curve obtained from the absorbance at 450nm of varying concentrations of GSH standards ranging from 3.9-500 pg/ml (R^2: Pearson Coefficient of Determination).

As shown in see (Table-10) and (Figure-42). The evaluation of the levels of this antioxidant component in the hippocampal homogenates over the course of time (4h, 24h, 3days, 1week and 2weeks) in bilateral adrenalectomized rats compared to sham operated indicated no significant increase in the first day following surgery. However, at day three a significant increase ($P<0.05$) in the level of GSH was observed in adrenalectomized rats compared to the sham. At one week postoperatively, no significant difference in the level of GSH was seen between the two groups, however, two weeks later we noticed a significant decrease ($P<0.05$) in GSH levels in adrenalectomized rats.

Table-10: Concentration of GSH levels in the hippocampal homogenates of adrenalectomized rats compared to the sham operated rats over the course of time (4h, 24h, 3days, 1week and 2weeks). Data are expressed as mean ± SEM.

Time / Group	SHAM	ADX	Statistical significance
4H	22.69±2.14	24.58±3.56	P>0.05
24H	14.39±1.47	17.42±1.13	P>0.05
72H	9.66±1.39	15.62±2.18	*P<0.05
1 Week	12.39±1.49	12.75±1.90	P>0.05
2 Weeks	10.66±1.75	6.18±0.85	*P<0.05

Unit of measurement: mol/ml

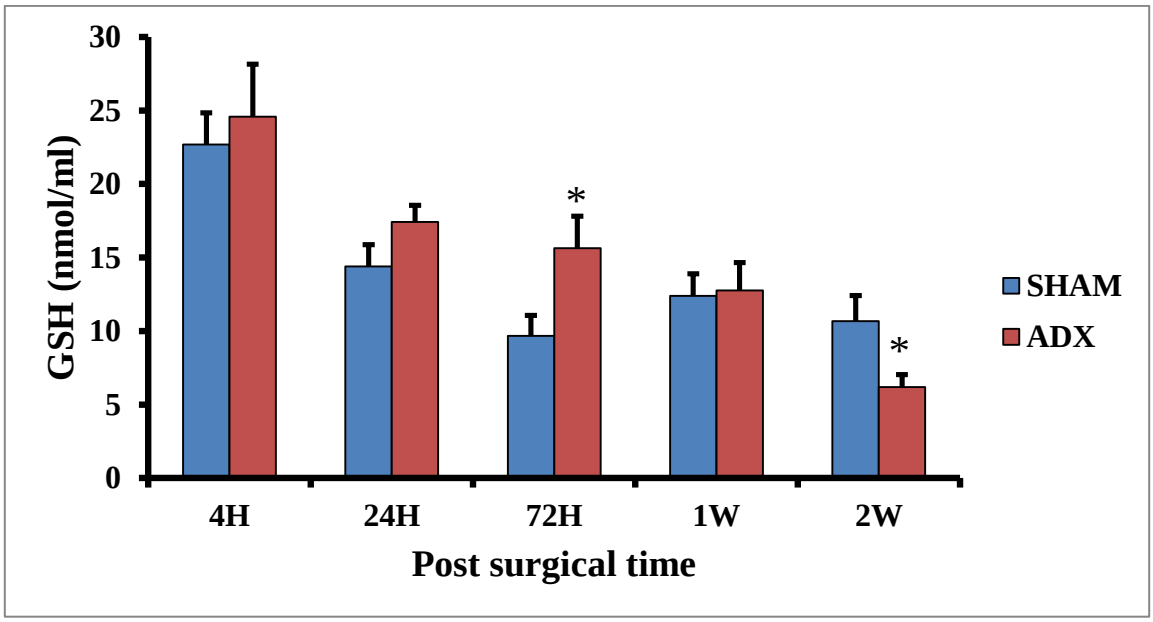

Figure-42: Bar graphs showing GSH levels in the hippocampus of adrenalectomized and Sham operated rats over course of time (4h, 24h, 3days, 1week and 2weeks) in adrenalectomized compared to sham operated rats .*P<0.05. Data are expressed as mean ± SEM.

5-2-Superoxide dismutase (SOD):

The measurement of the antioxidant enzyme, superoxide dismutase (SOD) activity was performed by a colorimetric assay in the hippocampal homogenates of adrenalectomized compared to sham operated rats and in order to determine the SOD concentration, a standard curve of the linearized rate (LR) of the standards that range 0.025-0.25 U/ml was constructed and the levels of SOD in the samples was determined by interpolation see (figure-43).

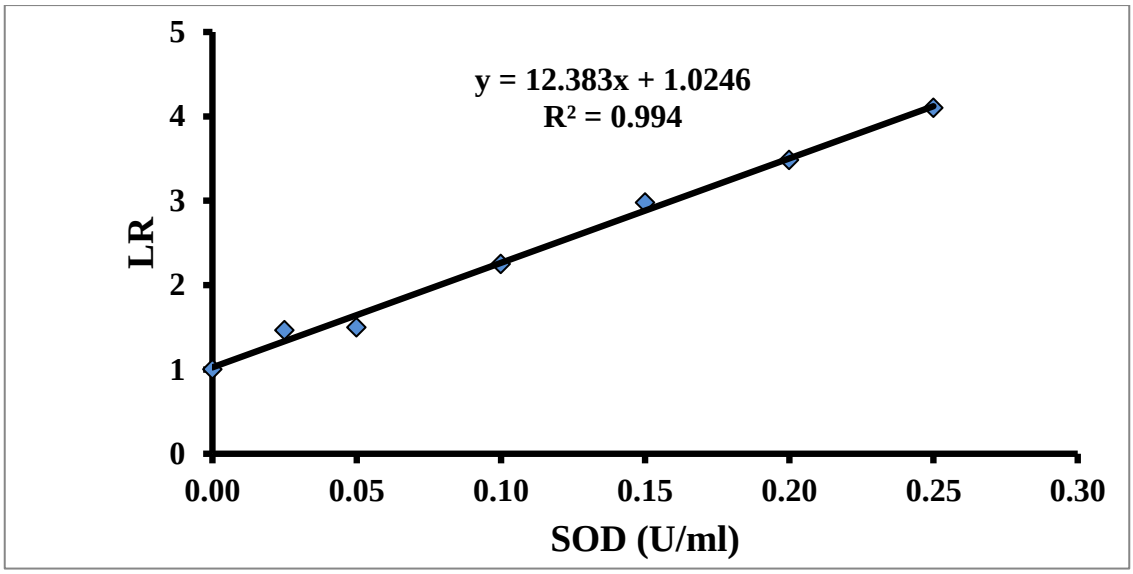

Figure-43: Superoxide dismutase Standard Curve. The curve obtained from the absorbance at 450nm of varying concentrations of SOD standards ranging from 0.025-0.25 U/ml (R^2: Pearson Coefficient of Determination).

Our results indicated no significant changes in SOD activity in the hippocampal homogenates of adrenalectomized compared to sham operated rats after 4h, 24h, 72h and 1week of adrenalectomy. However, two weeks after surgery a significant decrease in the enzyme activity ($P<0.01$) was revealed in the hippocampus of adrenalectomized compared to sham operated rats see (Table-11) and (Figure-44).

Table-11: Concentration of SOD levels in the hippocampal homogenates of adrenalectomized rats compared to the sham operated rats over the course of time (4h, 24h, 3days, 1week and 2weeks). Data are expressed as mean ± SEM.

Time / Group	SHAM	ADX	Statistical significance
4H	324.51±16.97	274.55±7.37	P>0.05
24H	276.61±21.07	299.38±11.82	P>0.05
72H	302.45±20.94	322.09±15.23	P>0.05
1 Week	288.12±20.23	304.46±24.06	P>0.05
2 Weeks	370.99±20.08	260.23±24.40	*P<0.05

Unit of measurement: U/ml

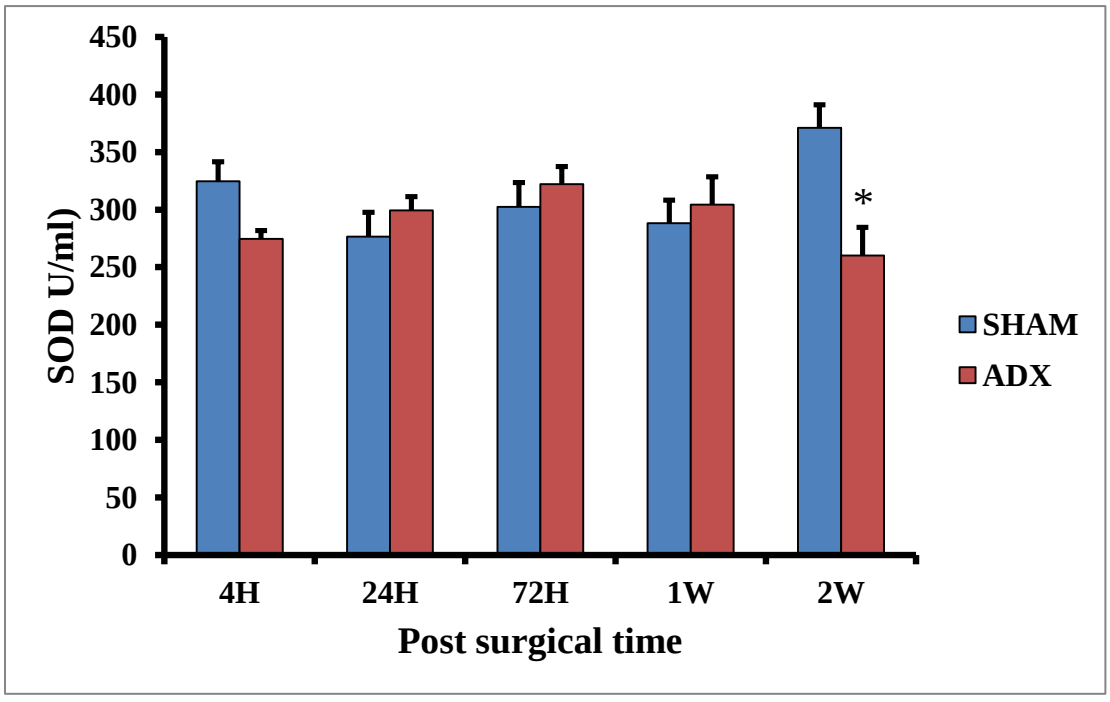

Figure-44: Bar graphs showing SOD activity in hippocampus of adrenalectomized and sham operated rats over the course of time (4h, 24h, 3days, 1week and 2weeks) in adrenalectomized compared to sham operated rats .*P<0.05. Data are expressed as mean ± SEM.

5-3-Malondialdehyde (MDA):

Lipid peroxidation is one of the most important manifestations of the imbalance between the antioxidants and the oxidants which leads to oxidative stress. We examined the occurrence of lipid peroxidation in the hippocampus by the measurement of malondialdehyde (MDA) levels and in order to determine the MDA concentration, a standard curve in the range 0.625-50 U/ml was constructed and the levels of MDA in the samples was determined by interpolation see (Figure-45).

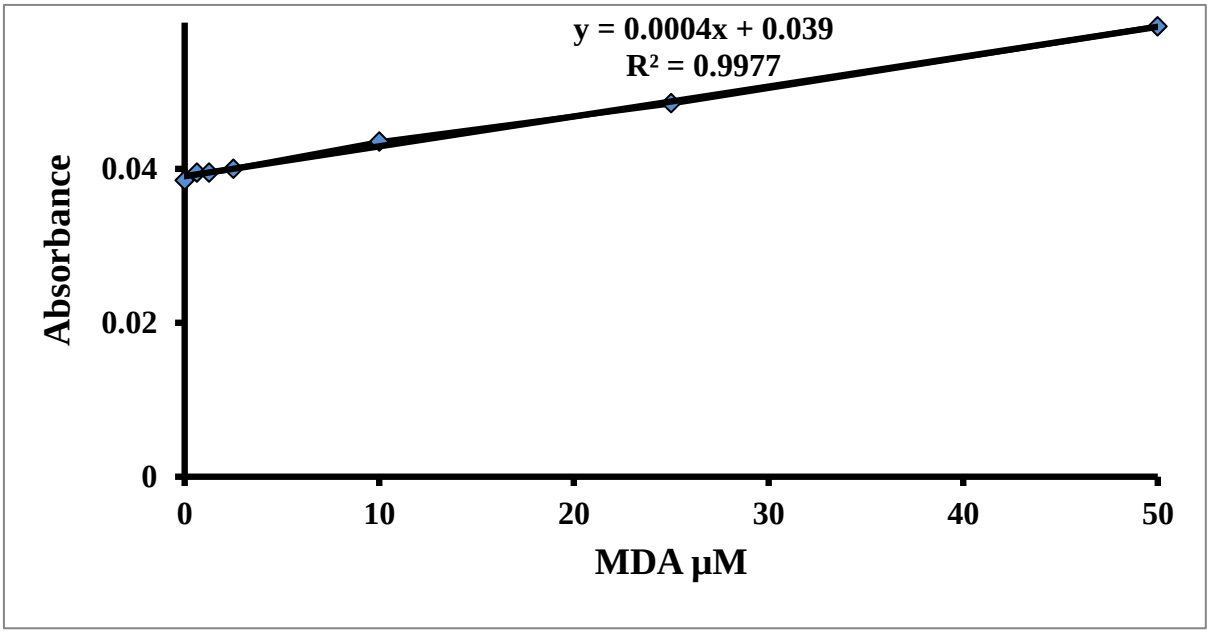

Figure-45: Malondialdehyde Standard Curve. The curve obtained from the absorbance at 450nm of varying concentrations of MDA standards ranging from 0.025-0.25 U/ml (R^2: Pearson Coefficient of Determination).

As shown see (Table-12) and (Figure-46) no statistical differences in the level of MDA until two weeks after surgery when a significant increase ($P<0.05$) in lipid peroxidation by-product MDA was seen in adrenalectomized rats compared to sham operated rats.

Table-12: Concentration of MDA levels in the hippocampal homogenates of adrenalectomized rats compared to the sham operated rats over the course of time (4h, 24h, 3days, 1week and 2weeks). Data are expressed as mean ± SEM.

Time / Group	SHAM	ADX	Statistical significance
4H	18.82±1.24	16.96±0.93	P>0.05
24H	26.02±2.07	25.13±1.74	P>0.05
72H	25.07±2.63	27.23±1.44	P>0.05
1 Week	23.77±1.73	25.93±2.05	P>0.05
2 Weeks	22.71±1.79	28.59±1.79	*P<0.05

Unit of measurement: µM

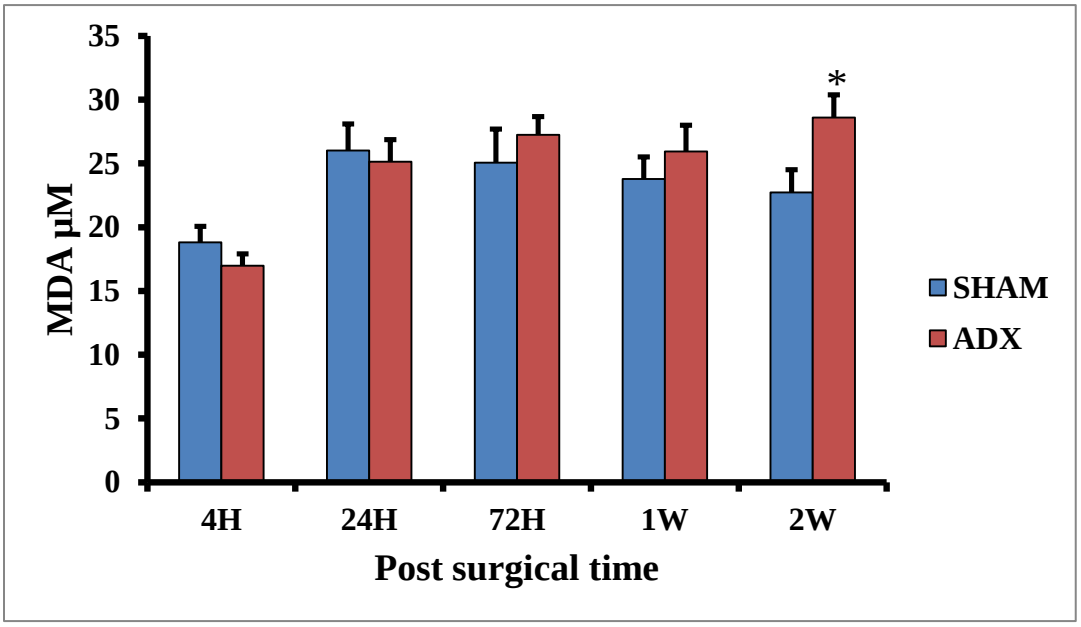

Figure-46: Bar graphs showing MDA levels in the hippocampus of adrenalectomized and Sham operated rats. Levels of MDA were measured by colorimetric assay over course of time (4h, 24h, 3days, 1week and 2weeks) in adrenalectomized rats compared to sham operated rats .*P<0.05. Data are expressed as mean ± SEM.

6- Animal Behavior

Based on what we have found on the histological and biochemical levels we thought such effects will leave its marks on the behavioral level, passive avoidance test was performed. The evaluation of the latency time for the both adrenalectomized and sham operated rats over the course of time (3days, 1week and 2weeks) indicated a significant increase on the third day following surgery ($P<0.05$) (Table-13A) and (Figure-47A).

Table-13A: Latency time of adrenalectomized rats compared to the sham operated rats after three days of adrenalectomy. Data are expressed as mean ± SEM.

	SHAM	ADX
Training day	30.61±6.93	300±00
Retention day	31.14±6.17	141.51±44.99

Unit of measurement: Seconds

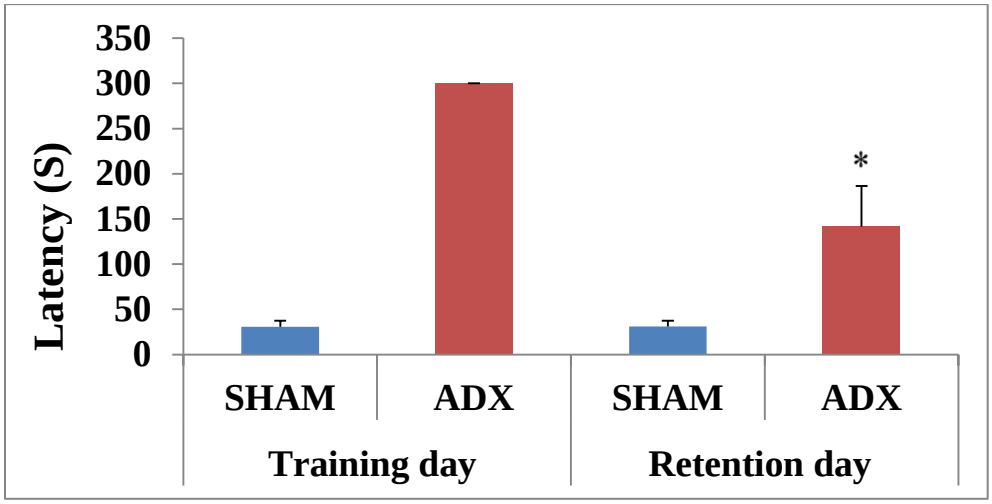

Figure-47A: Bar graphs showing latency time of adrenalectomized and Sham operated rats following three days of bilateral adrenalectomy .*$P<0.05$. Data are expressed as mean ± SEM.

Furthermore, at day seven a significant increase (P<0.05) in the latenecy time was observed in adrenalectomized rats compared to the sham (Table-13B) and (Figure-47B).

Table-13B: Latency time of adrenalectomized rats compared to the sham operated rats after one week of adrenalectomy. Data are expressed as mean ± SEM.

	SHAM	ADX
Training day	23.86±6.79	259.66±40.34
Retention day	25.76±6.25	146.11±52.85

Unit of measurement: Seconds

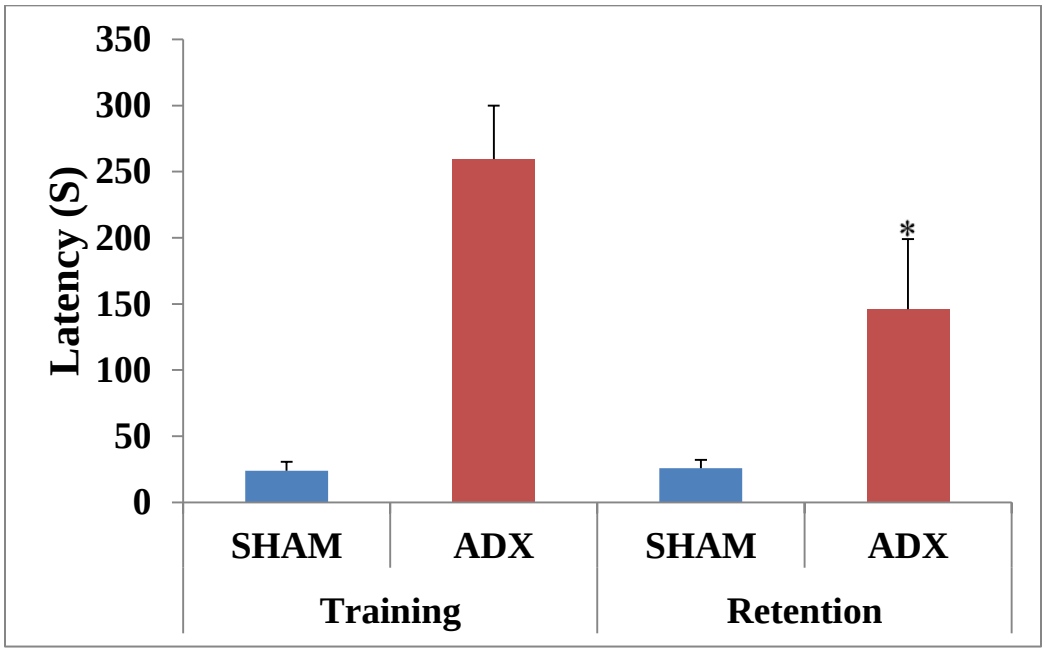

Figure-47B: Bar graphs showing latency time of adrenalectomized and Sham operated rats following one week of bilateral adrenalectomy .*P<0.05. Data are expressed as mean ± SEM.

At two weeks postoperatively, the significant increase persisted between the two groups (P<0.05) (Table-13C) and (Figure-47C).

Table-13C: Latency time of adrenalectomized rats compared to the sham operated rats after two weeks of adrenalectomy. Data are expressed as mean ± SEM.

	SHAM	ADX
Training day	14.38±3.66	281±19
Retention day	15.8±2.34	174.36±30.85

Unit of measurement: Seconds

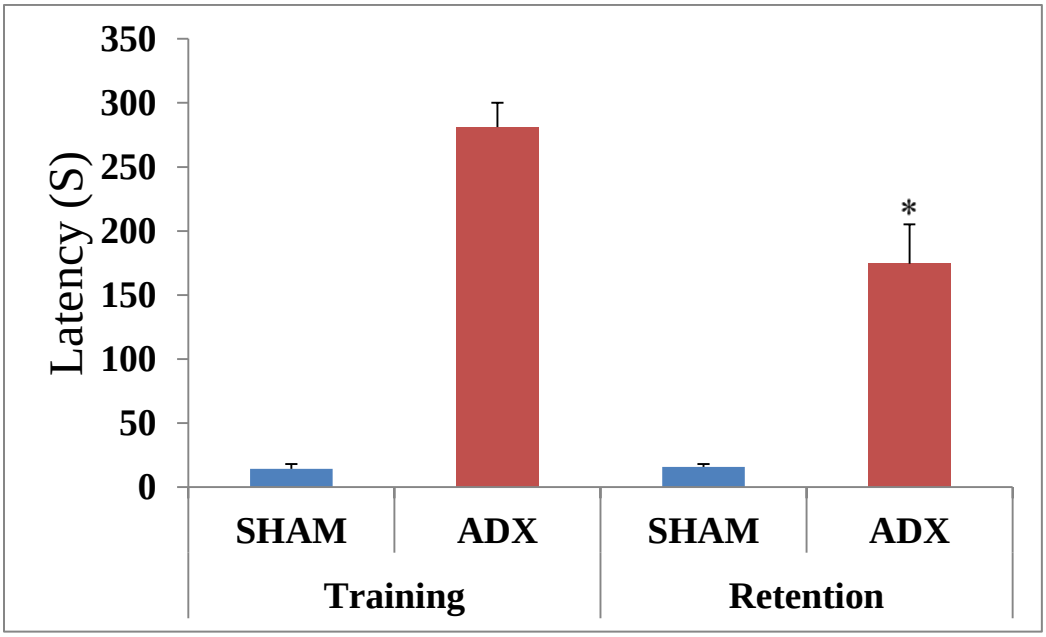

Figure-47C: Bar graphs showing latency time of adrenalectomized and Sham operated rats following two weeks of bilateral adrenalectomy.*P<0.05. Data are expressed as mean ± SEM.

DISCUSSION

The aim of this study was to investigate the effects of short-term bilateral adrenalectomy on the levels of pro-inflammatory cytokines IL-1β, IL-6 and TNF-α, the response of microglia and astrocytes to neuronal cell death as well as on oxidative stress markers GSH, SOD and MDA over the course of time (4h, 24h, 3days, 1week and 2weeks) in the hippocampus of Wistar rats.

Our results showed a significant decrease in the levels of corticosterone 4h following the adrenal gland removal and this decrease persisted over the course of the designated time of the experiment 24h, 3days, 1week and 2weeks in the adrenalectomized rats compared to the sham operated. A significant decrease in corticosterone following long-term adrenalectomy was also reported(Gould et al., 1990; Jaarsma et al., 1992; Sloviter et al., 1989, 1993a, 1993b; Spanswick et al., 2011).Regarding the pro-inflammatory cytokines IL-1β, IL-6 levels, our results showed transient elevation that lasts for three days in the hippocampus of adrenalectomized compared to sham operated rats. One week after adrenalectomy, the elevation of these cytokines dropped to sham levels. Both the sham operated and adrenalectomized rats showed significant elevated IL-1β and IL-6 levels compared to the naïve rats. The significant difference between the naïve and sham operated animals might be attributed to the surgical stress. However, the significant difference between the sham and adrenalectomized rats can only be attributed to the effect of adrenalectomy.

The occurrence of neuronal cell death in the hippocampus following adrenalectomy was confirmed by Fluoro-Jade B staining and electron microscopy. Our results showed that the induction of cell death in the granule cell layer of the dentate gyrus by adrenalectomy begun three days postoperatively where we have seen few FJB positive cells in the dorsal blade. the ultrastrucstural examination of the dorsal blade showed cell abnormalities appeared in condensed chromatin and

irregular cell membrane, such observation goes hand in hand with the finding of (Sloviter et al., 1989, 1993a, 1993b) where they showed granule cells degeneration after four days following adrenalectomy. In addition, we have made the same observation as Conrad et al. (Conrad and Roy, 1993; Sloviter et al., 1993a, 1993b) on the third day of adrenalectomy where no signs of degeneration were seen other than dentate gyrus that gives the impression that the current model of neurodegeneration seems to be a selective model for the exclusive loss of granule cells . The ultrastructural results showed degeneration of the pyramidal cells of the CA4 and CA3 after one week. After two weeks of adrenalectomy we observed a progression of cell death throughout the dorsal blade of the dentate gyrus. These findings are in line with those of Spanswick et al. (Spanswick et al., 2011) who reported, degenerated neurons throughout the granular layer of the dentate gyrus two weeks after adrenalectomy using Fluoro-Jade B staining.

In addition we observed a progression in pyramidal cells degeneration of CA3 and CA4 where more damages and affected cells were seen which goes in agreement with the observation of sapolsky et al. (Sapolsky et al., 1991) where they have observed degeneration up to 19% of pyramidal cells of the CA4 area. Subsequently, Prof. Adem and his team Islam et al.1999 demonstrated clearly different populations of neurons have been affected following long term adrenalectomy (5 months). Our findings are not in line with the observations that have been made by different groups where they found both short and long term adrenalectomy caused a selective cell death of the granule cells of the dentate gyrus (Conrad and Roy, 1993; Sloviter et al., 1993a, 1993b). We think the reason of that might returned to the sensitivity of different strains of animals or may be the sensitivity of the techniques used in different Labs. In addition, the close examination of the dentate gyrus indicates that adrenalectomy affects differentially

the dorsal and ventral blades of the dentate gyrus and suggest that the granule cells of the dorsal blade of the dentate gyrus are more vulnerable to adrenalectomy. The question that raises itself why this granule neurons are the most vulnerable to the absence of glucocorticoid hormones? There is strong evidence that those hormones are playing trophic role for this population of neurons, many studies from different groups confirmed the trophic crisis occurred in the absence of glucocorticoids.

In situ hybridization revealed DEX injection increase the NGF mRNA levels in the granule layer of the dentate gyrus however two weeks of adrenalectomy showed a significant reduction in the NGF expression (Mocchetti et al,1996). Chao et al,1994 showed BDNF and NT-3 mRNA decrease in pyramidal and granule cells of the dentate gyrus following seven days of adrenalectomy. Isalm et al. showed a significant reduction of IGF-1 receptors mRNA in the dentate, CA1, CA3 and CA4 areas.

To conclude regarding the cell death in the current model our results showed the vulnerability of different neuronal population to glucocorticoids absence on one hand and the non-selectivity of the current model of neurodegeneration. In addition, these findings might open the possibility to investigate the occurrence of neurodegeneration in other parts of the brain.

It is an issue of debate regarding the accurate time of cell death onset in the hippocampus and that returned to the idea of linking the raise in the inflammatory cytokines levels and neurodegeneration and to reach the conclusion if such increase precedes the cell death or it comes as a consequence to it. For that reason our findings are in line with the observations that have been made by several investigators that the earliest cell death occurs at least after three days of adrenalectomy (Gould et al., 1990; Nichols et al., 2005; Sloviter et al., 1989;

Spanswick et al., 2011; Stienstra et al., 1998). However, few investigators reported cell death on day two after adrenalectomy (Jaarsma et al., 1992; Nichols et al., 2005; Sloviter et al., 1993a).

It is interesting to note that the early elevation of the pro-inflammatory cytokines IL-1β, IL-6 and TNF-α was seen prior to neuronal death. Taken together our findings suggest that cell death was preceded by an increase of these pro-inflammatory cytokines. Similar findings have been reported in animal models of ischemia (Rothwell, 2003; Zhu et al., 2006), surgical injury (Tchelingerian et al., 1993), TMT (Trimethyltin) (Liu et al., 2005) KA (Kainic acid) (Minami et al., 1991) and cis-2,4-methanoglutamate (MGlu) (Pearson et al., 1999)where an early increase of different pro-inflammatory cytokines preceded neuronal damage.

Two studies reported the direct involvement of IL-1β in neurodegeneration. (Rothwell, 2003) reported the injection of low doses of IL-1β into the cerebral ventricles or brain parenchyma of mice or rats exposed to neurotoxins markedly exacerbates the damage. The second study showed the antagonism of IL-1β by co-infusion of IL-1β receptor antagonist with the neurotoxin N-Methyl-D-aspartate (NMDA) inhibits brain damage induced by such excitotoxin (Lawrence et al., 1998; Panegyres and Hughes, 1998). Moreover, IL-1β plays a crucial role in the exacerbation of acute neurodegeneration caused by ischemia, head trauma and stroke. In addition, it is implicated in the pathology of multiple sclerosis, Alzheimer's disease and other CNS chronic diseases (Allan and Rothwell, 2001; Boutin et al., 2001; Griffin and Mrak, 2002; Pearson et al., 1999).

IL-6 levels were found to be elevated in the serum and CSF of MS patients, locally around MS lesions (Malmeström et al., 2006; Stelmasiak et al., 2001) and in experimental auto-immune encephalitis (EAE) animal models (Gijbels et al.,

1990). IL-6 expression was significantly increased in the acute phase of cerebral ischemia (Berti et al., 2002). In AD patients, IL-6 is further increased locally around amyloid plaques and in the CSF (Blum-Degen et al., 1995; Lucin and Wyss-Coray, 2009). In agreement with the early increase of TNF-α that was observed in the current neurodegenerative model, several studies showed the same pattern of expression when elevation in the levels TNF-α mRNA were seen at early stage following different neuronal insults (Berti et al., 2002; Chiu et al., 2015; Liu et al., 2015; Zhu et al., 2006).

In summary, putting together the previous three finding regarding corticosterone, cytokines levels and neuronal cell death after short term adrenalectomy. Our results and others might suggest that the depletion in the levels of corticosterone after removal of the adrenal gland did not induce an immediate neuronal cells death However it was accompanied by an instant increase in the pro-inflammatory cytokines IL-1β, IL-6 and TNF-α. The transient elevation in these inflammatory components was followed directly by degeneration of the granule cells of the dentate gyrus of the adrenalectomized rats compared to the sham operated.

We think that the induction of the cell death was the result of both the increase of such cytokines which has been largely proved for their contribution in the exacerbation of the neuronal damage from one side and the depletion of the corticosterone which has been shown to play major role in the survival of the hippocampal neurons and the depletion in its levels like what is happening in the current model affects the production of essential factors for the survival of the hippocampal neurons on other side. several groups showed that the removal of the adrenal gland caused a depletion in the production of several neurotrophins such production of neurotrophin-3 (NT-3), Brain Derived Growth factor (BDNF), Nerve

Growth Factor (NGF) (Barbany and Persson, 1992; Nichols et al., 2005; Smith et al., 1995; Vollmayr et al., 2001).

In addition Prof. Adem and his colleagues demonstrated that the levels of IGF-1 were decreased after long term adrenalectomy. Taken together the aforementioned findings might lead us to suggest that after adrenalectomy IL-1β, IL-6 and TNF-α might contribute to the initiation of the biological cascade responsible for subsequent hippocampal neuronal cell death.

Synergistic effects of microglia and astrocytes are needed for tissue reconstitution after lesions, involving control of the BBB and invasion of haematogenous cells, removal of pro-inflammatory cytokines and their down regulation by TGF (Kreutzberg, 1996). Microglias are the main resident immune cells in the brain which presents 12% of the brain cells, playing a crucial role both in physiological and pathophysiological conditions (Polazzi and Monti,2010). Virtually ,every neurological disorder ,AD,PD,MS results in activation of these cells accompanied by biochemical and physiological changes leading to alteration in cell phenotype ,a phenomena generally termed "reactive gliosis" (Wenk, 2003). Moreover, acute neurodegenerative insults such as MPTP, TMT, Kainic acid, ischemia-reperfusion, colchicines induce the activation of these brain resident immune cells to compromise the neuronal survival and indirectly trigger neuroinflammation (Lalancette-He´et al.,2007; Lambertsen et al.,2009).

The activation of microglia is one of the major signs of neurodegeneration (Lucin and Wyss-Coray, 2009). Similar to Gould et al.(Gould et al., 1990) our results showed cell death starts in the dorsal blade of the dentate gyrus three days after adrenalectomy. Activated microglia were observed in the molecular and granular layers of the dorsal blade of the dentate gyrus three days after

adrenalectomy. One week after adrenalectomy as the cell death progresses in the dorsal blade the number of activated microglia are increased. Two weeks after adrenalectomy we showed that the whole dentate gyrus was invaded by activated microglia. In line with these findings quantitative analysis showed a progressive increase in the number of microglia in the hippocampus from day three with a further increase one and two weeks after adrenalectomy. Moreover, in addition to the invasion of activated microglia to the granule layer. we noted, the area bordered by granule layer and the hippocampal fissure, so-called molecular layer was occupied by these cells suggesting degeneration of the apical dendrites of the granule cells and this goes hand-in-hand with observation that (Jaarsma et al.,1992) made, using silver impregnation, a specific staining of neuron degeneration where they noticed argypholia at this layer.

Moreover, in a previous study Prof adem and his team in (Mulugeta et al., 2006) reported after two weeks of adrenalectomy the decrease in the concentration of the acetylcholine receptor M4, a receptor found on the presynaptic membrane of the perforant pathways in molecular layer of the dentate gyrus, where they synapse the apical dendrites of the granule cells. It is very important to mention the disintegration of synapses at this layer might lead to retrograde degeneration of the entorhinal cortex neurons and eventually microgliosis starting from the dentate gyrus back to the entorhinal cortex. To investigate this hypothesis and it is correlation with microgliosis, extension of the experiment survival timing one of our future plans.

Regarding the cornu amonis, we found invasion of activated microglia to the pyramidal layer of the CA4 which suggest vulnerability of this population of neurons at early stage of adrenalectomy. Nevertheless, no sign of microgliosis was seen in the pyramidal cells of CA3/CA2/CA1. However we noticed activated

microglia along the stratum lacunosum of the CA3, this layer where the mossy fibers get connected to the apical dendrites of big pyramidal cells of CA3 suggesting two weeks of glucocorticoids deprivation results in synapses disintegration which needs by standard the appearance of activated microglia for repairing and cleaning the debris of the degenerated axons.

Our current study showed a strong correlation between cell death and microglia activation over the course of time. Taken together our observations suggest a correlation between microgliosis and cell death.

Astrocytes are known to communicate with microglia, and such interaction is very important in pathological conditions (Verderio and Matteoli .,2001; Von Bernhardi and Ramirez.,2001). It is well known that brain injury is associated with increased astrocyte reactivity (Fiedorowicz et al., 2001). Reactive astrocytes synthesize a variety of cytokines, neurotrophins and components of the extracellular matrix, many of which are known to rescue damaged neurons after brain insults (Schwartz et al.,1993) and their scavenging effect for reactive oxygen species (Chen and Swanson,2003).

It is well known that brain injury is associated with increased astrocytes reactivity (Fiedorowicz et al., 2001). Astrocytes react profoundly to brain damage or disease by increasing both their number and size, a process referred to as reactive astrogliosis/astrocytosis which represents a remarkably homotypic response to CNS injuries (Penkowa et al., 2008). In this study, activation of astrocytes was observed throughout the dentate gyrus one week after adrenalectomy.

However, Krugers et al.(Krugers et al., 1994) found activation of astrocytes earlier, on the third day after adrenalectomy. Although we could not see activated

astrocytes at day three, it is possible that the activation of astrocytes takes place between day 3 and 7 after adrenalectomy. The observed astrogliosis in our study was predominantly in the molecular and polymorphous layers of the dentate gyrus whilst no apparent astrogliosis was seen in other areas of the hippocampus. Our findings are in line with those findings which showed astrocytes invasion of the dentate gyrus after TMT injection. TMT is a selective neurotoxin of granule cells (Fiedorowicz et al., 2001).

In addition to the activation of astrocytes after one week in the DG our results showed progressive activation of astrocytes in the CA4 and CA3 of the hippocampus two weeks after adrenalectomy. In line with these findings quantitative analysis showed a significant increase in the number of astrocytes in the hippocampus from one week until two weeks after adrenalectomy.

Astrocytes are known to communicate with microglia, and such interaction is very important in pathological conditions (von Bernhardi and Ramirez, 2001; Verderio and Matteoli, 2001). The progressive degeneration of granule cells correlated well with the activation of microglia and astroglia in the dentate gyrus over the course of two weeks. It is very important to note almost in all neurodegenerative models, microglia are the first cells to respond to neuronal damage and followed by activation of astrocytes , which leads us to suggest the important of cross talk between the two cell populations during neuronal damage and consider microglia as driving force in astroglia recruitment.These observations it goes hand in hand what we found in the current study where we noted microglia activation on the third day in first place and followed later by astrocytes activation on the seventh days.

Our results showed microglia activation on the third day followed by astrocytes activation on the seventh day after adrenalectomy. These findings are in

line with what has been found in different neurodegenerative models where microglia were found to be the first cells to respond to neuronal damage followed by activation of astrocytes (Frautschy et al., 1998; Gahtan and Overmier, 1999; Matsumoto et al., 1992; Reali et al., 2005). Taken together these findings suggest a cross talk between the two cell populations during neuronal damage and consider microglia as driving force in astroglia recruitment.

Oxidative stress occurs when there is an overproduction, or accumulation of reactive oxygen species (ROS) in conjunction with reduced antioxidant capacity within the cell (Sies, 1997). As a response to neuronal death, the quiescent microglia became functionally active and upregulate enzymes such as inducible nitric oxide synthase (iNOS) leading to an imbalance between free radicals production and the antioxidant defenses (Tran et al., 1997).

Our findings showed that a state of oxidative stress manifested in the decrease of reduced glutathione (GSH) two weeks after adrenalectomy. In addition, our study showed a significant decrease in the activity of the superoxide dismutase. In contrast to the decrease of the antioxidant defenses, malondialdehyde (MDA) the indicator of the plasma membrane disruption was significantly increased.

This imbalance, observed two weeks after adrenalectomy, reflects a state of oxidative stress which possibly resulted from the activated glial cells. It has been found after one week of adrenalectomy an overexpression of iNOS in activated microglia revealing these cells as source of the free radical in this model (Sugama et al., 2013). Taken together our findings are consistent with the literature showing that several neurodegenerative paradigms revealed the association between neuroinflammation accompanied by reactive gliosis and a state of oxidative stress (Zhu et al., 2004).

The hippocampus is well known for its role in cognition (Strange et al.2004; Zeidman and Maguire.2016), most importantly in learning and memory (Morgado-Bernal, 2011). As it was aforementioned due to the high concentration of glucocorticoids receptors in the hippocampus, it is considered the most targeted area of the brain by such hormones. Our study has shown the withdrawal of these hormones causes degeneration of different neuronal cell populations in the hippocampus. Several studies and most of them have investigated the impact of the neuronal damage caused by long term absence of such hormones on the behavior of the animals where Islam et al.1995 showed after 19 weeks of adrenalectomy a significant increase in the latency in the Morris maze task and significant lower rearing scores in the adrenalectomized rats compared to sham operated. In coherence with that Conrad and Roy.1995 showed that after long term adrenalectomy, the adrenalectomized rats exhibited difficulties in acquiring a new spatial memory. Furthermore Spanswick et al. 2007 showed the inability to reverse such deficit in the spatial memory by chronic treatment (6 weeks) with corticosterone or anther neurogenic compound called Fluoxetine of long term adrenalectomized rats, indicating the crucial role of hippocampal formation in building memories and acquiring new information. So far, we did not find in the literature the effect of adrenalectomy on cognitive functions following short-term adrenalectomy and in order to examine that we performed the passive avoidance test which is a legitimate test to verify the ability of the animals to learn and save new task that they have been taught recently. Our results showed the adrenalectomized rats failed to retain their cognitive capacity compared to the sham operated where we have seen from day 3 to day 7 and 14 a significant increase in the latency for the adrenalectomized rats revealing a cognitive decline similar to what had been seen after chronic adrenalectomy and suggested that such behavior impairement might start in day 3 following glucocorticoids

withdrawal and by that our results go hand in hand with the work of different research groups (Islam et al.1995; Conrad and Roy.1995; Spanswick et al. 2007).

The mechanisms underlying cell degeneration after bilateral adrenalectomy are not clear. We have previously suggested the possibility that adrenocortical hormones might have direct effects on the survival of hippocampal neurons. Hippocampal neurons might die when the mineralocorticoids (Type I) and /or glucocorticoid (Type II) receptors are not occupied by adrenocortical hormones (Adem et al., 1994; Islam et al., 1999). Subsequently, Hu et al. (Hu et al. 1997) reported that granule cell death after adrenalectomy was necessarily accompanied by the disappearance of glucocorticoid receptor immunoreactivity in the granule cell layer.

We have previously also suggested that the loss of adrenocortical hormones after adrenalectomy may cease to stimulate a factor(s), in the hippocampus or other tissues, that is (are) necessary for the survival of hippocampal neurons (Adem et al., 1994; Islam et al., 1999). It could be speculated that in several neurodegenerative diseases like Alzheimer's disease, chronic adrenal hormones and/or their receptors' decrease may result in inflammatory mechanisms which lead to hippocampal neurodegeneration (Heuser and Lammers, 2003; Landfield, 1978; McEwen, 1997; Woulfe et al., 2002).

CONCLUSION AND PERSPECTIVES

The removal of the adrenal gland leads to almost the depletion of glucocorticoids from the animals body, such change was assumed by many researchers around the world to cause an exclusive death of the granule cells in the hippocampus. However, in the current study we reached along with few aforementioned studies that there is another population of neurons different than the granule cells was affected by the absence of glucocorticoids called the pyramidal cells. This finding suggested that the cell death in the hippocampus is not selective to the granule cells as it was suggested before and opens the door for further investigation on the impact of such hormones on different cells in the brain.

The common believe that the inflammation is a phenomenon occurs as a result or response to cell death to get rid of the debris resulted from the cell degeneration which lead us to say that the cell death always precedes the inflammation. However, in the current study our results made us conclude that the inflammation does not play the usual beneficial effect in the current neurodegenerative model, on the contrary it might contribute or initiate the cell damage and this conclusion manifests in the early increase of different inflammatory cytokines before the neuronal death followed by the activation of another components of inflammation such as astrocytes and microglia cells.

In addition, our study revealed a strong correlation between the appearance of the inflammatory cells and the deterioration of the antioxidant defense from one side and the increase of the MDA, this later is a strong indicator of the oxidation and disruption of the cell membrane of neurons in the hippocampus which supports the idea that the inflammation has contributed to neuronal cell death. Furthermore, the neuronal cell death that was observed in the hippocampus has a direct impact on the cognitive capacity of the animal that manifested in memory shortage ollowing the removal of the adrenal gland (Figure-48).

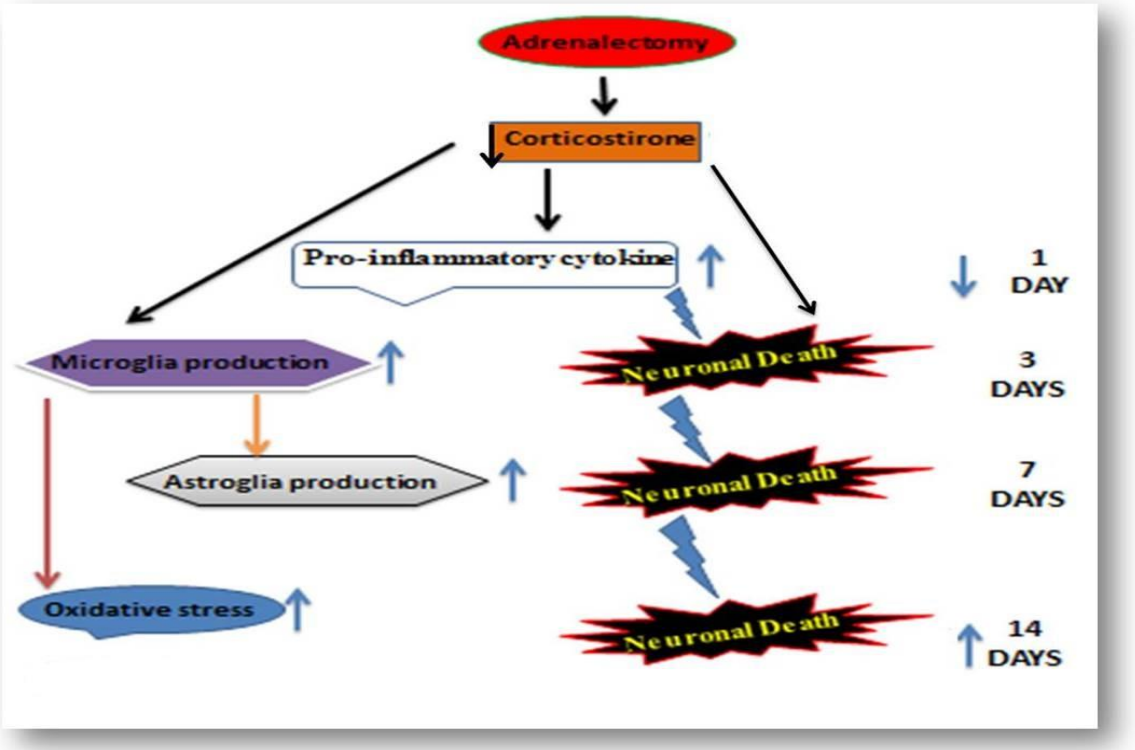

Figure-48: summary of our findings

In summary, our study showed that short-term bilateral adrenalectomy leads to an early increase in pro-inflammatory cytokines followed by neurodegeneration and activation of glial cells as well as oxidative stress and behavioral change. Taking all these findings together it could be suggested that the early inflammatory components might contribute to the initiation of the biological cascade responsible for subsequent hippocampal neuronal cell death and cognitive decline in the current neurodegenerative animal model.

Based on the results of the current work and the other eleven papers published by Prof. Adem et al. we are aiming in the future to go deep in our investigation conering the sources of the cytokines that appeared at the early satge following adrenalectomy. In addition to that we aime to investigate the impact of the removal of the adrenal gland on the production of a large group of growth

factors, since they are considered an essential components of cell survival. In order, to put our work in a medical sphere we planned to investigate the production of the APP (Amyloid precursor) in the hippocampus in attempt to relate it to the cell death occurring in the current model on one side and to Alzheimer,s diseases from another side .

ملخص باللغة العربية

مقدمة:

الهرمونات القشرية السكرية (Glucocorticoids) هي هرمونات ستيرويدية تصنع على مستوى الغدة الكظرية (adrenal gland) وتفرز في الدم تتبعا للساعة البيولوجية وكما تفرز أثناء حالات التوتر (Dickmeis, 2009).النسخة البشرية والقوارضية لهذه الهرمونات هي الكورتيزول والكورتيكوستيرون على الترتيب. لقد اثبت علميا منذ بداية النصف الثاني من القرن الماضي تواجد أعلى مستوى لمستقبلات هذه الهرمونات في الحصين (hippocampus).بالاضافة إلى العديد من المناطق الدماغية الأخرى مثل اللوزة (amygdala)، القشرة المخية الجديدة (neocortex)، تحت المهاد (hypothalamus) (Reul et al., 2015)، يعتبر الحصين المستهدف الرئيسي لهذه الهرمونات على مستوى الدماغ (McEwen et al., 1968) .

أظهرت الدراسات المناعية النسيجية (Immunohistochemistry) للدماغ وجود نوعين من المستقبلات للجلوكوكورتيكويد، مستقبلات المينيرالوكورتيكويد (mineralocorticoid) أو نوع 1 و غلوكوكورتيكويد أو نوع 2 (Reul and de Kloet, 1985). تختلف وفرة هذه المستقبلات في الحصين من نوع خلوي إلى آخر حيث تكون الخلايا الحبيبية (granule cells) غنية بالنوع 1 أما الخلايا العصبية الهرمية (pyramidal neurons) فهي غنية بالمستقبلات من النوع 2. إلى جانب تأثيرها الكبحي كوسطاء للالتهابات (MacLennan et al., 1998)، تلعب هذه الهرمونات دورا رئيسيا في المخ في إنتاج نيوروتروفين (neurotrophin-3)، مشتق عامل النمو المخي (Brain Derived Growth factor) وعامل نمو الأعصاب (Nerve Growth Factor) (Barbany and Persson, 1992; Nichols et al., 2005; Smith et al., 1995; Vollmayr et al., 2001).

أظهرت العديد من الدراسات التأثير المزدوج لهذه الهرمونات على مستوى الحصين، حيث أظهرت أن الحقن المزمن لجرعة عالية من الجلايكورتيكود تؤدي إلى تلاشي الخلايا العصبية الهرمية (Sapolsky and Pulsinelli, 1985). غير انه أظهرت العديد من الدراسات أن استئصال الغدة الكظرية (adrenalectomy) يسبب تلاشي هائل وانتقائي للخلايا الحبيبية للتلفيف المسنن (dentate gyrus) (Gould et al., 1990; (Sloviter et al., 1989, 1993a, 1993b) Nichols et al., 2005; Sloviter et al., 1989; Spanswick et al., 2011; Stienstra et al., 1998).

اضافة إلى تلاشي الخلايا الحبيبية، فقد لوحظ تلاشي الخلايا الهرمية في الحصين بعد استئصال الغدة الكظرية على المدى الطويل (Sapolsky et al., 1991) و(Adem et al., 1994). اكتشف سلوفيتر ومساعديه سنة 1989 (Sloviter et al., 1989). أن استئصال الغدة الكظرية يؤدي إلى موت الخلايا الحبيبية الحصينية و قد تم التوصل إلى نفس النتيجة من قبل عدة فرق بحث (Krugers et al., 1994; Nichols et al., 2005; Sousa et al., 1997; Sugama et al., 2013)، فضلا عن النتائج التي توصل إليها سابولسكي ومساعديه سنة 1991 (Sapolsky et al., 1991) و أدم ومساعديه سنة 1994 (Adem et al., 1994) التي أظهرت موت الخلايا الهرمية للحصين بعد استئصال الغدة الكظرية على المدى الطويل وقد اعتبر هذا النموذج كنموذج لدراسة موت الخلايا العصبية على مستوى الحصين. إن الموت الخلوي العصبي (neurodegeneration) والإستجابة الدبقية له (glial response) التي تحدث في هذا النموذج هو مماثل لما هو مبين في نماذج أخرى مثل الإقفارية-إعادة التروية (ischemia-reperfusion)(Rothwell, 2003; Zhu et al., 2006a)، و

الإصابة الجراحية (surgical injury) (Tchelingerian et al., 1993)، TMT (Trimethyltin) (Liu et al., 2005) KA (Kainic acid) (Minami et al., 1991) و cis-2,4-methanoglutamate (MGlu) (Pearson et al., 1999a). وبالتالي يمكن استخدام نموذج استئصال الغدة الكظرية كنموذج لدراسة موت الخلايا العصبية في الحصين والتي قد يكون نموذجا مماثلا لما يحدث في الأمراض العصبية المزمنة.

يتم إنتاج السيتوكينات الالتهابية (Pro-inflammatory cytokines) كالإنترلوكين-1β (IL-1β) (Rothwell and Luheshi, 2000a)، إنترليوكين-6 (IL-6) (Gadient and Otten, 1994; Godbout and Johnson, 2004) و عامل نخر الورم ألفا (TNF-α) (Perry et al., 2002; Sternberg, 1997a; Vitkovic et al., 2000a) من قبل خلايا عديدة في المخ (Rothwell, 2003).ولقد تم العثور على مستويات مرتفعة من هذه السيتوكينات في العديد من الأمراض التنكسية (degenerative diseases) مثل مرض الزهايمر (Alzheimer's)(Rubio-Perez and Morillas-Ruiz, 2012; Veerhuis et al., 1999)، التصلب الجانبي الضموري (Amyotrophic lateral sclerosis) (Rothwell and Luheshi, 2000a) ومرض الباركنسون (Parkinson's) (Blum-Degen et al., 1995; Nagatsu et al., 2000). وقد توصلت دراسات مختلفة الى الكشف عن الإفراز المبكر لهذه السيتوكينات في مختلف النماذج الحيوانية العصبية كنموذج KA (Yabuuchi et al., 1993)، TMT (Fiedorowicz et al., 2001)، نقص التروية (Sairanen et al., 1997; Yabuuchi et al., 1994)، 1-methyl-4-phenyl-1,2,3,6-tetrahydropyridine (MPTP) (Kumar et al., 2012; Selley, 2005). وقد ذكرت العديد من الدراسات أن هذه الوسائط الالتهابية تساهم في الشروع في التغيرات المورفولوجية التي تحدث أثناء موت الخلايا العصبية وتفاقم الأضرار الناجمة عن الإصابات المختلفة (Allan et al., 2000; Apelt and Schliebs, 2001; Berti et al., 2002a; Botchkina et al., 1997; Knoblach et al., 1999; Touzani et al., 2002). يعرف الإجهاد التأكسدي (Oxidative stress) بأنه ظاهرة خلوية سامة ناتجة عن اختلال في التوازن بين مضادات الأكسدة (antioxidants) والمواد المؤكسدة (oxidants) مما يؤدي إلى تعريض الأنسجة الى مخاطر مختلفة وبالتالي الإسهام في الموت العصبي (Halliwell, 2006; Lee et al., 2010a; Li et al., 2004; Murakami et al., 2011). غير أنه تملك هذه المواد المؤكسدة العديد من الوظائف الفسيولوجية المهمة (Hsieh and Yang, 2013; Schieber and Chandel, 2014). وقد يؤدي الإفراط في إنتاج مستويات عالية منها إلى الإجهاد التأكسدي. وهذا الاخير بدوره يمكن أن يسبب تلف خلوي ويعزز الالتهاب (Haddad, 2002) ولمواجهة ذلك تملك الخلايا مخزون من المركبات والأنزيمات المضادة للتأكسد للحيلولة دون تراكم هذه المواد المؤكسدة (van Horssen et al., 2011).

المواد وطرق العمل:

1-الهدف من الدراسة:

لقد وافقت اللجنة الأخلاقية الإقليمية لكلية الطب والعلوم الصحية (جامعة الإمارات العربية المتحدة) على هذه الدراسة (RECA/01/05). وكان الهدف من الدراسة الحالية هو بحث تأثير استئصال الغدة الكظرية على المدى القصير على موت الخلايا العصبية في مناطق مختلفة من الحصين، إنتاج السيتوكينات الالتهابية IL-1β، IL-6 و TNF-α، تنشيط مختلف الخلايا الدبقية النجمية (astrocytes) والدبقية الصغيرة (microglia) وعلى مؤشرات الإجهاد التأكسدي GSH، SOD و MDA وأثر غياب الهرمونات الكظرية على سلوك (animal's behavior) جرذان الويستار البيضاء.

2- الحيوانات و استئصال الغدة الكظرية:

انتقينا لهذه الدراسة جرذان الويستار البيضاء (albino Wistar) البالغة العمر ثمانية أسابيع و تتراوح أوزانها بين 170-220غ والتي تم الحصول عليها من المصلحة الحيوانية بكلية الطب والعلوم الصحية (العين، الامارات العربية المتحدة). وضعت جميع الحيوانات في أقفاص بلاستيكية (Plexiglas)، كل مجموعة تتكون من أربعة جرذان، وفي ظروف يتواتر الضوء والظلام فيها 12سا /12سا حيث درجة الحرارة تقدر 22°م، تركت الحيوانات حرة للوصول إلى الغذاء والماء طوال التجربة. وقد تم إعطاء الجرذان المستأصلة الغدة الكظرية ماء شرب مالح (saline) 0.9٪ بدلا من مياه الشرب العادية من أجل الحفاظ على توازن الأيونات ومنع الآثار الضارة الناتجة عن غياب كلوريد الصوديوم (sodium chloride).

خدرت الحيوانات باستعمال بينتوباربيتال (Pentobarbital) (35 مغ/كغ من وزن الجسم) ، تم حلق ظهور الحيوانات باستخدام آلة حلاقة كهربائية ثم قمنا سواء باستئصال الغدة الكظرية أو عمليات مزيفة (Sham surgery) كما وضحه سلوفيتر ومساعديه سنة 1989. من أجل إجراء عملية جراحية معقمة تم تنظيف ظهر الحيوان بالايثانول 70٪ وبعد ذلك قمنا بشق على مستوى الجلد والعضلة الظهرية للوصول إلى الجوف الصفاقي (peritoneal cavity) حيث يكون بالقدر الكافي الذي يسمح لنا برؤية الغدة الكظرية وبعض المساحة الحرة لإزالتها دون ترك أي بقايا منها. باستخدام ملقط حاد تم مسك الدهون المحيطة بالكظرية ثم استئصلت عن طريق قطع النسيج الضام الموجود بينها وبين الكلية بمساعدة ملقط حاد و مائل. بعد ذلك قمنا بخياطة الشق ووضع الحيوان في القفص. خضعت الحيوانات الشاهدة المزيفة (SHAM) لنفس الإجراءات السابقة باستثناء إزالة الغدة الكظرية (الشكل-6).

3-تحديد مستويات الكورتيكوستيرون في المصل بواسطة Enzyme Immunoassay (EIA):

الهدف من وراء هذه الخطوة هو معرفة مستويات الكورتيكوستيرون في المصل لتقييم فعالية عملية استئصال الغدة الكظرية، حصلنا من القلب حوالي 1مل من الدم مباشرة قبل تضحية الجرذان (Animal sacrifice) . وقد تمت التضحية من خلال قطع رأس الحيوان (decapitation) بعد فترات مختلفة من اجراء الجراحة 4 سا (ن = 24)، 24 سا (ن = 24)، 3 أيام (ن = 24)، اسبوع(ن = 24) و اسبوعين (ن = 24). خزنت عينات المصل (sera samples) عند درجة حرارة -80°م الى غاية موعد قياس مستويات الكورتيكوستيرون عن طريق تقنية (Enzyme Immunoassay) (Life sciences, Lausen, Switzerland). باختصار، في هذه التقنية ترتبط الاجسام المتعددة الانسال (polyclonal antibody) المضادة للكورتيكوستيرون بالاضداد المتعددة الانسال المصنعة في الحمار و المضادة للأغنام-(donkey anti sheep antibody) التي تكون مثبتة في حفر (wells) صفيحة بلاستيكية تدعى micro- plate.

غسلنا الصفيحة لإزالة الأجسام المضادة المتعددة الانسال الزائدة، يتنافس الكورتيكوستيرون الموجود في المصل مع كمية ثابتة من الكورتيكوستيرون الموسوم ببيروكسيديز الفجل (horseradish peroxidase) على المواقع الموجودة على الأجسام المضادة المتعددة الانسال. غسلنا الصفيحة مرة ثانية لإزالة العينات الزائدة والغير مرتبطة. اضفنا محلول الركيزة (substrate) إلى الحفر لتحديد نشاط الانزيم المرتبط. قمنا بوقف التفاعل باضافة محلولTMB stop solution لكل حفرة. رجت الصفيحة بهدوء وبعد ذلك قسنا الامتصاصية (absorbance) على طول الموجة 450 نانومتر بالمطياف (Spectrometer). كثافة اللون تتناسب عكسيا مع تركيز الكورتيكوستيرون في العينة. لحساب تركيز الكورتيكوستيرون في العينات تم إنشاء منحنى العيارية (Standard Curve) ضمن مجال يتراوح من 32 إلى 20،000 بيكوغرام/مل. ومن خلال هذا المنحني يتم استخراج معادلة المنحني العيارية. وبذلك يمكن قياس تركيز الكورتيكوستيرون اعتمادا على الكثافة الضوئية المقاسة بالمطياف.

4-الكيمياء الحيوية:

4-1-تحضير العينات:

قمنا بتضحية الجرذان (ن = 80) عن طريق قطع رأسها بعد أوقات مختلفة من اجراء الجراحة: 4 سا (ن = 16)، 24 سا (ن = 16)، 3 أيام (ن = 16)، اسبوع(ن = 16) و اسبوعين (ن = 16). بعد إزالة المخ قمنا بتشريحه وعزل الحصين على الفور فوق الجليد، وبعد ذلك جمد هذا الأخير في سائل النيتروجين (liquid nitrogen) و وضع في درجة حرارة -80°م إلى غاية موعد الفحص.

لتحضير جناسة العينات سحقت على الجليد أنسجة الحصين المذابة في محلول T-PER البارد (بيرس التكنولوجيا الحيوية، روكفورد، إيل، الولايات المتحدة الأمريكية)، المظاف اليه 1: 100 كوكتيل مثبط البروتياز (protease inhibitor cocktail) (Sigma-Aldrich, Missouri, USA). بعد صوتنة (sonication) العينات، تم تعريضها للطرد المركزي

(centrifugation) بسرعة 16000 دورة/الدقيقة لمدة 30 دقيقة في درجة حرارة 4°م. استرجعنا المحلول الطافي (supernatant) ثم قمنا بتخزينه في -80°م حتى موعد استعماله في تحديد كل من تركيز البروتين الإجمالي بواسطة اختبار برادفورد (Bradford's protein assay) (Bio-Rad, California, USA)) ، قياس مستوي السيتوكينات (IL-1β، IL-6 و TNF-α) عن طريق تقنية ELISA (R&D Systems; Minneapolis, USA) و مؤشرات الإجهاد التأكسدي GSH، SOD و MDA بواسطة تقنية قياس اللون (Colorimetry) .

4-2-تحديد تركيزالبروتين (Total protein) في العينات:

انطلاقا من محلول BSA (1%) (Bovine serum Albumine) قمنا بتكوين سلسلة من العينات المعيارية (standards) بشكل مضاعف تتراوح تراكيزها بين 0.2 و 1.4مغ/مل. خفف X5 كاشف برادفورد (Bradford Reagent) بنسبة 1: 4 بالماء المقطر ثم بواسطة ورقة ترشيح واتمان-1 رشح المحلول المخفف الناتج. أضفنا لكل أنبوب البوليسترين 1.25 مل من كاشف برادفورد المخفف. خففنا عينات الحصين في محلول التجانس (homogenation buffer) 10:1 كما استخدمنا هذا الأخير كمرجع (blank) خلال قياس الامتصاص. اضفنا 25 ميكرولتر من العينات المعيارية و عينات الحصين إلى الأنابيب التي تحتوي على كاشف برادفور. بعد 5 دقائق من التحضين (incubation) تم قياس الامتصاصية في 595 نانومتر. اعتمادا على امتصاصية العينات المعيارية قمنا برسم المنحنى العياري للبروتين . وعن طريق الاستيفاء منه حددنا تركيز البروتين في جناسة (Homogenate) الحصين لكل عينة.

4-3--تحديد مستوى السيتوكينات الالتهابية في الحصين (IL-1β، IL-6 و TNF-α) بواسطة ELISA:

استخدمنا صفيحة ELISA وهي عبارة عن صفيحة مكونة من 12 صف وكل واحد يتشكل من 8 حفر (well). اضفنا الى هذه الصفيحة الاجسام المضادة الخاصة بالسيتوكين المراد الكشف عنه وتترك لليلة كاملة في درجة حرارة المختبر. في اليوم التالي غسلنا الصفيحة للتخلص من الأجسام المضادة الغير ملتصقة ثم حظرت(block) بواسطة البومين مصل البقر 1٪ المذاب في محلول الفوسفات المالحة (Phosphate-buffered saline) وتركت للتحضين في درجة حرارة المختبر لمدة ساعتين. لتشكيل المنحنى العياري حضرنا العينات العيارية عن طريق التخفيف التسلسلي (serial dilution) لتراكيز معروفة من السيتوكين المراد قياسه (الشكل-7). وضعت كل من العينات العيارية و عينات الحصين في حفر الصفيحة ثم حضنت هذه الأخيرة في درجة حرارة الغرفة لليلة واحدة.

في اليوم التالي، غسلنا الصفيحة مرة ثانية للتخلص من العينات الغير ملتصقة ثم الأجسام المضادة الكاشفة المرتبطة بالبيوتين (Biotinylated goat) وتركت لمدة ساعة للتحضين في درجة حرارة المختبر. كمتفاعل ثالث تم اضافة الأجسام المضادة المرتبطة بالسترابدافيدين و بيروكسيديز الفجل (Streptavidin conjugated to horseradish peroxidase) للصفيحة وحضنت لمدة 20 دقيقة في في درجة حرارة المختبر. تم إضافة 100 ميكرولتر من Tetramethylbenzidine (41.6 ميلي مولارية) لكل حفرة للحصول على اللون. اوقفنا التفاعل بواسطة حامض الكبريتيك 2ملارية ($2N\ H_2SO_4$) و في غضون 10 دقائق من الوقف تم قياس الامتصاصية على طول الموجة 450 نانومتر بواسطة

المطياف (الشكل 8). اعتمادا على امتصاصية العينات المعيارية قمنا برسم المنحنى العياري لكل سيتوكين. وعن طريق الاستيفاء منه حددنا تركيز IL-1β، IL-6 و TNF-α لكل عينة. تم تقسيم تركيز السيتوكين لكل عينة على تركيز البروتين الاجمالي لنفس العينة لتعديل الإختلافات في حجم الأنسجة. يتم التعبير عن التركيز كالتالي بيكوغرام من سيتوكين/ملغ من البروتين.

4-4-تحديد مستويات مؤشرات الإجهاد التأكسدي (GSH، SOD و MDA) بواسطة تقنية قياس شدة اللون:

وانه لجدير بالذكر ان ننوه هنا أن نفس جناسة الحصين التي استخدمت لقياس السيتوكينات تم استخدامها لتحديد مستويات مؤشرات الإجهاد التأكسدي GSH، SOD MDA بواسطة تقنية قياس اللون.

**4-4-1-Superoxide dismutase: **

هي انزيمات معدنية تحفز عملية تفكيك الجذر الفائق ($O_2^{\bullet-}$) (dismutation of the superoxide radical -•) O_2) الى بيروكسيد الهيدروجين (H_2O_2) والأكسجين الجزيئي (O_2). ويستند قياس كمية SOD في جناسة الحصين على استخدام ملح تيترازوليوم (tetrazolium salt) للكشف عن الجذور الفوقية (superoxide radicals) التي تم إنشاؤها بواسطة xanthine oxidase و hypoxanthine (Cayman chemical, Michigan, USA)(الشكل -9).

أضيف حجم 10ميكرولتر من العينات والمعايير الى حفر الصفيحة. تلاها إضافة 200 ميكرولتر من الكاشف الجذري المخفف (محلول مخفف من 50 ميكرولتر من الملح تيترازوليوم مع 19.95 مل من الماء المقطر). وبمجرد الانتهاء من الخطوات السابقة تم إضافة 20 ميكرولتر من xanthine oxidase الى جميع الحفر من أجل الشروع في التفاعل. غطيت الصفيحة وحضنت على رجاجة (shaker) لمدة 20د في درجة حرارة الغرفة. تم قراءة الصفيحة على طول الموجة 440نانومتر. يتم تعريف وحدة واحدة من SOD كمقدار كمية الانزيم اللازمة لتطافر (dismutation) 50٪ من الجذر الفائق ($O_2^{\bullet-}$).

4-4-2- مالونديالدهيد (MDA):

ويستند قياس كمية TBARS في جناسة الحصين على تفاعل حمض الثيوباربيتوريك (thiobarbituric acid TBA) مع مالونديالدهيد (MDA) في ظروف حامضية (acetic acid) و درجة حرارة مرتفعة (95 درجة مئوية) (Cayman chemical, Michigan, USA). يتم خلط حجم 100ميكرولتر من جناسة الحصين مع نفس الكمية من محلول صوديوم دوديسيل الكبريتي (sodium dodecyl sulfate) وخلطها بشكل جيد مع 4مل من كاشف اللون المتشكل من (2120مغ من حمض TBA الذائب في خليط من 200 مل TBA- acetic acid و من 200 مل TBA- sodium hydroxide). تم غلي الخليط في أنبوب 5مل لمدة ساعة واحدة. مباشرة وبسرعة بعد انتهاء المدة الزمنية للغلي توضع الأنابيب على الجليد لمدة 10دقائق من أجل وقف التفاعل على الفور. بعد ذلك عرضت الأنابيب لطرد مركزي سرعته g16000 في درجة حرارة 4°م لمدة 10 دقائق. تم أخذ حجم 150 ميكرولتر من الطافي (supernatant) الناتج وإضافته الى الصفيحة. تم تطبيق إجراء مماثل للمعايير و جناسة الحصين (الشكل-10). تم قياس امتصاصية TBA-MDA في طول الموجة 530-540 نانومتر. استخدامنا امتصاصية المعايير في إنشاء المنحنى القياسي MDA. تم تحديد تركيز MDA في جناسة الحصين عن طريق الاستيفاء من منحنى القياسية.

4-4-3-الجلوتاثيون المرجع (GSH):

تم تحديد تركيز الجلوتاثيون المرجع (GSH) في جناسة الحصين باستخدام Commercial kit (Sigma-Aldrich, Missouri, USA). بدءا قمنا بنزع البروتونات من عينة الحصين بواسطة 5٪ من حمض 5-سلفوساليسيليك (5-Sulfosalicylic Acid) ثم تعرضت للطرد المركزي لإزالة البروتين المترسب وبعد ذلك تم قياس الجلوتاثيون.يعتمد قياس الجلوتاثيون على مقايسة الحركية (a kinetic assay) التي تعتمد على الكميات المحفزة (نانومول) من الجلوتاثيون التي تسبب إرجاع مستمر لمركب (DTNB) (5, 5'-dithiobis (2-nitrobenzoic acid TNB وGSSG. و GSSG المتشكل يتم تدويره (recycled) من قبل انزيم الجلوتاثيون ريدوكتاس (glutathione reductase) و NADPH. يتم قياس الناتج الأصفراللون المتمثل في حمض (5-TNB) 5-thio-2-nitrobenzoic acid طيفيا على طول الموجة 412 نانومتر (الشكل-11). يستخدم منحنى القياسية للجلوتاثيون المرجع لتحديد كمية الجلوتاثيون في العينة (Ellman, 1959).

5-الدراسة النسيجية:

5-1-إعداد أنسجة الحصين:

5-1-1-الإرواء-التثبيت Perfusion-fixation:

والغرض من هذا الإجراء هو الحصول على تثبيت سريع ومتجانس من جهة والحفاظ على سلامة محددات (epitopes) البروتين التي نسعى الى استهدافها في تقنية التلوين الهيستولوجي المَناعِيَّ (immunohistochemistrystaining). من أجل تجنب تخثر الدم، ولضمان سلاسة تدفق المحلول المثبت(fixative). تم إبقاء الحيوان على قيد الحياة عن طريق تخديريه بواسطة بنتوباربيتال 35مغ/كغ وبعد ذلك وضع على ظهره على لوحة

التشريح. باستخدام مقص حاد تم إجراء شق على مستوى البطن للوصول الى غشاء الحجاب الحاجز(diaphragm membrane) وبعناية تم قطع هذا الأخير لكشف القفص الصدري وبالتالي القلب. باستعمال مقص صغير تم احداث قطع في الأذين الأيمن وبسرعة جمعنا 1مل من الدم لقياس مستويات الكورتيزون في المصل. مباشرة بعد جمع الدم، يتم إدخال إبرة غير حادة من اسفل القلب الى غاية رؤيتها من خلال الشريان الأبهر (aorta). هذه الإبرة تكون مرتبطة بزجاجتين. واحدة تحتوي على محلول PBS 0.1مول (PH 7.4) والأخرى على محلول الفورمالين 10٪ (PH 7.4).

أولا تم ضخ حوالي 50مل من PBS حتى يظهر الكبد بلون شاحب دلالة على اخراج تقريبا كل الدم من الجسم. وبعد ذلك تمت عملية التثبيت بواسطة 300 مل من الفورمالين (10% formalin) لكل حيوان. وإنه لجدير بالذكر أن سرعة تدفق المحلول تكون 20ملل/دقيقة وهو يماثل تدفق الدم عند الجرذان (الشكل-12). مباشرة بعد الانتهاء من التثبيت، تم قطع رأس الحيوان وعلى الفور شرح الدماغ لاستخراج المخ ثم وضع في نفس المحلول المثبت بمقدار يفوق حجم المخ من 10-20 مرة ويترك لمدة واحد (الفترة المثلى التي وجدنا من خلالها يمكننا الحصول على أفضل نتائج للتلوين الهيستولوجي المَناعِيَّ).

5-1-2- التضمين بالبارافين (Paraffin Embedding):

هناك هدفان من هذه العملية، أولا التجفيف التدريجي لنسيج المخ ووضعه في قالب من البارافين وثانيا لجعل النسيج صلب وسهل للتقطيع بالمشراح (microtome). من أجل تحقيق الأغراض المذكورة أعلاه قمنا بالإجراء التالي.

ا-التجفيف (Dehydration): من خلال هذه الخطوة قمنا بتجفيف نسيج المخ تدريجيا من الماء من خلال وضعه في تراكيز مختلفة وتصاعدية للإيثانول (50، 70 و 90٪) حيث تستغرق كل خطوة ساعة واحدة تقريبا ثم يليها ثلاثة تغييرات في الإيثانول المطلق لكل 2 ساعة.

ب-التصفية (Clearing) : من خلال هذه الخطوة نهدف الى استبدال الكحول الذي تغلغل في النسيج اثناء الخطوة السابقة بالزيلين (xylene) من خلال ثلاثة تغييرات في الزيلين المطلق لكل ساعتين، وبما أن الكحول والبارافين غير قابلا للامتزاج تعتبر هذه الخطوة كخطوة تحضيرية للمرحلة التالية اين البارافين يصبح قادر على التسلل للنسيج.

ج-التشميع (Waxing): هذه هي الخطوة الأخيرة قبل القولبة (Embedding) حيث يوضع المخ في البارافين الذائب عند درجة حرارة تقارب 60°م للتخلص من جميع الزيلين الموجود في الأنسجة من خلال ثلاثة تغييرات في البارافين الذائب لكل ساعتين.

د-القولبة (Embedding): يحدث التضمين الفعلي عندما يتسلل البارافين الى نسيج المخ. يتم ضبط المخ في القالب بطريقة تتناسب وإمكانية الحصول على مقاطع عرضية.

5-1-3-تحضير مقاطع المخ:

نقوم بإزالة البارافين الزائد و تقليم أنسجة المخ الإضافية باستخدام مشراح (الشكل 9) حتى نصل الى منطقة اهتمامنا التي تسمى عادة بمنطقة الشارب (mustache area) التي تبعد تقريبا -3.7 ملم من البريجما وفقا لاطلس باكسينوس واتسون (Paxinos and Watson.2005) (الشكل -13). يرجع سبب اختيار هذه المنطقة من الحصين أنه على هذا المستوى تظهر جميع المناطق المشكلة للحصين بوضوح (DG، CA1، CA2، CA3 و CA4) و تكون جد محددة وسهلة للتمييز. للتأكد من أننا في المنطقة المخصصة استخدمنا التلوين السريع بالتولويدين الأزرق (toluidine blue). وبعد ذلك

أخذت مقاطع عرضية (Coronal sections) ذات سمك يقدر 1ميكرون. من أجل تسطيحها، يتم على الفور نقل هذه الأخيرة الى حمام مائي 50 درجة مئوية لازالة كل انكماشات الموجودة على النسيج. وبمجرد أن نتأكد من أن النسيج خال من الطي والتجاعيد، باستخدام شريحة مغلفة بالجيلاتين (slide coated by gelatin) يتم التقاط المقطع وتركه ليجف بوضع الشريحة بشكل عمودي على ورقة تجفيف. بمجرد تجفيف المقطع يتم نقل الشريحة الى لوحة التدفئة (heating plate) لضمان خلو المقطع من الماء وتجفيفه بشكل صحيح. يتم الاحتفاظ بجميع الشرائح حتى موعد استعمالها في مختلف التلوينات النسيجية.

5-2-التلوين FJB (Fluoro-Jade B):

تم إجراء تلوين FJB كما وصفه شميود و هوبكنز سنة 2000(Schmued and Hopkins, 2000). استخدم 32 حيوان لهذا التلوين، 4سا (ن=8)، 24سا (ن = 8)، 3أيام (ن = 8)، اسبوع(ن = 8) و اسبوعين (ن = 8). أولا تم نزع الشمع من المقاطع العرضية للمخ من خلال تغييرين في الزيلين 10د لكل منهما. يليها بعد ذلك الإرواء (rehydration) عبر وضع الشرائح في تراكيز متدرجة من الكحول (100 ،90 ، 80 ، 70 %).

تغمس الشرائح لمدة 5د في هيدروكسيد الصوديوم 1٪ المذاب في 80٪ كحول (20مل من 5٪ هيدروكسيد الصوديوم مضافة الى 80مل من الكحول المطلق). بعد ذلك توضع الشرائح في الكحول 70٪ ثم الماء المقطر لمدة 2د على التوالي. يتم نقل الشرائح الى محلول برمنجنات البوتاسيوم0.6٪ لمدة 10د. وبعد ذلك تغسل الشرائح في الماء المقطر لمدة دقيقتين وتغمس20د في محلول FJB 0.0004 ٪. تشطف الشرائح ثم تغسل بالماء المقطر ثلاثة مرات لمدة دقيقة واحدة لكل مرة. تجفف على شريحة تدفئة لمدة 10د. يتم تطهير الشرائح الجافة عن طريق الغمر في الزيلين لدقيقة على الأقل وبعد ذلك تغطى بمادة DPX.

5-3-دراسة نسيجية باستعمال المجهر الإلكتروني:

تمت إزالة منطقة الحصين من المخ ووضعها في قارورة زجاجية تحتوي على مثبت كارنوفسكي (KARNOVSKY'S fixative) PH 7.2 لمدة ليلة كاملة في 4°م. في اليوم التالي تم غسل الأنسجة ثلاث مرات في محلول PB 0.1 مول لمدة 30 دقيقة لكل منهما. اضيف حجم 1مل من محلول رباعي أكسيد الأوسميوم1 ٪ (osmium tetroxide %1) لكل قارورة وترج هذه الأخيرة لمدة ساعة. نتخلص من رباعي أكسيد الأوسميوم ثم بواسطة الماء المقطر نغسل النسيج ثلاثة مرات لمدة دقيقتين لكل منهما. نجفف العينات عن طريق وضعها في التراكيز المتدرجة من الكحول (30، 50، 70،80، 90، 95،100، 100%) 15د لكل تركيز وبعد ذلك تنقل الى محلول أكسيد البروبيلين- I (Propylene oxide 1) و أكسيد البروبيلين-II لمدة 15 دقيقة لكل منهما.

خلال آخر أكسيد البروبيلين، تم إعداد Agar100 epoxy resinلتكون جاهزة للمعالجة التالية:

Agar 100Resin: Propylene oxide 1:1 لمدة ساعة.

Agar 100Resin: Propylene oxide 2:1 لمدة ساعة.

Agar 100Resin: Propylene oxide 3:1 لمدة ساعة.

Agar 100Resin لليلة كاملة في درجة حرارة 4°م.

في اليوم التالي استخرجت قوالب resin من الثلاجة ووضعت في الفرن عند درجة حرارة 60°م لمدة 20 دقيقة وبعد ذلك واصلنا العملية على النحو التالي. تم ملء القوالب بمادة resin وتركت على الطاولة لمدة تتراوح بين 3-4 ساعات للتخلص من الفقاعات الهوائية وتسهيل تغلغل resin داخل النسيج بعد ذلك وضعت العينات في القوالب وتركت في الفرن لمدة 24سا عند 64°م. اخذت مقاطع عرضية من العينات على مستوى -3.7 ملم نسبة البريجما (bregma) وفقا لاطلس باكسينوس و واتسون سنة 2005. استخدم مشراح متناهي الحدة يسمى Reichert Ultracuts لأخذ مقاطع عرضية من الحصين سمكها يقدر 95 نانومتر، لونت المقاطع العرضية بواسطة 1٪ أزرق التوليدين للتأكد من المنطقة المرغوب دراستها. وضعت المقاطع العرضية الرفيعة على شبكة نحاسية-200 (mesh copper grids 200) ولونت بواسطة uranyl acetate ثم تلاها تلوين مضاعف بمحلول سترات الرصاص (lead citrate). فحصت الشرائح الشبكية واخذت صور من مناطق مختلفة للمقاطع العرضية للحصين تحت المجهر الإلكتروني النافذ نوعية فيليبس CM10 (Philips CM10 transmission electron microscope) لبحث و دراسة إمكانية حدوث موت الخلايا العصبية في النموذج الحالي.

4-5- تقنية كيمياء المناعة النسيجية (Immunoflurescent labeling):

نزع الشمع من شرائح العينات عن طريق غمسها في الزيلين، قمنا بعملية الإرواء لمقاطع المخ بوضعها في تراكيز مختلفة للإيثانول (100، 90، 80، و 70٪) وبعد ذلك غسلت في الماء المقطر. لكشف المحددات المستهدفة والحصول على نتائج مثالية لكيمياء المناعة النسيجية، تعرضت شرائح العينات لاسترجاع المستضد (antigen retrieval) باستعمال محلول سيترات الصوديوم 10ميلي مولار (10mM sodium citrate) (PH 6) يليه تسخين في الميكروويف (microwave) على أقصى قوة للجهاز لمدة دقيقة ثم أدنى قوة لمدة 10 دقائق. بعد هذا الإجراء تم غسل العينات بواسطةPBS 0.1 مول (PH 7.4) وتبريدها في درجة حرارة الغرفة.

للوسم المزدوج المناعي (double-immunofluorescence labeling) ، تم حظر (Block) المقاطع باستعمال BSA 1٪ في درجة حرارة الغرفة لمدة 30 دقيقة ثم حضنها مع كل الأجسام المضادة الأولية (primary antibodies) في 4 درجة مئوية لمدة ليلة كاملة. الأجسام المضادة الأولية المستخدمة كانت anti-ionized calcium-binding adaptor molecule 1 المستخلص من الأرنب (Iba1, Wako, Massachusetts, USA 1:2000) ممزوجة مع anti-neuronal nuclear antigen antibody المستخلص من الفأر (Neun, Millipore, Massachusetts,USA, 1:1000) و rabbit polyclonal anti-glial fibrillary acidic protein (GFAP, Dako, Copenhagen, Denmark, 1:1000). في اليوم التالي قمنا بغسل شرائح العينات ثلاث مرات في PBS حضنت مع أجسام مضادة ثانوية موسومة Alexa488 مستخلصة من الحمار مضادة للأجسام المضادة المستخرجة من الأرنب (Invitrogen,Paisley, UK, 1:200) ممزوجة بأجسام مضادة موسومة بالرودامين (Rhodamine) مستخرجة من الحمار (Jakson, Pennsylvania, USA, 1:100) مضادة للأجسام المضادة المستخرجة من الفأر المذابة في PBS-Triton X-100 0.3% لمدة ساعة في درجة حرارة الغرفة. بعد ذلك، تم غسل شرائح العينات عدة مرات فيPBS. تغطى الشرائح بمادة fluoromount.

واستخدمت إجراءات مماثلة لكيمياء المناعة النسيجية الثلاثية (triple-immunofluorescence labeling) من أجل تحديد تموضع الخلايا الدبقية الصغيرة، النجمية والخلايا العصبية بالنسبة لبعضها البعض، استخدم خليط من الأجسام المضادة الأولية التالية، GFAP أرنب مختلطة مع Neun الفأر و Iba1 الماعز وتركت في درجة 4°م لليلة واحدة. وفيما يتعلق بالأجسام المضادة الثانوية، حضنت شرائح الأنسجة مع اجسام مضادة للأرنب مستخرجة من الحمار موسومة Alexa488 ممزوجة بأجسام مضادة للفار مستخرجة من الحمار موسومة بالرودامين و أجسام مضادة للماعز مستخرجة من الحمار موسومة cy5 (Jakson, Pennsylvania, USA, 1:100).

تم التقاط الصور الرقمية (digital images) التمثيلية باستخدام الكاميرا الرقمية Zeiss AxioCamHRc مزودة ببرنامج AxioVision 3.0 . كما تم فحص بعض العينات باستعمال مجهر ليزرC1 البؤري الماسح (C1 laser scanning confocal microscope). استعملنا العدسات X4 و X20 لالتقاط الصور حيث اخترنا مقطع بصري واحد فقط. واستخدم فوتوشوب ShopCS6 لتعديل إضاءة الصور الملتقطة و من أجل التمييز بوضوح تموضع الخلايا العصبية، الخلايا النجمية والدبقية الصغيرة بالنسبة لبعضها البعض.

5-5-التحليل الكمي للخلايا الإيجابية Iba-1 وGFAP :

تتنشط الخلايا الدبقية الصغيرة استجابة لأي إصابة تحدث على مستوى الجهاز العصبي المركزي حيث تخضع لتغيرات مورفولوجية عديدة. في الدراسة الحالية قمنا ببحث إمكانية استجابة كل من هذه الخلايا الدبقية على مستوى الحصين بعد استئصال الغدة الكظرية. عادة، عندما تتنشط الخلايا الدبقية الصغيرة فإنها تأخذ شكل اميبي مع قصر وتوسع في التشعبات الطرفية. يمكن فحص هذه التغيرات المورفولوجية باستعمال تقنية كيمياء المناعة النسيجية باستعمال الأجسام المضادة Iba1 و GFAP للخلايا الدبقية الصغيرة والنجمية على الترتيب. في هذه الدراسة،اقتصرنا على عد الخلايا الدبقية الصغيرة و الخلايا التي يظهر جسمها الخلوي كليا اثناء التقاط الصورة. استخدمنا ثلاثة جرذان مستأصلة الغدة الكظرية و ثلاثة جرذان خاضعة لجراحة مزيفة لكل تجربة. من كل جرذ اخترنا ثلاثة مناطق من الحصين متباعدة فيما بينها بحوالي 30ميكرومتر. ومن كل منطقة تم اختيار ثلاثة حقول بصرية لعد الخلايا. اتخذت صور من أجزاء ملونة للحصين بالتكبير X20 باستخدام الكاميرا الرقميةAxioCam HRc AxioVision 3.0 3.0 (كارل زايس، ألمانيا). من أجل تفادي التحيز أثناء عملية العد، ثبتت أولا معايير الحصول على الصور في البرنامج بالنسبة للخلايا الدبقية الصغيرة و النجمية وأبقيت ثابتة بالنسبة لجميع النقاط الزمنية التي تم فحصها. قمنا بعد الخلايا المطابقة للمعايير المذكورة أعلاه يدويا باستخدام برنامج عد الخلايا (هيراكل بيوسوفت سرل، رومانيا). وبعد ذلك أجريت مقارنة بين عدد الخلايا الدبقية الصغيرة والنجمية عند الجرذان مستأصلة الغدة الكظرية و الجرذان الخاضعة لجراحة مزيفة.

6-دراسة سلوك الحيوان:

بغية تعود الحيوانات علينا تمت ملاطفتها والمسح على فروها يوميا لمدة 3 أيام على الأقل قبل التجارب. و اجرينا اختبار Passive Avoidance كما تم وصفه من طرف (Misane and Ahlander-Luttgen et al., 2003)باستخدام صندوق معياري مزدوج المقصورة (two-compartment standard shuttle box) (x25x2451 سم). يتكون من مقصورتين متساويتين في الحجم وأرضيتهما متكونة من شبكة مصنوعة من الفولاذ المقاوم للصدأ و يفصلهما باب انزلاق ابعاده 7x7 سم . تكون الحجرة اليمنى (مقصورة الصدمة) مصبوغة باللون الأسود للحصول على غرفة مظلمة، في حين أن المقصورة اليسرى كانت مضاءة بمصباح (24 فولت، 5 واط) مثبتة على الغطاء الزجاجي العلوي. وأجري التدريب على Passive Avoidance في جلسة واحدة (اليوم الأول) حيث وضعت الجرذان في حجرة مضاءة (مع استحالة الوصول الى الحجرة المظلمة) وسمح لها باستكشاف الغرفة لمدة 60 ثانية. عندما انتهت 60 ثانية، تم فتح الباب المنزلق تلقائيا و سمح لها بالعبور المقصورة المظلمة. بعد دخولها هذه الأخيرة بكافة الأرجل الأربعة، اغلق الباب المنزلق تلقائيا و اعطي تيار كهربائي ضعيف (تيار مستمر، شدته 0.3 مللي أمبير لمدة 3ثا) من خلال الشبكة الفولاذية. يسجل زمن العبور الى المقصورة المظلمة والذي يعرف بكمون التدريب (training latency). في حال امتنعت الحيوانات عن الانتقال إلى المقصورة المظلمة في غضون 300 ثانية أو ما يعرف بكمون القطع (cut off latency) يعاد فتح الباب وتدفع الجرذان بلطف خارج المقصورة المظلمة لتلقى الصدمة الكهربائية. بعد التعرض لصدمة القدم، يسمح للجرذان بالبقاء لمدة 30 ثانية في المقصورة المظلمة قبل تنحيتها من الجهاز وارجاعها الى قفصها.

تم اختبار الاحتفاظ (Retention) 24 ساعة بعد التدريب (اليوم 2). وضع الحيوان في المقصورة المضاءة مع ابقاء الباب مفتوح للسماح له بالمرور الى المقصورة المظلمة خلال 300 ثانية.قسنا الوقت الذي يستغرقه الحيوان لدخول المقصورة المظلمة بجميع الأرجل الأربعة تلقائيا (كمون الاحتفاظ). إذا امتنع الحيوان عن العبور الى المقصورة المظلمة في غضون 300 ثانية، يرجع الحيوان الى القفص و يقيم بالحد الأقصى للاختبار أي زمن الكمون الذي يقدر 300 ثانية (الشكل -14).

7-التحليل الاحصائي:

قمنا بالتعبير عن النتائج التي توصلنا عليها فيما يخص مستويات السيتوكينات الالتهابية (IL-1β، IL-6 و TNF-α)، مؤشرات الإجهاد التأكسدي (GSH، SOD وMDA) و عدد الخلايا الدبقية الصغيرة والخلايا النجمية بالمتوسط ± الخطأ المعياري المتوسطي (± SEM). و فيما يخص مقارنتها وتحليلها إحصائيا استخدمنا النسحة العشرون لبرنامج SPSS (IBM، الولايات المتحدة الأمريكية) واعتمدنا في ذلك على اختبار two-tail Student t test. اعتبرنا النتائج معنوية إحصائيا إذا كان $P \leq 0.05$. حددت مستوى المعنوية الإحصائية كالتالي:

$$(P^* \leq 0.05, P^{**} \leq 0.01, P^{***} \leq 0.001)$$

النتائج:

1-تركيز الكورتيزون في مصل الجرذان المستأصلة و الجرذان الخاضعة لجراحة مزيفة:

لقد قمنا بقياس مستويات كورتيزون في المصل بعد تضحية الجرذان للتأكد من فعالية عملية استئصال الغدة الكظرية. تم قياس تركيز الكورتيزون باستخدام الورق اللوغاريتمي التي تعتمد على نسبة الارتباط بدلالة تراكيز معروفة للكورتيزون التي تتراوح بين 32-20000 بيكوغرام / مل وبواسطة الاستيفاء من المنحنى يتم الحصول على تراكيز الكورتيزون في مصل الجرذان المستأصلة و الجرذان الخاضعة لجراحة مزيفة (الشكل- 15). لقد وجدنا أن مستويات الكورتيزون تراجعت بشكل ملحوظ ومعنوي احصائيا بعد 4 سا ($P = 0.001$) في مصل الجرذان المستأصلة مقارنة بالجرذان الخاضعة لجراحة مزيفة واستمر هدا الانخفاض في التركيز على مدى التجربة 24 سا($P <0.001$) ، 72سا($P <0.001$) ،اسبوع ($P <0.001$) واسبوعين ($P <0.001$) بعد الجراحة (الشكل- 16) و (الجدول-6).

2-الالتهاب العصبي:

2-1-انترلوكين- β1:

تعتبر السيتوكينات الالتهابية الثلاثة IL-1β، IL-6 و TNF-α من العوامل الرئيسية في مختلف الاستجابات المناعية للعديد من الاصابات. و ذلك أنها تلعب دورا هاما في مختلف الأمراض العصبية التنكسية. في النموذج الحالي لموت الخلايا العصبية هدفنا الى تقييم مستويات هذه السيتوكينات في حصين جرذان الويستار المستأصلة الغدة الكظرية و الجرذان الخاضعة لجراحة مزيفة باستخدام تقنية ELISA. قمنا بقياس مستويات السيتوكين الالتهابي الانترلوكين- β1 في جناسة الحصين على مدى (4 سا، 24 سا، 3أيام،اسبوع واسبوعين).

من أجل تحديد تركيز IL-1β بواسطة ELISA في العينات. اعتمدنا على المنحنى المعياري المشكل من نتائج الامتصاص لتراكيز معيارية معروفة للانترلوكين- β1 التي تتراوح بين 12.5 -600 بيكوغ/مل بدلالة هذه التراكيز نفسها. وعن طريق الاستيفاء من المنحى تم تحديد تركيز الانترلوكين-β1 في كل العينات (الشكل- 17).

وأظهرت النتائج التي توصلنا إليها أن مستويات IL-1β ازدادت بشكل ملحوظ ومعنوي احصائيا في عينات جناسة حصين الجرذان المستأصلة مقارنة بالجرذان الخاضعة لجراحة مزيفة بعد 4سا ($P <0.05$) ،24سا ($P <0.05$) و3أيام ($P <0.01$) من خضوع الحيوانات للعملية الجراحية .غير أنه، بعد مرور اسبوع واسبوعين عن عملية استئصال الغدة الكظرية لاحظنا أنه لا توجد أي فروق معنوية احصائيا في تراكيز IL-1βعلى مستوى حصين للمجموعتين (الجدول- 7) و (الشكل- 18).

2-2-انترلوكين-6 (IL-6):

تم قياس مستويات السيتوكين الالتهابي انترلوكين-6 في جناسة حصين الجرذان المستأصلة مقارنة بالجرذان الخاضعة لجراحة مزيفة على مدار (4 سا، 24 سا، 3أيام، اسبوع واسبوعين) .من أجل تحديد تركيز IL-6 بواسطةELISA، اعتمدنا على المنحنى المعياري المشكل من قياس امتصاص تراكيز معيارية معروفة لانترلوكين- β1 تتراوح بين 125-8000 بيكوغ/مل بدلالة هذه التراكيز نفسها. وعن طريق الاستيفاء من المنحى تم تحديد تركيز الانترلوكين- 6 في كل عينة (الشكل-19). وكانت النتائج مماثلة لما توصلنا ليه فيا يخص تراكيز IL-1β (الجدول- 8) و (الشكل- 20).

2-3-عامل نخر الورم (TNF-α) :

تم قياس مستويات السيتوكين الالتهابي TNF-α في جناسة حصين الجرذان المستأصلة مقارنة بالجرذان الخاضعة لجراحة مزيفة على مدار (4سا، 24سا، 3أيام،اسبوع واسبوعين) .من أجل تحديد تركيز TNF-α بواسطةELISA، اعتمدنا على المنحنى معياري المشكل من قياس امتصاص تراكيز معيارية معروفة TNF-α تتراوح بين 9.3-500 بيكوغ/مل بدلالة هذه التراكيز نفسها. وعن طريق الاستيفاء من المنحى تم تحديد تركيز TNF-α في كل عينة انظر (الشكل-21). لقد لاحظنا أن مستويات TNF-α ازدادت بشكل ملحوظ ومعنوي احصائيا في عينات جناسة حصين الجرذان المستأصلة مقارنة بالجرذان الخاضعة لجراحة مزيفة بعد 4سا ($P < 0.01$) فقط. غير أنها بقيت متقاربة عند الجرذان المستأصلة مقارنة بالجرذان الخاضعة لجراحة مزيفة بعد 24 سا، 3أيام، اسبوع واسبوعين من خضوعها للعملية الجراحية (الجدول-9) و (الشكل-22).

3- الموت الخلوي العصبي:

3-1-دراسة موت الخلايا العصبية باستخدام FJB:

من أجل دراسة حدوث موت الخلايا العصبية في الحصين بعد استئصال الغدة الكظرية على مدار (4 سا، 24 سا، 3أيام،اسبوع واسبوعين). لجأنا الى تقنية خاصة لتلوين الخلايا الميتة تدعى التلوين بصبغة FJB. و هوعبارة عن تلوين خاص للخلايا العصبية الميتة، بغض النظر عن آلية الموت الخلوي. بعد أربع ساعات و 24 سا من استئصال الغدة الكظرية أظهرت نتائج التلوين بصبغة FJB أنه لا توجد أي اثار للموت الخلوي على مستوى الحصين عند كل من الجرذان المستأصلة الغدة الكظرية والجرذان الخاضعة لجراحة مزيفة (الشكل-A23، 'A،E،'E).

بعد ثلاثة أيام من استئصال الغدة الكظرية لاحظنا بضع خلايا عصبية ميتة على مستوى الشفرة العلوية للتلفيف المسنن لحصين الجرذان المستأصلة الغدة الكظرية. غير أنه في المقابل لم نلاحظ أي تغير عند الجرذان الخاضعة لجراحة مزيفة (الشكل-B'23، B،F،'F). وعلاوة على ذلك، بعد اسبوع واحد من خضوع الحيوانات لعملية الاستئصال اظهرت نتائجنا زيادة في عدد الخلايا الميتة عند الحيوانات المستأصلة الغدة (الشكل-C'23،'G). وبقيت الحيوانات الخاضعة لجراحة مزيفة كما هي عليه بغياب تام لأي اثار للموت الخلوي (الشكل-C 23، G).بعد اسبوعين من استئصال الغدة الكظرية، اظهر التلوين بصبغة FJB تطور واضح للموت الخلوي على مستوى الشفرتين العلوية والسفلى للتلفيف المسنن لحصين الجرذان المستاصلة (الشكل-D'23 ،'H). و أنه لجدير بالذكر ان نشير هنا أن التلوين كان اكثر كثافة على مستوى الشفرة العلوية مقارنة بالشفرة السفلية موحيا على وجود تأثير تفاضلي لعملية الاستئصال على كلتا الشفرتين (الشكل 19). وفي الجهة المقابلة كانت نتائج التلوين بصبغة FJB سلبية على مستوى حصين الجرذان الخاضعة لجراحة مزيفة (الشكل-D23 ، H) و (الشكل 24).

3-2-دراسة موت الخلايا العصبية باستخدام المجهر الإلكتروني:

كان الدافع وراء هذه الدراسة التركيبية المجهرية تحديد الآثار المترتبة لغياب هذه الهرمونات على مختلف الخلايا الموجودة على مستوى الحصين بعد خضوع الحيوانات لاستئصال الغدة الكظرية على المدى القصير في نقاط زمنية مختلفة (3أيام،اسبوع واسبوعين). و قد نشر البروفيسور آدم وفريقه في دراسة سابقة أن غياب هذه الهرمونات على المدى الطويل (5 أشهر) يؤدي الى موت عدة أنواع خلوية في مختلف أجزاء الحصين.

أدى الفحص بالمجهر الإلكتروني لمقطع عرضي شديد الدقة لحصين جرذان مستأصلة الغدة الكظرية لمدة ثلاثة أيام الى ملاحظة اضمحلال و تلاشي للخلايا الحبيبية الموجودة على مستوى الشفرة العلوية للتلفيف المسنن حيث بدت بغشاء خلوي غير منتظم وبداية ظهور فجوات على مستوى السيتوبلازم تكدس وتكثف الكروماتين النووي. و المثير للاهتمام أننا لم نلاحظ اي تشوهات خلوية في باقي اجزاء التلفيف المسنن (الشكل-B25، D). وفيما يتعلق بامكانية حدوث تشوهات على مستوى قرن آمون (CA) فان التأثير كان منحصرا على الخلايا الهرمية للمنطقة CA4 (الشكل-26) في حين أن خلايا الهرمية لكل

منCA3، CA1 وخلايا CA2 لم تظهر أي علامات تنكس عصبي بعد ثلاثة أيام من ازالة الغدة الكظرية. الفحص المجهري الالكتروني لحصين الجرذان الخاضعة لجراحة مزيفة لم يكشف عن أي مؤشرات للموت الخلوي في جميع أجزاء الحصين (الشكل-A25 ، 1C، 2A و 2C).

اظهر الفحص المجهري الإلكتروني للحصين بعد اسبوع من ازالة الغدة الكظرية زيادة معتبرة في عدد الخلايا الميتة مقارنة باليوم الثالث. لم تقتصر الظاهرة على الشفرة العلوية للتلفيف المسنن بل انتقلت الى الشفرة السفلية (الشكل-27 A'). وعلى مستوى قرن امون لاحظنا توسع وانتشار للموت الخلوي في المنطقة CA4 (الشكل-27 B'). و لأول مرة لاحظنا ظهور خلايا ميتة ومضمحلة على مستوى الخلايا الهرمية للمنطقة CA3 (الشكل-27 C'). اظهرت نتائجنا انه بعد سبعة ايام من استئصال الغدة الكظرية عدم تأثر منطقة CA1. في الجهة المقابلة الفحص المجهري لحصين الجرذان الخاضعة لجراحة مزيفة لم يظهر اي تشهوات خلوية (الشكل-A27،B و C).

أظهرت نتائجنا انتشار واسع وكثيف للموت الخلوي على مستوى الشفرة العلوية للتلفيف المسنن مقارنة بالشفرة السفلية أين لاحظنا ان هذه الاخيرة اقل تضررا بعد اسبوعين من استئصال الغدة الكظرية. وقد شاهدنا تغيرات في المظهر و ظهور العديد من الفراغات على مستوى هذه الطبقة مما يوحي الى الموت الخلوي وظهور تغيرات تركيبية على مستوى الشفرتين (الشكل-28) أين لاحظنا تكدس وتكثف للكرماوتين النووي الى جانب انكماش وتلاشي الجسم الخلوي موحيا الى حدوث الموت الخلوي المبرمج والنيكروز من جهة و حساسية هدا النوع من الخلايا وسرعة تأثره بغياب الهرمونات الكظرية (الشكل-29). في الجهة المقابلة لاحظنا عند الجرذان الخاضعة لجراحة مزيفة استمرارية ووفرة وتماسك في الخلايا العصبية الحبيبية التي هي عبارة عن خلايا عصبية صغيرة أين تحتل النواة كامل الجسم الخلوي في حين يشغل السيتوبلازم حيز صغير محيط بهذه الأخيرة.

قمنا بتسجيل نفس الملاحظات تقريبا فيما يخص منطقة CA3 لحصين الجرذان المستأصلة حيث شاهدنا حدوث موت واضمحلال الخلايا الهرمية على طول الطبقة الرئيسية من هذه المنطقة اين لاحظنا تكدس الكروماتين النووي وظهور فجوات على مستوى السيتوبلازم حدوث تموجات في الغشاء النووي وتحجم الميتوكوندريا (الشكل 31). في المقابل ظهرت الخلايا الحبيبة للجرذان الغير المستأصلة الغدة الكظرية بشكل طبيعي أين كان الغشاء السيتوبلازمي و الغشاء النووي منتظمين جانب انتشار طبيعي للكروماتين على مستوى النواة. لم تظهر الخلايا الهرمية CA1 أي تشوهات بالنسبة للمجموعتين من الجرذان.

4- تنشيط الخلايا النجمية و الدبقية الصغيرة:

4-1-تنشيط الخلايا الدبقية الصغيرة:

تنشيط الخلايا الدبقية الصغيرة هو واحد من المعالم الكبرى لحدوث الموت الخلوي العصبي. من أجل بحث امكانية تنشيط هذه الخلايا كاستجابة لحدوث الموت الخلوي بعد استئصال الغدة الكظرية على المدى القصير ، اجرينا تقنية التلوين الهيستولوجي المَناعِيَّ المزدوج لكل من الخلايا العصبية باستعمال الجسم المضاد (Neun) و بالنسبة للخلايا الدبقية الصغيرة استخدمنا الجسم المضاد (Iba-1)على مدار (4 سا، 24 سا، 3أيام، اسبوع واسبوعين). بعد أربعة ساعات ويوم واحد من استئصال الغدة الكظرية لم تظهر نتائج التلوين الهيستولوجي المَناعِيَّ باستعمال الجسم المضاد (Iba-1) أي نشاط للخلايا الدبقية الصغيرة سواء عند الجرذان المستأصلة الغدة الكظرية او الجرذان الخاضعة لجراحة مزيفة (الشكل- 32 'A و A).

غيرانه ، بعد ثلاثة أيام لاحظنا تنشيط بعض الخلايا الدبقية الصغيرة في الشفرة العلوية للتلفيف المسنن عند الجرذان المستأصلة الغدة في حين لم تظهر أي علامات لنشاط هذه الخلايا عند الجرذان الخاضعة لجراحة مزيفة (الشكل- 32 'B وB). بعد مرور يوم واحد من إزالة الغدة الكظرية، لاحظنا نشاط الخلايا الدبقية الصغيرة على طول الشفرة العلوية للتلفيف المسنن للحصين دلالة على تطور وزيادة في نشاط هذه الخلايا الدبقية الصغيرة (الشكل- C'32) غير أنه في المقابل، لم نشاهد أي اثار مشابهة لتنشيط الخلايا الدبقية الصغيرة على مستوى حصين الجرذان الخاضعة لجراحة مزيفة (الشكل- C32).

بعد اسبوعين من استئصال الغدة الكظرية اظهرت نتائج التلوين الهيستولوجي المَناعِيَّ المزدوج لكل من الخلايا العصبية (Neun) والخلايا الدبقية الصغيرة (Iba-1) نشاط عالي جدا للخلايا الدبقية الصغيرة على مستوى الحصين وعلى وجه الخصوص في التلفيف المسنن (الشكل- 32 'D) والطبقة التي تدعى lucidum منCA3 (الشكل- H'32) عند مقارنتها مع مناطق مماثلة لحصين الجرذان الخاضعة لجراحة مزيفة (الشكل-32 D وH).

أظهرت نتائج التحليل الكمي لنشاط الخلايا الدبقية الصغيرة الموسومة بالأجسام المضادة (Iba-1) على مستوى حصين الجرذان المستأصلة الغدة الكظرية على عدد كبير ومتزايد لهذه الخلايا النشيطة بعد مرور ثلاثة أيام ($P <0.01$) ،اسبوع ($P <0.001$) و اسبوعين ($P <0.001$) مقارنة بالجرذان الخاضعة لجراحة مزيفة (الشكل-33). بينت نتائج التلوين باستعمال Iba-1 بعد اسبوعين من استئصال الغدة الكظرية عن انتشار تفاضلي لخلايا الدبقية الصغيرة في كافة أنحاء التلفيف المسنن حيث إنه يظهر بشكل مكثف في الطبقة الجزيئية والحبيبية من الشفرة العلوية خاصة عند النهاية الطرفية لهذه الاخيرة أين يظهر تلوين Neun النقص الواضح في الخلايا العصبية مقارنة بالشفرة السفلية (الشكل-34). وجدير بالذكر انه في نفس الوقت أي بعد اسبوعين من استئصال الغدة الكظرية لاحظنا و لأول مرة شريط من الخلايا الدبقية الصغيرة على مستوى الطبقة lucidum منCA3 (الشكل-34). بالمقابل لم نلاحظ اي نشاط لهذه الخلايا في مناطق مماثلة عند الجرذان الخاضعة لجراحة مزيفة بعد اسبوعين من العملية (الشكل-32 G، F، E و H).

2-4-تنشيط الخلايا النجمية:

من أجل دراسة تأثير إزالة الغدة الكظرية على التلوين الهيستولوجي المَناعِيَّ للخلايا النجمية في الحصين على مدار (4 سا، 24 سا، 3أيام،اسبوع واسبوعين) قمنا بالتلوين الهيستولوجي المَناعِيَّ المزدوج لكل من الخلايا العصبية (Neun) والخلايا النجمية (GFAP). من إزالة الغدة الكظرية لم بعد أربع ساعات، يوم واحد وثلاثة أيام نلاحظ اي اختلاف واضح في التلوين الهيستولوجي المَناعِيَّ للخلايا النجمية باستعمال الجسم المضاد (GFAP) على مستوى حصيني الجرذان المستأصلة الغدة و الجرذان الخاضعة لجراحة مزيفة (الشكل-35' A، A، B و'B).

غير انه، بعد مرور اسبوع واحد من استئصال الغدة الكظرية لاحظنا نشاط كبير للخلايا النجمية على مستوى التلفيف المسنن (الشكل-35 'C) ، في حين لم نشاهد اي نشاط لهذه الخلايا عند الجرذان الخاضعة لجراحة مزيفة (الشكل- C35). بعد اسبوعين من خضوع الجرذان لعملية الاستئصال لاحظنا نشاط كبير وواسع للخلايا النجمية في كافة أنحاء التلفيف المسنن (الشكل- 37) حيث شاهدنا خضوع الخلايا النجمية لتغيرات مورفولوجية تجلت في تضخم على مستوى الجسم الخلوي وزيادة في انتاج GFAP (الشكل-D'35). لجدير بالذكر هنا ان نشاط الخلايا النجمية كان اكثر على مستوى الطبقة الجزيئية والمتعددة مقارنة مع الطبقة الخلوية الحبيبية اين كان نشاط هذه الخلايا أقل (الشكل-37).وفيما يخص منطقة CA3 لاحظنا نشاط للخلايا النجمية على مستوى الطبقة المسماة lucidum (الشكل-H'35).

ومن ناحية أخرى، على المستوى الكمي لم يكن هناك فرق كبير في عدد الخلايا النجمية النشيطة في حصين الجرذان المستأصلة و الجرذان الخاضعة لجراحة مزيفة بعد ثلاثة أيام من استئصال الغدة الكظرية. غير انه مع مرور اسبوع واحد من خضوع الحيوانات للعملية الجراحية اظهرت نتائجنا زيادة كبيرة في عدد الخلايا النجمية ($P < 0.001$) وقمنا بتسجيل نفس الملاحظة بعد اسبوعين من عملية الاستئصال عند الجرذان المستأصلة مقارنة بالجرذان الخاضعة لجراحة مزيفة (الشكل-36).

وعلاوة على ذلك، أظهر التلوين الهيستولوجي المَناعِيَّ للخلايا النجمية باستعمال الجسم المضاد (GFAP) نشاط واسع لهذه الخلايا على مستوى منطقة CA4 وغياب تام لنشاطها على مستوى منطقة CA1 في حصين الجرذان المستأصلة و الجرذان الخاضعة لجراحة مزيفة (الشكل-37). من خلال النتائج التي توصلنا اليها فان الجرذان الخاضعة لجراحة مزيفة لم تبدي أي نشاط لهذه الخلايا النجمية على مستوى مختلف أجزاء الحصين كالتلفيف المسنن (الشكل-A35، B، C، D) ومنطقة CA3 (الشكل-E35، F، G و H) وباقي المناطق CA4، CA2 و CA1 (الشكل-37).

لقد كانت فكرة مثيرة للاهتمام والتي طرحت من طرف أحد المراجعين لمنشورنا حيث طلب منا التحقق من تأثير إزالة الغدة الكظرية على نشاط خلايا الدبق على طول المستوى الطولي للحصين إذا ما كان ثابت أم هناك اختلاف في هدا النشاط. وللقيام بذلك قررنا ان نجري التلوين الهيستولوجي المَناعِيَّ المزدوج لكل من الخلايا العصبية (Neun) والخلايا الدبقية الصغيرة (Iba-1) لمقاطع عرضية للمخ على مستويين مختلفين الاول يكون على بعد-4.68 مم والثاني -5.5مم من bregma حسب اطلس باكسينوس و وطسون سنة 2005.

في الواقع تحصلنا على نفس النتائج التي تحصلنا عليها في المستوى -3.7 أين لاحظنا نشاط للخلايا الدبقية الصغيرة على مستوى شفرتي التلفيف المسنن وبشكل أكبر على مستوى الشفرة العلوية لحصين الجرذان المستأصلة (الشكل 34). على غرار ما لاحظناه على المستوى -3.7 لم تظهر نتائجنا اي نشاط للخلايا الدبقية الصغيرة في حصين الجرذان الخاضعة لجراحة مزيفة على المستويين -4.68 مم (الشكل-38) و-5.5مم (الشكل-39). بينت نتائجنا نشاط مماثل لهذه الخلايا الدبقية الصغيرة على المستويين -4.68 مم و -5.5مم لما توصلنا على المستوى -3.7. وفيما يخص المنطقة CA3 لاحظنا نشاط الخلايا الدبقية الصغيرة على مستوى طبقة lucidum المحيطة بطبقة الخلايا الهرمية من CA3 . لم نلاحظ على هذين المستووين اي نشاط لهذه الخلايا النجمية في مختلف اجزاء الحصين بالنسبة الجرذان الخاضعة لجراحة مزيفة.

من أجل بحث نمط تموضع الخلايا الدبقية الصغيرة والخلايا النجمية بالنسبة للخلايا العصبية. اجرينا تقنية التلوين الهيستولوجي المَناعِيَّ الثلاثي لكل من الخلايا العصبية (Neun) ، الخلايا الدبقية الصغيرة (Iba-1) والخلايا النجمية (GFAP) بعد مرور اسبوعين من خضوع الحيوانات عملية استئصال الغدة الكظرية وقد اعطت نتائج الفحص تحت المجهر متحد البؤر تموضع متباين للخلايا الدبقية الصغيرة والخلايا النجمية على مستوى مختلف طبقات التلفيف المسنن (الشكل-40).

5- الإجهاد التأكسدي:

5-1- الجلوتاثيون المرجع (GSH):

الجلوتاثيون المرجع (GSH) هو المصدر الرئيسي للبروتونات لمعظم التفاعلات الكيميائية الحيوية لإزالة سمية الجذور الحرة داخل الخلية. من أجل تحديد تركيز GSH عن طريق فحص اللونية، اعتمدنا على المنحنى المعياري المشكل من قياس امتصاصية تراكيز معيارية معروفة للجلوتاثيون المرجع التي تتراوح بين 1.56 -50 نانومول/مل بدلالة هذه التراكيز نفسها. وعن طريق الاستيفاء من المنحى تم تحديد تركيز GSH في كل عينة (الشكل-41).

كما هو مبين في الجدول-10 والشكل 42. تقييم مستويات هذا العنصر المضاد للأكسدة في جناسة حصين الجرذان المستأصلة مقارنة بالجرذان الخاضعة لجراحة مزيفة على مدار (4 سا، 24سا، 3أيام،اسبوع واسبوعين). لاحظنا انه لم تكن فروق كبيرة التي ترقى ان تكون معنوية احصائيا في مستويات GSH بعد اليوم الأول من الجراحة. غير ان بعد ثلاثة أيام لاحظنا زيادة معتبرة في مستوى GSH ($P < 0.05$) عند الجرذان المستأصلة مقارنة بالجرذان الخاضعة لجراحة مزيفة. وبعد واحد من العملية الجراحية، لا يلاحظ اي فرق معنوي في مستوى GSH عند المجموعتين، غير انه بعد اسبوعين لاحظنا انخفاض معنوي في مستوى GSH عند الجرذان المستأصلة مقارنة بالجرذان الخاضعة لجراحة مزيفة.

5-2- Superoxide dismutase (SOD):

قمنا بقياس نشاط الانزيم المضاد للأكسدة (SOD) باستعمال تقنية فحص اللونية في جناسة حصين الجرذان المستأصلة مقارنة بالجرذان الخاضعة لجراحة مزيفة مدار (4 سا، 24سا، 3أيام،اسبوع واسبوعين). ومن أجل تحديد تركيز (SOD) ، شكلنا منحنى مستوى المعدل الخطي (LR) لتراكيز معيارية معروفة SOD تتراوح بين 0.25 -0.250 وحدة/مل بدلالة هذه التراكيز نفسها. وعن طريق الاستيفاء من المنحى تم تحديد تركيز SOD في كل عينة (الشكل-43). لم تشر نتائجنا الى تغير كبير في نشاط SOD في جناسة حصين الجرذان المستأصلة مقارنة بالجرذان الخاضعة لجراحة مزيفة مدار 4 سا، 24 سا، 3أيام واسبوع عن اجراء الجراحة. ومع ذلك، بعد اسبوعين من القيام بالعملية الجراحية لاحظنا انخفاض معنوي في نشاط انزيم ($P <0.01$) في جناسة حصين الجرذان المستأصلة مقارنة بالجرذان الخاضعة لجراحة مزيفة (الجدول-11) و (الشكل-44).

5-3- Malondialdehyde (MDA):

تعتبر أكسدة الليبيدات الغشائية واحدة من أهم مظاهر اختلال التوازن بين مضادات الأكسدة والجذور الحرة التي يؤدي الاجهاد التأكسدي. لقد حاولنا بحث امكانية حدوث أكسدة الليبيدات على مستوى حصين الجرذان المستأصلة مقارنة بالجرذان الخاضعة لجراحة مزيفة مدار (4سا، 24سا، 3أيام ،اسبوع واسبوعين) ومن أجل تحديد تركيز (MDA) اعتمدنا على المنحنى المعياري المشكل من قياس امتصاص تراكيز معيارية معروفة MDA تتراوح بين 1.56-50 نانومول/مل بدلالة هذه التراكيز نفسها. وعن طريق الاستيفاء من المنحى تم تحديد تركيز MDA في كل عينة (الشكل-45). كما هو موضح في (الجدول-12) و (الشكل-46) لم نلاحظ أي فروق معتبرة في تركيز MDA إلا بعد مرور اسبوعين عن استئصال الغدة الكظرية حيث لا حظنا زيادة كبيرة ومعنوية ($P <0.05$) في مستوى MDA في جناسة حصين الجرذان المستأصلة مقارنة بالجرذان الخاضعة لجراحة مزيفة.

6-سلوك الحيوان:

بناء على ما تحصلنا عليه على المستوى النسيجي والكيميائي الحيوي كنا نعتقد أن هذه التغيرات ستكون لها آثارا على على سلوك الحيوانات، ولبحث هذه الفرضية لجانا لتقنية passive avoidance. تقييم الفترة الكامنة للجرذان المستأصلة مقارنة بالجرذان الخاضعة لجراحة مزيفة على مدار (3أيام، اسبوع واسبوعين) أدى الى ملاحظة زيادة معنوية ($P <0.05$) في الفترة الكامنة للجرذان المستأصلة مقارنة بالجرذان الخاضعة لجراحة مزيفة في اليوم الثالث بعد الجراحة (الجدول-13A) و (الشكل-A 47). وعلاوة على ذلك، في اليوم السابع كانت الزيادة معتبرة في الفترة الكامنة ($P<0.05$) للجرذان المستأصلة مقارنة بالجرذان الخاضعة لجراحة مزيفة. بعد مرور اسبوع(الجدول-13B) و (الشكل-B 47) و اسبوعين (الجدول-C13) و (الشكل-C 47) من الجراحة، شاهدنا زيادة كبيرة ومعنوية في الفترة الكامنة عند الجرذان المستأصلة مقارنة بالجرذان الخاضعة لجراحة مزيفة ($P <0.05$).

مناقشة:

كان الهدف من هذه الدراسة بحث آثار استئصال الغدة الكظرية على المدى القصير على مستويات السيتوكينات الالتهابية IL-6 IL-1β و TNF-α، استجابة الخلايا الدبقية الصغيرة والخلايا النجمية موت الخلايا العصبية وكذلك مؤشرات الإجهاد التأكسدي GSH، SOD و MDA على مدار (4سا, 24سا, 72سا،اسبوع واسبوعين) في الحصين وامكانية تأثير الاستئصال على سلوك جرذان الويستار.

وأظهرت نتائجنا انخفاضا كبيرا في مستويات الكورتيكوستيرون 4سا بعد استئصال الغدة الكظرية واستمر هذا الانخفاض بعد 24سا من التجربة، 3 أيام، اسبوع واسبوعين عند الجرذان المستأصلة الغدة الكظرية مقارنة مع الجرذان الخاضعة لجراحة مزيفة. ولقد لوحظ الانخفاض الكبير في الكورتيكوستيرون بعد استئصال الغدة الكظرية على المدى الطويل في العديد من الدراسات (Gould et al., 1990; Jaarsma et al., 1992; Sloviter et al., 1989, 1993a, 1993b; Spanswick et al., 2011). فيما يتعلق السيتوكينات الالتهابية بمستويات IL-1β و IL-6، أظهرت نتائجنا ارتفاع عابر يستمر لمدة ثلاثة أيام على مستوى حصين الجرذان المستأصلة مقارنة مع الجرذان المزيفة. بعد واحد من استئصال الغدة الكظرية، لاحظنا عودة الارتفاع مستوى الجرذان الخاضعة لجراحة مزيفة. أظهرت كل من الجرذان المستأصلة و الجرذان الخاضعة لجراحة مزيفة ارتفاع كبيرفي مستويات IL-1β و IL-6 مقارنة مع الجرذان الشاهدة. ويمكن أن يعزى الفرق الكبير بين الجرذان الشاهدة و الجرذان الخاضعة لجراحة مزيفة اجهاد العملية الجراحية. غير انه لا يمكن أن يعزى الفرق الكبير بين الجرذان المستاصلة و الجرذان الخاضعة لجراحة مزيفة سوى تأثير استئصال الغدة الكظرية.

تم التأكد من حدوث موت الخلايا العصبية في الحصين بعد استئصال الغدة الكظرية عن طريق تلوين Fluoro-Jade B والمجهر الإلكتروني. وأظهرت نتائجنا حدوث الموت الخلوي في الطبقة الحبيبية من التلفيف المسنن بعد استئصال الغدة الكظرية بعد ثلاثة أيام من اجراء العملية الجراحية حيث لاحضنا القليل من الخلايا الملونة بصبغة FJB في الشفرة العلوية. أظهر الفحص بالمجهر الالكتروني للشفرة العلوية للتلفيف المسنن تشوهات خلوية تجلت في تكدس الكروماتين النووي وغشاء سيتوبلازمي غير منتظم وهذه الملاحظات تتفق تماما مع لاحظه العديد من فرق (Sloviter et al., 1989, 1993a, 1993b) اين لاحظوا ان موت الخلايا الحبيبية يحدث أربعة أيام من استئصال الغدة الكظرية. و ذلك، توصلنا نفس النتيجة التي تحصلت عليها كونراد ومساعديها التي تتمثل في عدم ظهور أي علامات اضمحلال على مستوى التلفيف المسنن للحصين الا بعد مرور ثلاثة أيام من استئصال الغدة الكظرية(Conrad and Roy, 1993; Sloviter et al., 1993a, 1993b). مما يعطي الانطباع بأن النموذج الحالي للتنكس العصبي على أنه نموذج انتقائي للموت الحصري للخلايا الحبيبية. أظهرت النتائج الفوق البنيوية موت الخلايا الهرمية على مستوى CA4 و CA3 بعد واحد. بعد اسبوعين من استئصال الغدة الكظرية لاحظنا تطور موت الخلايا في جميع أنحاء الشفرة العلوية من التلفيف المسنن. هذه النتائج تتماشى مع تلك التي نشرها

سبانزويك ومساعديه (Spanswick et al., 2011) فيما يخص حدوث الموت الخلوي في جميع أنحاء الطبقة الحبيبية من التلفيف المسنن بعد اسبوعين من استئصال الغدة الكظرية باستخدام تلوين FJB.

و ذلك لاحظنا زيادة في موت الخلايا الهرمية على مستوى المنطقتين CA3 و CA4 حيث لوحظ المزيد من الخلايا المتضررة وهذه النتائج تتفق مع ملاحظة سابولسكي ومساعديه (Sapolsky et al., 1991) حيث لاحظوا موت خلوي يصل 19٪ من الخلايا الهرمية لمنطقة CA4. وفي وقت لاحق، أظهر البروفيسور أدم وفريقه المتكون من إسلام وآخرون سنة 1999 Islam et al.1999 تأثر وموت واضح لمجموعات مختلفة من الخلايا العصبية جراء عملية استئصال الغدة الكظرية على المدى الطويل (5 أشهر). نتائجنا لا تتماشى مع الملاحظات التي قدمتها فرق بحث مختلفة حيث وجدوا أن كلا من استئصال الغدة الكظرية على المدى القصير والطويل تسبب في الموت الانتقائي للخلايا الحبيبية للتلفيف المسنن (Conrad and Roy, 1993; Sloviter et al., 1993a, 1993b). نعتقد أن السبب في ذلك قد يعود الحساسية سلالات مختلفة من الحيوانات أو قد تكون حساسية التقنيات المستخدمة في مختبرات مختلفة. و ذلك الفحص الدقيق للتلفيف المسنن يشير إلى أن استئصال الغدة الكظرية يؤثر بشكل تفاضلي على الشفرة العلوية والسفلية للتلفيف المسنن وتشير إلى أن الخلايا الحبيبية للشفرة العلوية من التلفيف المسنن أكثر تحسسا لاستئصال الغدة الكظرية. ونخلص في دراستنا الحالية بتعرض مختلف الخلايا العصبية للموت الخلوي جراء استئصال الغدة الكظرية من جهة وبالتالي عدم انتقائية الموت الخلوي في النموذج الحالي. و ذلك، فإن هذه النتائج قد تفتح إمكانية التحقيق في حدوث موت خلوي في أجزاء أخرى من الدماغ.

تعتبر مسالة معرفة الوقت الدقيق لبدأ حدوث الموت الخلوي في الحصين موضوع نقاش واهتمام العلماء وذلك يعود لمحاولة الربط بين ظاهرتي الزيادة في مستويات السيتوكينات الالتهابية و الموت الخلوي والوصول نتيجة ما إذا كانت هذه الزيادة في مستويات السيتوكينات تسبق موت الخلايا أو أنه تكون كنتيجة له. لهذا السبب تتوافق النتائج التي توصلنا إليها مع العديد من الملاحظات التي أبداها الكثير من الباحثين بأن الموت المبكر للخلايا يحدث على الأقل بعد ثلاثة أيام من استئصال الغدة الكظرية (Gould et al., 1990; Nichols et al., 2005; Sloviter et al., 1989; Spanswick et al., 2011; Stienstra et al., 1998). ومع ذلك، قلة من الباحثين أشاروا ان الموت الخلوي يحدث في اليوم الثاني بعد استئصال الغدة الكظرية(Jaarsma et al., 1992; Nichols et al., 2005; Sloviter et al., 1993a). ومن المثير للاهتمام أننا لاحظنا أن الارتفاع المبكر للسيتوكينات الالتهابية IL-6 IL-1β و TNF-α يسبق حدوث الموت الخلوي. وتشير مجمل النتائج التي توصلنا إليها أن موت الخلايا كان مسبوق بزيادة في مستويات هذه السيتوكينات الالتهابية. وقد نشرت نتائج مماثلة في نماذج حيوانية مختلفة كنقص التروية (Rothwell, 2003; Zhu et al., 2006a)، الإصابة الجراحية (Tchelingerian et al., 1993)، TMT (Trimethyltin) ، KA (Kainic acid) (حمض الكاينيك) (Pearson et al., 1999a) و cis-2,4-methanoglutamate (MGlu)(بيرسون وآخرون، 1999a) حيث كانت الزيادة المبكرة لمختلف السيتوكينات الالتهابية تسبق الموت الخلوي.

ولقد اظهرت بوضوح دراستين علميتين المساهمة المباشرة IL-1β في الموت العصبي(Rothwell, 2003). حيث جاء في الأولى ان حقن جرعات منخفضة من IL-1β في البطينين الايمن والايسر للمخ أو في برنشيم المخ لفئران محقونة مسبقا بسموم عصبية يؤدي تفاقم الضرر بشكل ملحوظ. وأظهرت الدراسة الثانية ضخ كل من مثبط مستقبلات IL-1β و السم العصبي N-Methyl-D-aspartate (NMDA) يؤدي تثبيط سمية الاخير وبالتالي لا يلاحظ حدوث للموت خلوي

(Lawrence et al., 1998b; Panegyres and Hughes, 1998). وعلاوة على ذلك، يلعب IL-1β دورا هاما في تفاقم الموت العصبي الحاد الناجم عن نقص التروية، صدمات الرأس والسكتة الدماغية. و ذلك، فإنه يدخل في باثولوجيا العديد من الامراض كالتصلب المتعدد، مرض الزهايمر وغيرها من الأمراض المزمنة التي تصيب الجهاز العصبي المركزي (Allan and Rothwell, 2001b; Boutin et al., 2001b; Griffin and Mrak, 2002b; Pearson et al., 1999a). وفيما يخص IL-6 عثر على مستويات مرتفعة له في مصل الدم و السائل المخي الشوكي لمرضى التصلب العصبي المتعدد في انحاء وقوع التصلبات العصبية (Malmeström et al., 2006; Stelmasiak et al., 2001) وفي نماذج تجريبية للمناعة الذاتية لالتهاب المخ (Gijbels et al., 1990). العثور على تراكيز عالية للستوكين IL-6 أثناء المرحلة الحادة من نقص التروية الدماغية (Berti et al., 2002a). و عند مرضى الزهايمر، يزداد IL-6 في محيط تكتلات صفائح الأميلويد على مستوى النسيج العصبي وفي السائل المخي الشوكي للمصابين ب المرض (Blum-Degen et al., 1995; Lucin and Wyss-Coray, 2009). توافقا مع الزيادة المبكرة IL-6 التي لوحظت في النموذج العصبي الحالي، أظهرت العديد من الدراسات نفس النمط من الزيادة أين ا لوحظ ارتفاع في مستوياتTNF-α في مراحل مبكرة في العديد من الاصابات العصبية (Berti et al., 2002b; Chiu et al., 2015; Liu et al., 2015; Zhu et al., 2006b).

وباختصار، ربط النتائج الثلاثة السابقة فيما بينها بشأن الكورتيزون، مستويات السيتوكينات وموت الخلايا العصبية بعد استئصال الغدة الكظرية على المدى القصير يقودنا ان استنزاف مستويات الكورتيزون بعد إزالة الغدة الكظرية لم يحفز مباشرة موت الخلايا العصبية بل رافقه زيادة فورية في السيتوكينات الالتهابية IL-1β، IL-6 و TNF-α. ثم تلى الارتفاع العابر في هذه المكونات الالتهابية مباشرة موت الخلايا الحبيبية للتلفيف المسنن لحصين الجرذان المستأصلة مقارنة مع الجرذان الخاضعة لجراحة مزيفة. نحن نعتقد أن تحريض موت الخلايا كان نتيجة لكل من زيادة هذه السيتوكينات التي ثبت حد كبير مساهمتها في تفاقم الضرر العصبي من جانب واحد واستنزاف الكورتيزون التي ثبت أنه يلعب دور رئيسي في بقاء الخلايا العصبية الحصينية وتاثيره المباشر في إنتاج العوامل الأساسية لبقاء الخلايا العصبية الحصين على الجانب الآخر. كما أظهرت عدة فرق أن إزالة الغدة الكظرية تسبب في استنفاذ إنتاج العديد من عوامل النمو مثل إنتاج نيوروتروفين-3 (NT-3)، مشتق عامل النمو المخي (BDNF)، عامل نمو الأعصاب (NGF) (Barbany and Persson, 1992; Nichols et al., 2005; Smith et al., 1995; Vollmayr et al., 2001).

وذلك، أظهر البروفسور أدم وزملاؤه أن مستويات IGF-1 قد انخفضت بعد استئصال الغدة الكظرية على المدى الطويل. ان ربط جميع النتائج المذكورة أعلاه قد يقودنا أن نقترح أن استئصال الغدة الكظرية يؤدي الزيادة في مستويات كل من IL-1β، IL-6 و TNF-α التي بدورها قد تساهم في الشروع في سلسلة بيولوجية مسؤولة عن موت الخلايا العصبية الحصينية بعد ثلاثة أيام من الاستئصال.

تنشيط الخلايا الدبقية الصغيرة هي واحدة من العلامات الرئيسية للموت العصبي (Lucin and Wyss-Coray, 2009). على غرار غولد ومساعديها (Gould et al., 1990) أظهرت نتائجنا موت الخلايا يبدأ في الشفرة العلوية من التلفيف المسنن بعد ثلاثة أيام من استئصال الغدة الكظرية. لوحظت الخلايا الدبقية الصغيرة النشطة بعد ثلاثة أيام من الاستئصال على مستوى الطبقات الجزيئية والحبيبية للشفرة العلوية للتلفيف المسنن. بعد واحد من استئصال الغدة الكظرية لاحظنا زيادة في الموت الخلوي على مستوى الشفرة العلوية ويوافقها زيادة في عدد الخلايا الدبقية الصغيرة النشيطة. بعد اسبوعين من استئصال

الغدة الكظرية أظهرنا غزو كامل للتلفيف المسنن للخلايا الدبقية الصغيرة المنشطة. وتماشيا مع هذه النتائج أظهر التحليل الكمي زيادة تدريجية في عدد الخلايا الدبقية الصغيرة في الحصين انطلاقا من اليوم الثالث مع زيادة تدريجية بعد مرور اسبوع واسبوعين من استئصال الغدة الكظرية. لاحظ جارسما ومساعديه(Jaarsma et al., 1992) باستخدام تلوين التشريب الفضي، أرجيروفيليا على مستوى الجسم والتشعبات الخلوية في الطبقة الحبيبية والجزيئية على التوالي وفي المنطقة الطرفية لألياف موسي Mossy fibers.

وفيما يتعلق قرن أمون، بعد اسبوعين من استئصال الغدة الكظرية لاحظنا غزو منطقة CA4 بواسطة الخلايا الدبقية الصغيرة النشيطة. في المقابل، لم يلاحظ أي اثار لهذه الخلايا على مستوى الخلايا الهرمية CA3، CA2 و CA1. ومع ذلك، لاحظنا الخلايا الدبقية الصغيرة النشيطة على طول الطبقة المتوسطة من CA3. أظهرت دراستنا الحالية وجود علاقة قوية بين موت الخلايا وتنشيط الخلايا الدبقية الصغيرة على مر الزمن. مجملا من خلال الملاحظات التي قمنا بها يمكن القول انه توجد علاقة بين تفاعل الدبقية الصغيرة والموت الخلوي. ومن المعروف عن وجود ارتباط وثيق بين إصابات المخ و الزيادة في نشاط الخلايا النجمية (Fiedorowicz et al., 2001). تستجيب الخلايا النجمية بشكل كبير للإصابات والامراض المخية عن طريق زيادة كل من حجمها وحجم تشعباتها، وهي ظاهرة تعرف باسم النجمية المتفاعلة التي تمثل استجابة نمطية ملحوظة لإصابات الجهاز العصبي المركزي (Penkowa et al., 2008). في هذه الدراسة، لوحظ تنشيط الخلايا النجمية في جميع أنحاء التلفيف المسنن بعد واحد من استئصال الغدة الكظرية.

ومع ذلك، وجد كروجرز ومساعديه في وقت سابق تنشيط الخلايا النجمية في اليوم الثالث بعد استئصال الغدة الكظرية (Krugers et al., 1994). على الرغم من أننا لم نتمكن من ملاحظة النشاط في اليوم الثالث، فمن الممكن أن تفعيل الخلايا النجمية يحدث بين يوم 3 و 7 بعد استئصال الغدة الكظرية. لاحظنا في دراستنا الحالية ظهور بارز للخلايا النجمية النشيطة على مستوى الطبقات الجزيئية ومتعددة الأشكال من التلفيف المسنن في حين شاهدنا غيابه في باقي مناطق الحصين. نتائجنا تتماشى مع تلك النتائج التي أظهرت ان الخلايا النجمية تغزو التلفيف المسنن بعد حقن السم العصبي TMT الذي بدوره يحدث موت انتقائي للخلايا العصبية الحبيبية (Fiedorowicz et al., 2001). تنشيط الخلايا النجمية بعد واحد على مستوى التلفيف المسنن أظهرت نتائجنا نشاط تدريجي للخلايا النجمية على مستوى كل من CA4 و CA3 من الحصين بعد اسبوعين من استئصال الغدة الكظرية. وتماشيا مع هذه النتائج أظهر التحليل الكمي زيادة كبيرة في عدد الخلايا النجمية في الحصين من اسبوع واحد حتى اسبوعين بعد استئصال الغدة الكظرية.

ومن المعروف أن الخلايا النجمية في تفاعل وظيفي مستمر مع الخلايا الدبقية الصغيرة، وهذا التفاعل مهم خلال الظروف المرضية (von Bernhardi and Ramirez, 2001; Verderio and Matteoli, 2001). ولقد لاحظنا ان الموت التدريجي للخلايا الحبيبية في النموذج الحالي يرتبط طرديا مع نشاط الخلايا الدبقية الصغيرة و النجمية في التلفيف المسنن على مدى اسبوعين. أظهرت نتائجنا تنشيط الخلايا الدبقية الصغيرة في اليوم الثالث يليها تفعيل الخلايا النجمية في اليوم السابع بعد استئصال الغدة الكظرية. هذه النتائج تتماشى مع ما تم العثور عليه في نماذج تنكس عصبي مختلفة حيث تم العثور اولا على تنشيط الخلايا الدبقية الصغيرة كاستجابة لتلف الخلايا العصبية يليها تنشيط الخلايا النجمية (Frautschy et al., 1998; Gahtan and Overmier, 1999; Matsumoto et al., 1992; Reali et al., 2005). وبصورة عامة ربط هذه النتائج مع بعضها يسوقنا القول بحدوث تفاعل بين هذين النوعين من الخلايا الدبقية استجابة لحدوث التلف العصبي من جهة واعتبار

ان الخلايا الدبقية الصغيرة قوة دافعة لتوظيف الخلايا النجمية. عادة يكون الإجهاد التأكسدي نتاج لتراكم أو ارتفاع مفرط لأنواع الأوكسجين التفاعلية (ROS) من جهة وانخفاض الدفاعات التؤكسدية من جهة اخرى داخل الخلية (Sies, 1997). كنتيجة لموت الخلايا العصبية، عندما تتنشط الخلايا الدبقية الصغيرة وظيفيا تزيد في صناعة العديد من الإنزيمات التؤكسدية مثل محفز(nitric oxide synthase (iNOS مما يؤدي اختلال في التوازن بين إنتاج الجذور الحرة والدفاعات المضادة للأكسدة (Tran et al., 1997).

وأظهرت نتائجنا حالة من الإجهاد التأكسدي تجلت في انخفاض الجلوتاثيون (GSH) بعد اسبوعين من استئصال الغدة الكظرية. و ذلك، انخفاض كبير في نشاط SOD. وعلى النقيض من انخفاض الدفاعات المضادة للأكسدة،لاحضنا زيادة معتبرة في تركيز مالونديالدهيد (MDA). هذا الاختلال، الذي لوحظ بعد اسبوعين من استئصال الغدة الكظرية، يعكس حالة من الاكسدة التي قد تنتج عن الخلايا الدبقية المنشطة. وقد لاحظ سوغاما ومساعديه سنة 2013 ارتفاع في تركيز iNOS في الخلايا الدبقية الصغيرة النشيطة بعد من استئصال الغدة الكظرية ملمحا ان هذه الخلايا تعتبر كمصدر للجذور الحرة في هذا النموذج (Sugama et al., 2013) . وتتفق نتائجنا مع المنشورات التي تبين أن العديد من النماذج العصبية كشفت عن وجود تلازم بين التهاب النسيج العصبي الذي يرافقه تنشيط خلايا الدبق وحالة من الإجهاد التأكسدي (Zhu et al., 2004).

الآليات الكامنة وراء تلف الخلايا بعد استئصال الغدة الكظرية ليست واضحة. لقد اقترحنا في السابق إمكانية أن الهرمونات القشرية التي تنتجها الغدة الكظرية قد تكون لها آثار مباشرة على بقاء الخلايا العصبية للحصين. قد تموت الخلايا العصبية للحصين في حالة عدم ارتباط هذه الهرمونات القشرية الكظرية بالمستقبلات الخاصة بها مينيرالوكورتيكويدز (النوع الأول) و/أو جلايكورتيكود (النوع الثاني) (Adem et al., 1994; Islam et al., 1999). وفي وقت لاحق، هو ومساعدوه سنة 1997. (Hu et al. 1997) لاحظوا أن موت الخلايا الحبيبية بعد استئصال الغدة الكظرية كان مصحوبا بسلبية الوسم المناعي لمستقبلات جلايكورتيكويد في طبقة الخلايا الحبيبية (Hu et al. 1997).لقد اقترحنا سابقا أن غياب هرمونات القشرة الكظرية بعد استئصال الغدة الكظرية قد يؤدي توقف تنشيط عامل (عوامل) اساسية لبقاء الخلايا العصبية للحصين أو على مستوى أنسجة أخرى (Adem et al., 1994; Islam et al., 1999). يمكن التكهن بأنه في العديد من الأمراض العصبية مثل مرض الزهايمر انه قد يؤدي الانخفاض المزمن لهرمونات الغدة الكظرية و/أو انخفاض مستقبلاتها آليات التهابية تؤدي تنكس عصبي لخلايا الحصين (Heuser and Lammers, 2003; Landfield, 1978; Landfield et al., 1978; McEwen, 1997; Woulfe et al., 2002)

خلاصة:

ظهرت دراستنا أن استئصال الغدة الكظرية المزدوج على المدى القصير يؤدي زيادة مبكرة في السيتوكينات الالتهابية يليها موت الخلايا العصبية وتنشيط الخلايا الدبقية وكذلك الإجهاد التأكسدي. وفي بناء على كله يمكننا من أن نقترح ان ظهور المكونات الالتهابية في وقت مبكر قد يساهم في الشروع في سلسلة بيولوجية مسؤولة عن موت الخلايا العصبية الحصينية في النموذج الحيواني العصبي الحالي. وتشير هذه النتائج أن الآليات الالتهابية تسبق الموت الخلوي العصبي وتنشيط الدبقية.

REFERENCES

1-Research Articles:

1. Adam, M. P. Miller, Lindsey C. Vedder, L. Matthew Law.,David M. Smith. (2014). Cues, context, and long-term memory: the role of the retrosplenial cortex in spatial cognition. Front Hum Neurosci.; 8: 586.
2. Adem, A., Islam, A., Bogdanovic, N., Carlström, K., and Winblad, B. (1994). Loss of neurones after long-term adrenalectomy in the adult rat hippocampal formation. Neuroreport *5*, 2285–2288.

3. Agostinho, P., Cunha, R.A., and Oliveira, C. (2010). Neuroinflammation, oxidative stress and the pathogenesis of Alzheimer's disease. Curr. Pharm. Des. *16*, 2766–2778.

4. Ahlander-Luttgen, M., Madjid, N., Schott, P.A., Sandin, J., Ögren, S.O. (2003). Analysis of the role of the 5-HT1B receptor in spatial and aversive learning in the rat.Neuropsychopharmacology.1642-1655

5. Allan, S.M., and Rothwell, N.J. (2001). Cytokines and acute neurodegeneration. Nat. Rev. Neurosci. *2*, 734–744.

6. Allan, S.M., Parker, L.C., Collins, B., Davies, R., Luheshi, G.N., and Rothwell, N.J. (2000). Cortical cell death induced by IL-1 is mediated via actions in the hypothalamus of the rat. Proc. Natl. Acad. Sci. U. S. A. *97*, 5580–5585.

7. Amaral, D. G., Scharfman, H. E., Lavenex, P. (2007). The dentate gyrus: fundamental neuroanatomical organization (dentate gyrus for dummies). Prog. Brain Res. 163, 3–22

8. Apelt, J., and Schliebs, R. (2001). Beta-amyloid-induced glial expression of both pro- and anti-inflammatory cytokines in cerebral cortex of aged transgenic Tg2576 mice with Alzheimer plaque pathology. Brain Res. *894*, 21–30.

9. Arszovszki, A., Borhegyi, Z., Klausberger, T. (2014). Three axonal projection routes of individual pyramidal cells in the ventral CA1 hippocampus. Front Neuroanat. 2014 Jun 25;8:53.

10. Auron, P.E., Webb, A.C., Rosenwasser, L.J., Mucci, S.F., Rich, A., Wolff, S.M., and Dinarello, C.A. (2007). Nucleotide sequence of human monocyte

interleukin 1 precursor cDNA. Proc. Natl. Acad. Sci. USA 1984. 81: 7907-7911. J. Immunol. Baltim. Md 1950 *178*, 5413–5417.

11. Babateen O, Korol SV, Jin Z, Bhandage AK, Ahemaiti A, Birnir B. (2017). Liraglutide modulates GABAergic signaling in rat hippocampal CA3 pyramidal neuronspredominantly by presynaptic mechanism. BMC Pharmacol Toxicol. Dec 16;18(1):83.

12. Barbany, G., and Persson, H. (1992). Regulation of Neurotrophin mRNA Expression in the Rat Brain by Glucocorticoids. Eur. J. Neurosci. *4*, 396–403.

13. Bauer, S., Kerr, B.J., and Patterson, P.H. (2007). The neuropoietic cytokine family in development, plasticity, disease and injury. Nat. Rev. Neurosci. *8*, 221–232.

14. Benedek, G., Zhang, J., Nguyen, H., Kent, G., Seifert, H., Vandenbark, A.A., Offner, H. (2017). Novel feedback loop between M2 macrophages/microglia and regulatory B cells in estrogen-protected EAE mice.J Neuroimmunol. 2017 Apr 15;305:59-67. doi: 10.1016/j.jneuroim.2016.12.018. Epub Jan 28.

15. Berliner, J.A., and Heinecke, J.W. (1996). The role of oxidized lipoproteins in atherogenesis. Free Radic. Biol. Med. *20*, 707–727.

16. Beutler, B., Cerami, A. (1988).Tumor necrosis, cachexia,shock, and inflammation: A common mediator. Ann. Rev.Biochem. 57: 505-518.

17. Berti, R., Williams, A.J., Moffett, J.R., Hale, S.L., Velarde, L.C., Elliott, P.J., Yao, C., Dave, J.R., and Tortella, F.C. (2002). Quantitative real-time RT-PCR analysis of inflammatory gene expression associated with ischemia-reperfusion brain injury. J. Cereb. Blood Flow Metab. Off. J. Int. Soc. Cereb. Blood Flow Metab. *22*, 1068–1079.

18. Betz, A.L., Schielke, G.P., and Yang, G.Y. (1996). Interleukin-1 in cerebral ischemia. Keio J. Med. *45*, 230–237; discussion 238.

19. Blasko, I., Marx, F., Steiner, E., Hartmann, T., and Grubeck-Loebenstein, B. (1999). TNFalpha plus IFNgamma induce the production of Alzheimer beta-

amyloid peptides and decrease the secretion of APPs. FASEB J. Off. Publ. Fed. Am. Soc. Exp. Biol. *13*, 63–68.

20. Block, M.L., and Hong, J.-S. (2005). Microglia and inflammation-mediated neurodegeneration: multiple triggers with a common mechanism. Prog. Neurobiol. *76*, 77–98.

21. Blum-Degen, D., Müller, T., Kuhn, W., Gerlach, M., Przuntek, H., and Riederer, P. (1995). Interleukin-1 beta and interleukin-6 are elevated in the cerebrospinal fluid of Alzheimer's and de novo Parkinson's disease patients. Neurosci. Lett. *202*, 17–20.

22. Bondy, S.C., and Lee, D.K. (1993). Oxidative stress induced by glutamate receptor agonists. Brain Res. *610*, 229–233.

23. Botchkina, G.I., Meistrell, M.E., Botchkina, I.L., and Tracey, K.J. (1997). Expression of TNF and TNF receptors (p55 and p75) in the rat brain after focal cerebral ischemia. Mol. Med. Camb. Mass *3*, 765–781.

24. Boutin, H., LeFeuvre, R.A., Horai, R., Asano, M., Iwakura, Y., and Rothwell, N.J. (2001). Role of IL-1alpha and IL-1beta in ischemic brain damage. J. Neurosci. Off. J. Soc. Neurosci. *21*, 5528–5534.

25. Bradley, J.R. (2008). TNF-mediated inflammatory disease. J. Pathol. *214*, 149–160.

26. Brown, A.M., and Ransom, B.R. (2007). Astrocyte glycogen and brain energy metabolism. Glia *55*, 1263–1271.

27. Bruijn, L.I., Becher, M.W., Lee, M.K., Anderson, K.L., Jenkins, N.A., Copeland, N.G., Sisodia, S.S., Rothstein, J.D., Borchelt, D.R., Price, D.L., et al. (1997). ALS-linked SOD1 mutant G85R mediates damage to astrocytes and promotes rapidly progressive disease with SOD1-containing inclusions. Neuron *18*, 327–338.

28. Burgess, N., Maguire, E.A., O'Keefe, J. (2002). The human hippocampus and spatial and episodic memory. Neuron. 15;35(4):625-41.

29. Bushong, E.A., Martone, M.E., and Ellisman, M.H. (2003). Examination of the relationship between astrocyte morphology and laminar boundaries in the molecular layer of adult dentate gyrus. J. Comp. Neurol. *462*, 241–251.

30. Butterfield, D.A., Castegna, A., Lauderback, C.M., and Drake, J. (2002). Evidence that amyloid beta-peptide-induced lipid peroxidation and its sequelae in Alzheimer's disease brain contribute to neuronal death. Neurobiol. Aging *23*, 655–664.

31. Buttini, M., Appel, K., Sauter, A., Gebicke-Haerter, P.J., and Boddeke, H.W. (1996). Expression of tumor necrosis factor alpha after focal cerebral ischaemia in the rat. Neuroscience *71*, 1–16.

32. Campbell, I.L., Abraham, C.R., Masliah, E., Kemper, P., Inglis, J.D., Oldstone, M.B., and Mucke, L. (1993). Neurologic disease induced in transgenic mice by cerebral overexpression of interleukin 6. Proc. Natl. Acad. Sci. U. S. A. *90*, 10061–10065.

33. Cao B, Passos IC, Mwangi B, Amaral-Silva H, Tannous J, Wu MJ, Zunta-Soares GB1, Soares JC. (2017). Hippocampal subfield volumes in mood disorders. Mol Psychiatry. 22(9):1352-1358. doi: 10.1038/mp.2016.262. Epub 2017 Jan 24

34. Claiborne, B.J., Amaral, D.G., Cowan, W.M. (1990). "A quantitative three-dimensional analysis of granule cell dendrites in the rat dentate gyrus". The Journal of Comparative Neurology. 206–219.

35. Cardenas, H., and Bolin, L.M. (2003). Compromised reactive microgliosis in MPTP-lesioned IL-6 KO mice. Brain Res. *985*, 89–97.

36. Carson, M.J., Doose, J.M., Melchior, B., Schmid, C.D., and Ploix, C.C. (2006). CNS immune privilege: hiding in plain sight. Immunol. Rev. *213*, 48–65.

37. Carswell, E.A., Old, L.J., Kassel, R.L., Green, S., Fiore, N., and Williamson, B. (1975). An endotoxin-induced serum factor that causes necrosis of tumors. Proc. Natl. Acad. Sci. U. S. A. *72*, 3666–3670.

38. Chance, B., Sies, H., and Boveris, A. (1979). Hydroperoxide metabolism in mammalian organs. Physiol. Rev. *59*, 527–605.

39. Chen Y, Swanson R A. (2003). Astrocytes and Brain Injury. Journal of Cerebral Blood Flow & Metabolism 23:137–149.

40. Chiang, C.S., Stalder, A., Samimi, A., and Campbell, I.L. (1994). Reactive gliosis as a consequence of interleukin-6 expression in the brain: studies in transgenic mice. Dev. Neurosci. *16*, 212–221.

41. Chiu, K.M., Wu, C.C., Wang, M.J., Lee, M.Y., and Wang, S.J. (2015). Protective Effects of Bupivacaine against Kainic Acid-Induced Seizure and Neuronal Cell Death in the Rat Hippocampus. Biol. Pharm. Bull. *38*, 522–530.

42. Ciesielska, A., Joniec, I., Kurkowska-Jastrzebska, I., Cudna, A., Przybyłkowski, A., Członkowska, A., and Członkowski, A. (2009). The impact of age and gender on the striatal astrocytes activation in murine model of Parkinson's disease. Inflamm. Res. Off. J. Eur. Histamine Res. Soc. Al *58*, 747–753.

43. Conrad, C.D., and Roy, E.J. (1993). Selective loss of hippocampal granule cells following adrenalectomy: implications for spatial memory. J. Neurosci. Off. J. Soc. Neurosci. *13*, 2582–2590.

44. Conrad, C.D., Roy, E.J.(1995). Dentate gyrus destruction and spatial learning impairment after corticosteroid removal in young and middle-aged rats. Hippocampus. 5(1):1-15.

45. Craft, J.M., Watterson, D.M., Frautschy, S.A., and Van Eldik, L.J. (2004). Aminopyridazines inhibit beta-amyloid-induced glial activation and neuronal damage in vivo. Neurobiol. Aging *25*, 1283–1292.

46. Curello, S., Ceconi, C., Bigoli, C., Ferrari, R., Albertini, A., and Guarnieri, C. (1985). Changes in the cardiac glutathione status after ischemia and reperfusion. Experientia *41*, 42–43.

47. ***D***almau, I., Finsen, B., Zimmer, J., González, B., and Castellano, B. (1998). Development of microglia in the postnatal rat hippocampus. Hippocampus *8*, 458–474.

48. Davalos, D., Grutzendler, J., Yang, G., Kim, J.V., Zuo, Y., Jung, S., Littman, D.R., Dustin, M.L., and Gan, W.-B. (2005). ATP mediates rapid microglial response to local brain injury in vivo. Nat. Neurosci. *8*, 752–758.David, G.A., Helen, E. S, Pierre, L. (2007). The dentate gyrus: fundamental neuroanatomical organization (dentate gyrus for dummies). Prog Brain Res. 3–22.

49. Davies, K.J. (2000). Oxidative stress, antioxidant defenses, and damage removal, repair, and replacement systems. IUBMB Life *50*, 279–289.

50. Davis, J.B., McMurray, H.F., and Schubert, D. (1992). The amyloid beta-protein of Alzheimer's disease is chemotactic for mononuclear phagocytes. Biochem. Biophys. Res. Commun. *189*, 1096–1100.

51. Day JJ., Jones JL., Carelli RM. (2011). Nucleus accumbens neurons encode predicted and ongoing reward costs in rats. Eur J Neurosci. 308-21.

52. Deverman, B.E., and Patterson, P.H. (2009). Cytokines and CNS development. Neuron *64*, 61–78.

53. Dickmeis, T. (2009). Glucocorticoids and the circadian clock. J. Endocrinol. *200*, 3–22.

54. Dinarello, C.A. (1996). Biologic basis for interleukin-1 in disease. Blood *87*, 2095–2147.

55. Dudai, Y. (2012). The restless engram: consolidations never end. Annu. Rev. Neurosci. 35, 227–247. doi: 10.1146/annurev-neuro-062111-150500

56. Dudek, F.E. (2004). Seizure-induced neurogenesis and epilepsy: involvement of ectopic granule cells?Epilepsy Curr. 103-4.

57. Duguid, I., Branco, T., Chadderton, P., Arlt, C., Powell, K., Häusser, M. (2015).Control of cerebellar granule cell output by sensory-evoked Golgi cell inhibition. Proc Natl Acad Sci U S A. 13099-104.

58. Eichenbaum H. (2000). A cortical-hippocampal system for declarative memory. Nat Rev Neurosci. 1:41–50.

59. **E**l Falougy, H., Kubikova, E., Benuska, J. (2008). The microscopical structure of the hippocampus in the rat.Bratisl Lek Listy. 106-110.

60. Egger V., Svoboda K., Mainen ZF.(2005).Dendrodendritic synaptic signals in olfactory bulb granule cells: local spine boost and global low-threshold spike.J Neurosci. 3521-30.

61. Ellman, G.L. (1959). Tissue sulfhydryl groups. Arch. Biochem. Biophys. *82*, 70–77.

62. Esterbauer, H. (1993). Cytotoxicity and genotoxicity of lipid-oxidation products. Am. J. Clin. Nutr. *57*, 779S–785S; discussion 785S–786S.

63. Eugster, H.P., Frei, K., Kopf, M., Lassmann, H., and Fontana, A. (1998). IL-6-deficient mice resist myelin oligodendrocyte glycoprotein-induced autoimmune encephalomyelitis. Eur. J. Immunol. *28*, 2178–2187.

64. Fann, M.J., and Patterson, P.H. (1994). Neuropoietic cytokines and activin A differentially regulate the phenotype of cultured sympathetic neurons. Proc. Natl. Acad. Sci. U. S. A. *91*, 43–47.

65. ***F***attori, E., Lazzaro, D., Musiani, P., Modesti, A., Alonzi, T., and Ciliberto, G. (1995). IL-6 expression in neurons of transgenic mice causes reactive astrocytosis and increase in ramified microglial cells but no neuronal damage. Eur. J. Neurosci. *7*, 2441–2449.

66. Fedoroff, S., Zhai, R., and Novak, J.P. (1997). Microglia and astroglia have a common progenitor cell. J. Neurosci. Res. *50*, 477–486.

67. Fendler, K., G. Karmos., G. Telegdy. (1961). The effect of hippocampal lesion on pituitary-adrenal function. Acta Physiol. 20:283-297.

68. Ferretti, V., Roullet P., Sargolini, F., Rinaldi, A., Perri, V., Del Fabbro, M., Costantini, V.J., Annese, V., Scesa, G., De Stefano, M.E., Oliverio, A.,Mele, A. (2010). Ventral striatal plasticity and spatial memory.Proc Natl Acad Sci U S A. 7945-50.

69. Fiedorowicz, A., Figiel, I., Kamińska, B., Zaremba, M., Wilk, S., and Oderfeld-Nowak, B. (2001). Dentate granule neuron apoptosis and glia activation in murine hippocampus induced by trimethyltin exposure. Brain Res. *912*, 116–127.

70. Fiske, B.K., and Brunjes, P.C. (2000). Microglial activation in the developing rat olfactory bulb. Neuroscience *96*, 807–815.

71. Floyd, R.A., and Carney, J.M. (1992). Free radical damage to protein and DNA: mechanisms involved and relevant observations on brain undergoing oxidative stress. Ann. Neurol. *32 Suppl*, S22-27.

72. Forloni, G., Mangiarotti, F., Angeretti, N., Lucca, E., and De Simoni, M.G. (1997). Beta-amyloid fragment potentiates IL-6 and TNF-alpha secretion by LPS in astrocytes but not in microglia. Cytokine *9*, 759–762.

73. Frautschy, S.A., Yang, F., Irrizarry, M., Hyman, B., Saido, T.C., Hsiao, K., and Cole, G.M. (1998). Microglial response to amyloid plaques in APPsw transgenic mice. Am. J. Pathol. *152*, 307–317.

74. Frei, K., Siepl, C., Groscurth, P., Bodmer, S., Schwerdel, C., and Fontana, A. (1987). Antigen presentation and tumor cytotoxicity by interferon-gamma-treated microglial cells. Eur. J. Immunol. *17*, 1271–1278.

75. Fridovich, S.E., and Porter, N.A. (1981). Oxidation of arachidonic acid in micelles by superoxide and hydrogen peroxide. J. Biol. Chem. *256*, 260–265.

76. Friedman, J.M., and Halaas, J.L. (1998). Leptin and the regulation of body weight in mammals. Nature *395*, 763–770.

77. **G**adient, R.A., and Otten, U. (1993). Differential expression of interleukin-6 (IL-6) and interleukin-6 receptor (IL-6R) mRNAs in rat hypothalamus. Neurosci. Lett. *153*, 13–16.

78. Gadient, R.A., and Otten, U. (1994). Expression of interleukin-6 (IL-6) and interleukin-6 receptor (IL-6R) mRNAs in rat brain during postnatal development. Brain Res. *637*, 10–14.

79. Gahtan, E., and Overmier, J.B. (1999). Inflammatory pathogenesis in Alzheimer's disease: biological mechanisms and cognitive sequeli. Neurosci. Biobehav. Rev. *23*, 615–633.

80. Galiano, M., Liu, Z.Q., Kalla, R., Bohatschek, M., Koppius, A., Gschwendtner, A., Xu, S., Werner, A., Kloss, C.U., Jones, L.L., et al. (2001). Interleukin-6 (IL-6) and cellular response to facial nerve injury:

effects on lymphocyte recruitment, early microglial activation and axonal outgrowth in IL-6-deficient mice. Eur. J. Neurosci. *14*, 327–341.

81. Gao, H.-M., Liu, B., and Hong, J.-S. (2003). Critical role for microglial NADPH oxidase in rotenone-induced degeneration of dopaminergic neurons. J. Neurosci. Off. J. Soc. Neurosci. *23*, 6181–6187.

82. Gery, I., and Waksman, B.H. (1972). Potentiation of the T-lymphocyte response to mitogens. II. The cellular source of potentiating mediator(s). J. Exp. Med. *136*, 143–155.

83. Giaume, C., Koulakoff, A., Roux, L., Holcman, D., and Rouach, N. (2010). Astroglial networks: a step further in neuroglial and gliovascular interactions. Nat. Rev. Neurosci. *11*, 87–99.

84. Gibbs, M.E., Hutchinson, D., and Hertz, L. (2008). Astrocytic involvement in learning and memory consolidation. Neurosci. Biobehav. Rev. *32*, 927–944.

85. Gijbels, K., Van Damme, J., Proost, P., Put, W., Carton, H., and Billiau, A. (1990). Interleukin 6 production in the central nervous system during experimental autoimmune encephalomyelitis. Eur. J. Immunol. *20*, 233–235.

86. Giralt, M., Penkowa, M., Hernández, J., Molinero, A., Carrasco, J., Lago, N., Camats, J., Campbell, I.L., and Hidalgo, J. (2002). Metallothionein-1+2 deficiency increases brain pathology in transgenic mice with astrocyte-targeted expression of interleukin 6. Neurobiol. Dis. *9*, 319–338.

87. Godbout, J.P., and Johnson, R.W. (2004). Interleukin-6 in the aging brain. J. Neuroimmunol. *147*, 141–144.

88. Gordon, G.R.J., Mulligan, S.J., and MacVicar, B.A. (2007). Astrocyte control of the cerebrovasculature. Glia *55*, 1214–1221.

89. Gould, E., Woolley, C.S., and McEwen, B.S. (1990). Short-term glucocorticoid manipulations affect neuronal morphology and survival in the adult dentate gyrus. Neuroscience *37*, 367–375.

90. Gould, E., McEwen, BS., Tanapat, P., Galea, L.A.M., Fuchs, E. (1997). Neurogenesis in the dentate gyrus of the adult tree shrew is regulated by psychosocial stress and NMDA receptor activation. The Journal of Neuroscience 17:2492-2498.

91. Gourine, A.V., Kasymov, V., Marina, N., Tang, F., Figueiredo, M.F., Lane, S., Teschemacher, A.G., Spyer, K.M., Deisseroth, K., and Kasparov, S. (2010). Astrocytes control breathing through pH-dependent release of ATP. Science 329, 571–575.

92. Graeber, M.B., and Streit, W.J. (2010). Microglia: biology and pathology. Acta Neuropathol. (Berl.) *119*, 89–105.

93. Graves AR., Moore SJ., Bloss EB., Mensh BD., Kath WL., Spruston N. (2012).Hippocampal pyramidal neurons comprise two distinct cell types that are countermodulated by metabotropic receptors. Neuron. 776-89.

94. Gregus, Z., Fekete, T., Halászi, E., and Klaassen, C.D. (1996). Lipoic acid impairs glycine conjugation of benzoic acid and renal excretion of benzoylglycine. Drug Metab. Dispos. Biol. Fate Chem. 24, 682–688.

95. Griffin, W.S.T., and Mrak, R.E. (2002). Interleukin-1 in the genesis and progression of and risk for development of neuronal degeneration in Alzheimer's disease. J. Leukoc. Biol. 72, 233–238.

96. Gutiérrez, R. (2003).The GABAergic phenotype of the "glutamatergic" granule cells of the dentate gyrus. Prog Neurobiol. 337-58.

97. ***H***abib, P., Beyer, C. (2015) Regulation of brain microglia by female gonadal steroids.J Steroid Biochem Mol Biol. 146:3-14.

98. Haddad, J.J. (2002). Oxygen-sensitive pro-inflammatory cytokines, apoptosis signaling and redox-responsive transcription factors in development and pathophysiology. Cytokines Cell. Mol. Ther. *7*, 1–14.

99. Hakkoum, D., Stoppini, L., and Muller, D. (2007). Interleukin-6 promotes sprouting and functional recovery in lesioned organotypic hippocampal slice cultures. J. Neurochem. *100*, 747–757.

100. Halassa, M.M., Florian, C., Fellin, T., Munoz, J.R., Lee, S.-Y., Abel, T., Haydon, P.G., and Frank, M.G. (2009). Astrocytic modulation of sleep homeostasis and cognitive consequences of sleep loss. Neuron *61*, 213–219.

101. Halliwell, B. (1999). Establishing the significance and optimal intake of dietary antioxidants: the biomarker concept. Nutr. Rev. *57*, 104–113.

102. Halliwell, B. (2006). Oxidative stress and neurodegeneration: where are we now? J. Neurochem. *97*, 1634–1658.

103. Halliwell, B., and Gutteridge, J.M. (1984). Oxygen toxicity, oxygen radicals, transition metals and disease. Biochem. J. *219*, 1–14.

104. Hammad, L.A., Wu, G., Saleh, M.M., Klouckova, I., Dobrolecki, L.E., Hickey, R.J., Schnaper, L., Novotny, M.V., and Mechref, Y. (2009). Elevated levels of hydroxylated phosphocholine lipids in the blood serum of breast cancer patients. Rapid Commun. Mass Spectrom. RCM *23*, 863–876.

105. Herman, J.P., Schäfer, M.K., Young, E.A., Thompson, R., Douglass, J., Akil, H., Watson, S.J. (1989).Evidence for hippocampal regulation of neuroendocrine neurons of the hypothalamo-pituitary-adrenocortical axis. J Neurosci. 3072-82.

106. Harry, G.J., and Kraft, A.D. (2012). Microglia in the developing brain: a potential target with lifetime effects. Neurotoxicology *33*, 191–206.

107. Hauber W., Sommer S. (2009). Prefrontostriatal circuitry regulates effort-related decision making. Cereb Cortex. 2240-7.

108. Heuser, I., and Lammers, C.-H. (2003). Stress and the brain. Neurobiol. Aging *24 Suppl 1*, S69-76; discussion S81-82.

109. Hirano, T., Yasukawa, K., Harada, H., Taga, T., Watanabe, Y., Matsuda, T., Kashiwamura, S., Nakajima, K., Koyama, K., and Iwamatsu, A. (1986). Complementary DNA for a novel human interleukin (BSF-2) that induces B lymphocytes to produce immunoglobulin. Nature *324*, 73–76.

110. Höfflin F, Jack A, Riedel C, Mack-Bucher J, Roos J, Corcelli C, Schultz C1, Wahle P, Engelhardt M. (2017). Heterogeneity of the Axon Initial Segment in Interneurons and Pyramidal Cells of Rodent Visual Cortex. Front Cell Neurosci. 11:332.

111. Hofmann, K.W., Schuh, A.F.S., Saute, J., Townsend, R., Fricke, D., Leke, R., Souza, D.O., Portela, L.V., Chaves, M.L.F., and Rieder, C.R.M. (2009). Interleukin-6 serum levels in patients with Parkinson's disease. Neurochem. Res. *34*, 1401–1404.

112. Hsieh, H.-L., and Yang, C.-M. (2013). Role of redox signaling in neuroinflammation and neurodegenerative diseases. BioMed Res. Int. *2013*, 484613.

113. Hu, Z., Yuri, K., Ozawa, H., Lu, H., Yang, Y., Ito, T., Kawata, M.(1997). Adrenalectomyinduced granule cell death is predicated on the disappearance of glucocorticoid receptor immunoreactivity in the rat hippocampal granule cell layer. Brain Res. 293–301.

114. Hu, X., Leak, R.K., Shi, Y., Suenaga, J., Gao, Y., Zheng, P., Chen, J. (2015). Microglial and macrophage polarization—new prospects for brain repair. Nat Rev Neurol. 56-64.

115. Hurst, S.M., Wilkinson, T.S., McLoughlin, R.M., Jones, S., Horiuchi, S., Yamamoto, N., Rose-John, S., Fuller, G.M., Topley, N., and Jones, S.A. (2001). Il-6 and its soluble receptor orchestrate a temporal switch in the pattern of leukocyte recruitment seen during acute inflammation. Immunity *14*, 705–714.

116. Humphries, M.D., Prescott, T.J. (2010). The ventral basal ganglia, a selection mechanism at the crossroads of space, strategy, and reward. Prog Neurobiol. 385-417.

117. Iadecola, C., and Nedergaard, M. (2007). Glial regulation of the cerebral microvasculature. Nat. Neurosci. *10*, 1369–1376.

118. Imai, Y., Kuba, K., Neely, G.G., Yaghubian-Malhami, R., Perkmann, T., van Loo, G., Ermolaeva, M., Veldhuizen, R., Leung, Y.H.C., Wang, H., et al. (2008). Identification of oxidative stress and Toll-like receptor 4 signaling as a key pathway of acute lung injury. Cell *133*, 235–249.

119. Islam, A., Westman, J., Bogdanovic, N., Suliman, I.A., Lindell, I., Winblad, B., and Adem, A. (1999). Ultrastructural analysis of the hippocampus of adult rats after long-term adrenalectomy. Brain Res. *849*, 226–230.

120. Islam, A., Henriksson, B., Mohammed, A., Winblad, B., Adem, A. (1995).Behavioural deficits in adult rats following long-term adrenalectomy. Neurosci Lett. 194(1-2):49-52.

121. Ito M, Kato M, Kawabata M. (1998). Premature bifurcation of the apical dendritic trunk of vibrissa-responding pyramidal neurones of X-irradiated rat neocortex. J Physiol. 15;512 (Pt 2):543-53.

122. Isaacson, R. L. (1972). Hippocampal destruction in man and other animals. Neuropsychologia l0,47-64.

123. Jaarsma, D., Postema, F., and Korf, J. (1992). Time course and distribution of neuronal degeneration in the dentate gyrus of rat after adrenalectomy: a silver impregnation study. Hippocampus *2*, 143–150.

124. Jiang, C., Ting, A.T., and Seed, B. (1998). PPAR-gamma agonists inhibit production of monocyte inflammatory cytokines. Nature *391*, 82–86.

125. Jones, D.P. (2002). Redox potential of GSH/GSSG couple: assay and biological significance. Methods Enzymol. *348*, 93–112.

126. O'Keefe,J., Nadel,L. (1978). hippocampus as cognitive map.Clarendon press. Oxford.

127. Jones, S.A. (2005). Directing transition from innate to acquired immunity: defining a role for IL-6. J. Immunol. Baltim. Md 1950 *175*, 3463–3468.

128. Kee, N.,Teixeira, C.M., Wang, A.H., Frankland, P.W. (2007).Preferential incorporation of adult-generated granule cells into spatial memory networks in the dentate gyrus. Nat Neurosci. 355-62.

129. Kempermann, G., Jessberger, S., Steiner, B., and Kronenberg, G. (2004). Milestones of neuronal development in the adult hippocampus. Trends Neurosci. *27*, 447–452.

130. Kettenmann, H., Hanisch, U.-K., Noda, M., and Verkhratsky, A. (2011). Physiology of microglia. Physiol. Rev. *91*, 461–553.

131. Kim, W.G., Mohney, R.P., Wilson, B., Jeohn, G.H., Liu, B., and Hong, J.S. (2000). Regional difference in susceptibility to

lipopolysaccharide-induced neurotoxicity in the rat brain: role of microglia. J. Neurosci. Off. J. Soc. Neurosci. *20*, 6309–6316.

132. Kjelstrup, K. B., Solstad, T., Brun, V. H., Hafting, T., Leutgeb, S., Witter, M. P., et al. (2008). Finite scale of spatial representation in the hippocampus. Science 321, 140–143. doi: 10.1126/science.1157086.

133. Kim, Y.-H., Chun, Y.-S., Park, J.-W., Kim, C.-H., and Kim, M.-S. (2002). Involvement of adrenergic pathways in activation of catalase by myocardial ischemia-reperfusion. Am. J. Physiol. Regul. Integr. Comp. Physiol. *282*, R1450-1458.

134. Klein, M.A., Möller, J.C., Jones, L.L., Bluethmann, H., Kreutzberg, G.W., and Raivich, G. (1997). Impaired neuroglial activation in interleukin-6 deficient mice. Glia *19*, 227–233.

135. Knigge, K. M. (196 1). Adrenocortical response to stress in rats with lesions in hippocampus and amygdala. Proc. Sot. Exp. Biol. Med. 108: 67-69.

136. Knoblach, S.M., Fan, L., and Faden, A.I. (1999). Early neuronal expression of tumor necrosis factor-alpha after experimental brain injury contributes to neurological impairment. J. Neuroimmunol. *95*, 115–125.

137. Koistinaho, M., Lin, S., Wu, X., Esterman, M., Koger, D., Hanson, J., Higgs, R., Liu, F., Malkani, S., Bales, K.R., et al. (2004). Apolipoprotein E promotes astrocyte colocalization and degradation of deposited amyloid-beta peptides. Nat. Med. *10*, 719–726.

138. Kopelman, M.D. (1993). The neuropsychology of remote memory. In: Boller F, Grafman J (eds) Handbook of neuropsycho-biology. 215–238.

139. Krueger, J.M., Obál, F.J., Fang, J., Kubota, T., and Taishi, P. (2001). The role of cytokines in physiological sleep regulation. Ann. N. Y. Acad. Sci. *933*, 211–221.

140. Krugers, H.J., Medema, R.M., Postema, F., and Korf, J. (1994). Induction of glial fibrillary acidic protein immunoreactivity in the rat dentate gyrus after adrenalectomy: comparison with neurodegenerative changes using silver impregnation. Hippocampus *4*, 307–314.

141. Kreutzberg GW. (1996). Microglia: a sensor for pathological events in the CNS. Trends Neurosci 19:312–318.

142. Kumar, A., Sharma, N., Gupta, A., Kalonia, H., and Mishra, J. (2012). Neuroprotective potential of atorvastatin and simvastatin (HMG-CoA reductase inhibitors) against 6-hydroxydopamine (6-OHDA) induced Parkinson-like symptoms. Brain Res. *1471*, 13–22.

143. Kunwar, A., and Priyadarsini, K.I. (2011). Free radicals, oxidative stress and importance of antioxidants in human health. J. Med. Allied Sci. *1*, 53–60.

144. Landfield, P.W., Waymire, J.C., and Lynch, G. (1978). Hippocampal aging and adrenocorticoids: quantitative correlations. Science *202*, 1098–1102.

145. Lalancette-He´ bert M, Gowing G, Simard A, Weng YC, Kriz J. (2007). Selective ablation of proliferating microglial cells exacerbates ischemic injury in the brain. J Neurosci 27:2596–2605.

146. Lathe R. (2001).Hormones and the hippocampus. J Endocrinol. 169(2):205–31.

147. Lavine, S.D., Hofman, F.M., and Zlokovic, B.V. (1998). Circulating antibody against tumor necrosis factor-alpha protects rat brain from reperfusion injury. J. Cereb. Blood Flow Metab. Off. J. Int. Soc. Cereb. Blood Flow Metab. *18*, 52–58.

148. Lambertsen KL, Clausen BH, Babcock AA, Gregersen R, Fenger C, Nielsen HH, Haugaard LS, Wirenfeldt M, Nielsen M, Dagnaes-Hansen F, Bluethmann H,Faergeman NJ, Meldgaard M, Deierborg T, Finsen B. (2009). Microglia protect neurons against ischemia by synthesis of tumor necrosis factor. J Neurosci. 29:1319–1930.

149. Lawrence, C.B., Allan, S.M., and Rothwell, N.J. (1998). Interleukin-1beta and the interleukin-1 receptor antagonist act in the striatum to modify excitotoxic brain damage in the rat. Eur. J. Neurosci. *10*, 1188–1195.

150. Lee, M., Cho, T., Jantaratnotai, N., Wang, Y.T., McGeer, E., and McGeer, P.L. (2010). Depletion of GSH in glial cells induces neurotoxicity:

relevance to aging and degenerative neurological diseases. FASEB J. Off. Publ. Fed. Am. Soc. Exp. Biol. *24*, 2533–2545.

151. Li, C., Zhao, R., Gao, K., Wei, Z., Yin, M.Y., Lau, L.T., Chui, D., and Yu, A.C.H. (2011). Astrocytes: implications for neuroinflammatory pathogenesis of Alzheimer's disease. Curr. Alzheimer Res. *8*, 67–80.

152. Li, F., Calingasan, N.Y., Yu, F., Mauck, W.M., Toidze, M., Almeida, C.G., Takahashi, R.H., Carlson, G.A., Flint Beal, M., Lin, M.T., et al. (2004). Increased plaque burden in brains of APP mutant MnSOD heterozygous knockout mice. J. Neurochem. *89*, 1308–1312.

153. Liu T, Clark RK, McDonnell PC, Young PR, White RF, Barone FC, Feuerstein GZ.(1994).Tumor necrosis factor-alpha expression in ischemic neurons.Stroke. 25(7):1481-8.

154. Liu, Z.G., and Han, J. (2001). Cellular responses to tumor necrosis factor. Curr. Issues Mol. Biol. *3*, 79–90.

155. Liu, H., Song, Z., Liao, D., Zhang, T., Liu, F., Zhuang, K., Luo, K., and Yang, L. (2015). Neuroprotective effects of trans-caryophyllene against kainic acid induced seizure activity and oxidative stress in mice. Neurochem. Res. *40*, 118–123.

156. Liu, Y., Imai, H., Sadamatsu, M., Tsunashima, K., and Kato, N. (2005). Cytokines participate in neuronal death induced by trimethyltin in the rat hippocampus via type II glucocorticoid receptors. Neurosci. Res. *51*, 319–327.

157. Loew, O. (1900). A NEW ENZYME OF GENERAL OCCURRENCE IN ORGANISMIS. Science *11*, 701–702.

158. Lopez-Rojas, J., Kreutz, M.R. (2016). Mature granule cells of the dentate gyrus--Passive bystanders or principal performers in hippocampal function? Neurosci Biobehav Rev. 167-74.

159. Lorincz, A., and Nusser, Z. (2010). Molecular identity of dendritic voltagegated sodium channels. Science 328, 906–909.

160. Lovell, M.A., Ehmann, W.D., Butler, S.M., and Markesbery, W.R. (1995). Elevated thiobarbituric acid-reactive substances and antioxidant

enzyme activity in the brain in Alzheimer's disease. Neurology *45*, 1594–1601.

161. Lucin, K.M., and Wyss-Coray, T. (2009). Immune activation in brain aging and neurodegeneration: too much or too little? Neuron *64*, 110–122.

162. Lull, M.E., Block, M.L. (2010). Microglial activation and chronic neurodegeneration. Neurotherapeutics. 354-65.

163. MacLennan, K.M., Smith, P.F., and Darlington, C.L. (1998). Adrenalectomy-induced neuronal degeneration. Prog. Neurobiol. *54*, 481–498.

164. Magistretti, P.J. (2006). Neuron-glia metabolic coupling and plasticity. J. Exp. Biol. *209*, 2304–2311.

165. Malmeström, C., Andersson, B.A., Haghighi, S., and Lycke, J. (2006). IL-6 and CCL2 levels in CSF are associated with the clinical course of MS: implications for their possible immunopathogenic roles. J. Neuroimmunol. *175*, 176–182.

166. Marklund, S. (1980). Distribution of CuZn superoxide dismutase and Mn superoxide dismutase in human tissues and extracellular fluids. Acta Physiol. Scand. Suppl. *492*, 19–23.Marsha R. P., Sheri J. Y. (2012). Mizumori Age-associated changes in the hippocampal-ventral striatum-ventral tegmental loop that impact learning, prediction, and context discrimination.Front Aging Neurosci. 4: 22.

167. März, P., Cheng, J.G., Gadient, R.A., Patterson, P.H., Stoyan, T., Otten, U., and Rose-John, S. (1998). Sympathetic neurons can produce and respond to interleukin 6. Proc. Natl. Acad. Sci. U. S. A. *95*, 3251–3256.

168. Matos, M., Augusto, E., Oliveira, C.R., and Agostinho, P. (2008). Amyloid-beta peptide decreases glutamate uptake in cultured astrocytes: involvement of oxidative stress and mitogen-activated protein kinase cascades. Neuroscience *156*, 898–910.

169. Matsumoto, Y., Ohmori, K., and Fujiwara, M. (1992). Microglial and astroglial reactions to inflammatory lesions of experimental autoimmune

encephalomyelitis in the rat central nervous system. J. Neuroimmunol. *37*, 23–33.

170. Matthews, V.B., Allen, T.L., Risis, S., Chan, M.H.S., Henstridge, D.C., Watson, N., Zaffino, L.A., Babb, J.R., Boon, J., Meikle, P.J., et al. (2010). Interleukin-6-deficient mice develop hepatic inflammation and systemic insulin resistance. Diabetologia *53*, 2431–2441.

171. Matyash, V., and Kettenmann, H. (2010). Heterogeneity in astrocyte morphology and physiology. Brain Res. Rev. *63*, 2–10.

172. McEwen, B.S. (1997). Possible mechanisms for atrophy of the human hippocampus. Mol. Psychiatry *2*, 255–262.

173. McEwen, B.S., Weiss, J.M., and Schwartz, L.S. (1968). Selective retention of corticosterone by limbic structures in rat brain. Nature *220*, 911–912.

174. McGeer, P.L., and McGeer, E.G. (1995). The inflammatory response system of brain: implications for therapy of Alzheimer and other neurodegenerative diseases. Brain Res. Brain Res. Rev. *21*, 195–218.

175. Meda, L., Cassatella, M.A., Szendrei, G.I., Otvos, L., Baron, P., Villalba, M., Ferrari, D., and Rossi, F. (1995). Activation of microglial cells by beta-amyloid protein and interferon-gamma. Nature *374*, 647–650.

176. Meister, A., and Anderson, M.E. (1983). Glutathione. Annu. Rev. Biochem. *52*, 711–760.

177. Mendel, I., Katz, A., Kozak, N., Ben-Nun, A., and Revel, M. (1998). Interleukin-6 functions in autoimmune encephalomyelitis: a study in gene-targeted mice. Eur. J. Immunol. *28*, 1727–1737.

178. Mihara, M., Hashizume, M., Yoshida, H., Suzuki, M., and Shiina, M. (2012). IL-6/IL-6 receptor system and its role in physiological and pathological conditions. Clin. Sci. Lond. Engl. 1979 *122*, 143–159.

179. Miller, L.J., Kurtzman, S.H., Anderson, K., Wang, Y., Stankus, M., Renna, M., Lindquist, R., Barrows, G., and Kreutzer, D.L. (2000). Interleukin-1 family expression in human breast cancer: interleukin-1 receptor antagonist. Cancer Invest. *18*, 293–302.

180. Minami, M., Kuraishi, Y., and Satoh, M. (1991). Effects of kainic acid on messenger RNA levels of IL-1 beta, IL-6, TNF alpha and LIF in the rat brain. Biochem. Biophys. Res. Commun. *176*, 593–598.

181. Misane,I., Ögren, S.O. (2003). Selective 5-HT1A antagonists WAY 100635 and NAD-299 attenuate the impairment of passive avoidance caused by scopolamine in the rat.Neuropsychopharmacology.253-264

182. Moberg, G. P., V. Scapagnini., J. deGroot., W. F. Ganong. (1971). Effect of sectioning the fomix on diurnal fluctuations in plasma corticosterone levels in the rat. Neuroendocrinology 7: 11-15.

183. Mocchetti, I., Spiga, G., Hayes, V. Y., Isackson, P. J. and Colangelo, A. (1996) Glucocorticoids di€erentially increase nerve growth factor and basic broblast growth factor ex-pression in the rat brain. Journal of Neuroscience 16, 2141±2148.

184. Montine, T.J., Montine, K.S., McMahan, W., Markesbery, W.R., Quinn, J.F., and Morrow, J.D. (2005). F2-isoprostanes in Alzheimer and other neurodegenerative diseases. Antioxid. Redox Signal. *7*, 269–275.

185. Morgado-Bernal, I. (2011). Learning and memory consolidation: Linking molecular and behavioral data. Neuroscience. 176:12–9.

186. Munoz, D.G., Dickson, D.W., Bergeron, C., Mackenzie, I.R.A., Delacourte, A., and Zhukareva, V. (2003). The neuropathology and biochemistry of frontotemporal dementia. Ann. Neurol. *54 Suppl 5*, S24-28.

187. Murakami, K., Murata, N., Noda, Y., Tahara, S., Kaneko, T., Kinoshita, N., Hatsuta, H., Murayama, S., Barnham, K.J., Irie, K., et al. (2011). SOD1 (copper/zinc superoxide dismutase) deficiency drives amyloid β protein oligomerization and memory loss in mouse model of Alzheimer disease. J. Biol. Chem. *286*, 44557–44568.

188. Muramatsu, Y., Kurosaki, R., Watanabe, H., Michimata, M., Matsubara, M., Imai, Y., and Araki, T. (2003). Cerebral alterations in a MPTP-mouse model of Parkinson's disease--an immunocytochemical study. J. Neural Transm. Vienna Austria 1996 *110*, 1129–1144.

189. Murzin, A.G., Lesk, A.M., and Chothia, C. (1992). beta-Trefoil fold. Patterns of structure and sequence in the Kunitz inhibitors interleukins-1 beta and 1 alpha and fibroblast growth factors. J. Mol. Biol. *223*, 531–543.

190. Nagatsu, T., Mogi, M., Ichinose, H., and Togari, A. (2000). Changes in cytokines and neurotrophins in Parkinson's disease. J. Neural Transm. Suppl. 277–290.

191. Nagele, R.G., D'Andrea, M.R., Lee, H., Venkataraman, V., and Wang, H.-Y. (2003). Astrocytes accumulate A beta 42 and give rise to astrocytic amyloid plaques in Alzheimer disease brains. Brain Res. *971*, 197–209.

192. Nakashiba, T., Young, JZ., McHugh, T.J., Buhl D.L., Tonegawa, S. (2008). Transgenic inhibition of synaptic transmission reveals role of CA3 output in hippocampal learning. Science. 1260-4.

193. Oberheim, N.A., Takahiro, T., Xiaoning, Han., Wei, He., Jane, H. C. L., Fushun, W., Qiwu, X., Jeffrey, D. W., Webster, P., Jeffrey, G. O., Bruce, R. R., Steven A. G., Maiken, N. (2009). Uniquely Hominid Features of Adult Human Astrocytes. Journal of Neuroscience.29 (10) 3276-3287.

194. Nedergaard, M., Ransom, B., and Goldman, S.A. (2003). New roles for astrocytes: redefining the functional architecture of the brain. Trends Neurosci. *26*, 523–530.

195. Neves, G., Cooke, S.F., Bliss, T.V. (2008). Synaptic plasticity, memory and the hippocampus: a neural network approach to causality. Nat Rev Neurosci. 65-75.

196. Nichols, N.R., Agolley, D., Zieba, M., and Bye, N. (2005). Glucocorticoid regulation of glial responses during hippocampal neurodegeneration and regeneration. Brain Res. Brain Res. Rev. *48*, 287–301.

197. Nicholson, D.W., and Thornberry, N.A. (1997). Caspases: killer proteases. Trends Biochem. Sci. *22*, 299–306.

198. Nimmerjahn, A., Kirchhoff, F., and Helmchen, F. (2005). Resting microglial cells are highly dynamic surveillants of brain parenchyma in vivo. Science *308*, 1314–1318.

199. Nonas, S., Miller, I., Kawkitinarong, K., Chatchavalvanich, S., Gorshkova, I., Bochkov, V.N., Leitinger, N., Natarajan, V., Garcia, J.G.N., and Birukov, K.G. (2006). Oxidized phospholipids reduce vascular leak and inflammation in rat model of acute lung injury. Am. J. Respir. Crit. Care Med. *173*, 1130–1138.

200. Okuda, Y., Nakatsuji, Y., Fujimura, H., Esumi, H., Ogura, T., Yanagihara, T., and Sakoda, S. (1995). Expression of the inducible isoform of nitric oxide synthase in the central nervous system of mice correlates with the severity of actively induced experimental allergic encephalomyelitis. J. Neuroimmunol. *62*, 103–112.

201. Olanow, C.W., and Tatton, W.G. (1999). Etiology and pathogenesis of Parkinson's disease. Annu. Rev. Neurosci. *22*, 123–144.

202. Orihuela, R.,McPherson, C.A.,Harry, G.J.(2016). Microglial M1/M2 polarization and metabolic states.Br J Pharmacol. 173(4):649-65.

203. Panegyres, P.K., and Hughes, J. (1998). The neuroprotective effects of the recombinant interleukin-1 receptor antagonist rhIL-1ra after excitotoxic stimulation with kainic acid and its relationship to the amyloid precursor protein gene. J. Neurol. Sci. *154*, 123–132.

204. Pappolla, M.A., Chyan, Y.J., Omar, R.A., Hsiao, K., Perry, G., Smith, M.A., and Bozner, P. (1998). Evidence of oxidative stress and in vivo neurotoxicity of beta-amyloid in a transgenic mouse model of Alzheimer's disease: a chronic oxidative paradigm for testing antioxidant therapies in vivo. Am. J. Pathol. *152*, 871–877.

205. Parpura V, Verkhratsky A. Astrocytes revisited: concise historic outlook on glutamate homeostasis and signaling.Croat Med J. 2012 Dec;53(6):518-28.

206. Patten, A.R., Yau, S.Y., Fontaine, C.J., Meconi, A.W., Ryan, C.C., Brian R. (2015).The Benefits of Exercise on Structural and Functional Plasticity in the Rodent Hippocampus of Different Disease Models. Brain Plasticity. 97-127.

207. Paxinos, G., Watson, C. (2005).The Rat Brain in Stereotaxic Coordinates. Elsevier Academic Press, 166pp.

208. Pearson, V.L., Rothwell, N.J., and Toulmond, S. (1999). Excitotoxic brain damage in the rat induces interleukin-1beta protein in microglia and astrocytes: correlation with the progression of cell death. Glia *25*, 311–323.

209. Pedersen, B.K., and Febbraio, M.A. (2008). Muscle as an endocrine organ: focus on muscle-derived interleukin-6. Physiol. Rev. *88*, 1379–1406.

210. Pedersen, B.K., Steensberg, A., Fischer, C., Keller, C., Keller, P., Plomgaard, P., Febbraio, M., and Saltin, B. (2003). Searching for the exercise factor: is IL-6 a candidate? J. Muscle Res. Cell Motil. *24*, 113–119.

211. Pekny M, Pekna M. (2014).Astrocyte reactivity and reactive astrogliosis: Costs and benefits. Physiol Rev94:1077–1098.

212. Pfeffer, K.(2003).Biological functions of tumor necrosis factor cytokines and their receptors.Cytokine Growth Factor Rev. 14(3-4):185-91.

213. Piirainen, S.,Youssef, A.,Song, C.,Kalueff, A.V.,Landreth, G.E.,Malm, T.,Tian, L. (2017). Psychosocial stress on neuroinflammation and cognitive dysfunctions in Alzheimer's disease: the emerging role for microglia?Neurosci Biobehav Rev. 77:148-164.

214. Placone, A.L., McGuiggan, P.M., Bergles, D.E., Guerrero-Cazares, H., Quiñones-Hinojosa, A., Searson, P.C. (2015) Human astrocytes develop physiological morphology and remain quiescent in a novel 3D matrix.Biomaterials. 42:134-43.

215. Pelegrin, P., and Surprenant, A. (2006). Pannexin-1 mediates large pore formation and interleukin-1beta release by the ATP-gated P2X7 receptor. EMBO J. *25*, 5071–5082.

216. Penkowa, M., and Hidalgo, J. (2000). IL-6 deficiency leads to reduced metallothionein-I+II expression and increased oxidative stress in the brain stem after 6-aminonicotinamide treatment. Exp. Neurol. *163*, 72–84.

217. Penkowa, M., Moos, T., Carrasco, J., Hadberg, H., Molinero, A., Bluethmann, H., and Hidalgo, J. (1999a). Strongly compromised inflammatory response to brain injury in interleukin-6-deficient mice. Glia *25*, 343–357.

218. Penkowa, M., Carrasco, J., Giralt, M., Moos, T., and Hidalgo, J. (1999b). CNS wound healing is severely depressed in metallothionein I- and II-deficient mice. J. Neurosci. Off. J. Soc. Neurosci. *19*, 2535–2545.

219. Penkowa, M., Hidalgo, J., and Aschner, M. (2008). Immune and Inflammatory Responses in the Central Nervous System: Modulation by Astrocytes. In NeuroImmune Biology, P. and Korneva, ed. (Elsevier), pp. 275–288.

220. Perea, G., Navarrete, M., and Araque, A. (2009). Tripartite synapses: astrocytes process and control synaptic information. Trends Neurosci. *32*, 421–431.

221. Perry, S.W., Dewhurst, S., Bellizzi, M.J., and Gelbard, H.A. (2002). Tumor necrosis factor-alpha in normal and diseased brain: Conflicting effects via intraneuronal receptor crosstalk? J. Neurovirol. *8*, 611–624.

222. Perry, V.H., Hume, D.A., and Gordon, S. (1985). Immunohistochemical localization of macrophages and microglia in the adult and developing mouse brain. Neuroscience *15*, 313–326.

223. Perry, V.H., Newman, T.A., and Cunningham, C. (2003). The impact of systemic infection on the progression of neurodegenerative disease. Nat. Rev. Neurosci. *4*, 103–112.

224. Pfeffer, K.,Matsuyama, T.,Kündig, T.M.,Wakeham, A.,Kishihara, K.,Shahinian, A.,Wiegmann, K.,Ohashi, P.S.,Krönke, M.,Mak, T.W.(1993).Mice deficient for the 55 kd tumor necrosis factor receptor are resistant to endotoxic shock, yet succumb to L. monocytogenes infection.Cell. 7;73(3):457-67.

225. Placone AL, McGuiggan PM, Bergles DE, Guerrero-Cazares H, Quiñones-Hinojosa A, Searson PC. Human astrocytes develop physiological morphology and remain quiescent in a novel 3D matrix.Biomaterials. 2015 Feb;42:134-43.

226. Polazzi E, Monti B. (2010). Microglia and neuroprotection: From in vitro studies to therapeutic applications.Progress in Neurobiology 92:293–315.

227. Porter, F.D., Scherrer, D.E., Lanier, M.H., Langmade, S.J., Molugu, V., Gale, S.E., Olzeski, D., Sidhu, R., Dietzen, D.J., Fu, R., et al. (2010).

Cholesterol oxidation products are sensitive and specific blood-based biomarkers for Niemann-Pick C1 disease. Sci. Transl. Med. *2*, 56ra81.

228. Pratt, D.A., Tallman, K.A., and Porter, N.A. (2011). Free radical oxidation of polyunsaturated lipids: New mechanistic insights and the development of peroxyl radical clocks. Acc. Chem. Res. *44*, 458–467.

229. Probert, L., Akassoglou, K., Kassiotis, G., Pasparakis, M., Alexopoulou, L., and Kollias, G. (1997). TNF-alpha transgenic and knockout models of CNS inflammation and degeneration. J. Neuroimmunol. *72*, 137–141.

230. Raivich, G., Bohatschek, M., Kloss, C.U., Werner, A., Jones, L.L., and Kreutzberg, G.W. (1999). Neuroglial activation repertoire in the injured brain: graded response, molecular mechanisms and cues to physiological function. Brain Res. Brain Res. Rev. *30*, 77–105.

231. Ransohoff, R.M., and Perry, V.H. (2009). Microglial physiology: unique stimuli, specialized responses. Annu. Rev. Immunol. *27*, 119–145.

232. Rasband, M. N. (2010). The axon initial segment and the maintenance of neuronal polarity. Nat. Rev. Neurosci. 11, 552–562.

233. Reali, C., Scintu, F., Pillai, R., Donato, R., Michetti, F., and Sogos, V. (2005). S100b counteracts effects of the neurotoxicant trimethyltin on astrocytes and microglia. J. Neurosci. Res. *81*, 677–686.

234. Reiter, R.J., Tan, D.X., Osuna, C., and Gitto, E. (2000). Actions of melatonin in the reduction of oxidative stress. A review. J. Biomed. Sci. *7*, 444–458.

235. Renno, T., Krakowski, M., Piccirillo, C., Lin, J.Y., and Owens, T. (1995). TNF-alpha expression by resident microglia and infiltrating leukocytes in the central nervous system of mice with experimental allergic encephalomyelitis. Regulation by Th1 cytokines. J. Immunol. Baltim. Md 1950 *154*, 944–953.

236. Reul, J.M., and de Kloet, E.R. (1985). Two receptor systems for corticosterone in rat brain: microdistribution and differential occupation. Endocrinology *117*, 2505–2511.

237. Reul, J.M.H.M., Collins, A., Saliba, R.S., Mifsud, K.R., Carter, S.D., Gutierrez-Mecinas, M., Qian, X., and Linthorst, A.C.E. (2015). Glucocorticoids, epigenetic control and stress resilience. Neurobiol. Stress *1*, 44–59.

238. Romero, J., Muñiz, J., Logica Tornatore, T., Holubiec, M., González, J., Barreto, G.E., Guelman, L., Lillig, C.H., Blanco, E., and Capani, F. (2014). Dual role of astrocytes in perinatal asphyxia injury and neuroprotection. Neurosci. Lett. *565*, 42–46.

239. Rothwell, N. (2003). Interleukin-1 and neuronal injury: mechanisms, modification, and therapeutic potential. Brain. Behav. Immun. *17*, 152–157.

240. Rothwell, N.J. (1997). Sixteenth Gaddum Memorial Lecture December 1996. Neuroimmune interactions: the role of cytokines. Br. J. Pharmacol. *121*, 841–847.

241. Rothwell, N.J., and Luheshi, G.N. (2000). Interleukin 1 in the brain: biology, pathology and therapeutic target. Trends Neurosci. *23*, 618–625.

242. Rothwell, N., Allan, S., and Toulmond, S. (1997). The role of interleukin 1 in acute neurodegeneration and stroke: pathophysiological and therapeutic implications. J. Clin. Invest. *100*, 2648–2652.

243. Rothwell, N.J., Luheshi, G., and Toulmond, S. (1996). Cytokines and their receptors in the central nervous system: physiology, pharmacology, and pathology. Pharmacol. Ther. *69*, 85–95.

244. Rubio-Perez, J.M., and Morillas-Ruiz, J.M. (2012). A review: inflammatory process in Alzheimer's disease, role of cytokines. ScientificWorldJournal *2012*, 756357.

245. Sairanen, T.R., Lindsberg, P.J., Brenner, M., and Sirén, A.L. (1997). Global forebrain ischemia results in differential cellular expression of interleukin-1beta (IL-1beta) and its receptor at mRNA and protein level. J. Cereb. Blood Flow Metab. Off. J. Int. Soc. Cereb. Blood Flow Metab. *17*, 1107–1120.

246. Sandström, J., Nilsson, P., Karlsson, K., and Marklund, S.L. (1994). 10-fold increase in human plasma extracellular superoxide dismutase

content caused by a mutation in heparin-binding domain. J. Biol. Chem. *269*, 19163–19166.

247. Sapolsky, R.M., and Pulsinelli, W.A. (1985). Glucocorticoids potentiate ischemic injury to neurons: therapeutic implications. Science *229*, 1397–1400.

248. Sapolsky, R.M., Stein-Behrens, B.A., and Armanini, M.P. (1991). Long-term adrenalectomy causes loss of dentate gyrus and pyramidal neurons in the adult hippocampus. Exp. Neurol. *114*, 246–249.

249. Sasaki, A., Yamaguchi, H., Ogawa, A., Sugihara, S., and Nakazato, Y. (1997). Microglial activation in early stages of amyloid beta protein deposition. Acta Neuropathol. (Berl.) *94*, 316–322.

250. Scheller, J., Chalaris, A., Schmidt-Arras, D., and Rose-John, S. (2011). The pro- and anti-inflammatory properties of the cytokine interleukin-6. Biochim. Biophys. Acta *1813*, 878–888.

251. Schieber, M., and Chandel, N.S. (2014). ROS function in redox signaling and oxidative stress. Curr. Biol. CB *24*, R453-462.

252. Schwartz JP, Sheng JG, Mitsuo K, Shirabe S, Nishiyama N. (1993). Trophic factors production by reactive astrocytes in injured brain Ann NY Acad Sci 679 226–234.

253. Schmued, L.C., and Hopkins, K.J. (2000). Fluoro-Jade B: a high affinity fluorescent marker for the localization of neuronal degeneration. Brain Res. *874*, 123–130.

254. Schneider, H., Pitossi, F., Balschun, D., Wagner, A., del Rey, A., and Besedovsky, H.O. (1998). A neuromodulatory role of interleukin-1beta in the hippocampus. Proc. Natl. Acad. Sci. U. S. A. *95*, 7778–7783.

255. Schöbitz, B., de Kloet, E.R., Sutanto, W., and Holsboer, F. (1993). Cellular localization of interleukin 6 mRNA and interleukin 6 receptor mRNA in rat brain. Eur. J. Neurosci. *5*, 1426–1435.

256. Schofield, E., Kersaitis, C., Shepherd, C.E., Kril, J.J., and Halliday, G.M. (2003). Severity of gliosis in Pick's disease and frontotemporal lobar degeneration: tau-positive glia differentiate these disorders. Brain J. Neurol. *126*, 827–840.

257. Selley, M.L. (2005). Simvastatin prevents 1-methyl-4-phenyl-1,2,3,6-tetrahydropyridine-induced striatal dopamine depletion and protein tyrosine nitration in mice. Brain Res. *1037*, 1–6.

258. Selmaj, K., Raine, C.S., Cannella, B., and Brosnan, C.F. (1991). Identification of lymphotoxin and tumor necrosis factor in multiple sclerosis lesions. J. Clin. Invest. *87*, 949–954.

259. Shechter, R., Miller, O., Yovel, G., Rosenzweig, N., London, A., Ruckh, J., Kim, K.-W., Klein, E., Kalchenko, V., Bendel, P., et al. (2013). Recruitment of beneficial M2 macrophages to injured spinal cord is orchestrated by remote brain choroid plexus. Immunity *38*, 555–569.

260. Shigetomi, E., Bowser, D.N., Sofroniew, M.V., and Khakh, B.S. (2008). Two forms of astrocyte calcium excitability have distinct effects on NMDA receptor-mediated slow inward currents in pyramidal neurons. J. Neurosci. Off. J. Soc. Neurosci. *28*, 6659–6663.

261. Sica, A., and Mantovani, A. (2012). Macrophage plasticity and polarization: in vivo veritas. J. Clin. Invest. *122*, 787–795.

262. Sies, H. (1997). Oxidative stress: oxidants and antioxidants. Exp. Physiol. *82*, 291–295.

263. Silverstein, R.L., and Febbraio, M. (2009). CD36, a scavenger receptor involved in immunity, metabolism, angiogenesis, and behavior. Sci. Signal. *2*, re3.

264. Sloviter, R.S., Valiquette, G., Abrams, G.M., Ronk, E.C., Sollas, A.L., Paul, L.A., and Neubort, S. (1989). Selective loss of hippocampal granule cells in the mature rat brain after adrenalectomy. Science *243*, 535–538.

265. Sloviter, R.S., Sollas, A.L., Dean, E., and Neubort, S. (1993a). Adrenalectomy-induced granule cell degeneration in the rat hippocampal dentate gyrus: characterization of an in vivo model of controlled neuronal death. J. Comp. Neurol. *330*, 324–336.

266. Sloviter, R.S., Dean, E., and Neubort, S. (1993b). Electron microscopic analysis of adrenalectomy-induced hippocampal granule cell degeneration in the rat: apoptosis in the adult central nervous system. J. Comp. Neurol. *330*, 337–351.

267. Smith, M.A., Makino, S., Kvetnansky, R., and Post, R.M. (1995). Stress and glucocorticoids affect the expression of brain-derived neurotrophic factor and neurotrophin-3 mRNAs in the hippocampus. J. Neurosci. Off. J. Soc. Neurosci. *15*, 1768–1777.

268. Sedger, L.M.,McDermott, M.F.(2014).TNF and TNF-receptors: From mediators of cell death and inflammation to therapeutic giants - past, present and future.Cytokine Growth Factor Rev. 25(4):453-72.

269. Schafer, D.P.,Stevens, B. (2015). Microglia Function in Central Nervous System Development and Plasticity.Cold Spring Harb Perspect Biol. 17;7(10):a020545.

270. Spanswick, S.C., Epp J.R., Keith, J.R., Sutherland RJ. (2007).Adrenalectomy-induced granule cell degeneration in the hippocampus causes spatial memory deficits that are not reversed by chronic treatment with corticosterone or fluoxetine. Hippocampus. 17(2):137-46.

271. Sofroniew, M.V, Vinters, H.V.(2010) Astrocytes: biology and pathology.Acta Neuropathol. 119(1):7-35.

272. Sousa, N., Madeira, M.D., Paula-Barbosa, M.M. (1997). Structural alterations of the hippocampal formation of adrenalectomized rats: an unbiased stereological study. J Neurocytol. 423–38.

273. Sousa, N., Madeira, M.D., and Paula-Barbosa, M.M. (1997). Structural alterations of the hippocampal formation of adrenalectomized rats: an unbiased stereological study. J. Neurocytol. *26*, 423–438.

274. Spanswick, S.C., Epp, J.R., and Sutherland, R.J. (2011). Time-course of hippocampal granule cell degeneration and changes in adult neurogenesis after adrenalectomy in rats. Neuroscience *190*, 166–176.

275. Spruston N1. (2008). Pyramidal neurons: dendritic structure and synaptic integration. Nat Rev Neurosci. 9(3):206-21. doi: 10.1038/nrn2286.

276. Speranza, M.J., Bagley, A.C., and Lynch, R.E. (1993). Cells enriched for catalase are sensitized to the toxicities of bleomycin, adriamycin, and paraquat. J. Biol. Chem. *268*, 19039–19043.

277. Stelmasiak, Z., Kozioł-Montewka, M., Dobosz, B., and Rejdak, K. (2001). IL-6 and sIL-6R concentration in the cerebrospinal fluid and serum of MS patients. Med. Sci. Monit. Int. Med. J. Exp. Clin. Res. *7*, 914–918.Stepan, J., Dine, J., Eder, M. (2015). Functional optical probing of the hippocampal trisynaptic circuit in vitro: network dynamics, filter properties, and polysynaptic induction of CA1 LTP.Front Neurosci. 6;9:160.

278. Stepan, J., Dine, J., Eder, M. (2015). Functional optical probing of the hippocampal trisynaptic circuit in vitro: network dynamics, filter properties, and polysynaptic induction of CA1 LTP.Front Neurosci. 6;9:160.

279. Sternberg, E.M. (1997). Neural-immune interactions in health and disease. J. Clin. Invest. *100*, 2641–2647.

280. Stienstra, C.M., Van Der Graaf, F., Bosma, A., Karten, Y.J., Hesen, W., and Joëls, M. (1998). Synaptic transmission in the rat dentate gyrus after adrenalectomy. Neuroscience *85*, 1061–1071.

281. Strange BA, Witter MP, Lein ES, Moser EI. (2014). Functional organization of the hippocampal longitudinal axis. Nat Rev Neurosci. 15(10):655–69.

282. Sugama, S., Takenouchi, T., Fujita, M., Kitani, H., Conti, B., and Hashimoto, M. (2013). Corticosteroids limit microglial activation occurring during acute stress. Neuroscience *232*, 13–20.

283. Sugiura, S., Lahav, R., Han, J., Kou, S.Y., Banner, L.R., de Pablo, F., and Patterson, P.H. (2000). Leukaemia inhibitory factor is required for normal inflammatory responses to injury in the peripheral and central nervous systems in vivo and is chemotactic for macrophages in vitro. Eur. J. Neurosci. *12*, 457–466.

284. Sumner, J.B., and Dounce, A.L. (1937). CRYSTALLINE CATALASE. Science *85*, 366–367.

285. Swanson, L.W., Wyss, J.M., Cowan, W.M. (1978). An autoradiographic study of the organization of intrahippocampal association pathways in the rat.J Comp Neurol. 681-715.

286. Tracey, K.J. and Cerami, A. (1993).Tumor necrosis factor,other cytokines and disease. Annu. Rev. Cell Biol. 9: 317-43.

287. Tchelingerian, J.L., Quinonero, J., Booss, J., and Jacque, C. (1993). Localization of TNF alpha and IL-1 alpha immunoreactivities in striatal neurons after surgical injury to the hippocampus. Neuron *10*, 213–224.

288. Touzani, O., Boutin, H., Chuquet, J., and Rothwell, N. (1999). Potential mechanisms of interleukin-1 involvement in cerebral ischaemia. J. Neuroimmunol. *100*, 203–215.

289. Touzani, O., Boutin, H., LeFeuvre, R., Parker, L., Miller, A., Luheshi, G., and Rothwell, N. (2002). Interleukin-1 influences ischemic brain damage in the mouse independently of the interleukin-1 type I receptor. J. Neurosci. Off. J. Soc. Neurosci. *22*, 38–43.

290. Tran, E.H., Hardin-Pouzet, H., Verge, G., and Owens, T. (1997). Astrocytes and microglia express inducible nitric oxide synthase in mice with experimental allergic encephalomyelitis. J. Neuroimmunol. *74*, 121–129.

291. Tremblay, M.-È., Stevens, B., Sierra, A., Wake, H., Bessis, A., and Nimmerjahn, A. (2011). The role of microglia in the healthy brain. J. Neurosci. Off. J. Soc. Neurosci. *31*, 16064–16069.

292. Tsacopoulos, M., and Magistretti, P.J. (1996). Metabolic coupling between glia and neurons. J. Neurosci. Off. J. Soc. Neurosci. *16*, 877–885.

293. Turner D.A., Buhl E.H., Hailer N.P., Nitsch R. (1998). Morphological features of the entorhinal-hippocampal connection. Prog Neurobiol. 537-62

294. Ueda, Y., Yokoyama, H., Niwa, R., Konaka, R., Ohya-Nishiguchi, H., and Kamada, H. (1997). Generation of lipid radicals in the hippocampal extracellular space during kainic acid-induced seizures in rats. Epilepsy Res. *26*, 329–333.

295. Uttara, B., Singh, A.V., Zamboni, P., and Mahajan, R.T. (2009). Oxidative stress and neurodegenerative diseases: a review of upstream and

downstream antioxidant therapeutic options. Curr. Neuropharmacol. *7*, 65–74.

296. Van Horssen, J., Witte, M.E., Schreibelt, G., and de Vries, H.E. (2011). Radical changes in multiple sclerosis pathogenesis. Biochim. Biophys. Acta *1812*, 141–150.

297. Van Antwerp, D.J., Martin, S.J., Kafri, T., Green, D.R., and Verma, I.M. (1996). Suppression of TNF-alpha-induced apoptosis by NF-kappaB. Science *274*, 787–789.

298. Veerhuis, R., Janssen, I., De Groot, C.J., Van Muiswinkel, F.L., Hack, C.E., and Eikelenboom, P. (1999). Cytokines associated with amyloid plaques in Alzheimer's disease brain stimulate human glial and neuronal cell cultures to secrete early complement proteins, but not C1-inhibitor. Exp. Neurol. *160*, 289–299.

299. Verderio, C., and Matteoli, M. (2001). ATP mediates calcium signaling between astrocytes and microglial cells: modulation by IFN-gamma. J. Immunol. Baltim. Md 1950 *166*, 6383–6391.

300. Vicenová, B., Vopálenský, V., Burýsek, L., and Pospísek, M. (2009). Emerging role of interleukin-1 in cardiovascular diseases. Physiol. Res. Acad. Sci. Bohemoslov. *58*, 481–498.

301. Vitkovic, L., Bockaert, J., and Jacque, C. (2000). "Inflammatory" cytokines: neuromodulators in normal brain? J. Neurochem. *74*, 457–471.

302. Vollmayr, B., Faust, H., Lewicka, S., and Henn, F.A. (2001). Brain-derived-neurotrophic-factor (BDNF) stress response in rats bred for learned helplessness. Mol. Psychiatry *6*, 471–474, 358.

303. Von Bernhardi, R., and Ramirez, G. (2001). Microglia-astrocyte interaction in Alzheimer's disease: friends or foes for the nervous system? Biol. Res. *34*, 123–128.

304. Voorn P., Vanderschuren LJ., Groenewegen HJ., Robbins TW., Pennartz CM. (2004). Putting a spin on the dorsal-ventral divide of the striatum. Trends Neurosci. 468-74.

305. Wallach, D., Boldin, M., Varfolomeev, E., Beyaert, R., Vandenabeele, P., and Fiers, W. (1997). Cell death induction by receptors of the TNF family: towards a molecular understanding. FEBS Lett. *410*, 96–106.

306. Wake, H., Moorhouse, A.J., Miyamoto, A., and Nabekura, J. (2013). Microglia: actively surveying and shaping neuronal circuit structure and function. Trends Neurosci. *36*, 209–217.

307. Wang, D. D., Bordey, A. (2008) The astrocyte odyssey. Prog.Neurobiol.86, 342–367.

308. Wang, D., Ayers, M.M., Catmull, D.V., Hazelwood, L.J., Bernard, C.C.A., and Orian, J.M. (2005). Astrocyte-associated axonal damage in pre-onset stages of experimental autoimmune encephalomyelitis. Glia *51*, 235–240.

309. Wenk GL. (2003). Neuropathologic changes in Alzheimer's disease. J Clin Psychiatry 64: 7–10.

310. Wiens, G.D., Glenney, G.W.(2011). Origin and evolution of TNF and TNF receptor superfamilies. Dev Comp Immunol.1324-35.

311. Williams, K., Ulvestad, E., and Antel, J. (1994). Immune regulatory and effector properties of human adult microglia studies in vitro and in situ. Adv. Neuroimmunol. *4*, 273–281.

312. Wolf, J.S., Chen, Z., Dong, G., Sunwoo, J.B., Bancroft, C.C., Capo, D.E., Yeh, N.T., Mukaida, N., and Van Waes, C. (2001). IL (interleukin)-1alpha promotes nuclear factor-kappaB and AP-1-induced IL-8 expression, cell survival, and proliferation in head and neck squamous cell carcinomas. Clin. Cancer Res. Off. J. Am. Assoc. Cancer Res. *7*, 1812–1820.

313. Woulfe, J.M., Hammond, R., Richardson, B., Sooriabalan, D., Parks, W., Rippstein, P., and Munoz, D.G. (2002). Reduction of neuronal intranuclear rodlets immunoreactive for tubulin and glucocorticoid receptor in Alzheimer's disease. Brain Pathol. Zurich Switz. *12*, 300–307.

314. Wu, R.P., Hayashi, T., Cottam, H.B., Jin, G., Yao, S., Wu, C.C.N., Rosenbach, M.D., Corr, M., Schwab, R.B., and Carson, D.A. (2010). Nrf2

responses and the therapeutic selectivity of electrophilic compounds in chronic lymphocytic leukemia. Proc. Natl. Acad. Sci. U. S. A. *107*, 7479–7484.

315. Witter, M.P. (1993). Organization of the entorhinal-hippocampal system: a review of current anatomical data. Hippocampus. 33–44.

316. Wu, X.-F., Block, M.L., Zhang, W., Qin, L., Wilson, B., Zhang, W.-Q., Veronesi, B., and Hong, J.-S. (2005). The role of microglia in paraquat-induced dopaminergic neurotoxicity. Antioxid. Redox Signal. *7*, 654–661.

317. Wyss-Coray, T., Loike, J.D., Brionne, T.C., Lu, E., Anankov, R., Yan, F., Silverstein, S.C., and Husemann, J. (2003). Adult mouse astrocytes degrade amyloid-beta in vitro and in situ. Nat. Med. *9*, 453–457.

318. **Y**abuuchi, K., Minami, M., Katsumata, S., and Satoh, M. (1993). In situ hybridization study of interleukin-1 beta mRNA induced by kainic acid in the rat brain. Brain Res. Mol. Brain Res. *20*, 153–161.

319. Yabuuchi, K., Minami, M., Katsumata, S., Yamazaki, A., and Satoh, M. (1994). An in situ hybridization study on interleukin-1 beta mRNA induced by transient forebrain ischemia in the rat brain. Brain Res. Mol. Brain Res. *26*, 135–142.

320. Yang, L., Latchoumycandane, C., McMullen, M.R., Pratt, B.T., Zhang, R., Papouchado, B.G., Nagy, L.E., Feldstein, A.E., and McIntyre, T.M. (2010). Chronic alcohol exposure increases circulating bioactive oxidized phospholipids. J. Biol. Chem. *285*, 22211–22220.

321. **Z**aleska, M.M., and Floyd, R.A. (1985). Regional lipid peroxidation in rat brain in vitro: possible role of endogenous iron. Neurochem. Res. *10*, 397–410.

322. Zeidman P, Maguire EA. (2016). Anterior hippocampus: the anatomy of perception, imagination and episodic memory. Nat Rev Neurosci. 17(3):173–82.

323.

324. Zhu, X., Raina, A.K., Lee, H.-G., Casadesus, G., Smith, M.A., and Perry, G. (2004). Oxidative stress signalling in Alzheimer's disease. Brain Res. *1000*, 32–39.

325. Zhu, Y., Saito, K., Murakami, Y., Asano, M., Iwakura, Y., and Seishima, M. (2006). Early increase in mRNA levels of pro-inflammatory cytokines and their interactions in the mouse hippocampus after transient global ischemia. Neurosci. Lett. *393*, 122–126.

2-Websites:

- https://www.radiantthinking.us/memory-theory/ii-behavioral-assessments-in-rodents.html
- http://voltagegate.blogspot.ae/2013/07/at-heart-of-matter-introduction-to.html

Abstract

Bilateral adrenalectomy has been shown to damage the hippocampal neurons. Although the effects of long-term adrenalectomy have been studied extensively there are few publications on the effects of short-term adrenalectomy. In the present study we aimed to investigate the effects of short-term bilateral adrenalectomy on the levels of pro-inflammatory cytokines IL-1β, IL-6 and TNF-α; the response of microglia and astrocytes to neuronal cell death animal behavior as well as oxidative stress markers GSH, SOD and MDA over the course of time (4h, 24h, 3days, 1week and 2weeks) in the hippocampus of Wistar rats.

Our results showed a transient significant elevation of pro-inflammatory cytokines IL-1β and IL-6 from four hours to three days in the adrenalectomized compared to sham operated rats. After one week, the elevation of both cytokines returns to the sham levels. Surprisingly, TNF-α levels were significantly elevated at four hours only in adrenalectomized compared to sham operated rats. The occurrence of neuronal cell death in the hippocampus following adrenalectomy was confirmed by Fluoro-Jade B staining. Our results showed a time dependent increase in degenerated neurons in the dorsal blade of the dentate gyrus from three days to two weeks after adrenalectomy. Our results revealed an early activation of microglia on day three whereas activation of astroglia in the hippocampus was observed at one week postoperatively. A progression of microglia and astroglia activation all over the dentate gyrus and their appearance for the first time in CA3 of adrenalectomized rats hippocampi compared to sham operated was seen after two weeks of surgery. Quantitative analysis revealed a significant increase in the number of microglia (3, 7 and 14 days) and astrocytes (7 and 14 days) of ADX compared to sham operated rats. Our study revealed no major signs of oxidative stress until two weeks after adrenalectomy when a significant decrease of GSH levels and SOD activity as well as an increase in MDA levels were found in adrenalectomized compared to sham rats. In the current study we used passive avoidance test to evaluate the cognitive functions of the ADX rats, we have found that the removal of the adrenal gland caused a behavioral deficit in the adrenalectomized rats compared to the sham over the time (3, 7 and 14 days).

Our study showed an early increase in the pro-inflammatory cytokines followed by neurodegeneration and activation of glial cells as well as oxidative stress. Taking these findings together it could be speculated that the early inflammatory components might contribute to the initiation of the biological cascade responsible for subsequent neuronal death in the current neurodegenerative animal model. These findings suggest that inflammatory mechanisms precede neurodegeneration and glial activation.

Keywords: Adrenalectomy, Hippocampus, Neuroinflammation, Neurodegeneration, Oxidative stress

Résumé

Il a été montré que la surrenalectomie bilatérale capable d'endommager les neurones de l'hippocampe. Bien que les effets de la surrénalectomie à long terme ont été largement étudiés, il y a peu de publications sur les effets de la surrénalectomie à court terme. Notre but Dans la présente étude a été de déterminer les effets de la surrénalectomie bilatérale à court terme sur les niveaux de cytokines pro-inflammatoires IL- 1β , IL- 6 et de TNF – α, la réponse de la microglie et les astrocytes, la mort des cellules neuronales ainsi que les marqueurs du stress oxydatif GSH , SOD et MDA au cours d'une période du temps (4h , 24h , 3 jours , 1 semaine et 2 semaines) dans l'hippocampe de rats Wistar .

Nos résultats ont montré une élévation significative transitoire de cytokines pro-inflammatoires IL-1B et IL-6 à partir de quatre heures à trois jours dans les rats surrénalectomisé par rapport aux rats subi une opération fictive. Après une semaine, cette élévation de ces deux cytokines revient aux niveaux fictifs. Étonnamment, les niveaux de TNF-α ont été significativement plus élevés à quatre heures seulement en rats surrénalectomisé par rapport aux rats subi une opération fictive. Nos résultats ont révélé une activation de la microglie début de la troisième journée. Alors que l'activation des astrocytes dans l'hippocampe a été observée à une semaine après l'opération. On a vu Une progression de l'activation de la microglie et des astrocytes dans le gyrus denté et leur apparition pour la première fois dans CA3 de l'hippocampe du rats surrénalectomisés par rapport à opéré fictivement après deux semaines de l'intervention chirurgicale. Notre étude n'a pas révélé de signes majeurs de stress oxydatif que deux semaines après surrénalectomie qui il été apparait dans une baisse importante des niveaux de GSH et de l'activité de la SOD ainsi une augmentation des niveaux de MDA dans les rats surrénalectomisé par rapport rats subi une opération fictive. Dans l'étude en cours, nous avons utilisé un test d'évitement passif pour évaluer les fonctions cognitives des rats ADX, nous avons constaté que l'élimination de la glande surrénale entraînait un déficit de comportement chez les rats adrénalectomisés par rapport au controles au cours du temps (3, 7 et 14 journées).

Notre étude a montré une augmentation rapide dans les cytokines pro-inflammatoires et la neurodégénérescence suivie par l'activation de cellules gliales, ainsi que le stress oxydatif. Compte tenu de ces constatations et il pourrait être suggéré que les composants inflammatoires pourraient contribuer à l'initiation de la cascade biologique responsable de la mort ultérieure des cellules neuronales dans ce modèle neurodégénérative. Ces résultats suggèrent que les mécanismes inflammatoires précèdent la neurodégénérescence et l'activation des cellules gliales. Il peut être supposé que, dans plusieurs maladies neurodégénératives comme la maladie d'Alzheimer, les changements chroniques dans les hormones surrénales et / ou leurs récepteurs pourrait entamait les mécanismes inflammatoires qui conduisent ultérieurement à la neurodégénérescence hippocampique.

Mots-clés: surrénalectomie, Hippocampe, Neuroinflammation, neurodégénérescence, stress oxydatif.

ملخص

لقد بينت الدراسات العلمية ان استئصال الغدة الكظرية (adrenalectomy-ADX) من الجانبين يؤدي إلى تلف الخلايا العصبية للحصين (hippocampus) . وعلى الرغم من أن آثار استئصال الغدة الكظرية على المدى الطويل قد درس على نطاق واسع غير ان هناك عدد قليل من المنشورات حول آثاره على المدى القصير. كنا نهدف في هذه الدراسة لبحث آثار استئصال الغدة الكظرية على المدى القصير على مستويات السيتوكينات الالتهابية (pro-inflammatory cytokines) IL-1β و IL-6 و TNF-α، استجابة الخلايا الدبقية الصغيرة (microglia) و الخلايا النجمية (astrocytes) لموت الخلايا العصبية، على مؤشرات الاجهاد التأكسدي (oxidative stress) المتمثلة في GSH, SOD و MDA على مستوى حصين وعلى سلوك جرذان (animal behavior) الويستار على مدى فترات مختلفة من الزمن (4سا, 24سا, 72سا, اسبوع و اسبوعين).

لقد أظهرت نتائجنا ارتفاع كبير و عابر للسيتوكينات الالتهابية IL-1β وIL-6 من أربع ساعات إلى ثلاثة أيام عند الجرذان المستأصلة الغدة الكظرية (ADX) مقارنة بالجرذان الخاضعة لجراحة مزيفة (sham). بعد اسبوع لاحظنا عودة هدا الارتفاع الى مستوى الجردان الخاضعة لجراحة مزيفة. والمثير للدهشة ان مستوي TNF-α ارتفع بشكل ملحوظ في أربع ساعات فقط عند *الجرذان* المستأصلة الغدة الكظرية مقارنة بالجرذان الخاضعة لجراحة مزيفة. كشفت نتائجنا عن تنشيط مبكر للخلايا الدبقية الصغيرة في اليوم الثالث. و بعد أسبوع واحد من الجراحة لوحظ تنشيط خلايا الدبق النجمية في الحصين. بعد اسبوعين لاحظنا انتشار واسع للخلايا النجمية و الدبق الصغيرة في معظم اجزاء التلفيف المسنن للحصين وظهورها لأول مرة في منطقة CA3 عند الجرذان المستأصلة الغدة الكظرية مقارنة بالجر*ذان الخاضعة لجراحة مزيفة*. كشفت دراستنا ان استئصال الغدة الكظرية من الجانبين لا يحدث اي تغيرات ملحوظة في مختلف مؤشرات الاجهاد التأكسدي الا بعد فترة اسبوعين اين لاحظنا انخفاض كبير في مستويات GSH ونشاط انزيم SOD بالإضافة الى زيادة في مستويات MDA عند الجرذان المستأصلة الغدة الكظرية مقارنة بالجرذان الخاضعة لجراحة مزيفة. في الدراسة الحالية استخدمنا اختبار passive avoidance لتقييم الوظائف المعرفية عند الجرذان المستأصلة الغدة الكظرية ، وجدنا أن إزالة الغدة الكظرية تسببت فيعجز سلوكي عند الجرذان المستأصلة الغدة الكظرية مقارنة بالجرذان الخاضعة لجراحة مزيفة خلال (3، 7 و 14 أيام).

أظهرت دراستنا زيادة مبكرة في مستويات السيتوكينات الالتهابية يليها موت الخلايا العصبية و تنشيط الخلايا الدبقية وكذلك الاجهاد التأكسدي . أن ربط كل هذه النتائج يقودنا الى الاستنباط أن الحدوث المبكر للالتهاب قد يساهم في الشروع في السلسلة البيولوجية المسؤولة عن موت الخلايا العصبية الدي يحدث في النموذج الحيواني الحالي للموت العصبي. هذه النتائج تشير إلى أن الآليات الالتهابية تسبق التلف العصبي وتفعيل الدبقية . يمكن التكهن أنه في العديد من الأمراض العصبية مثل مرض الزهايمر ، التغييرات المزمنة في هرمونات الغدة الكظرية و/ أو مستقبلاتها قد تؤدي إلى آليات التهابية التي تؤدي بدورها إلى تلف الخلايا العصبية للحصين.

كلمات البحث: استئصال الغدة الكظرية ، الحصين ، التهابات عصبية ، تلف الخلايا العصبية ، الاجهاد التأكسدي.

Conferences and Publications:

1-Conferences

1. Neuroethology: Behavior, Evolution & Neurobiology. Tuscany Il Ciocco in Lucca (Barga) Italy. 06/28/2015 - 07/03/2015. **Naserddine Hamadi, Azimullah Sheikh, Nather Madjid, Loai Lubbad, Naheed Amir, Safa Al-Deen Saudi Shehab, Fatima Khelifi-Touhami, Abdu Adem*.Neuro-Inflammation, Glia Activation And Oxidative Stress In The Hippocampus Of The Adrenalectomized Rats.**

2. 1st international conference on educational neuroscience. Abu Dhabi, United Arab Emirates. 28-29 February, 2016. **Naserddine Hamadi, Azimullah Sheikh, Nather Madjid, Loai Lubbad, Naheed Amir, Safa Al-Deen Saudi Shehab, Fatima Khelifi-Touhami, Abdu Adem*. Hippocampal Neuroinflammation, Neurodegeneration, Gliosis in Wistar rats Following Adrenal Gland Removal.**

3. The Annual Research and Innovation Conference. United Arab Emirates University, Al Ain. 21-22 November, 2016. **Naserddine Hamadi, Azimullah Sheikh, Nather Madjid, Loai Lubbad, Naheed Amir, Safa Al-Deen Saudi Shehab, Fatima Khelifi-Touhami, Abdu Adem*. Increased pro-inflammatory cytokines, glial activation and oxidative stress in the hippocampus after short-term bilateral adrenalectomy.**

4. 2nd International Conference on Educational Neuroscience, Abu Dhabi, United Arab Emirates, 05 - 06 March, 2017. **Naserddine Hamadi, Saeed Tariq, Nather Madjid, Fatima Khelifi-Touhami, Abdu Adem*. Behavioral deficit and hippocampal neurodegeneration following short-term adrenalectomy.**

5. Innovations and State of the Art in Dementia Research, Rome, Italy, 07- 09 September, 2017. **Naserddine Hamadi, Azimullah Sheikh, Nather Madjid, Loai Lubbad, Naheed Amir, Safa Al-Deen Saudi Shehab, Fatima Khelifi-Touhami,Abdu Adem*. Neuroinflammation, glial activation, oxidative stress and behavioral deficit in the hippocampus following short-term adrenalectomy.**

2-Publications:

Abstracts:

1. **Hamadi N, Adem A, Khelifi-touhami F, Sheikh A, Amir N and Shehab S (2016).** Hippocampal Neuroinflammation, Neurodegeneration, Gliosis in Wistar rats Following Adrenal Gland Removal. Front. Neurosci. International Conference-Educational Neuroscience. doi: 10.3389/conf.fnins.2016.92.00007.

2. **Hamadi N, Minhas ST, Madjid N, Khelifi-touhami F and Adem A (2017).**Behavioral deficit and hippocampal neurodegeneration following short-term adrenaectomy. Front. Hum. Neurosci. Conference. 2nd International Conference on Educational Neuroscience. doi: 10.3389/conf.fnhum.2017.222.00032.

Research papers:

1. **NaserddineHamadi, Azimullah Sheikh, NatherMadjid, LoaiLubbad, Naheed Amir,Safa Al‑Deen Saudi Shehab, Fatima Khelifi‑Touhami and Abdu Adem.**Increased pro-inflammatory cytokines, glial activation and oxidative stress in the hippocampus after short-term bilateral adrenalectomy. BMC Neurosci. 2016 Sep 1; 17(1):61. doi: 10.1186/s12868-016-0296-1.

2. **NaserddineHamadi, NatherMadjid, Saeed Tariq, Fatima Khelifi‑Touhami and Abdu Adem.** Behavioral deficit and hippocampal neurodegeneration following short-term adrenalectomy (In process).

Prenom: Naserddine

Nom: Hamadi

EN VUE DE L'OBTENTION DU DIPLOME DE DOCTORAT EN SCIENCE EN BIOLOGIE ANIMALE

Neurodegeneration, inflammation, oxidative stress and behavioral deficit followingbilateral short term adrenalectomy in the nervous system of albino Wistar rats

Abstract

Bilateral adrenalectomy has been shown to damage the hippocampal neurons. Although the effects of long-term adrenalectomy have been studied extensively there are few publications on the effects of short-term adrenalectomy. In the present study we aimed to investigate the effects of short-term bilateral adrenalectomy on the levels of pro-inflammatory cytokines IL-1β, IL-6 and TNF-α; the response of microglia and astrocytes to neuronal cell death animal behavior as well as oxidative stress markers GSH, SOD and MDA over the course of time (4h, 24h, 3days, 1week and 2weeks) in the hippocampus of Wistar rats.

Our results showed a transient significant elevation of pro-inflammatory cytokines IL-1β and IL-6 from four hours to three days in the adrenalectomized compared to sham operated rats. After one week, the elevation of both cytokines returns to the sham levels. Surprisingly, TNF-α levels were significantly elevated at four hours only in adrenalectomized compared to sham operated rats. The occurrence of neuronal cell death in the hippocampus following adrenalectomy was confirmed by Fluoro-Jade B staining. Our results showed a time dependent increase in degenerated neurons in the dorsal blade of the dentate gyrus from three days to two weeks after adrenalectomy. Our results revealed an early activation of microglia on day three whereas activation of astroglia in the hippocampus was observed at one week postoperatively. A progression of microglia and astroglia activation all over the dentate gyrus and their appearance for the first time in CA3 of adrenalectomized rats hippocampi compared to sham operated was seen after two weeks of surgery. Quantitative analysis revealed a significant increase in the number of microglia (3, 7 and 14 days) and astrocytes (7 and 14 days) of ADX compared to sham operated rats. Our study revealed no major signs of oxidative stress until two weeks after adrenalectomy when a significant decrease of GSH levels and SOD activity as well as an increase in MDA levels were found in adrenalectomized compared to sham rats. In the current study we used passive avoidance test to evaluate the cognitive functions of the ADX rats, we have found that the removal of the adrenal gland caused a behavioral deficit in the adrenalectomized rats compared to the sham over the time (3, 7 and 14 days).

Our study showed an early increase in the pro-inflammatory cytokines followed by neurodegeneration and activation of glial cells as well as oxidative stress. Taking these findings together it could be speculated that the early inflammatory components might contribute to the initiation of the biological cascade responsible for subsequent neuronal death in the current neurodegenerative animal model. These findings suggest that inflammatory mechanisms precede neurodegeneration and glial activation.

Keywords: Adrenalectomy, Hippocampus, Neuroinflammation, Neurodegeneration, Oxidative stress

Laboratoire: Ethnobotanie-Palynologie and Ethnopharmacologie-Toxicologie, Département de Biologie animale, Université les frères Mentouri Constantine-1.

Devant le jury :

Présidente :	Pr. AMEDAH SOUAD	Université des frères Mentouri Constantine1
Directrice de thèse :	Pr. KHELIFI-TOUHAMI FATIMA	Université des frères Mentouri Constantine1
Examinateurs:	Pr. BAGHIANI ABDERRAHMANE	Universite Abbas Ferhat setif-1
	Pr. ARRAR LEKHMICI	Université Abbas Ferhat Sétif-1
	Pr. KHENNOUF SEDDIK	Université Abbas Ferhat Sétif-1
	Dr. CHETTOUM AZIEZ	Universite des freres mentouri Constantine1